Activity of oncolytic vaccinia virus vectors in ovarian cancer

Lynsey May Whilding

A thesis submitted for the degree of Doctor of Philosophy

March 2012

Centre for Molecular Oncology
Barts Cancer Institute
Queen Mary, University of London
Charterhouse Square
London
United Kingdom

Declaration

The work presented in this thesis was done by the author, Lynsey May Whilding, at the Centre for Molecular Oncology, Barts Cancer Institute, Barts and The London School of Medicine and Dentistry, Queen Mary University of London. All external sources have been properly acknowledged.

Acknowledgments

I am grateful to Prof. Nick Lemoine for giving me the opportunity to work at the Barts Cancer Institute. It has been a wonderful place in which to undertake a PhD and this is due to both the facilities and the supportive and friendly nature of everyone who works here. It is a great Institute and one that I have been very proud to be associated with.

I have two supervisors that I could not have done this without. To Daniel Öberg, my supervisor for the first half of this PhD. Thank you for everything; your initial ideas, your enthusiasm and your unwavering support and belief in me from day one. You have been sorely missed! I am truly grateful for all you have done for me. To Iain McNeish, who graciously adopted another student and made me feel like one of his team: I now have a branded mug to make it official. Thank you for all your support, the shared enthusiasm for pretty pictures, and your help in seeing this through. It has been invaluable to me and I really appreciate it.

There are far too many people at the Barts Cancer Institute to thank individually but I will attempt to. Thanks to Jerome for helping me in the early days, and to Julie for help with furry things. To everyone in Team McNeish past and present, thank you Katrina, Carin, Kyra, Michelle, Laura, Darren, AM, Maggie and Michael. Thanks for the scientific help, your company in the lab and the seemingly endless supply of cake and chocolate!

Special mentions must go to Katrina Pirlo, Katrina Sweeney and Kate Lines for their friendship outside of the lab. There have been countless holidays, nights out, lunch breaks and gossip. You have always been there for me and I count you as very good friends. Thanks for making it so much fun! Thanks also for sharing wine/cocktails/coffee and listening when it wasn't so fun. And to my best drinking partner Mark Ferguson, cheers! To Sab, thank you for all of the above and for a million and one other things. I hope you know how much it means to me. I couldn't have done this without you and, more importantly, nor would I have wanted to.

Last, but definitely not least, thank you to all my family, to my parents and to my brothers and sisters, Michelle, Diana, David and Jack. It has always been nice having everyone so close and knowing that I could always pop round. Thanks for tempting me away from the lab with tea, cake, roast dinners, celebrations and multiple trips away (Michelle!). Most of all, thank you for always being there and reminding me of the all the things that are more important than a PhD!

Abstract

Oncolytic vaccinia virus has great potential in the treatment of cancer and two engineered strains have entered clinical trials. As the advent for oncolytic vaccinia virus as an approved therapy beckons, it is critical to consider some of the barriers that may hinder this progress. These include suboptimal delivery of the virus to tumour sites, incomplete destruction of the tumour mass, and a lack of full understanding of the way in which oncolytic vaccinia kills its target cells. This thesis attempts to address these issues, with a particular focus on ovarian cancer.

As ovarian cancer is generally restricted to the peritoneal cavity, intraperitoneal delivery may be preferable over intravenous delivery. Here, it is shown that Lister-dTK, an engineered vaccinia strain, is able to selectively replicate in ovarian tumours, including metastases to the liver following intraperitoneal delivery. To determine whether Lister-dTK could potentially be used in combination with current therapies for ovarian cancer, the effect of cisplatin and Lister-dTK together was assessed *in vitro* but showed no improvement in overall cell death.

In an attempt to further improve the anti-tumour efficacy of Lister-dTK, the extracellular matrix protein (ECM) decorin was expressed from the virus. Decorin interacts with various signalling pathways and is proposed to enhance virus spread. However, abrogation of EGFR and TGFβ signalling could not be demonstrated *in vitro*, nor could improved virus spread. In an intraperitoneal model of ovarian cancer, Lister-mDCN did not demonstrate enhanced efficacy over a control virus.

To determine the mechanisms of ovarian cancer cell death induced by Lister-dTK, the roles of apoptosis, autophagy and necrosis were investigated. Whilst some features of both apoptosis and autophagy were observed, inhibition of these pathways did not attenuate Lister-dTK. It is proposed that necrosis is the primary cause of cell death but that this process may occur in a regulated manner.

Abbreviations

3-MA	3-methyladenine
5-FC	5-fluorocytosine
5-FU	5-fluorouracil
6-MPDR	6-methylpurine deoxyriboside
Ad	adenovirus
AIF	apoptosis-inducing factor
AMP	adenosine monophosphate
AMPK	AMP-activated protein kinase
Apaf-1	apoptotic protease activating factor 1
APC	antigen-presenting cell
APS	ammonium persulphate
AST	aspartate transaminase
ATP	adenosine triphosphate
BCI	Barts Cancer Institute
BSA	bovine serum albumin
BSU	Biological Services Unit
CAD	Caspase activated DNase
CAR	coxsackievirus-adenovirus receptor
CBP	chemokine binding protein
CD	cytosine deaminase
CEV	cell-associated enveloped virus
CHO	Chinese Hamster Ovary
CO2	carbon dioxide
COX-2	cyclooxygenase-2
CPE	cytopathic effect
CQ	chloroquine
CS	chondroitin sulphate
DAPI	4',6-diamidino-2-phenylindole
DCN	decorin

DLT	dose limiting toxicity
DMEM	Dulbecco's modified eagle medium
DMSO	dimethyl sulphoxide
DNA	deoxyribonucleic acid
DS	dermatan sulphate
dsRNA	double-stranded RNA
DTT	dithiothreitol
EC50	efficient concentration 50%
ECL	enhanced chemiluminescence
ECM	extracellular matrix
EEV	extracellular enveloped virus
EFC	entry-fusion complex
EGF	epidermal growth factor
EGFR	epidermal growth factor receptor
ELISA	enzyme linked immunosorbent assay
Est	estimated
FADD	Fas-Associated protein with Death Domain
FBS	foetal bovine serum
FDA	Food and Drug Administration
FGF	fibroblast growth factor
FLIP	FLICE-like inhibitory protein
FSC	forward scatter
GAG	glycosaminoglycan
GM-CSF	granulocyte macrophage colony-stimulating factor
H&E	hematoxylin and eosin
H_2O	water
HBSS	Hank's buffered salt solution
HGF	hepatocyte growth factor
HMGB1	high-mobility group protein B1
hr	hour
HRP	horseradish peroxidase

HSV	herpes simplex virus
hTERT	human telomerase reverse transcriptase
IAP	inhibitor of apoptosis protein
iCAD	inhibitor of Caspase activated DNase
IFN	interferon
IL	interleukin
IMV	intracellular mature virus
IOSE	immortalised ovarian surface epithelial
ip	intraperitoneal
IRES	internal ribosomal entry site
it	intratumoural
iv	intravenous
IV	immature virion
LB	liquid broth
LC3	light chain 3
MCMV	murine cytomegalovirus
mDCN	murine decorin
MFI	mean fluorescent intensity
MHC	major histocompatibility complex
MMP	matrix metalloproteinase
mRNA	messenger RNA
MTD	maximum tolerated dose
MTS	3-(4,5-dimethylthiazol-2-yl)-5-(3-carboxymethoxyphenyl)-2-(4-sulfophenyl)-2H-tetrazolium)
MTT	(3-(4,5-Dimethylthiazol-2-yl)-2,5-diphenyltetrazolium bromide)
MV	mature virus
MVA	modified Ankara strain
Nec-1	Necrostatin-1
NK	natural killer
NT	non-targeting
NTC	non template control

NYCBOH	New York City Board of Health
NYVAC	New York vaccinia strain
OD	optical density
PAMP	pathogen-associated molecular pattern
PARP	Poly (ADP-ribose) polymerase
PBS	phosphate buffered saline
PBST	phosphate buffered saline tween
PCD	programmed cell death
PCR	polymerase chain reaction
PD	progressive disease
PDCD4	programmed cell death 4
PDGF	platelet derived growth factor
pEGFR	phosphorylated epidermal growth factor receptor
pfu	plaque forming unit
PKR	RNA-dependent protein kinase
PMS	phenazine methosulphate
PNP	purine nuceloside phosphorylase
PR	partial response
PRR	pathogen recognition receptor
PS	phosphatidylserine
qPCR	quantitative PCR
RAGE	receptor for advanced glycation end products
RECIST	Response Evaluation Criteria In Solid Tumours
RFP	red fluorescent protein
RIP1	receptor interacting protein 1
RIP3	receptor interacting protein 3
rmDCN	recombinant murine decorin
RNA	ribonucleic acid
SD	stable disease
SD	standard deviation
SDS	sodium dodecyl sulphate

SEM	standard error of the mean
SGLT1	sodium/glucose co transporter
siRNA	small interfering RNA
SPI	serine protease inhibitor
SSC	side scatter
TBST	Tris-buffered saline Tween
TCA	trichloroacetic acid
TCID50	tissue culture inhibitory dose 50%
TGFβ	transforming growth factor β
TK	thymidine kinase
TLR	toll-like receptor
TNFR	tumour necrosis factor receptor
TNFα	tumour necrosis factor α
TRADD	Tumor necrosis factor receptor type 1-associated DEATH domain
TRAIL	TNF-related apoptosis-inducing ligand
TTP	thymidine triphosphate
Tyr	tyrosine
UK	United Kingdom
UV	ultra violet
VCP	vaccinia complement control protein
VEGF	vascular endothelial growth factor
VEGFR	vascular endothelial growth factor receptor
VGF	vaccinia growth factor
VSV	vesicular stomatitis virus
WR	Western Reserve
wt	wild-type

Contents

Chapter 1

Introduction

1. Introduction

Cancer is a leading cause of death worldwide and, in 2008, accounted for 13% of all deaths (Globocan 2008 database). This figure is projected to continue to rise and, despite significant advances in diagnosis, reductive surgery and therapeutic intervention, cancer remains a global concern. It is estimated that, worldwide, almost one in five people will develop cancer before the age of 75, rising to at least one in three in developed countries (Globocan 2008 database). Sadly, many of these will die from the disease, as conventional chemo- or radiotherapy remain fairly ineffective in treating metastatic disease and fail to cure patients who have been diagnosed at a late stage. Furthermore, current treatment options are typically associated with adverse side effects and potential therapeutic benefit must be weighed against quality of life. It is perhaps no surprise given these statistics that numerous awareness and screening programmes are in place in the developed world, and that there is extensive research undertaken covering the causes, prevention and early diagnosis of cancer. Whilst these attempts are admirable, and indeed potentially hugely effective, there remains an ongoing need to develop improved and innovative treatments. This is of particular importance in cancers where symptoms are vague, and diagnosis is therefore delayed until cancer has progressed beyond the point of surgical intervention or the window of effective conventional therapeutic treatment; one such cancer is ovarian cancer.

1.1 Ovarian Cancer

Ovarian cancer was diagnosed in approximately 6500 women in the UK in 2008 and, in the same year, 4400 women died from the disease (CancerResearchUK 2011). The incidence has decreased slightly across all age groups since the early 2000's, possibly due to widespread use of the contraceptive pill which decreases the risk of ovarian cancer (Rodriguez 2003; Hannaford, Iversen et al. 2010), and has coincided with a small decrease in mortality. However, the long-term survival (>5yrs) is still relatively low at 41% and has not seen significant increases over the past decades. In contrast, the 1-year survival rate currently stands at 70% in patients diagnosed between 2003-2007 and has increased significantly from 42% in 1971-75 diagnoses, 52% in 1980-1984, and 67% in those diagnosed between 2000-2004 (CancerResearchUK 2011). It is believed that these increases are due to the increased use of platinum-based therapy; however the improvement in the 1-year survival rate appears to be levelling out since the beginning of the century. Similarly, the 5-year survival has only increased from 38% to 41% in the last decade, and the increase here is mainly in those diagnosed at an earlier stage.

In patients who are diagnosed with stage 1 disease (confined to the ovaries) the 5-year survival is 90%, although only 30% of patients are in this category. A further 5% are diagnosed at stage II (metastasized to the pelvic organs only), and the majority of patients at either stage III (metastasized beyond the pelvis area and/or regional lymph node metastases) or stage IV (distant metastases beyond the peritoneal cavity). Patients who are diagnosed at these later stages (III and IV) have 5-year survival rates of just 22% and 6% respectively, and it is in these patient populations particularly that there is an urgent need for novel, more effective therapies.

Current treatment for ovarian cancer consists of surgery to remove the tumour. Even at later stages, when complete resection is not possible, primary 'de-bulking' of the tumour is performed as there is a belief that this, followed by chemotherapy, may increase survival, although this is still under debate (Schorge, Garrett et al. 2011). It has been reported that interval debulking as opposed to primary debulking results in improved survival in patients with stage IIIC/IV disease, with fewer complications (Rauh-Hain, Rodriguez et al. 2011). The majority of patients besides those with stage IA or IB disease receive adjuvant chemotherapy, invariably platinum-based and this is administered immediately following surgery. In patients with early stage disease, adjuvant chemotherapy has been shown to increase survival (Colombo, Guthrie et al. 2003; Trimbos, Parmar et al. 2003); in late stage disease it is the only standard treatment option available, although the majority of patients relapse after an initial response. If a patient relapses within 6 months of platinum treatment they are deemed platinum-resistant; relapse after this timepoint generally results in repeat platinum-based chemotherapy. This cycle of relapse and subsequent further chemotherapy continues, sometimes with a favourable outcome, but inevitably to the point where tumours are refractory to treatment and disease progresses.

There is an argument for intraperitoneal (ip) delivery of chemotherapeutics as ovarian cancer is constrained to the peritoneal cavity except in stage IV disease. The high local concentration of drug that ip delivery achieves can result in improved outcome compared to intravenous delivery. Compared to intravenous (iv) delivery, ip delivery improved progression-free survival by 5 months and overall survival by 15 months (Armstrong, Bundy et al. 2006), and a meta-analysis studying the results of nine trials comparing ip to iv therapy also supported the view that ip delivery improved survival. In addition, a recent study confirmed that several cycles (<6) of ip chemotherapy could be administered to patients with advanced stage disease (stage IIA-IV) (Skaznik-Wikiel, Lesnock et al. 2011).

Despite the late diagnosis (stage III-IV) of 60% of patients that might suggest otherwise, ovarian cancer is not an asymptomatic disease. It has been suggested that symptoms are present at all stages of disease progression (Bankhead, Collins et al. 2008) but without a doubt these are vague, and include pelvic and abdominal pain, fatigue, back pain and urinary symptoms amongst others. Whilst persistant abdominal pain may lead to further clinical investigation, other transient symptoms are easily confused with less severe health problems, and this may contribute to the late diagnosis of the majority of patients. Diagnostic tests include ultrasound and measurement of serum levels of CA125 (also known as MUC16), which is elevated in many ovarian cancers, and histological confirmation of disease.

The lack of clearly defined symptoms of ovarian cancer which leads to advanced disease at the time of diagnosis, subsequent dissemination resulting in an unresectable tumour burden, and the development of chemo-resistance means that there is a need for novel therapeutics for the treatment of advanced ovarian cancer. Viral gene therapy is one such strategy that may be of therapeutic benefit.

1.2 Viral gene therapy for cancer

Viruses are obligate intracellular parasites, which have evolved to behave as biological delivery vehicles capable of self-amplification within the host, and generally lead to the eventual death of infected cells. Their frequently immunogenic nature also gives rise to the possibility that their presence may initiate or potentiate an anti-tumour host immune response. Increased understanding of the pathogenesis of cancer, and the molecular pathways underlying malignant transformation have prompted the design of rationally developed therapeutics that can specifically target aspects of tumour progression. This, coupled with increased knowledge of virus behaviour and advances in molecular biology techniques, has accelerated the manipulation of viruses for therapeutic benefit.

The idea that viral infection can lead to tumour clearance is not a novel concept and dates back to at least 1912, when De Pace described tumour regression in one patient with cervical carcinoma following inoculation with a live attenuated rabies vaccine (described by Sinkovics and Horvath (Sinkovics and Horvath 2008)). Since then, there have been several reports of spontaneous tumour regression, all of which were described following infection with measles virus (Bluming and Ziegler 1971; Pasquinucci 1971; Zygiert 1971; Taqi, Abdurrahman et al. 1981). In addition, deliberate injection of wild-type vaccinia virus into lesions of melanoma several decades ago (Burdick and Hawk 1964; Hunter-Craig, Newton et al. 1970; Roenigk, Deodhar et al. 1974) resulted in regression, although understandably, the reasons behind this response were not understood. Increased knowledge of the molecular mechanisms behind cancer has led to a resurged interest in viral gene therapy, as it becomes possible to target cancer cells directly with specific genetic abnormalities/mutations using viral delivery vectors. In contrast, conventional therapy frequently targets rapidly dividing cells rather than specific molecular targets to cause cell growth arrest or cell death. As a result, treatment is restricted by dose-limiting toxicity to normal proliferating cells.

Viruses can be genetically engineered to replicate selectively in tumour cells and, as replication is aborted in normal tissue, in theory they represent a safe means of treatment. Additionally, as they replicate and cause cell lysis, spreading from one cell to the next, they have the potential to kill a large tumour mass from an initial low dose. Almost 70% of all gene therapy clinical trials target cancer (Young, Searle et al. 2006) and, although they have proved safe, few have shown success in terms of an advantage in survival when used as mono-therapeutic agents. In contrast, when combined with conventional chemotherapeutics, or when viruses are armed with transgenes, response rates are higher (Young, Searle et al. 2006). Two clinical trials in particular have shown the potential of viral gene therapy as a realistic treatment option for cancer. A randomised trial showed a significant survival advantage in patients with human malignant glioma who were treated with adenovirus, although this was replication defective. Following tumour resection patients received doses of the virus, which was armed with a transgene to convert a non-toxic drug into its toxic form. This treatment led to an increase in median survival of over 65% (Immonen, Vapalahti et al. 2004) when compared to the standard treatment of radiotherapy post-resection.

Further successful trials led to the worlds first approved oncolytic agent for the treatment of cancer in 2004: a replicating adenovirus expressing p53 (H101) is now an approved therapy for head and neck squamous cell carcinoma and oesophageal cancer in China in combination with chemotherapy. The success of H101 is now attempting to be duplicated in glioblastoma with promising early results (Song, Zhou et al. 2009) and shows how the development of oncolytic viruses may be applied across many cancers.

1.3 Vaccinia Virus

Vaccinia virus is a member of the *Orthopoxvirus* genus and, together with variola virus, cowpox virus, monkeypox virus, ectromelia virus, raccoonpox virus, camelpox virus and ataterapoxvirus, forms part of the *poxviridae* family. Genome sequencing of these viruses identifies them as morphologically indistinguishable and antigenically related to one another

(Smith, Vanderplasschen et al. 2002), providing the basis for which cowpox and then vaccinia virus were able to vaccinate so successfully against variola virus, the cause of smallpox, leading to its global eradication in 1979.

1.3.1 Structure

Vaccinia is a large, enveloped, double-stranded DNA virus that replicates exclusively in the cytoplasm of host cells. The vaccinia virus virion comprises double-stranded DNA within a biconcave core particle flanked by two lateral bodies (Hruby 1990; Kuznetsov, Gershon et al. 2008). This entire structure is enclosed by an outer envelope to make up a large brick shaped mature virus (MV) measuring approximately 400 x 240 x 200nm in size (Michael T. Madigan 2000). A second form of the virus exists which has an extra lipid bilayer, and is termed the extracellular enveloped virus (EEV).

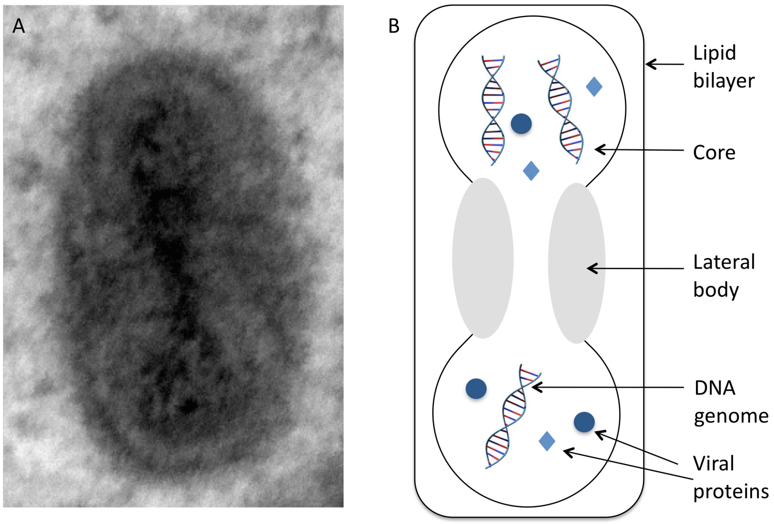

Figure 1: Structure of mature vaccinia virus. A) Electron microscopy of a mature virion. B) Schematic diagram of vaccinia virus.

1.3.2 Cell entry

The mechanisms of cell entry are still unclear and differ between the two forms of infectious vaccinia virus, the intracellular mature virus (IMV) and the extracellular enveloped virus (EEV). IMV are virions enclosed within a single membrane and are predominantly released upon cell lysis. However, between 5 and 20% are transported to the cell surface before cell lysis and acquire an extra membrane to form either cell-associated enveloped virus (CEV) or EEV. CEV are responsible for cell-to-cell spread and drive virions towards uninfected cells by inducing the formation of actin tails at the cell surface. In contrast, EEV, which represent only a small proportion of virions formed during replication, are released from the cell surface and are responsible for long-range dissemination (Roberts and Smith 2008).

Three main mechanisms for virus entry have been proposed: direct fusion, endocytosis and macropinocytosis (depicted in Figure 2). Electron microscopy images generated within this thesis (Figure 2) also show virions between cells, presumably spreading from one cell to the next. It has been reported that IMV and EEV bind to cells through different receptors (Vanderplasschen and Smith 1997) and enter via distinct pathways, either pH-independent or pH-dependent respectively (Vanderplasschen, Hollinshead et al. 1998). A minority of IMV enter cells through direct fusion with the plasma membrane (Carter, Law et al. 2005); however, a second, low pH-dependent pathway where IMV is internalised by endocytosis has also been described (Townsley and Moss 2007). In addition, there is evidence to suggest that both forms of vaccinia virus enter cells by macropinocytosis (Huang, Lu et al. 2008; Mercer and Helenius 2008; Mercer, Knebel et al. 2009; Sandgren, Wilkinson et al. 2010; Schmidt, Bleck et al. 2011), a process normally reserved for the intake of fluid. Macropinocytosis is accompanied by actin-mediated membrane ruffling and blebbing, followed by the formation of large vacuoles at the plasma membrane. As almost all cell types are capable of macropinocytosis, this may allow virus entry into a huge range of host cells, and indeed vaccinia can infect a wide range of cells.

An entry-fusion complex (EFC) has been proposed for vaccinia based on the identification of at least 8 proteins that have been determined as essential for cell entry. These include the A28L (Senkevich, Ward et al. 2004), H2 (Senkevich and Moss 2005), A21 (Townsley, Senkevich et al. 2005), L5R (Townsley, Senkevich et al. 2005), G3L (Izmailyan, Huang et al. 2006), G9 (Ojeda, Domi et al. 2006) and A16L proteins (Ojeda, Senkevich et al. 2006). More recently, another component of the complex has been identified following investigation into smaller open reading frames within the vaccinia virus genome (Satheshkumar and Moss 2009). These proteins are all surface components of the IMV that are expressed late in infection. Individual null mutants produce phenotypes that are indistinguishable from each other; virions look normal but are non-infectious, with particles attaching to cells but not penetrating into the cytoplasm (Moss 2006).

Entry of EEV requires shedding of both membranes and it is proposed that the outer envelope is shed first allowing the inner IMV membrane to fuse with the plasma membrane (Law, Carter et al. 2006). The process of macropinocytosis is also implicated in the entry of EEV

(Sandgren, Wilkinson et al. 2010; Schmidt, Bleck et al. 2011), and indeed this pathway may be more important for the EEV form than the IMV form, as IMV entry is less sensitive to inhibition of the pathway by rottlerin and dimethy amiloride (Sandgren, Wilkinson et al. 2010). Despite the presence of an additional membrane, fusion is more efficient and occurs more rapidly for the EEV form than the IMV (Doms, Blumenthal et al. 1990). Additionally, whilst the entry of IMV initiates a signalling cascade, EEV do not (Locker, Kuehn et al. 2000), suggesting that different receptors or mechanisms are involved.

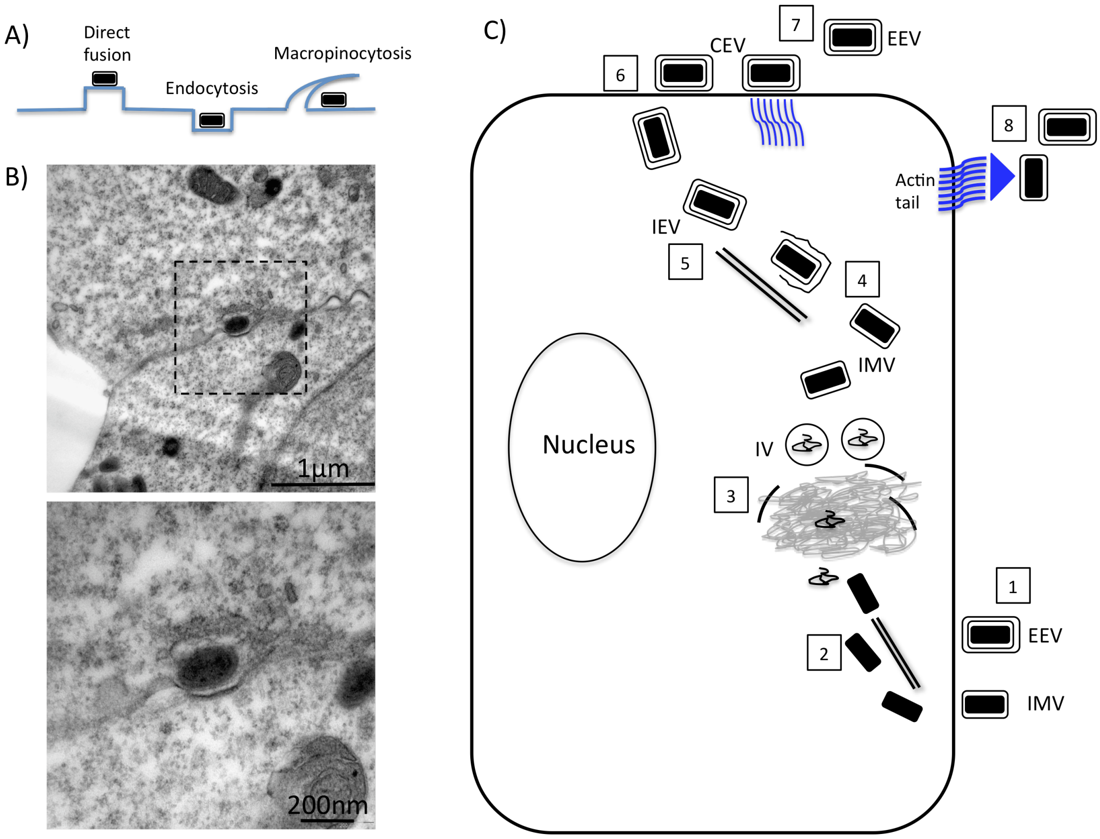

Figure 2: Entry and life cycle of vaccinia virus. A) Vaccinia virus can enter by either direct fusion with the cell membrane, endocytosis or macropinocytosis. B) Electron microscopy of vaccinia cell to cell spread in A2780 ovarian cancer cells. Cells were infected with 10pfu/cell of Lister-dTK and fixed 72hrs post-infection. A virion can be seen between two cells within a dip in the cell membrane. EM images were generated by the author, with assistance (see Materials and Methods) C) Schematic diagram of vaccinia virus replication. Intracellular mature virions (IMV) or extracellular enveloped virions (EEV) enter cells (1), lose their outer membrane and the virus core moves further into the cytoplasm by transport along microtubules (2). Here, the core is uncoated and DNA replication takes place within a virus factory (3), where immature virions (IV) assemble and are processed to form IMV (4), the majority of which are released upon cell lysis. Some IMV are wrapped by a double membrane to form intracellular enveloped virions (IEV) (5) and are transported to the cell membrane. The outer IEV membrane fuses with the plasma membrane to expose cellular enveloped virions (CEV) at the cell surface (6), which are either driven by an actin tail towards neighbouring cells or released as EEV (7). Once a cell is infected there is rapid repulsion of external virions towards uninfected neighbouring cells by actin tails to prevent re-infection of the same cell.

1.3.3 Replication and life cycle

The vaccinia virus genome is 195 kb long and encodes nearly 200 genes. Replication takes place exclusively within the cytoplasm and, although vaccinia is remarkable in its self-reliance compared to nuclear viruses, it is apparent that some host cell proteins are utilised during mRNA synthesis, and that there is a requirement for the host cell nucleus (reviewed by Moyer (Moyer 1987)). A virus-encoded RNA polymerase transcribes four distinct classes of genes: early, early/intermediate, intermediate and late. Approximately 50% are early genes whose products include enzymes necessary for uncoating of the virion core and DNA replication, and proteins involved in immune evasion, and are transcribed within minutes of virus entry. Transcription of early genes takes place within the virion core, where the enzymes and proteins required to synthesise mature mRNA reside alongside the viral genome.

The life cycle of vaccinia is summarised in Figure 2 and, following virus entry, DNA replication is initiated three hours post-infection within distinct sites that are surrounded by membranes derived from rough endoplasmic reticulum (Schramm and Locker 2005) and which are known as viral factories (Figure 3, panel A). Here, the most primitive form of virion begins to assemble with the formation of virus crescents (Figure 3, panel A). Proteins involved in virion morphogenesis and assembly are expressed from the late class of genes (Broyles 2003), and immature virions start to move away from the factory to be packaged into intracellular mature virions (IMV) within 5 hours of infection (Figure 3, panel B).

Replication is rapid and efficient and, after just 5-6 hours, it is possible for virions to be released from the cell surface, before cell lysis has occurred. Recently, live cell imaging has revealed a novel mechanism identifying the presence of ‘superinfecting virions’ that, remarkably, are able to spread across one cell every 75 minutes (Doceul, Hollinshead et al. 2010), far quicker than replication kinetics allow. Newly infected cells that have not yet set up viral factories express two surface proteins, A33 and A36, which exploit cellular machinery to induce actin tail formation before new virions are formed. These actin tails repel the CEV/EEV from the initial infection towards neighbouring uninfected cells, allowing viral spread to distant cells without the need to replicate first in each one. It also serves to repel other infecting virions. Thus, it appears that vaccinia has developed sophisticated methods to limit the number of virions that enter each cell, and instead promotes infection of neighbouring unoccupied cells.

As infection progresses, the number of IMV within the cell increases and membrane rupture occurs (Figure 3, panel C) before the host cell eventually succumbs to cell lysis, releasing IMV which go on to infect neighbouring cells (Figure 3, panel D).

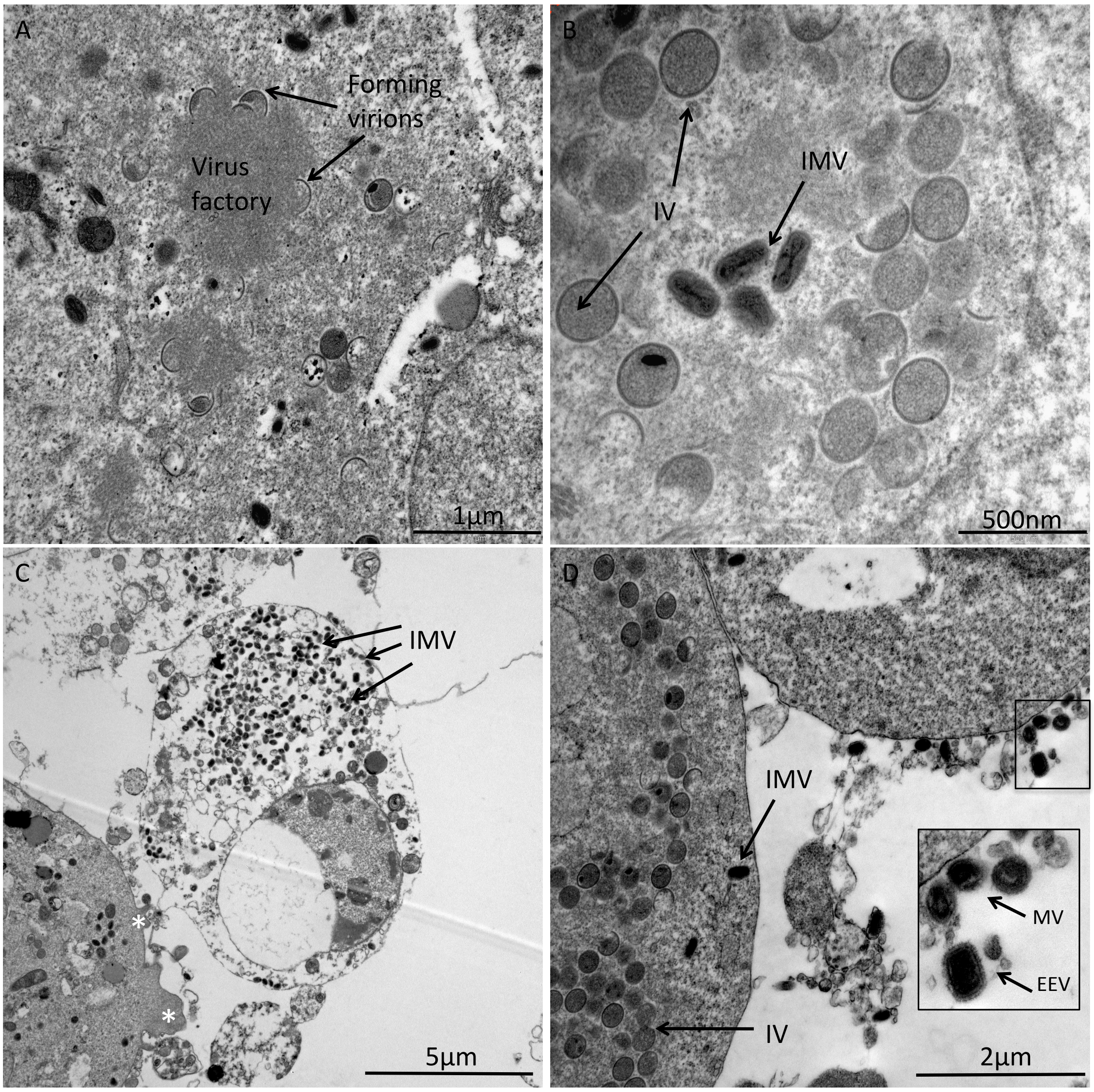

Figure 3: Early and late replication of vaccinia virus in A2780 ovarian cancer cells. Mixed populations of cells in the early stages of infection (A and B) and later stages of infection (C and D) were observed by electron microscopy following infection with 10pfu/cell Lister-dTK. A virus factory can be seen in panel A where virus crescents depict forming virions. These assemble into immature virions (IV) and intracellular mature virions (IMV) (panel B). In the later stages of infection (panel C), a cell is seen full of IMV and with a ruptured cell membrane. A neighbouring cell in an earlier stage of infection shows signs of membrane ruffling (marked with *). Cell debris from a dead cell is observed in panel D and the two forms of virus (IM and EEV) can be seen near the surface of a neighbouring cell. Electron microscopy images were generated by the author, with assistance from Graham McPhail, Nanovision Centre, Queen Mary University of London (see Materials and Methods).

1.4 Vaccinia as an oncolytic virus

Vaccinia possesses numerous properties that make it an attractive candidate for use in viral gene therapy, including a proven safety record, a wide host range, rapid cytoplasmic replication, immuno-evasion and the capacity to incorporate inserted genes, all of which are described in more detail in section 1.4.1. In addition to early observations that wild-type vaccinia virus could lead to tumour regression (Hunter-Craig, Newton et al. 1970; Roenigk, Deodhar et al. 1974), multiple groups have studied the effect of engineered viruses in pre-clinical and clinical models. The success of these pre-clinical studies in mice still remains to be seen in patients, although it is true that most clinical trials to date have focused on determining the maximum tolerated dose and documenting any adverse side effects rather than aim for efficacious treatment. By far the most promising, or certainly the most advanced, of these engineered viruses is the JX-594 engineered strain, which has shown safety and some efficacy in several clinical trials, summarised in section 1.4.5.

1.4.1 Advantages of using vaccinia

Vaccinia has been widely used during the worldwide vaccination programme against smallpox and so has a proven record of safety in humans spanning centuries, with well documented side effects (Lane, Ruben et al. 1969). Subsequent clinical trials in humans using vaccinia as an oncolytic virus have also demonstrated limited toxicity (Mastrangelo, Maguire et al. 1999; Park, Hwang et al. 2008). In the rare incidence that the virus could cause complications due to uncontrolled replication, approved drugs such as cidofovir (De Clercq 2002) or vaccinia immunoglobulin (Wittek 2006) exist to combat symptoms.

An advantage of vaccinia over other virus competitors, such as adenovirus, is its ability to infect a wide variety of species, enabling its use in pre-clinical animal models, the results of which may facilitate progression into human trials. Additionally, due to presumed ubiquitous receptors for virus entry, or via the process of macropinocytosis, vaccinia is able to infect almost all human tissue and cells (Moss 2001). Not only does this greatly expand the range of pre-clinical work that can be performed in a laboratory, but it also implies that vaccinia could be used successfully to treat a wide range of cancers originating from different tissue.

Although some strains of vaccinia virus show natural tumour tropism (discussed further in section 1.4.3.1) it is generally necessary, and perceived far safer, to ensure tumour-specificity by deletion of certain viral genes that are required for replication in normal cells but not in tumour cells.

Unlike smaller DNA viruses, there appear to be no constraints on the absolute size of vaccinia virus for efficient packaging and replication, allowing deletion of up to 20 kilobases from the viral genome (Panicali, Davis et al. 1981). Although viral gene deletions promote tumour specificity they may also attenuate the virus in target tissue. Inserting therapeutic genes, which aim to increase overall toxicity to cancer cells, into the virus can combat this and, as vaccinia virus can also incorporate up to 25 kilobases of foreign DNA (Smith and Moss 1983), multiple genes may be inserted without compromising replication.

Vaccinia virus replication takes place strictly in the cytoplasm of cells eliminating the risk of integration into the host genome. Dependence on host RNA polymerases is not required for vaccinia virus replication (Broyles 2003) and foreign genes inserted into the genome are capped and polyadenylated by viral enzymes ensuring efficient translation. Additionally, cytoplasmic replication means export signals to transport foreign DNA from the nucleus to the cytoplasm where translation takes place are not required. As vaccinia virus does not splice its primary transcripts, there is no need to consider consensus splice signals in the correct locations (Hruby 1990).

The life cycle of vaccinia virus is summarised in Figure 2**.** There is complete inhibition of host cell protein synthesis within 2 hours of the virus entering the cell (Shen and Nemunaitis 2005; Thorne, Bartlett et al. 2005), viral replication factories are initiated within 5 hours of infection and a single replication cycle producing mature virions takes just 10-12 hours (Hruby 1990). This rapid replication and release of infectious progeny means a lower dose can initially be given, yet effective infection of neighbouring cells and spread within the tumour is retained. Rapid replication also maximises tumour cell death in the time it takes the immune system to mount an attack against the virus.

Dissemination of virus particles to distant sites following delivery has so far been a limitation in viral gene therapy and, furthermore, rapid clearance of some viruses delivered systemically restricts accessible tumour tissue to predominantly primary lesions that can be targeted by intratumoural delivery. In mice, 90% of systemically delivered adenovirus 5 is cleared by Kuppfer cells in the liver within 24hrs (Alemany, Suzuki et al. 2000) and, whilst there are unpublished data to suggest that the spleen is involved in early clearance of vaccinia virus (James Tysome et al, unpublished data, Barts Cancer Institute, Queen Mary University of London) intravenous delivery of vaccinia has been shown effective in treating various pre-clinical models (Kirn, Wang et al. 2007; Thorne, Hwang et al. 2007; Zhang, Yu et al. 2007; Yu, Galanis et al. 2009; Gentschev, Donat et al. 2010; Gentschev, Muller et al. 2011).

Recently, a small trial involving 23 patients with various tumours demonstrated tumour selective virus replication following intravenous delivery of vaccinia, and stable disease in 12 patients with a partial response in another patient (Breitbach, Burke et al. 2011). This encouraging response from a dose-escalating Phase I trial designed to determine effective delivery only, together with pre-clinical data, suggests that vaccinia may be effective in treating metastatic disease. Furthermore, the EEV produced during natural vaccinia infection has naturally evolved to mediate long range dissemination within the host and, crucially, is resistant to neutralisation both by antibodies (Vanderplasschen, Hollinshead et al. 1997) and complement (Vanderplasschen, Mathew et al. 1998). A recent study has shown that increased production of EEV leads to enhanced intratumoural spread and spread to distant tumours following systemic delivery without compromising safety (Kirn, Wang et al. 2008).

1.4.2 Vaccinia virus strains

Multiple variants of vaccinia virus exist owing to the use of different vaccine strains during the smallpox eradication programme, and all of these strains have unique properties. Some strains, such as modified Ankara strain (MVA) and New York vaccinia strain (NYVAC), do not replicate in mammalian cells. Thus, whilst they are suited for vaccination purposes, they have no oncolytic potential. The different strains that have potential as oncolytic agents are summarised in **Table 1**; of these the most widely used to date are the Wyeth, New York City Board of Health (NYCBOH), Western Reserve and Lister strains.

Table 1: Replication competent vaccinia virus strains.

Strain	Background	Characteristics	Ref.
Wyeth or NYCBOH	North American vaccine strain	Minimal inherent tumour selectivity but commonly used, including in clinical trials as an oncolytic virus	(Park, Hwang et al. 2008; Breitbach, Burke et al. 2011)
Western Reserve	Laboratory strain derived from Wyeth after passaging in mice	Has high tumour selectivity, reported to have increased lytic ability. Limited clinical use in humans	(Thorne, Hwang et al. 2007)
Lister	European (UK) vaccine strain	Extensive use in humans during eradication of smallpox, also in clinical trials as oncolytic virus. Some inherent tumour selectivity. Unpublished data suggests Lister strain has higher oncolytic potential than WR (Hughes et al, Barts Cancer Institute, Queen Mary University of London).	(Lane, Ruben et al. 1969; Tysome, Wang et al. 2011)
Copenhagen	Northern European vaccine strain	Inherent tumour selectivity but withdrawn during smallpox eradication programme due to high incidence of adverse events	(Kretzschmar, Wallinga et al. 2006)
Tian Tan	Chinese vaccine strain	Extensive use in China during eradication of smallpox, less virulent than WR strain but unknown oncolytic potential	(Fang, Yang et al. 2005)

1.4.3 Mechanisms of tumour specificity

Some strains of vaccinia virus demonstrate inherent tropism for tumour tissue (***Table 1***) without the need for viral gene deletions to ensure tumour specificity; however, this is not a defining feature in selecting a strain for clinical use as an oncolytic virus, as the Wyeth strain most often used demonstrates minimal natural tropism. In order to ensure tumour specificity and limit toxicity in normal tissue, it is usually necessary to delete certain viral genes that are required for replication in normal cells but not in tumour cells. This is made possible by the fact that the genes and pathways that viruses modify in host cells in order to replicate successfully are often already deregulated in cancer cells. Viral genes encoding these modifying proteins are therefore redundant for replication in tumour cells and may be deleted.

1.4.3.1 Inherent tumour tropism

The mechanisms of tumour tropism are poorly understood, but may include preferential extravasation of the large vaccinia virus into tissue with leaky tumour vasculature, enhanced uptake of the virus and preferential replication in an already dividing cell that has aberrant growth pathways.

One characteristic of cancer is the leaky vasculature within tumours and the large vaccinia virus virions may preferentially infect tumour tissue due to easy access. This may also explain why biodistribution studies in mice following virus delivery show increased titres in the ovaries (Zhang, Yu et al. 2007; Chalikonda, Kivlen et al. 2008; Yu, Galanis et al. 2009) compared to other tissue, as ovarian follicles also have leaky vasculature (Neeman, Abramovitch et al. 1997). In addition, it has been shown that vaccinia virus uptake is increased in areas of hyperthermia (Chang, Chalikonda et al. 2005) which increases vascular permeability, and smallpox virus has also been described as replicating in areas of increased vascular permeability (McCart, Ward et al. 2001). As both tumours and ovaries are known to secrete vascular endothelial growth factor (Reynolds, Grazul-Bilska et al. 2000), which also increases vascular permeability, this may be a further contributing factor to their tendency to support virus infection.

The rapidly dividing nature of tumour cells may also be a contributing factor in the tumour tropism of vaccinia. Vaccinia virus encodes vaccinia growth factor (VGF) to stimulate cell proliferation (Buller, Chakrabarti et al. 1988) and the ready pool of nucleotides in already dividing tumour cells may encourage preferential replication in these over normal cells. However, it appears that dividing cells appear to support viral replication rather than be a critical factor in dictating tumour tropism as vaccinia is not toxic to other rapidly dividing cells, such as bone marrow-derived cells and gastrointestinal mucosa (Harrington 2008). This contrasts sharply with conventional chemotherapy that targets dividing cells. The epidermal growth factor receptor (EGFR) and subsequent signalling through the Ras/MAPK/ERK pathway is essential for vaccinia replication, as demonstrated by Yang et al (Yang, Kim et al. 2005), who showed that an EGFR tyrosine kinase inhibitor was able to delay or prevent death in mice following a lethal dose of vaccinia virus. Overexpression of the EGFR and constitutive activation of Ras are present in more than 50% and 20% respectively of all human cancers (Downward 2003), most notably in pancreatic cancer, where Ras mutations exist in nearly all cases (Almoguera, Shibata et al. 1988; Pellegata, Sessa et al. 1994). Activation of the EGFR-Ras pathway in cancer may further facilitate vaccinia virus replication and may contribute to tumour tropism.

1.4.3.2 Genetic engineering to ensure tumour selective replication

As not all vaccinia strains demonstrate inherent tumour tropism, and to increase the specificity of those that do further, a number of approaches are possible to achieve selective replication in tumour cells.

1.4.3.3 Tumour targeting by modifiying viral surface proteins

Attempts to ensure tumour specificity by modifying binding to cells have been largely unsuccessful (Galmiche, Rindisbacher et al. 1997; Katz, Wolffe et al. 1997) due to the complexity of vaccinia virus cell entry. Whilst understanding has increased over recent years, the mechanisms behind viral binding and entry remain inconclusive. The receptors responsible for virus attachment have not yet been identified for vaccinia virus and this makes it unlikely that tumour targeting by modification of surface proteins and their interactions with host cell proteins will be sufficient for selective replication yet. Additionally, cell entry appears both virus strain (Bengali, Townsley et al. 2009) and host cell type (Whitbeck, Foo et al. 2009) dependent, further complicating efforts to manipulate this process. It is also known that the intracellular and extracellular forms of vaccinia bind to distinct (unknown) receptors (Vanderplasschen and Smith 1997) and it is proposed that they enter cells by different mechanisms (Vanderplasschen, Hollinshead et al. 1998). The EEV has a fragile membrane that is easily damaged by purification, sonification or freeze thawing and so is difficult to isolate in the laboratory. Moreover, it is antigenically distinct from the IMV available in the lab (Boulter 1969) and therefore modification of IMV surface proteins may not have an effect on viral targeting *in vivo.*

1.4.3.4 Deletion of host range genes

Vaccinia can infect virtually all cell types, yet cell specific replication is possible via the interactions of host range gene products that selectively interact with cells to allow replication. Two such identified genes are SPI-1 and SPI-2, which are serine protease inhibitors (Kotwal and Moss 1989) implicated in the inhibition of apoptosis. The normal host defence mechanisms to viral infection include the induction of apoptosis; the function of these genes is to inhibit this process to permit viral replication. As one of the hallmarks of cancer is a resistance to cell death (Hanahan and Weinberg 2000), deletion of these genes is an approach that has been used to produce a tumour-selective virus with preferential replication in p53-null or transformed cells over normal cells (Guo, Naik et al. 2005). To date, only deletion of the SPI-1 and SPI-2 host range genes has been studied. By far, the most widely used approach in achieving tumour selectivity is the deletion of genes required for replication in normal cells, such as thymidine kinase and vaccinia growth factor.

1.4.3.5 Deletion of genes required for replication

Transformed cells typically already meet optimal conditions for viral replication as they have uncontrolled entry into S phase, disruption of apoptotic pathways and loss of ability to respond to immune factors. Vaccinia genes that induce these conditions in normal cells are therefore dispensable for successful replication in cancer cells and deletion of these genes to provide tumour specificity has proved successful for many tumour models including colon (McCart, Ward et al. 2001), pancreatic (Yu, Galanis et al. 2009), ovarian (Chalikonda, Kivlen et al. 2008), breast (Zhang, Yu et al. 2007), liver (Park, Hwang et al. 2008) and prostate cancers (Thorne, Hwang et al. 2007). The thymidine kinase (TK), vaccinia growth factor (VGF) and B18R genes are common deletions in vaccinia tumour-selectivity.

Type I interferons (IFNs) have profound anti-viral effects and the B18R gene encodes a protein that neutralises their effects. As tumour cells frequently do not produce IFN or are unresponsive to it, viral replication is enhanced in cancer cells (Kirn, Wang et al. 2007) regardless of the presence or absence of the B18R gene.

Cellular TK exists in both cytosolic and mitochondrial forms; the cytosolic form is responsible for the regulation of the precursor pool for DNA synthesis and the latter for the low but constant activity of resting cells. Cytosolic TK is almost undetectable in normal quiescent cells but increases at least 30-fold as cells enter S-phase (Hengstschlager, Knofler et al. 1994). In contrast, it is constitutively high in tumour cells (Hengstschlager, Knofler et al. 1994). Wild-type vaccinia virus encodes its own TK in order to increase the nucleotide pool required for DNA replication: a deletion in the viral TK gene creates a dependency on cellular thymidine triphosphate (TTP) from the nucleotide pool present in dividing cells or constitutively active tumour cells, thus restricting successful viral replication to these cells only.

VGF is a protein secreted early during viral infection that is closely related to epidermal growth factor (EGF) (Buller, Chakrabarti et al. 1988) and acts to prime neighbouring cells for infection by binding to the EGF receptor (EGFR) to stimulate cell proliferation and increase the nucleotide pool. Deletion of the gene reduces virulence in normal cells (Buller, Chakrabarti et al. 1988) but allows replication in tumour cells that frequently have activating mutations of the EGFR (Downward 2003). A vaccinia virus with deletions in both TK and

VGF genes was first described in 2001 (McCart, Ward et al. 2001), and was followed by the construction of other mutants comprising double deletions and insertion of various therapeutic genes (Kirn, Wang et al. 2007; Thorne, Hwang et al. 2007; Chalikonda, Kivlen et al. 2008), all of which have been shown to replicate selectively in tumour cells. It is possible to combine multiple deletions of both host range genes and replication-essential genes but this may attenuate viral activity in both tumour cells and normal cells, as a triple-deleted virus demonstrated reduced oncolytic potential (Yang, Guo et al. 2007) .

1.4.4 Optimisation of vaccinia virus oncolytic therapy

A number of approaches exist that aim to improve the potency of vaccinia as an oncolytic agent. These include expression of transgenes from the virus that can enhance tumour cell death or aid imaging of the virus as it replicates in tumour sites, targeting metastatic or inaccessible tumours by intravenous delivery, approaches that allow repeated administration, and combining vaccinia virus with conventional therapies.

1.4.4.1 Transgene expression

In an effort to make vaccinia virus more potent and cytotoxic to tumour cells, a number of transgenes expressed from vaccinia virus have been evaluated. The potential of vaccinia virus to incorporate a large amount of foreign DNA into the genome, and the emergence of strong endogenous or synthetic promoters that allow high levels of transgene expression have already been discussed (section 1.4.1). Transgene expression within the infected cell is transient, and lasts only as long as the cell is viable. As vaccinia virus infection eventually leads to the death of infected cells, it is beneficial to express a transgene capable of having a bystander effect on surrounding uninfected cells, or one which is secreted and can enhance the overall cytotoxic effect through complementary mechanisms of action. As such, the majority of transgenes expressed from vaccinia virus have aimed to take advantage of these features and include pro-drug converting enzymes (Puhlmann, Gnant et al. 1999; McCart, Puhlmann et al. 2000; Erbs, Findeli et al. 2007; Chalikonda, Kivlen et al. 2008), anti-angiogenic agents (Frentzen, Yu et al. 2009; Guse, Sloniecka et al. 2010), cytokines to stimulate the anti-tumour immune response (Kim, Oh et al. 2006; Kirn, Wang et al. 2007; Thorne, Hwang et al. 2007) and pro-apoptotic agents (Ziauddin, Guo et al. 2011). In addition, the expression of imaging genes from vaccinia has allowed the delivery and replication of vaccinia virus to be studied, and can provide some indication of therapeutic action without disrupting the efficacy of the virus (Andrea McCart, Mehta et al. 2004; Brader, Kelly et al. 2009; Haddad, Chen et al. 2011).

The expression of a pro-drug converting enzyme from an oncolytic virus, which converts a non-toxic drug to its toxic form, is attractive in that it can lead to the death of uninfected cells in the surrounding area and thus a lower dose of virus can be administered with greater effect. The cytosine-deaminase (CD)/5-fluorocytosine (5-FC) (Gnant, Puhlmann et al. 1999) and purine nucleoside phosphorylase (PNP)/6-methylpurine deoxyriboside (6-MPDR) (Puhlmann, Gnant et al. 1999) prodrug systems, when expressed from a conditionally replicating vaccinia virus, have shown a survival advantage compared to the virus alone in colon and melanoma cancer models respectively when delivered locally. More recently, systemic delivery of VV in combination with CD/5-FC treatment proved effective in reducing tumour growth, showing its application for more advanced cancers with metastases (Foloppe, Kintz et al. 2008). However, an antiviral effect of the converted prodrug (5-FC to 5-FU) has been implied and no therapeutic advantage was seen when high doses of virus were given along with the prodrug (McCart, Puhlmann et al. 2000).

Expression of granulocyte macrophage colony-stimulating factor (GM-CSF) from oncolytic vaccinia has led to the development of JX-594 as the most successful strain in the clinic to date. GM-CSF stimulates anti-tumour immunity (Dranoff, Jaffee et al. 1993) and may contribute to the intra-tumoural vascular shutdown induced by vaccinia (Breitbach, Paterson et al. 2007); the success of JX-594 in controlling tumour growth in pre-clinical work has led to its development in several clinical trials (Table 2, section 1.4.5). The approach of using anti-angiogenic agents to enhance cytotoxic effect had also been studied through the expression of a soluble vascular endothelial growth factor (VEGF) receptor 1 (sVEGFR-1) (Guse, Sloniecka et al. 2010) and of an antibody against VEGF (GLAF-1) (Frentzen, Yu et al. 2009). Expression of VEGFR-1 from vaccinia blocks the action of the high levels of VEGF observed in renal cell cancers and led to tumour clearance or regression following intratumoural or systemic delivery respectively (Guse, Sloniecka et al. 2010). Similarly, expression of the anti-VEGF single chain antibody GLAF-1 from vaccinia virus has shown improved efficacy compared to the already successful parental strain GLV-1h68, which has entered clinical trials (Table 2).

1.4.4.2 Delivery of vaccinia

It is obviously advantageous to expose as much tumour tissue to vaccinia virus as possible, to ensure sufficient infection, replication and subsequent cell death. One of the major advantages of vaccinia virus is its ability to travel systemically through the blood (McCart, Ward et al. 2001; Kim, Oh et al. 2006; Thorne, Hwang et al. 2007) and the regression of distant, uninjected lesions in patients following injection at other sites has been demonstrated in a recent clinical trial (Park, Hwang et al. 2008). The EEV form of vaccinia virus is already well suited to long range dissemination due to its ability to evade recognition by both complement (Vanderplasschen, Mathew et al. 1998) and neutralising antibodies (Vanderplasschen, Hollinshead et al. 1997).

Despite the natural ability of vaccinia to spread systemically, only a small proportion of the virus will reach the target tissue, and in a recent clinical trial only high doses of virus delivered systemically led to replication at tumour sites (Breitbach, Burke et al. 2011). This has led to approaches to try and improve virus delivery, one of which is to increase production of the EEV form by genetic modification, which has been shown to improve virus spread following systemic delivery (Kirn, Wang et al. 2008). Another approach is to use carrier cells (reviewed in (Guo, Thorne et al. 2008)) and/or immunosuppression (Guo, Parimi et al. 2011), although immunosuppression carries some safety concerns and it can be argued that it negates any anti-tumour immune response initiated by infection.

A further consideration in the delivery of vaccinia virus is pre-existing immunity in immunized patients, or a host immune response after the first delivery that leads to rapid clearance of virus on subsequent doses. Several strategies exist to combat this including immunosuppression and use of carrier cells in combination (Guo, Parimi et al. 2011), delivery of different viruses in succession which synergise with each other to increase tumour cell death (Le Boeuf, Diallo et al. 2010; Zhang, Tsai et al. 2010) and treatment with cyclooxygenase-2 (COX-2) inhibitors, anti-inflammatory drugs, that have been shown to prevent the generation of neutralizing antibodies to allow repeated and effective administration of vaccinia virus (Chang, Ma et al. 2009).

1.4.4.3 Combination therapies

Despite tumour eradication in mice and some partial responses in human, vaccinia virus as a single agent therapy is unlikely to be approved in the clinic, at least initially. Systemic delivery is the only viable option in treating metastatic disease, or tumours that are inaccessible to intratumoural injections, and only a small proportion of intravenously injected virus reaches the tumour. This insufficient infection, coupled with virus elimination by the host immune response, and the fact that every clinical trial to date is tested on treatment refractory patients, means that in order to see a survival advantage in this challenging patient group it is likely that viral gene therapy will have to be combined with the best other supporting care, normally chemotherapeutic drugs. As vaccinia virus and traditional therapies target different properties of tumour cells and have different mechanisms of action, it is likely that they will work effectively in combination to increase overall tumour cell death and reduce resistance to therapy. In this respect a number of studies have been performed that investigate the anti-tumour response to oncolytic vaccinia plus a combination of drugs.

Recently, a small trial was undertaken on three patients who had progressive disease after treatment with the oncolytic vaccinia virus JX-594 and then went on to receive sorafenib, a small molecule inhibitor of B-raf and vascular endothelial growth factor receptor (Heo, Breitbach et al. 2011). As JX-594 and sorafenib have different mechanisms of action, it was hypothesised that some clinical benefit might be obtained by combination treatment and indeed all three patients had stable disease by RECIST after combined treatment, one of which was still alive and disease-free 4 years later. Although this was a small study, the combination of JX-594 with sorafenib did result in 100% response rate compared to just 40% in a larger group (n=15) of patients treated with sorafenib alone. This implies that, although the mechanisms of sensitisation to treatment with sorafenib are not understood, combination therapy may be of therapeutic advantage even when treatment with virus alone does not lead to a response. The importance of combined therapy in the development of oncolytic vaccinia as an approved therapy is further highlighted by an upcoming clinical trial combining oncolytic vaccinia (JX-594) with chemotherapy compared to placebo plus chemotherapy (Table 2); this Phase 2 trial is the first to measure survival as a primary outcome following treatment with vaccinia virus.

To pave the way for further clinical development a number of pre-clinical studies have looked at the efficacy of oncolytic vaccinia in combination with chemotherapeutics. Vaccinia virus has shown synergy in combination with paclitaxel in colorectal and ovarian cancer cells (Huang, Sikorski et al. 2010), with oxaliplatin in colorectal cancer (Ziauddin, Guo et al. 2011) and with rapamycin or cyclophosphamide in malignant glioma (Lun, Jang et al. 2009). In addition, GLV-1h68, a vaccinia strain currently in clinical trails as GL-ONC1 (Table 2) that encodes β-galactosidase shows improved efficacy in combination with a β-galactosidase activated prodrug in breast cancer (Seubert, Stritzker et al. 2011) and in combination with cisplatin and gemcitabine in pancreatic cancer (Yu, Galanis et al. 2009).

1.4.5 Clinical trials involving oncolytic vaccinia virus

By far, the most advanced oncolytic vaccinia virus in clinical development is the JX-594 strain which has already completed several Phase I and Phase II clinical trials, with more pending (Table 2). The only other oncolytic vaccinia virus in clinical trials at the time of writing is GL-ONC1, which was known as GLV-1h68 in pre-clinical studies (Zhang, Yu et al. 2007; Yu, Galanis et al. 2009; Gentschev, Muller et al. 2011). JX-594 expresses granulocyte macrophage colony-stimulating factor (GM-CSF), which stimulates anti-tumour immunity (Dranoff, Jaffee et al. 1993) and may contribute to the intra-tumoural vascular shutdown induced by vaccinia (Breitbach, Paterson et al. 2007), whilst GL-ONC1 is a triple-deleted virus.

To date, completed trials using JX-594 have been designed to primarily investigate the safety and maximum tolerated dose (MTD) of virus, with tumour response a secondary outcome. Despite this, there have been reports of either partial response or stable disease (Park, Hwang et al. 2008; Breitbach, Burke et al. 2011) following virus delivery, which is encouraging for future trials. Crucially, delivery of virus to tumour tissue has been shown following intravenous injection, albeit generally only in patients treated at higher doses ($>10^7$ pfu) (Breitbach, Burke et al. 2011) and there are several other trials on-going that are further investigating the safety and efficacy of oncolytic vaccinia virus delivered intravenously (Table 2). As intravenous delivery remains the most attractive way of targeting both primary tumour and inaccessible or metastatic disease, the findings from these trials are likely to be key to future viral gene therapy research. Furthermore, a Phase II trial of JX-594 in hepatocellular carcinoma is currently recruiting patients and aims to measure survival as a primary outcome (Table 2). This trial is designed to show improved survival of patients treated with JX-594 plus best supportive care compared to best supportive care alone; the outcome of this is sure to be of huge interest as, if successful, it will be the first clinical report to show a survival advantage following treatment with oncolytic vaccinia virus.

Table 2: Completed and on-going clinical trials using oncolytic vaccinia virus

Virus strain	Modifications	Route/Phase and NCI Reference	Cancer type and patient number	Doses	Safety	Efficacy	Ref.
Vaccinia (Wyeth)	JX-594 TK deleted; hGM-CSF expression under control of synthetic E/L promoter	Intravenous Phase I complete NCT00625456	Solid tumours Treatment refractory n=23	Single dose Dose escalation 10^5 pfu kg^{-1} (n=3) 10^6 pfu kg^{-1} (n=3) 3 x10^6 pfu kg^{-1} (n=4) 10^7 pfu kg^{-1} (n=4) 1.5x10^7 pfu kg^{-1} (n=5) 3 x10^7 pfu kg^{-1} (n=3)	DLT not reached Grade 1-2 flu-like symptoms	Evidence of replication in 87% tumours treated with $\geq$ 1.5x10^7 pfu kg^{-1} RECIST: 8 PD; 12 SD, 1 PR, 1 ND Choi: 23% response	(Breitbach, Burke et al. 2011)
Vaccinia (Wyeth)	JX-594 (as above)	Intratumoural Phase I/II complete NCT00629759	Primary Liver tumours and solid tumour liver mets Treatment refractory n=14	Repeat dosing every 3 weeks (2-8 cycles) Dose escalation 1x10^8 pfu (n=3) 3x10^8 pfu (n=3) 1x10^9 pfu (n=6) 3x10^9 pfu (n=2)	MTD defined: 1x10^9 pfu DLT: Grade 3 hyperbilirubinemia Grade 1-3 flu-like symptoms, Grade 1-3 thrombocytopenia, lymphopenia	RECIST: 30% PR 60% SD 10% PD Choi: 80% response Non-injected distant tumours 1 PR, 4 SD, 1 PD Choi: 33% response	(Liu, Hwang et al. 2008; Park, Hwang et al. 2008)
Vaccinia (Wyeth)	JX-594 (as above)	Intratumoural Phase I complete NCT00429312	Melanoma-cutaneous Treatment refractory n=7	Pre-vaccinated 4 days prior to treatment Dose ranging 10^4 - 8 x 10^7 pfu Repeat dosing three times weekly x 6 weeks	Flu-like symptoms, injected tumour inflammation	5 of 7 objective response, 100% regression of non-injected cutaneous metastases (n=4)	(Mastrangelo, Maguire et al. 2000)
Vaccinia (Lister)	GL-ONC1 (known as GLV-1h68 previously) TK deleted, F14.5L and A56R deleted; expression of Renilla luciferase-Aequorea green fluorescent protein fusion, β-galactosidase, and β-glucuronidase	Intravenous Phase I ongoing NCT00794131	Advanced solid tumours Treatment refractory n=24 to date	Single or multiple dose Dose escalation 1x10^5 pfu ,1x10^6 pfu 1x10^7 pfu ,1x10^8 pfu 1x10^9 pfu, 3 x10^9 pfu 1.667x10^7pfu or 1.667x10^8 pfu on days 1-3 1x10^9 pfu on days 1-5	Grade 1-2 flu-like symptoms Dose-limiting grade 3 rise in AST levels (n=1) Grade 3 femoral artery embolism (n=1)	Best response so far SD at 24 weeks (n=4) and 8-12 weeks (n=4)	Corral, Biondo et al. 2011) Poster A54, MCRI conference 2011
Virus strain	**Modifications**	**Route/Phase and NCI Reference**	**Cancer type and patient number**	**Doses**	**Safety**	**Efficacy**	**Ref.**
Vaccinia (Lister)	GL-ONC1 (as above)	Infusion within abdominal cavity by inserted catheter	Advanced peritoneal carcinomatosis	Every 4 weeks for 4 cycles Dose escalation	pending	pending	

		Phase I/II recruiting NCT 01443260	Treatment refractory Est n=30				
Vaccinia (Wyeth)	JX-594 (as above)	Intratumoural Phase II ongoing NCT00554372	Unresectable primary hepatocellular carcinoma, at least one prior treatment Est n=30	Repeat dosing every 2 weeks x 3 10^8 pfu or 10^9 pfu total dose	pending	pending	
Vaccinia (Wyeth)	JX-594 (as above)	Intravenous followed by intratumoural boosts Phase I/IIa recruiting NCT01394939	Metastatic, refractory colorectal carcinoma Est n=42	5 IV infusions +/- up to 3 IT boosts alone or in combination with irinotecan Dose escalation	pending	pending	
Vaccinia (Wyeth)	JX-594 (as above)	Intravenous Phase IIb recruiting NCT01387555	Advanced hepatocellular carcinoma, failed sorafenib treatment Est n=120	Six doses over 18 weeks, 10^9 pfu total dose plus best supportive care Placebo controlled	pending	pending	
Vaccinia (Wyeth)	JX-594 (as above)	Intratumoural Phase I recruiting NCT01169584	Advanced, unresectable solid tumours in paediatric patients Treatment refractory Est n=15	Single IT dose to 1-3 injectable tumours Dose escalation	pending	pending	

1.4.6 Limitations of oncolytic vaccinia virus

Oncolytic vaccinia virus has great potential in the treatment of cancer, particularly due to its ability to infect and replicate in almost every cell type, including those that are resistant to standard chemotherapy. In addition, the potential for safe systemic delivery to target metastatic disease has also been demonstrated, although efficacy has so far only been shown in pre-clinical studies. Despite the promise of oncolytic virotherapy, there remain hurdles in its development if it is to be approved in the clinic. There has been tremendous progress in the understanding of tumour pathogenesis and vaccinia virus biology, which, leading on from historical observations, have allowed the development of new modified strains which are tumour specific and can target various molecular aspects of cancer. Several Phase I trials have confirmed the potential of oncolytic vaccinia to reach tumour sites following systemic delivery (Breitbach, Burke et al. 2011), and to spread to distant metastases after replication in injected tumour sites elsewhere (Park, Hwang et al. 2008). However, as with any novel therapy, there remain challenges to overcome.

These include sub-optimal delivery of the virus to tumour sites, incomplete destruction of the tumour mass, clearance of the virus from the body and the problems associated with repeat dosing, such as neutralising antibodies, all of which have been touched on in various sections so far. In addition, it has been proposed that tumour cell lysis is the most important factor in late-phase tumour regression and that the ability of vaccinia to infect and destroy cells is more critical than initiation of an immune response or vascular collapse (Weibel, Raab et al. 2011). This means that novel ways to increase virus spread and enhance cell killing are likely to be of importance. Furthermore, if oncolytic virotherapy is to be used to its full potential, either alone or in combination with other therapies, increased understanding of the mechanisms of tumour cell death are needed. This may pave the way for manipulation of the death process to enhance cell killing, or the rational design of future combination therapies that potentiate tumour destruction without attenuating the action of vaccinia.

1.5 The tumour microenvironment

It is accepted that tumour cells themselves do not exclusively contribute to the malignancy of cancer and that their ability to grow, invade and metastasise is dependent on their surroundings. These surroundings are termed the tumour microenvironment and comprise all the non-malignant cell components of cancer, such as the extracellular matrix (ECM), immune and inflammatory cells, fibroblasts and endothelial cells (Hanna, Quick et al. 2009). The ECM is a complex network that provides structural support for the tumour and consists primarily of a collagen scaffold interspersed with bound glycoproteins and proteoglycans that interact with cells within the matrix via matrix receptors (Bosman and Stamenkovic 2003). Far from a static structure, the ECM is constantly remodelling, mainly through the actions of secreted matrix metalloproteinases (MMPs), which have an important role in the degradation of ECM. There is evidence to suggest that the mechanical rigidity of the ECM may influence tumour progression, as a more rigid ECM correlates with increased motility and proliferation of glioma cells (Ulrich, de Juan Pardo et al. 2009). However, the ECM components are also involved in signalling between the tumour and its surroundings and it is this communication that can greatly affect the progression of cancer.

Tumour cells release growth factors such as transforming growth factor β (TGFβ), platelet derived growth factor (PDGF), vascular endothelial growth factor (VEGF), basic fibroblast growth factor (bFGF) and epidermal growth factor receptor (EGFR) ligands to modify the microenvironment in such a way as to facilitate tumour growth (Mueller and Fusenig 2004). The induction of angiogenesis is essential not only for metastasis but also to enable delivery of oxygen and nutrients to the tumour, and VEGF is a major pro-angiogenic factor. The release of TGFβ and PDGF activates stromal fibroblasts to become myofibroblasts, which subsequently secrete growth factors, pro-migratory ECM components and MMPs to promote tumour progression (Mueller and Fusenig 2004). Myofibroblasts are suggested to be the driving force behind invasion (De Wever and Mareel 2003) and it has previously been shown that the breakdown of the ECM is initiated by enzymes released from stromal cells rather than tumour cells (Jodele, Blavier et al. 2006).

The microenvironment is proposed to be a critical factor in the development of metastases. Whilst many metastases simply form downstream of the primary tumour in the direction of blood flow, establishment of metastases in distant sites supports the “seed and soil” theory proposed by Stephen Paget in 1889 (reviewed by Fidler (Fidler 2003)) that cancer cells require a suitable ‘fertile’ environment in which to flourish. Despite this early suggestion that the tumour microenvironment plays an important role in tumour establishment and growth, it was not until fairly recently that the targets in cancer therapy were expanded to include not just tumour cells but components of the tumour microenvironment. A number of approaches have been employed to modify the tumour microenvironment to prevent tumour growth and progression and are well summarised in several recent reviews (Mueller and Fusenig 2004; Hanna, Quick et al. 2009; Efstathiou and Logothetis 2010). These include inhibitors of VEGF signalling, and bevacizumab, a monoclonal antibody against VEGF, was the first anti-angiogenic drug approved by the FDA for treatment of colorectal cancer in 2004. Other targets include inhibition of signalling pathways known to contribute to cancer progression through the use of small molecule tyrosine kinase inhibitors that target the receptors, or soluble receptors or antibodies that bind and neutralise cytokines themselves. Combination therapies that target multiple components of the tumour microenvironment have demonstrated improved efficacy over single agents in colon, melanoma and pancreatic cancer models (Blansfield, Caragacianu et al. 2008) and re-iterate the crosstalk of signalling pathways that exist between stromal cells and tumour cells. Blocking one component of the microenvironment may lead to upregulation of other pathways in response, which may counteract any therapeutic benefit.

1.5.1 Role of the microenvironment in oncolytic therapy

These strategies to target the microenvironment have also translated into the field of oncolytic therapy; some of these involve the expression of anti-angiogenic or immune-stimulatory cytokines from a replicating virus (discussed briefly in section 1.4.4.1). These strategies aim to combine the direct cell killing of vaccinia virus with complementary mechanisms to increase the overall anti-tumour efficacy. Other strategies involve targeting the microenvironment, and the barriers it presents to effective oncolytic therapy, to improve the spread of virus with the aim of reaching and subsequently destroying a larger tumour area.

Oncolytic vaccinia virus has seen some success following intratumoural delivery, including infection and replication in distant uninfected metastases (Park, Hwang et al. 2008), However, complete tumour regression is seldom seen, even in pre-clinical models, and this may be due to inadequate tumour penetration by the virus. Intravenous delivery is preferable over intratumoural delivery in advanced disease where tumours are inaccessible and have metastasized. However, this is problematic as only a small percentage of injected virus reaches the tumour, the remainder being cleared by circulating antibodies and/or the liver and spleen. Furthermore, once reaching the tumour (and presumably gaining access via the leaky vasculature associated with tumours), virus particles have to contend with high interstitial fluid pressure within tumours, which limits their diffusion to the periphery of the tumour, and a varying ECM which can also restrict their spread (Smith, Breznik et al. 2011). In addition, intravenous delivery depends on functional vasculature to deliver the virus to the initial site where it can replicate and then spread to metastases via the vascular system.

The tumour mass can contain a mixture of tumour cells, normal cells and stromal cells; this heterogeneity may hinder virus spread, as non-tumour cells do not support virus replication and may halt replicative spread. Additionally, the sheer mass of cells within a dense network may also prevent spread, as physically the large virus may not be able to move freely between cells to disseminate. These issues are not only associated with intravenous delivery but also intratumoural delivery. There are several strategies that target the microenvironment and aim to improve overall virus distribution and therapeutic efficacy, including modification of tumour vasculature and degradation of the ECM to facilitate virus spread. Strategies to target the tumour microenvironment to increase the efficacy of oncolytic viruses are discussed in more detail in the next section.

1.5.2 Targeting the tumour microenvironment to improve virus spread

Targeting the ECM for degradation, either by co-administration of degrading enzymes or by their expression from a replicating virus, is one way of overcoming the physical barriers to virus spread. To date, these strategies have been utilised with other oncolytic viruses besides vaccinia virus. However, despite the presence of the vaccinia EEV, which enables long-range dissemination in the face of an immune response, vaccinia is a large virus whose spread may be hindered in highly dense areas. It is therefore conceivable that oncolytic vaccinia therapy could benefit from targeting the tumour microenvironment. Whilst the majority of tumour microenvironment modulating viruses express cytokines to regulate the immune response, or anti-angiogenic genes (Kaur, Cripe et al. 2009), it is the remainder that target the ECM for degradation that are discussed in more detail here.

In vivo imaging of herpes simplex virus (HSV) showed that virus particles were primarily distributed around collagen-free areas of melanoma tumours, and a negative correlation between the amount of collagen fibrils and the amount of virus was observed (McKee, Grandi et al. 2006). This inhibition of virus spread was also shown to be size dependent; 20nm dextran tracer molecules were able to penetrate into collagen-rich areas, whereas 150nm microspheres (similar to the size of HSV particles) showed the same distribution as that of HSV. When collagenase was co-adminstered, viral distribution was increased three-fold, and there was significantly delayed tumour growth in the combination group compared to virus alone (McKee, Grandi et al. 2006). Given that, at 200nm, vaccinia virus is larger than HSV, it is likely that collagen also inhibits the spread of vaccinia virus.

Similarly, matrix metalloproteases (MMPs) are also able to degrade collagen and it has been shown that soft tissue sarcoma tumours stably transfected with MMP-1 or MMP-8 showed a significant growth delay upon treatment with HSV whereas mock transfected tumours did not (Mok, Boucher et al. 2007). Another study reported a decrease in collagen I following delivery of MMP-8 to lung and pancreatic tumours, and the combination of oncolytic adenovirus and a replication-defective adenovirus expressing MMP-8 was better able to control tumour growth *in vivo* than controls in both tumour models (Cheng, Sauthoff et al. 2007).

Relaxin can also regulate the ECM by decreasing collagen expression and increasing MMP expression (Unemori, Pickford et al. 1996; Brown, McKee et al. 2003). Its expression from a replicating oncolytic adenovirus decreased collagen content in a model of cervical cancer, and was associated with increased virus spread and persistence (Kim, Lee et al. 2006). When compared to a control virus, an adenovirus expressing relaxin was also able to reduce tumour growth (or halt it completely) and increase survival in five different subcutaneous tumour models (Kim, Lee et al. 2006). This was also demonstrated in another report, where the expression of relaxin from an oncolytic adenovirus 5 backbone resulted in increased virus spread and a significant delay in tumour progression in a melanoma model (Ganesh, Gonzalez Edick et al. 2007). Interestingly, it is suggested in this same paper that relaxin may only enhance virus spread under conditions where infectivity and replication is sub-optimal. Its expression from an oncolytic adenovirus retargeted towards the CD46 receptor readily expressed on tumour cells did not improve efficacy compared to a control virus (Ganesh, Gonzalez Edick et al. 2007). This may have implications for the use of ECM degrading molecules in oncolytic vaccinia, which generally is better equipped for entry and spread compared to adenovirus.

Other components in the ECM besides collagen can also be targeted to improve virus spread; co-expression of heparanase (which degrades heparan sulfate) from a non-replicating adenovirus in combination with an oncolytic adenovirus, improved survival in a model of mesothelioma and enhanced penetration of the virus into tumour spheroids (Watanabe, Kojima et al. 2010). Similarly, co-delivery of hyaluronidase (which degrades hyaluronan) with an oncolytic adenovirus was able to increase survival in pancreatic and melanoma models, (Ganesh, Gonzalez-Edick et al. 2008). When expressed from an oncolytic adenovirus, it also showed improved efficacy over a control virus in mice bearing subcutaneous melanoma tumours following both intratumoural and intravenous delivery (Guedan, Rojas et al. 2010), and this corresponded to increased spread of the virus.

Finally, decorin is a component of the ECM that associates with collagen fibrils. Its expression from a replicating oncolytic adenovirus was recently shown to increase virus penetration and decrease levels of collagen I and elastin (Choi, Lee et al. 2010). Furthermore, survival was increased compared to the control virus. Decorin also has an anti-proliferative effect on many tumour cell lines (see section 1.5.3.1) and can interact with signalling pathways to inhibit growth, angiogenesis and metastasis (sections 1.5.3.2 and 1.5.3.3).

As an aside, it is worth noting here that, despite concerns that degradation of the ECM could enhance tumour metastasis and a recent paper suggesting that relaxin is involved in the invasiveness of thyroid cancer cells (Bialek, Kunanuvat et al. 2011), there has been no increase in metastasis observed when the ECM is targeted for degradation alongside oncolytic virotherapy. In contrast, the number of metastases *in vivo* was actually reduced (Kim, Lee et al. 2006; Ganesh, Gonzalez Edick et al. 2007; Choi, Lee et al. 2010; Watanabe, Kojima et al. 2010). In addition, decorin as a single agent has been shown to inhibit metastasis in breast cancer and osteosarcoma models (Reed, Waterhouse et al. 2005; Goldoni, Seidler et al. 2008; Shintani, Matsumine et al. 2008).

1.5.3 Decorin

Decorin is a small leucine-rich proteoglycan whose protein core interacts with numerous ECM proteins, growth factors and their receptors. It consists of a protein core that consists of tandem repeats, each 24 amino acids long and rich in leucine. The 40kDa core is glycosylated with several small oligosaccharides, and the protein is completed with a 50kDa glycosaminoglycan (GAG) chain (Figure 4), which differs depending on the tissue location and is either chondroitin sulphate or dermatan sulphate.

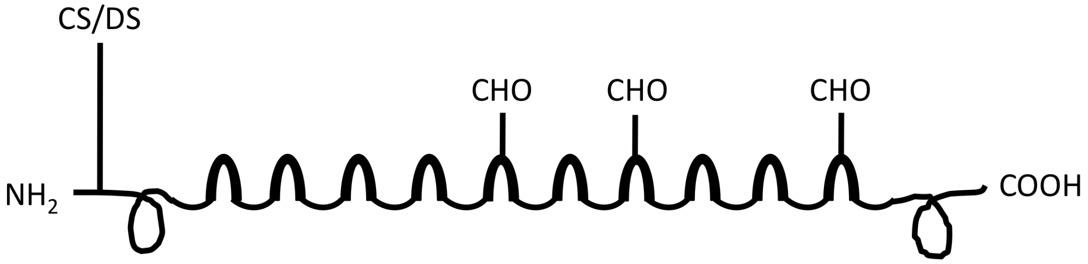

Figure 4: Structure of decorin. Decorin consists of a protein core comprising the leucine-rich tandem repeats that are linked to small carbohydrate chains (CHO). A single glycosaminoglycan chain of either chondroitin sulphate (CS) or dermatan sulphate (DS) is attached to a serine residue near the N-terminus.

Decorin is a secreted, highly soluble protein that is predominantly synthesised by fibroblasts and myofibroblasts and as such is commonly located in the microenvironment of tumours. Whilst decorin is not confirmed as a tumour suppressor gene, its deletion alongside p53 leads to accelerated tumour development in mice in a spontaneous lymphoma model, suggesting that absence of this gene is permissive for tumour development (Iozzo, Chakrani et al. 1999). More recent research has demonstrated that loss of decorin is also permissive for metastatic spread and that this can be reversed by stable transfection (Shintani, Matsumine et al. 2008) or delivery of decorin to cells, either intratumourally or systemically (Reed, Waterhouse et al. 2005; Goldoni, Seidler et al. 2008).

1.5.3.1 Decorin expression in cancer

Decorin is able to inhibit cell growth through induction of p21, an inhibitor of cyclin-dependent kinases (De Luca, Santra et al. 1996) that arrests cells in the G1 phase of the cycle. It can also trigger apoptosis via caspase-3 activation (Seidler, Goldoni et al. 2006). Considering these features, it is perhaps not surprising that expression of decorin is downregulated in many tumour cells, including breast, ovarian and pancreatic cancers (Nash, Deavers et al. 2002; Troup, Njue et al. 2003; Koninger, Giese et al. 2004). The mechanisms of downregulation are not clear but, in the case of ovarian cancer, treatment with proteasome inhibitors re-establishes expression of decorin (Nash, Deavers et al. 2002), suggesting that expression is controlled by means of rapid degradation rather than inhibition at the mRNA level. Despite downregulation by tumour cells, forced expression of decorin has an anti-proliferative effect in many cell lines (Santra, Skorski et al. 1995; Reed, Gauldie et al. 2002; Koninger, Giese et al. 2004; Hu, Sun et al. 2009) implying that cancer cells retain responsiveness to its growth-inhibitory effects. The only exception to date is the human

MG63 osteosarcoma cell line, where decorin has no effect on tumour growth and appears to promote cell migration instead (Zafiropoulos, Nikitovic et al. 2008).

In contrast to the downregulation in cancer cells, decorin is upregulated in the stroma of pancreatic and colon cancer (Adany, Heimer et al. 1990; Adany and Iozzo 1991; Koninger, Giese et al. 2004; Koninger, Giese et al. 2004); the amount of decorin is directly proportional to the amount of stroma and high levels may be seen in pancreatic cancer, which is typically accompanied by a pronounced desmoplastic reaction. It is proposed that the accumulation of decorin in the tumour microenvironment may represent a host response in an attempt to prevent spread, and that it is not a promoter of malignancy. This is supported by the fact that pancreatic cancer cells secrete factors that suppress the expression of decorin from myofibroblasts (Koninger, Giese et al. 2004) and instead promote expression of versican, another proteoglycan, which has been shown to enhance metastasis in several cancers (Labropoulou, Theocharis et al. 2006; Ricciardelli, Russell et al. 2007). An increase in decorin around the surrounding tissue of malignant vascular neoplasms, despite its loss in tumour cells themselves, was also hypothesised to be a protective response by the host to prevent spread (Salomaki, Sainio et al. 2008).

1.5.3.2 Decorin as a Multi-Receptor Tyrosine Kinase Inhibitor

A huge number of small molecule tyrosine kinase inhibitors, some of which are already approved therapies or are in clinical trials, abrogate signalling pathways that are known to promote tumourigenesis or metastasis. These include the c-met, TGFβ, VEGF and ErbB family signalling pathways. However, it is becoming increasingly acknowledged that targeting just one signalling pathway is not generally sufficient to inhibit the growth and spread of such a complex disease as cancer. Sorafenib is a multi kinase inhibitor that targets Raf, VEGF and PDGF signalling pathways and is approved for use against renal cell carcinoma; other multi-targeting agents are under investigation and include MK-2461 which predominantly targets c-met but also the FGFR and PDGFR (Pan, Chan et al. 2010) and ZD6474 which targets the EGFR and VEGFR-2 (Sarkar, Mazumdar et al. 2010). Decorin has been shown to have both autocrine and paracrine actions on cells to downregulate the EGFR, HER2 (ErbB2) and c-met receptor and so can be viewed as a natural, secreted multi-kinase inhibitor.

Decorin has no homology to EGF but is a biological ligand for the EGFR (De Luca, Santra et al. 1996; Iozzo, Moscatello et al. 1999), and binds in an overlapping but distinct region from that of the natural EGF ligand (Santra, Reed et al. 2002). In contrast to the mitogenic signalling stimulated by EGFR, this initiates a different signalling cascade that results in induction of p21 to cause growth arrest (De Luca, Santra et al. 1996). The binding of decorin to EGFR results in a sustained down-regulation of the receptor, with total levels decreasing by 40% and the phosphorylated form by 95% (Csordas, Santra et al. 2000). This sustained downregulation of the EGFR is due to the different fate of the internalised receptor following dimerisation by either decorin or EGF. Ultimately, both pathways converge at the transfer of EGFR to late endosomes for lysosomal degradation. However, EGF binding leads to clathrin-dependent internalisation of EGFR and some recycling of the receptor by $Rab11^+$ endosomes (Zhu, Goldoni et al. 2005). In contrast, decorin binding results in caveolae-mediated endocytosis of the EGFR, where it is transported to large vesicles known as caveosomes and eventually degraded without entering a recycling pathway (Zhu, Goldoni et al. 2005). This leads to a decrease in the amount of EGFR at the cell surface, thus reducing the available binding sites for EGF and so cell growth is suppressed. Similarly, decorin is also able to bind other members of the ErbB kinase family and downregulates HER2, the preferred dimerisation partner for all ErbB family members, and the most oncogenic family member, by 40% in a breast cancer model (Santra, Eichstetter et al. 2000). As with binding to the EGFR, decorin leads to long lasting downregulation, although suppression is indirect and assumed to be through decorin binding to the HER4 receptor, thus altering the heterodimer that forms, rather than HER2 itself (Santra, Eichstetter et al. 2000).

This dual targeting of ErbB family members by decorin may be of therapeutic importance in the inhibition of their combined mitogenic effects. The reported expression of EGFR in ovarian cancer varies considerably between studies but is 48% across all studies combined (Lafky, Wilken et al. 2008). Likewise, the reported frequency of HER2 expression varies but is expressed in up to 35% of epithelial ovarian cancer (Bookman, Darcy et al. 2003; Steffensen, Waldstrom et al. 2007; Tuefferd, Couturier et al. 2007) and is associated with poorer prognosis (Serrano-Olvera, Duenas-Gonzalez et al. 2006). Furthermore, HER2 is expressed in 20 immortal ovarian cancer cell lines derived from patients with stage III or IV disease, suggesting that expression is more frequent in advanced stage disease (Hellstrom, Goodman et al. 2001). Although therapies directed against ErbB family members are attractive for ovarian cancer, they have had limited success to date (Bookman, Darcy et al. 2003; Gordon, Finkler et al. 2005; Schilder, Sill et al. 2005; Schilder, Pathak et al. 2009) and this may reflect a need to target the extended ErbB network rather than individual family members. In support of this, resistance to ErbB targeted therapies in other cancers is often mediated by up-regulated expression or signalling of non-targeted family members (Wang, Narasanna et al. 2006; Ritter, Perez-Torres et al. 2007; Sergina, Rausch et al. 2007), and trastuzumab, a monoclonal antibody against HER2 sensitises ovarian cancer cells to gefitinib and cetuximab (EGFR targeted therapies). Expression of decorin from vaccinia virus, as well as potentially improving virus spread as discussed in section 1.5.2, may also therefore contribute to tumour growth inhibition by its dual actions on EGFR and HER2 in ovarian cancer.

Furthermore, decorin also has interactions with the hepatocyte growth factor (HGF) receptor c-met, another potential target in ovarian cancer therapy. Recently, a small molecule tyrosine kinase inhibitor of c-met was shown to reduce tumour burden and metastasis in a pre-clinical model of ovarian cancer (Zillhardt, Christensen et al. 2010) and decorin has also recently been identified as an antagonist ligand for c-met (Goldoni, Humphries et al. 2009). The c-met receptor is involved in the migration and invasion of cancer cells (Gentile, Trusolino et al. 2008) and is the target for several therapeutic drugs due to its role in metastasis (Stellrecht and Gandhi 2009). Decorin binds directly to c-met with very high affinity (Kd≈1.5nM) (Goldoni, Humphries et al. 2009) and, although the receptor is phosphorylated upon decorin binding the outcome is very different to that following HGF binding. It is proposed that decorin and HGF may induce different receptor conformations, and that differential phosphorylation of the receptor ensues, with decorin inhibiting phosphorylation of Tyr1349, the sole Tyr associated with downstream signalling events. The β-catenin pathway is activated downstream of c-met signalling, and levels of β-catenin protein in HeLa cells were decreased by 90% after 24hrs treatment with decorin (Goldoni, Humphries et al. 2009). In addition, levels of myc, a downstream target of β-catenin were also downregulated by decorin in a separate study (Buraschi, Pal et al. 2010). In both cases, downregulation was through proteasomal degradation.

As well as inhibiting downstream signalling pathways of c-met activation, decorin also causes downregulation of the receptor itself by inducing both ectodomain shedding and internalisation (Goldoni, Humphries et al. 2009). Previously, decorin has been shown to inhibit metastatic spread in various *in vivo* pre-clinical models (Reed, Waterhouse et al. 2005; Goldoni, Seidler et al. 2008; Shintani, Matsumine et al. 2008) and this may be mediated via the interactions with c-met described above.

1.5.3.3 Angiogenesis and decorin

Disruption of tumour vasculature has been observed following infection with vaccinia virus and this may be due to destruction of tumour endothelial cells, which are shown to be infected after systemic delivery (Kirn, Wang et al. 2007), or production of pro-inflammatory cytokines

(Breitbach, Paterson et al. 2007). In contrast, Weisel et al showed that endothelial cells were not infected and that tumour vasculature remained functional after vaccinia delivery (Weibel, Raab et al. 2011). If tumour vasculature shutdown were to occur, this may be of therapeutic benefit and the development of anti-angiogenic therapies in their own right is an area of much research. Whilst it may be true that vascular collapse might limit future intravenous delivery of oncolytic virus or chemotherapeutics, strategies to enhance this process in oncolytic virotherapy are of interest. Expression of anti-angiogenic agents from vaccinia virus, such as an anti-VEGF antibody (Frentzen, Yu et al. 2009) or a soluble VEGF receptor (Guse, Sloniecka et al. 2010) have shown superior anti-tumour efficacy over control viruses in prostate and renal cancer pre-clinical models respectively.

Decorin has also been reported to have anti-angiogenic effects and osteosarcoma, fibrosarcoma and cervical carcinoma cells stably transfected with full-length decorin protein show reduced production of the pro-angiogenic VEGF and reduced neovascularisation *in vivo* (Grant, Yenisey et al. 2002). Similarly, treatment of the wild type cells with recombinant decorin also suppressed VEGF expression by 80-95%. The mechanism of VEGF suppression is unknown, although it may be a consequence of ErbB family member down-regulation by decorin, as activation of these pathways is known to induce VEGF expression (Petit, Rak et al. 1997). Additionally, purified decorin and a leucine-rich repeat of the protein core were able to induce apoptosis in endothelial cells and inhibit VEGF stimulated migration and attachment to fibronectin (Sulochana, Fan et al. 2005).

However, there are contradictory reports on the role of decorin on angiogenesis and it has recently been suggested that decorin may regulate angiogenesis in a positive or negative manner depending on cues from the local environment (Fiedler and Eble 2009) due to the contradiction of several studies investigating the function of decorin on endothelial cell migration, adhesion and tube formation, summarised in the same paper. As decorin can interact with multiple signalling molecules, including receptor tyrosine kinases and components of the ECM, it is difficult to determine a precise role for decorin in angiogenesis *in vitro,* and the idea that decorin could have contradictory roles *in vivo* may well be true. Nonetheless, there is certainly some evidence to suggest that expression of decorin from an oncolytic vaccinia virus could potentiate vascular shutdown.

1.5.3.4 Modulation of the ECM by decorin

Further to its role in regulating cell growth and extracellular signalling, decorin is also able to modulate the ECM via its interactions with collagen and other ECM components. There are at least 2 binding sites for collagen I, and these are distinct from other binding sites, such as that for TGFβ, meaning that multiple interactions may take place simultaneously. Decorin binds to collagen type I via its protein core and delays the initiation of collagen fibrillogenesis (Vogel, Paulsson et al. 1984; Neame, Kay et al. 2000) resulting in collagen fibrils with a decreased diameter. Decorin null mice ($DCN^{-/-}$) demonstrate an irregular collagen fibril structure with reduced organisation and, although the mean diameter of fibrils remains similar to wild type (wt) mice, there is a greater range in size (Danielson, Baribault et al. 1997).

Recently, treatment of glioma tumours with a replicating adenovirus expressing decorin (Ad-ΔE1B-DCNG) led to significantly reduced levels of collagen type I, collagen type III and elastin compared to a control virus (Choi, Lee et al. 2010). In addition, tumours treated with Ad-ΔE1B-DCNG appeared devoid of collagen fibres, indicating that decorin has a role in reducing collagen content within the tumour mass. Expression of decorin from a non-replicating adenovirus also led to increased virus spread throughout glioma xenografts and, through the expression of point-mutant decorin genes from the same virus backbone that had no or reduced binding affinity to collagen type I fibrils, this enhanced tumour penetration was shown to be collagen-binding dependent (Choi, Lee et al. 2010).

Decorin also interacts with matrix metalloproteases (MMPs) and TGFβ within the tumour microenvironment and these interactions may contribute to the improved spread of virus within the tumour. MMPs are capable of degrading collagen and decorin has been reported to induce MMP-1 under certain conditions (Huttenlocher, Werb et al. 1996). Furthermore, interactions between decorin and TGFβ, possibly as part of a feedback loop, (Yamaguchi, Mann et al. 1990) may also affect ECM composition.

1.5.3.5 Rationale for expression of decorin from vaccinia

The role of decorin in inhibiting tumour growth and progression has been under scrutiny for several years, and as further mechanisms are uncovered it is becoming a novel therapeutic possibility. It has a defined role in ECM modulation, inhibition of several tyrosine kinase receptor signalling pathways and inhibition of tumour promoting growth factors such as TGFβ. Decorin has also been shown to inhibit tumour growth in prostate cancer by interactions with the androgen receptor (Hu, Sun et al. 2009), indicating that there may be other as yet undiscovered mechanisms of action. A recent paper also suggested that decorin may control tumour growth by inducing a proinflammatory response that favours anti-tumour activity by interactions with toll-like receptors on macrophages (Merline, Moreth et al. 2011). It is proposed that this is mediated through decreased expression of TGFβ, and oncogenic miR-21, both of which inhibit programmed cell death 4 (PDCD4), a pro-inflammatory molecule. The increased production of PDCD4 in turn leads to decreased expression of the anti-inflammatory cytokine interleukin-10 and enhanced expression of the pro-inflammatory cytokines TNFα, and these cytokines were detected at lower and higher levels respectively in decorin treated lung cancer xenografts (Merline, Moreth et al. 2011).

The multiple mechanisms of decorin in inhibiting tumour growth and metastasis, coupled with its ability to apparently enhance viral delivery and spread, make it a promising transgene of choice for expression from a replication-selective oncolytic vaccinia virus.

1.6 Mechanisms of cell death induced by vaccinia

There are three distinct routes of cellular death, namely apoptosis, autophagy and necrosis, that have been defined and classified in a recent review (Kroemer, Galluzzi et al. 2009). Of these, apoptosis and necrosis are pathways that result in cell death whereas autophagy results in degradation of cellular content but it is unclear if autophagy truly is a mode of cell death. Each of these processes has been implicated in vaccinia infection to varying degrees; cell lysis is a common endpoint of infection, apoptosis has been observed in some cell lines and autophagy may have a role in virus replication and maturation. Whilst modified vaccinia virus strains have demonstrated selective tumour cell death in pre-clinical models, the mechanisms of tumour cell death following infection are not well characterised.

Areas of necrosis are commonly seen in tumours infected with modified tumour-selective oncolytic vaccinia strains and it is assumed that this is a direct result of virus infection, which causes cell lysis. However, other modes of cell death, albeit mostly in non-malignant cells, have been described following infection with vaccinia. Despite encoding various genes that inhibit apoptosis, vaccinia virus is capable of inducing apoptosis in certain cell types. These include immune cells such as immature B lymphocytes, dendritic cells and macrophages (Baixeras, Cebrian et al. 1998; Engelmayer, Larsson et al. 1999; Humlova, Vokurka et al. 2002), and HeLa G cells derived from epithelial cervical carcinoma (Liskova, Knitlova et al. 2011). Apoptosis is associated with aborted replication in some cells (Baixeras, Cebrian et al.

1998; Ramsey-Ewing and Moss 1998; Engelmayer, Larsson et al. 1999), and viral DNA replication does not proceed beyond early gene expression. Whilst the induction of apoptosis is attributed to the presence of the immunogenic vaccinia protein L1R in non-permissive Chinese hamster ovary (CHO) cells (Ramsey-Ewing and Moss 1998), active induction of apoptosis triggered by early gene expression is proposed in permissive murine macrophages, as the presence of inactivated (but still immunogenic) virus did not lead to apoptotic demise (Humlova, Vokurka et al. 2002).

Autophagy, the degradation of a cell's own components though lysosomal machinery, is a process that is induced upon conditions of nutrient starvation, withdrawal of growth factors or external triggers such as infection. Generally, it is thought of as a survival mechanism, whereby the cell can recycle nutrients and maintain energy production under stressful conditions, although it can eventually lead to cell death (Scarlatti, Granata et al. 2009). Whilst autophagic cell death has not yet been described for vaccinia virus, there is evidence to suggest that it may be induced upon infection with other double-stranded DNA viruses such as cytomegalovirus and herpes simplex virus (McFarlane, Aitken et al. 2011; Rodriguez-Rocha, Gomez-Gutierrez et al. 2011; Tian, Sir et al. 2011; Zhang, Xi et al. 2011) and in adenovirus (Rodriguez-Rocha, Gomez-Gutierrez et al. 2011) where it is suggested that autophagy correlates with enhanced virus replication and oncolytic cell death. In contrast, Baird et al note the induction of autophagy but do not conclude it to be a mode of cell death and suggest that adenovirus induces a novel, and as yet undetermined, form of programmed cell death (Baird, Aerts et al. 2007).

Finally, the distinction between programmed cell death pathways such as apoptosis, and the traditionally regarded unregulated process of necrosis has recently been challenged with the emergence of programmed necrotic pathways (Hitomi, Christofferson et al. 2008; Christofferson and Yuan 2010; Vandenabeele, Galluzzi et al. 2010). Whilst vaccinia is regarded as producing a lytic (ie. necrotic) infection, programmed necrosis may have a role in the fate of vaccinia-infected cells (Cho, Challa et al. 2009), as well as those infected with other viruses such as cytomegalovirus (Brune 2011).

It is worth re-iterating that much of the work described above attempting to characterise vaccinia-induced cell death was not performed in malignant cells. Two exceptions are the induction of apoptosis in HeLa G cells (Liskova, Knitlova et al. 2011) although this was shown to be strain-specific, as wild type Western Reserve (wt-WR) induced apoptosis whereas the vaccination Wyeth strain did not, and in melanoma cells following infection with both wt-WR and the highly attenuated modified virus Ankara (MVA) strain (Greiner, Humrich et al. 2006). It is clear then that, whilst the majority of malignant cells show signs of necrotic injury following infection with tumour-selective vaccinia strains, other mechanisms of cell death may be involved and these may be both strain and cell-type specific. Given that oncolytic vaccinia is in clinical trials for the treatment of cancer, greater understanding of the exact mechanisms by which tumour cell death occurs is warranted, particularly as this may lead to the rational selection of complementary chemotherapy or the development of strategies to manipulate the cell death pathway to augment synergistic effect. Furthermore, evasion of apoptosis is a hallmark of cancer (Hanahan and Weinberg 2000) and understanding the mechanisms by which a novel anti-cancer agent induces death in malignant cells which are likely to have aberrant cell death pathways is an exciting phenomenon. Finally, deciphering these mechanisms can lead to investigation into how and why resistance occurs, both *de novo* and potentially acquired, as has been recently described to oncolytic herpes simplex virus (Song, Haddad et al. 2012).

Vaccinia virus can contribute to tumour regression either by direct cell destruction or stimulation of an immune response that may be directed against tumour cells. Generation of an immune response, primarily the activation of antigen-presenting cells, is strongly affected by the apoptotic or necrotic origin of the antigen, and so it is important to understand the mechanisms of tumour cell death in the context of oncolytic virotherapy. The EEV form of vaccinia virus, which is released prior to cell lysis and thought to be primarily responsible for long range dissemination within the host, is resistant to both neutralizing antibodies and complement (Vanderplasschen, Hollinshead et al. 1997; Vanderplasschen, Mathew et al. 1998). In contrast, the IMV form released upon cell lysis is highly immunogenic and may attract infiltrating lymphocytes to the tumour. In addition, the release of cellular content upon cell membrane rupture is also key to activation of the immune response. In contrast, apoptotic cell death is largely non-immunogenic and dying cells are phagocytosed in the absence of an inflammatory response.

Furthermore, it is well described that vaccinia can act synergistically with various chemotherapeutics including paclitaxel, cisplatin and cyclophosphamide (Lun, Jang et al. 2009; Yu, Galanis et al. 2009; Huang, Sikorski et al. 2010; Ziauddin, Guo et al. 2011). Various explanations have been offered for this including that immunosuppression by cyclophosphamide enhances virus replication and spread or, conversely, that factors released from infected cells such as interferon and high-mobility group protein B1 (HMGB1) are able to sensitise surrounding cells to paclitaxel (Huang, Sikorski et al. 2010). In addition, it has been proposed for another large oncolytic virus (herpes simplex virus) that the space created by apoptotic cells killed by chemotherapy enables enhanced spread of virus within the tumour (Nagano, Perentes et al. 2008). However, certain combination therapies can inhibit virus replication (McCart, Puhlmann et al. 2000) and, in order to select rational and optimised combination therapies, it is important to fully understand the mechanisms of vaccinia cell death so that additional therapies can have complementary modes of action.

1.6.1 Counteraction of the host immune response by vaccinia

Vaccinia encodes a multitude of proteins that are capable of dampening the host immune response and inhibiting apoptosis. These include secreted viroceptors that are able to bind and inhibit the signalling of pro-inflammatory cytokines such as IL-1 and TNFα, inhibitors of complement proteins and chemokines, and intracellular proteins that can modulate the cells ability to undergo apoptosis (Figure 5).

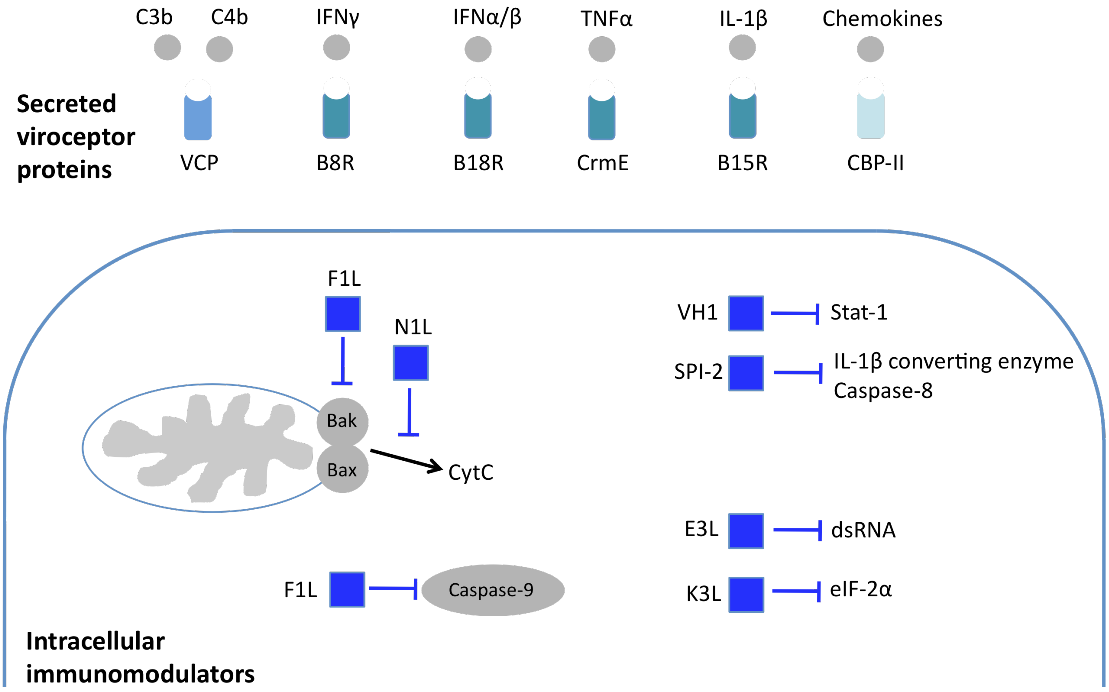

Figure 5: Intracellular and secreted immunoregulators encoded by vaccinia virus. Vaccinia encodes a number of secreted viroceptors that bind and inhibit cytokines, chemokines and complement factors. Intracellularly, the vaccinia proteins VH1 and SPI-2 can inhibit the IL-1 signalling pathway through inhibition of the transcription factor Stat-1 and the IL-1β converting enzyme (ICE). In addition, SPI-2 may inhibit caspase-8. The vaccinia proteins encoded by E3L and K3L bind and sequester dsRNA and eIF-2α respectively to prevent the inhibition of viral gene translation and apoptosis. Vaccinia can also inhibit the intrinsic pathway of apoptosis by inhibiting the dimerisation of Bak and Bax, inhibiting the release of cytochrome c from the mitochondria and inhibiting caspase-9. Note that this is not an exhaustive list of vaccinia proteins involved in immune evasion.

Complement is a critical part of the innate immune response and is involved in the control of viral pathogens such as vaccinia virus. Activation of complement leads to production of both pro-inflammatory peptides (C3a and C5a) and peptides which can mediate virus neutralization by opsonization (C3b and C4b). The presence of C3b targets viral particles for phagocytosis and also leads to downstream activation pathways and formation of the membrane attack complex, which lyses infected cells. Vaccinia virus encodes the vaccinia complement control protein (VCP) which limits complement activation by binding to C3b and C4b to inhibit the classical and alternative pathways of complement, and also promotes the degradation of C3 convertases (Kotwal, Isaacs et al. 1990). Recently, it has also been demonstrated that deletion of VCP from vaccinia virus leads to decreased virus titres, and a corresponding increase in both neutralizing antibodies and accumulation of CD4+ and CD8+ T cells at the site of infection (Girgis, Dehaven et al. 2011), suggesting that VCP may also have a role in suppressing the adaptive immune response.

During virus infection, chemokines are produced which co-ordinate the activation and migration of leukocytes to the area of infection. Vaccinia virus encodes the chemokine binding protein CBP-II which binds with high affinity to 26 out of 80 CC-chemokines (Burns, Dairaghi et al. 2002) to block the binding site for their respective G-protein coupled receptors (Alcami, Symons et al. 1998). Chemokine signalling usually results in an increase in intracellular calcium levels that triggers the activation of subsequent signalling pathways to promote the migration of immune cells to the site of infection. Thus sequestration of chemokines by CBP-II prevents this signalling to inhibit infiltrating immune cells.

Furthermore, vaccinia virus also encodes numerous decoy receptors for cytokines with anti-viral properties such as IFNγ, the type I interferons IFNα and IFNβ, TNFα and the interleukin-1 (IL-1) family. The viroceptors CrmE and B15R bind the pro-inflammatory cytokines TNFα and IL1-β respectively. CrmE is a homolog of the TNF receptor (TNFR) (Reading, Khanna et al. 2002) and similarly, B15R encodes a decoy receptor that is able to bind and block the effects of IL-1β but not IL-1α (Alcami and Smith 1992). IFNγ has several anti-viral properties including the activation of macrophages, neutrophils and natural killer (NK) cells and increased production of MHC class I and II molecules and co-stimulatory molecules by antigen-presenting cells (APC). To circumvent these effects, the vaccinia virus B8R gene encodes an IFNγ receptor homolog (Alcami and Smith 1995). Finally, type I interferons produced following recognition of viral PAMPs (pathogen-associated molecular patterns) are also capable of inducing potent anti-viral effects through their signalling with IFN receptors, which include elimination of virus, induction of apoptosis and conferring resistance to infection in neighbouring uninfected cells. The B18R gene of vaccinia encodes a soluble receptor for IFNα and IFNβ (Symons, Alcami et al. 1995) that, once secreted, binds to the surface of both infected and uninfected cells to block the activity of the interferons and render cells susceptible to virus infection (Alcami, Symons et al. 2000).

In addition to the secreted proteins involved in immune evasion, vaccinia is also able to modulate the effects of interferon intracellularly. PKR (RNA-dependent protein kinase) is an intracellular target of IFN and activation of PKR by dsRNA inhibits the translation of viral proteins and can lead to apoptosis. Vaccinia virus encodes two proteins that can counteract this process; E3L binds directly to dsRNA to sequester it and prevent activation of PKR (Chang, Watson et al. 1992; Kibler, Shors et al. 1997) and K3L has homology to eIF-2α (eukaryotic translation initiation factor) which is downstream of PKR signalling (Davies, Elroy-Stein et al. 1992; Carroll, Elroy-Stein et al. 1993). Activated PKR phosphorylates the α subunit of eIF-2 and alters its function to prevent initiation of translation; K3L therefore acts as a competitive inhibitor of phosphorylation to allow viral protein synthesis to continue. Furthermore, vaccinia also inhibits IFN signalling indirectly by encoding VH1, a phosphatase that prevents IFN-induced activation of Stat-1, a transcription factor downstream of IFNγ signalling (Najarro, Traktman et al. 2001).

Vaccinia virus also encodes several inhibitors of apoptosis including F1L, N1L and SPI-2 (Figure 5), which are rapidly expressed in the early phase of infection to prevent the early clearance of infected cells before completion of virus replication and the release of new progeny. These are discussed further in section 1.6.2.1.

1.6.2 Apoptosis

Apoptosis is a form of programmed cell death and is an effective means of removing defective cells, including those infected with virus. Apoptosis is characterised morphologically by cell shrinkage, chromatin condensation, nuclear fragmentation and plasma membrane blebbing (Kroemer, Galluzzi et al. 2009). Biochemically, it may also be associated with internucleosomal DNA cleavage, caspase activation, and activation or cleavage of targets of caspases. Apoptotic bodies are rapidly engulfed and cleared by phagocytes, partly through recognition of apoptotic ligands such as phosphatidylserine on the surface of apoptotic cells and, as cells are eliminated with an intact cell membrane, inflammation is not triggered by the presence of intracellular content or danger signals (Taylor, Cullen et al. 2008).

Apoptosis can be initiated by death receptor signalling or cellular stress/DNA damage and then proceeds down either the extrinsic or intrinsic pathway respectively (Figure 6). Both pathways converge at the activation of the major effector caspases 3, 6 and 7, which mediate many of the events of apoptosis. Vaccinia encodes a TNFR homolog that can prevent the binding of TNFα to TNFR at the cell surface, and the subsequent activation of apoptosis through the extrinsic pathway. In addition, vaccinia encodes several proteins that act intracellularly to prevent apoptosis.

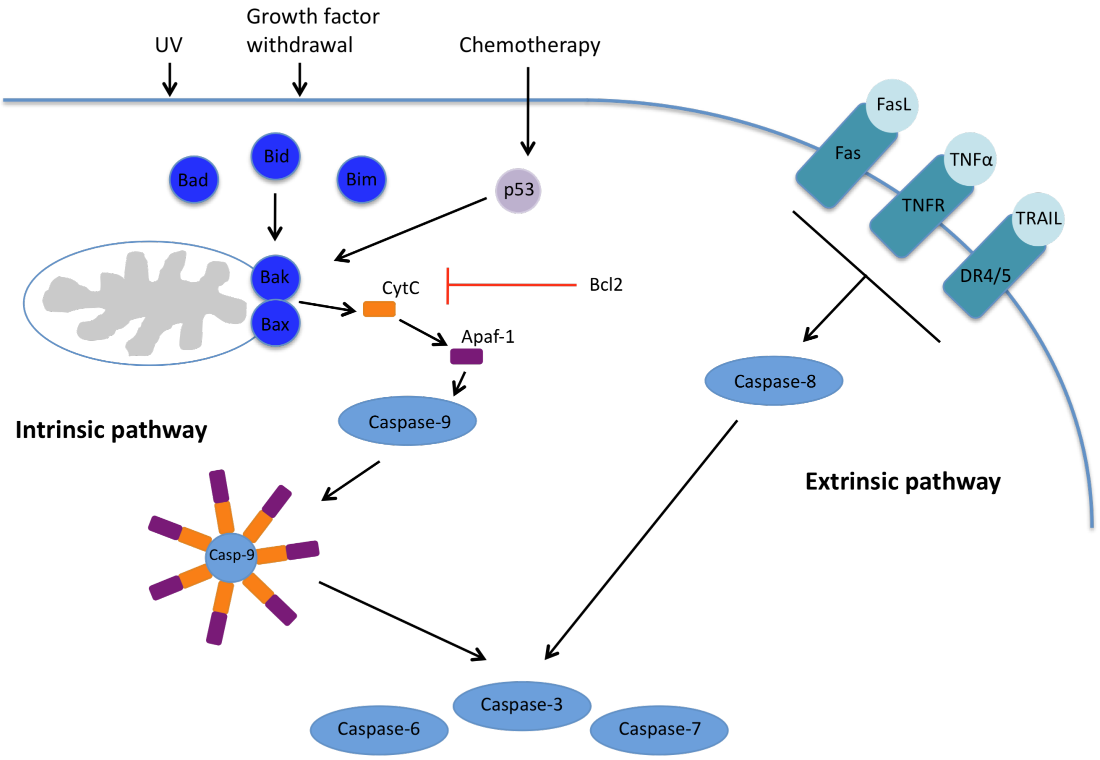

Figure 6: Apoptotic signalling. Apoptosis can be induced by binding of extracellular death ligands such as FasL, TNFα or TRAIL to their respective transmembrane receptors. Activation of the receptors leads to caspase-8 activation. Alternatively, the intrinsic pathway of apoptosis is initiated through range of stimuli including UV, growth factor withdrawal or DNA damage induced by chemotherapy. This leads to activate of pro-apoptotic proteins such as Bad, Bim and Bid. These proteins promote dimerisation of Bak and Bax at the mitochondrial membrane which leads to the release of cytochrome C into the cytosol. The binding of cytochrome C to Apaf-1 initiates formation of the apoptosome, which recruits and activates caspase-9. Both the intrinsic and the extrinsic pathway converge at activation of caspases 3, 6 and 7. These caspases mediate apoptotic demise by initiating DNA fragmentation, dismantling of the cell and the formation of apoptotic bodies.

1.6.2.1 Counteraction of apoptosis by vaccinia

Given that premature removal of infected cells before replication is complete may limit infection, vaccinia encodes several proteins that act to prevent apoptosis. Apoptosis is a highly regulated affair and controlled by several proteins, one of which is the anti-apoptotic protein Bcl2 that prevents the release of cytochrome c from the mitochondria (Yang, Liu et al. 1997), a key event in the intrinsic pathway. Vaccinia virus encodes two Bcl2-like proteins, N1L and F1L, which are able to interact with the BH3 peptides in pro-apoptotic members of the Bcl2 family to prevent their activity. Vaccinia virus N1L is an intracellular 14kDa protein that is able to bind with high affinity to pro-apoptotic proteins (Aoyagi, Zhai et al. 2007) and whose deletion attenuates vaccinia replication in the brain (Billings, Smith et al. 2004) and in intranasal and intradermal models (Bartlett, Symons et al. 2002). In addition to the anti-apoptotic activity of N1L it is also described as having an effect on the immune response during infection. N1L reduces the levels of secreted cytokines, including the pro-inflammatory cytokines TNFα, IL-1β and IFNα/β, from infected monocytes (Zhang, Abrahams et al. 2005) and its deletion, whilst not affecting either CD4$^+$ or CD8$^+$ T-cell infiltration, does increase natural killer (NK) cells activity (Jacobs, Bartlett et al. 2008).

Another protein F1L, despite having no obvious BH domains, is also able to interact with members of the Bcl2 family. First identified in 2003 for its ability to prevent the release of cytochrome-c from the mitochondria (Wasilenko, Stewart et al. 2003), it was later shown to achieve this through its interaction with Bak to prevent activation of the pro-apoptotic protein Bax and subsequent disruption of the mitochondrial membrane (Wasilenko, Banadyga et al. 2005). The interaction of F1L with Bak is similar to that of cellular proteins such as Mcl-1 and Bcl-xL, which also function to restrict apoptosis. Mcl-1 is usually in a complex with Bak to prevent apoptosis in the absence of apoptotic stimuli and, following infection with vaccinia, is displaced by F1L but remains localised to the mitochondria (Campbell, Hazes et al. 2010). It is proposed that the vaccinia protein F1L has functional similarity to Mcl-1 and, as the expression of Mcl-1 is upregulated following infection, its release from Bak may enable it to bind to other BH3-only proteins such as Bim, Puma and Bik in order to sustain a pro-survival environment (Campbell, Hazes et al. 2010).

F1L has recently also been identified as having a dual role in the inhibition of apoptosis. The release of cytochrome c is critical in the apoptotic cascade as it binds to and initiates the oligomerization of Apaf-1 to form the apoptosome (Figure 6). The apoptosome then recruits and activates caspase-9 to initiate downstream activation and cleavage of the executioner caspases 3 and 7. F1L, as well as inhibiting the release of cytocrome-c, is an inhibitor of caspase-9 and therefore prevents two key steps in the mitochondrial pathway of apoptosis. F1L binds directly to caspase-9 and is thought to act in a similar manner to the cellular apoptosis inhibitor XIAP, although unlike XIAP F1L is able to bind caspase-9 irrespective of whether it has been cleaved or not (Zhai, Yu et al. 2010).

The mechanisms of inhibition of apoptosis by N1L and F1L relate solely to the mitochondrial pathway of apoptosis but a third protein, SPI-2 (also known as B13R), is able to inhibit the extrinsic pathway. SPI-2 belongs to the serine protease inhibitor (serpin) family and is a 39kDa protein that bears 93% homology to the potent inhibitor of apoptosis encoded by coxpox, CrmA (Dobbelstein and Shenk 1996). Similar to CrmA, SPI-2 is able to offer protection from TNFα or Fas mediated apoptosis (Dobbelstein and Shenk 1996) and also inhibits IL-1β converting enzyme (ICE) to prevent the cleavage of pro-IL-1β into its mature form (Kettle, Alcami et al. 1997).

1.6.2.2 Apoptosis and oncolytic vaccinia for the treatment of ovarian cancer

Reports of apoptosis as a direct cause of vaccinia infection are rare, particularly in the context of viral gene therapy, although this may be in part due to a lack of investigation into the precise mechanisms of cell death. Whilst it can be argued that tumour cell death by any means is the end therapeutic goal, the mode of cell death is not a trivial issue and can determine which cells respond and the side effects. Evasion of apoptosis is one of the original hallmarks of cancer described by Hanahan and Weinberg (Hanahan and Weinberg 2000) and maintains its inclusion on an expanding list (Hanahan and Weinberg 2011). Despite this, patients with ovarian cancer do initially respond to cisplatin, a DNA damaging agent that is generally accepted to initiate apoptosis, although it has been reported that cisplatin also causes death by necrosis (Gonzalez, Fuertes et al. 2001) and that the route to cell death depends on the dose (Sancho-Martinez, Piedrafita et al. 2011).

Apoptosis and necrosis exert entirely different effects on the surrounding tissue and the organism as a whole, notably an inflammatory response that is absent in apoptosis but triggered by necrosis. This response may aid tumour regression but almost certainly contributes to toxic side effects, some of which can be dose limiting. In terms of oncolytic vaccinia, side effects observed in clinical trials suggest an inflammatory response that may arise from necrotic cell injury. However, this is not to suggest that necrosis is the only or indeed the predominant mode of tumour cell death. Following administration with cisplatin, both necrotic and apoptotic cells were observed in the same population of treated cells

(Pestell, Hobbs et al. 2000), suggesting that several mechanisms of cell death can ensue from the same stimuli. This is supported by the crosstalk between apoptotic and autophagic pathways (Levine, Sinha et al. 2008), between apoptotic and necrotic pathways (Vandenabeele, Galluzzi et al. 2010), and between autophagic and necrotic pathways (Zhang, Chen et al. 2011), and suggests that the mode of cell death may depend on intracellular components and signalling pathways following the original stimulus. As tumours are generally heterogenous in nature it is conceivable that different cells within the same population may die by different means, or indeed not die at all. In addition, the mode of cell death also depends on ATP availability (a requirement for apoptosis) (Eguchi, Shimizu et al. 1997) and on oxygen availability, both of which may be dysregulated in tumour cells due to tumour hypoxia and alterations in tumour cell metabolism (Vander Heiden, Cantley et al. 2009).

Apoptosis may be important in oncolytic vaccinia treatment for several reasons. Firstly, apoptotic death may lead to fewer side effects although this may be counter-balanced by a lack of immune response that could be directed towards the tumour. Secondly, it has been suggested that apoptosis in some cells may enhance virus spread, as the space created by dead cells reduces interstitial pressure and increases virus dissemination within the tumour (Nagano, Perentes et al. 2008). Conversely, initiation of apoptosis following infection with vaccinia has so far been described mainly in non-permissive cell lines (Baixeras, Cebrian et al. 1998; Ramsey-Ewing and Moss 1998; Engelmayer, Larsson et al. 1999) suggesting that it may be a host response that limits virus replication and spread. In this case, apoptosis may reduce viral titres. Finally, the main limitation of current chemotherapy in the treatment of ovarian cancer is acquired resistance. In order to understand potential resistance to oncolytic vaccinia virus it is important to understand how vaccinia kills tumour cells, and what pathways are involved.

1.6.3 Autophagy

Autophagy is an evolutionarily conserved process by which long-lived and/or large cellular proteins are sequestered within a double-membrane vesicle known as the autophagosome and subsequently degraded upon fusion of the autophagosome with the lysosome. Autophagy does occur at a basal level to eliminate damaged or aggregated proteins and intracellular pathogens, but dysregulation of the pathway has been implicated in a number of diseases including cancer (Levine and Kroemer 2008). It is also an important regulator of the host response to virus infection and, although some viruses appear to use autophagy for their own benefit, autophagy has a critical role in the detection and removal of virions and in mediating the innate immune response (Jordan and Randall 2011).

Autophagy is upregulated in response to nutrient starvation or withdrawal of growth factors. In addition, autophagy can also be initiated as a cellular response during oxidative stress or infection. Under these conditions, autophagy can either allow the cell time to adapt and survive or it can lead to type II (autophagic) cell death, although the very concept of autophagic death is one that is still under scrutiny (Shen, Kepp et al. 2012).

The mammalian target of rapamycin (mTOR) is the main regulator of autophagy that, as a result of signalling initiated by growth factors with their respective receptors, acts to repress autophagy. Under conditions where growth factors are removed, or when AMP-activated protein kinase (AMPK) senses low ATP, nutrient or oxygen levels (Mihaylova and Shaw 2012), mTOR is inactivated and autophagy is initiated. This begins with the formation/activation of an autophagy complex containing Atg1, Atg11, Atg13 and Atg17 (Figure 7), which in turn leads to activation of a class III PI3K and its subsequent association with beclin-1. Formation of the autophagosome is dependent on the formation of this beclin-1 containing complex and of another comprising Atg5, Atg7, Atg12 and Atg1; the latter complex is critical for the recruitment of LC3B. During autophagy, LC3B-I is converted to LC3B-II through lipidation by a ubiquitin-like system involving Atg7 (Ichimura, Kirisako et al. 2000) and incorporated into the autophagosome membrane. Both the conversion of LC3B and its localisation to the autophagic vesicle are considered indicators of autophagy. Finally, the autophagosome and lysosome fuse (through mechanisms which are not clearly understood) resulting in the degradation of the contents of the autophagic vesicle (Figure 7).

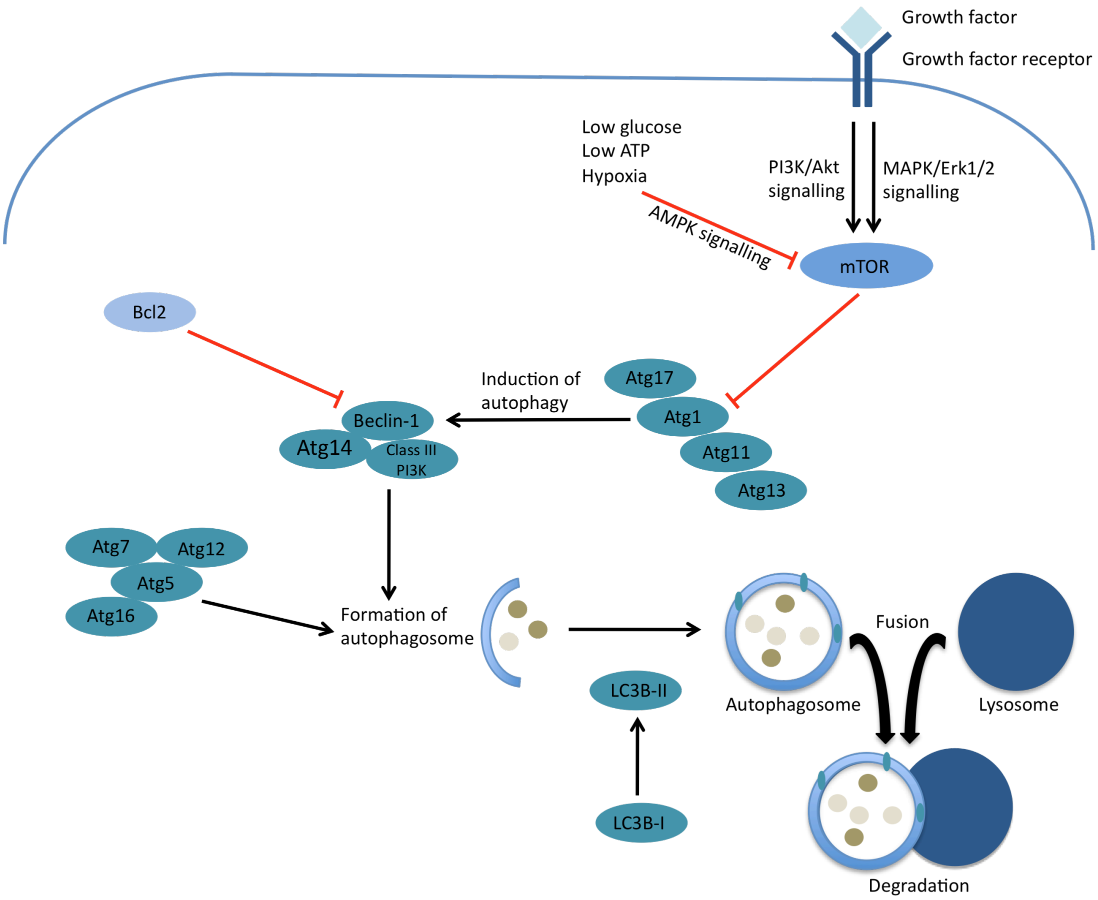

Figure 7: Autophagy signalling. In the presence of growth factor signalling autophagy is inhibited by the activity of mTOR. Under conditions of nutrient deprivation, or cellular stress detected by the energy sensor AMPK, mTOR is inactivated and the Atg1/Atg17/Atg11/Atg13 complex forms which initiates autophagy. Formation of the autophagosome is dependent on the formation of two complexes, the first containing Beclin-1, class III PI3K and Atg14 and the second involving Atg7, Atg5, Atg12 and Atg16. Upon induction of autophagy, LC3-I is cleaved to LC3-II and recruited to the autophagosome where it is sequestered. Mechanisms of autophagosome and lysosome fusion are less well understood but, upon fusion, the contents are degraded and the autophagic vesicle breaks down.

It is worth noting that autophagy can also be regulated by the anti-apoptotic protein Bcl-2, which inhibits autophagy through binding to Beclin-1 (Levine, Sinha et al. 2008). This highlights the crosstalk between apoptosis and autophagy and it has been proposed that impairment of both apoptosis and autophagy may promote necrotic cell death (Degenhardt, Mathew et al. 2006). As vaccinia virus encodes several inhibitors of apoptosis including Bcl-2 homologs (see section 1.6.2.1), these and any direct effects of infection on autophagy will certainly influence the mechanism of tumour cell death and any ensuing inflammation and immune response.

1.6.3.1 Vaccinia and autophagy

There is some controversy for the requirement of autophagy for virus replication. There is evidence to suggest that autophagy induction aids replication, and inhibition of autophagy decreases release of infectious enterovirus (Zhang, Xi et al. 2011) and replication of hepatitis B virus in the liver following liver specific knockout of the autophagy protein Atg5 (Tian, Sir et al. 2011). Studies on adenovirus, a virus frequently used in gene therapy of cancer, also conflict on the role of autophagy, with some groups showing induction of autophagy that is involved in viral structural protein expression, virus replication and induction of cell death (Jiang, White et al. 2011; Rodriguez-Rocha, Gomez-Gutierrez et al. 2011). In contrast, others demonstrate that autophagy is a cell survival mechanism in response to adenovirus and in fact cell death is enhanced when this pathway is inhibited (Baird, Aerts et al. 2007).

The role of autophagy in the life cycle of vaccinia infection is even less clear. The biogenesis of vaccinia virions has long been a topic of interest, and in particular the formation of the vaccinia envelope and its origin from within the host cell. One of the early steps in the virus life cycle is the formation of immature virions (IV), spherical structures that consist of dense viroplasm that is first surrounded by a crescent shaped double membrane and then fully engulfed. Given the morphological similarity between the formation of immature virions and of the autophagosome, which also originates from a crescent shaped, double-layered membrane, it was thought that autophagic machinery might play a role in virus morphogenesis. However, it has been shown (at least in embryonic stem cells and mouse fibroblasts) that the vaccinia virus strain NCYBH does not require cellular autophagy machinery for virion formation, and is able to mature and replicate in autophagy-deficient cell lines (Zhang, Monken et al. 2006). In addition, it has also been shown that vaccinia infection of mouse fibroblasts leads to massive LC3 lipidation, although this was not involved in membrane biogenesis or virus proliferation (Moloughney, Monken et al. 2011). It was concluded that vaccinia virus disrupts autophagy in these cells rather than induce it; neither autophagosome formation nor autophagy flux were observed despite LC3 lipidation.

These observations on autophagy following infection with vaccinia are based on embryonic stem cells or fibroblasts, and the consequences of either autophagy induction or disruption by vaccinia in cancer cells is not known. These findings may have relevance to the outcome of viral gene therapy and tumour progression, although it is still not known whether autophagy is favourable or detrimental to cancer cell survival. It has been suggested that higher levels of autophagy correlate with increased resistance to chemotherapy and shorter survival in patients with melanoma (Ma, Piao et al. 2011). Another study covering nearly 1400 tumours from 20 types of cancer including ovarian cancer also supported the view that inhibition of autophagy should be a target in the treatment of cancer and noted an association between punctate LC3B expression and increased proliferation and invasion, with an overall worse outcome (Lazova, Camp et al. 2011). Ovarian cancer cells have shown decreased levels of the autophagy proteins Beclin-1 and LC3 (Shen, Li et al. 2008), but retain the ability to induce autophagy as a protective mechanism against necrosis caused by some therapeutics (Zhang, Qi et al. 2010). In addition, autophagy may be used as a survival mechanism and has been reported to induce tumour dormancy in ovarian cancer cells (Lu, Luo et al. 2008). In contrast, autophagic cell death has been described for ovarian cancer (Le, Mao et al. 2010) and induction of autophagy associated with prolonged overall survival (Bartholomeusz, Rosen et al. 2008).

The ability of autophagy to either cause cell death or promote survival may be determined by the tumour microenvironment as, *in vitro*, autophagy induction by disruption of P13K signalling leads to cell death whereas *in vivo*, induction of autophagy by the same mechanism leads to tumour cell survival (Amaravadi 2008). It is suggested that there may be a threshold level of autophagy that determines the fate of cells, and that this is influenced by factors in the microenvironment such as growth factors, cytokines, angiogenic factors and ECM proteins. The role of autophagy may therefore differ depending on the stage of cancer progression (Kondo, Kanzawa et al. 2005).

Increased understanding of the role that autophagy plays in cancer means that it may become a therapeutic target for novel approaches, and thus the interaction between oncolytic vaccinia virus and autophagy warrants further investigation to avoid potential conflicting actions on both tumourigenesis and virus efficacy.

1.6.4 Necrosis

Traditionally, necrosis has been defined in a negative manner in the absence of morphological traits of apoptosis and autophagy, and was deemed an unregulated and accidental affair. However, there are now a multitude of papers that describe necrosis as a regulated affair (Hitomi, Christofferson et al. 2008; Cho, Challa et al. 2009; Vandenabeele, Galluzzi et al. 2010; Feoktistova, Geserick et al. 2011; Tenev, Bianchi et al. 2011) and even describe different pathways of programmed necrosis that are reliant upon specific proteins (Zhang, Shao et al. 2009; Upton, Kaiser et al. 2010).

1.6.4.1 Programmed necrosis

The most well studied pathway of programmed necrosis is that via the TNF receptor. It was first observed in 1988 that TNF could induce both apoptosis or necrosis in different cell types (Laster, Wood et al. 1988), and it has since been proposed that these differing mechanisms of cell death depend on the activity of caspase-8 (Vandenabeele, Galluzzi et al. 2010). Upon stimulation by its ligands TNFR is internalised and leads to the formation of a death inducing signalling complex (complex II) comprising of TRADD, FADD, RIP1, RIP3 and caspase 8. Caspase 8 inactivates RIP1 and RIP3 by proteolytic cleavage and initiates the apoptotic cascade; in contrast, when caspase 8 is deleted or inhibited (by viral encoded proteins for example), programmed necrosis can instead be initiated (Figure 8). RIP1 appears to be essential for initiation of necrosis as has been demonstrated by chemical inhibition by necrostatin-1, which inhibits RIP1 kinase activity (Degterev, Hitomi et al. 2008). RIP3 also appears an essential protein as knockdown in NIH3T3 cells prevents programmed necrosis in the presence of zVAD (Zhang, Shao et al. 2009). Furthermore, embryonic fibroblasts from RIP3 knockout mice are resistant to necrosis and cell lines devoid of RIP3 do not undergo necrosis upon treatment with TNFα in contrast to cells where RIP3 expression is evident (He, Wang et al. 2009). As well as RIP1 kinase activity, RIP3 kinase activity is also required for programmed necrosis (Cho, Challa et al. 2009) and removal of the kinase domain by cleavage of RIP3 by caspase 8 is thought to be one of the mechanisms for inactivation of the pathway (Feng, Yang et al. 2007).

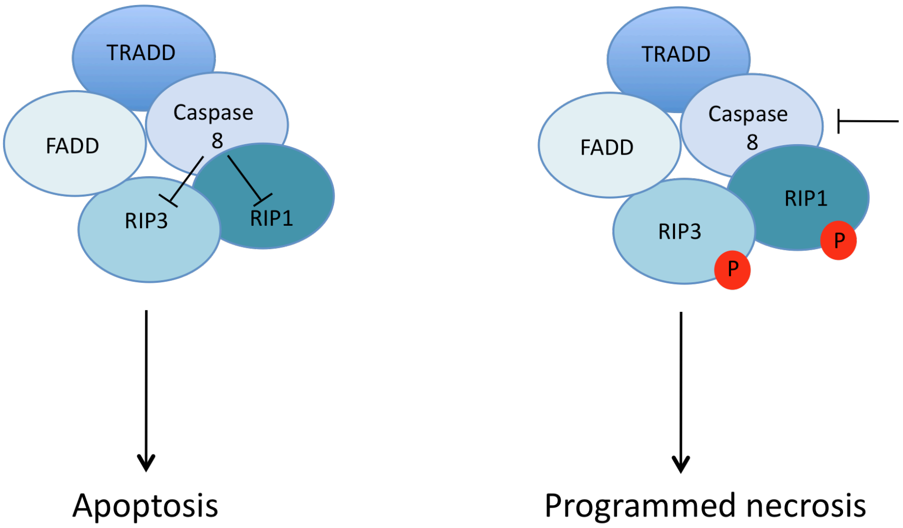

Figure 8: Death domain receptor mediated programmed necrosis leads to the formation of complex II. The outcome of this signalling complex is regulated by caspase-8. In the presence of caspase 8, RIP1 and RIP3 are inactivated and apoptosis can occur. Under conditions where caspase 8 is either deleted or inhibited, both RIP1 and RIP3 are phosphorylated and the cell proceeds down a necrotic pathway instead.

A second complex that forms independently of TNF, TRAIL and/or CD95L involvement is termed the ripoptosome and comprises of RIP1, FADD and caspase-8 at the core and FLIP$_L$ and RIP3 in certain cells (Tenev, Bianchi et al. 2011). In addition, caspase 10 has also been described within the complex although the biological significance and activity of this protein within the ripoptosome is still under investigation (Feoktistova, Geserick et al. 2011). Similar to complex II, which arises as a result of death receptor signalling, the ripoptosome can also lead to either apoptosis or necrosis. In the absence of CIAPs, just as with complex II, caspase 8 is the main regulator of whether the cell undergoes apoptosis or necrosis (Feoktistova, Geserick et al. 2011). When IAPs including cIAP1, cIAP2 and XIAP are present however, they target RIP1 and RIP3 for degaradtion by ubiquitylation (Tenev, Bianchi et al. 2011). Ripoptosome activity is also regulated by c-FLIP, which forms a heterodimer with caspase 8 and limits the activity of the ripoptosome (Tenev, Bianchi et al. 2011), and cells with low RIP1 and high cFLIP expression are resistant to ripoptosome formation and subsequent cell death (Feoktistova, Geserick et al. 2011).

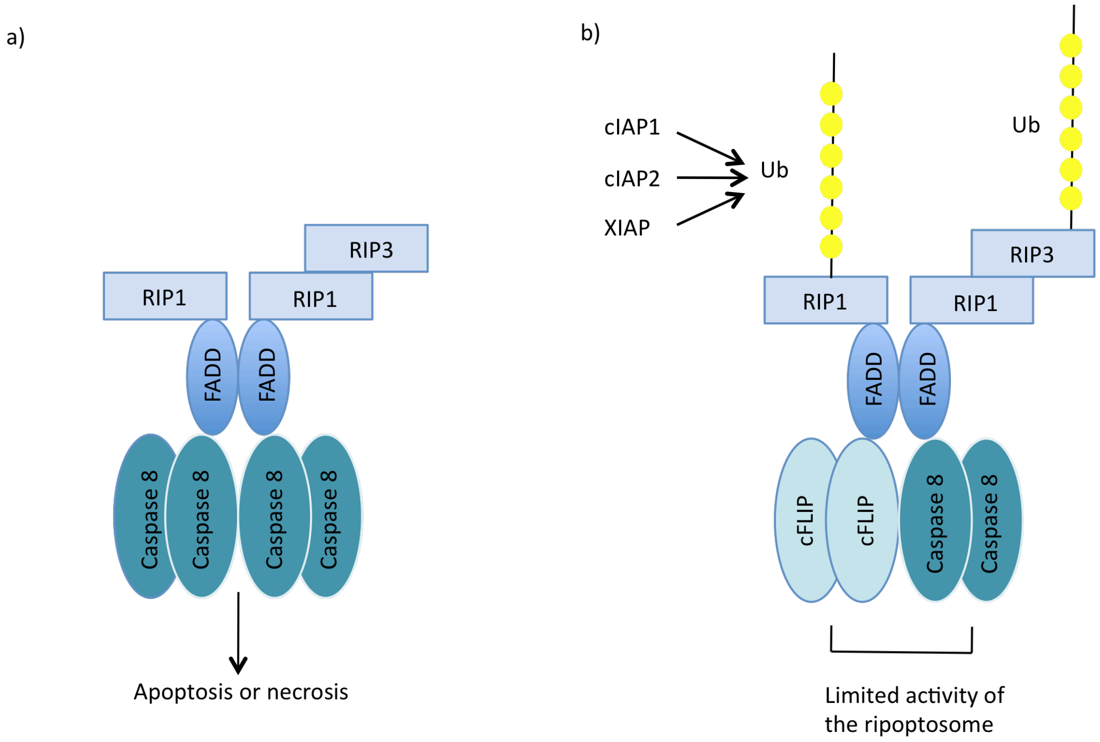

Figure 9: The ripoptosome. a) Active ripoptosome that leads to either apoptotic or necrotic death depending on cellular factors b) Regulation of ripoptosome assembly by IAPs which target components of the ripoptosome for proteasomal degradation and by cFLIP which limits ripoptosome activity by forming a heterodimer with caspase 8.

1.6.4.2 Vaccinia and programmed necrosis

Little has been described regarding the role of programmed necrosis in vaccinia infection, and its significance to cell death. The pro-necrotic RIP1/RIP3 complex has been detected in the liver of wild-type mice within 24hrs of infection with vaccinia virus (Cho, Challa et al. 2009). Comparison of infection in wild-type and RIP3$^{-/-}$ mice showed significantly reduced inflammation in RIP3$^{-/-}$ mice which corresponded to increased viral titres in the liver and spleen (Cho, Challa et al. 2009). These mice succumbed to virus infection, suggesting that RIP3 is required for the control of virus infection. Similarly, RIP3 has also been implicated as a key protein involved in the antiviral response of the host to murine cytomegalovirus (MCMV) (Upton, Kaiser et al. 2010), and viral proteins encoded by MCMV act to inhibit RIP3 dependent necrosis. Together, both these data suggest that inhibition of programmed necrosis, in addition to the well-established inhibition of apoptosis by viral proteins, may be a viral strategy to evade host defences.

1.7 Aims

Oncolytic viral therapy has shown promise for the treatment of various human cancers in pre-clinical models and has demonstrated that it is safe in Phase I and II clinical trials. The aim of this project was to investigate the potential of oncolytic vaccinia as a novel therapeutic agent for the treatment of ovarian cancer. This overall goal was subdivided into three more specific research aims:

1) Construction of a thymidine kinase deleted virus (Lister-dTK) and determination of its activity and specificity in a panel of ovarian cancer cell lines. In addition, investigation of the feasibility of combining Lister-dTK with cisplatin, an approved therapy for ovarian cancer.

2) Construction of a novel oncolytic vaccinia virus expressing decorin, an extracellular matrix protein, and evaluation of its activity compared to the control Lister-dTK virus in ovarian cancer cell lines. Decorin has many reported anti-tumourigenic properties including inhibition of tumour growth, inhibition of several tyrosine kinase receptor signalling pathways and inhibition of metastasis. Furthermore, decorin is proposed to enhance viral spread throughout the tumour.

3) Investigation into the mechanisms of vaccinia induced cell death in ovarian cancer, specifically apoptosis, autophagy and necrosis. This aimed to increase knowledge of the actions of Lister-dTK, with a long-term view of selecting complementary therapies and deciphering mechanisms of resistance to oncolytic vaccinia therapy.

Chapter 2

Materials and Methods

2. Methods and Materials

2.1 Cell Lines and Culture

All cell lines were cultured in Dulbecco's modified Eagle Medium (DMEM) (PAA Laboratories) supplemented with 10% heat-inactivated foetal bovine serum (FBS) (Biosera), 100 units/ml penicillin and 100µg/ml streptomycin (PAA Laboratories) unless stated otherwise. Cell lines were maintained at 37°C in a humidified atmosphere with 5% CO_2 and routinely passaged twice a week using 0.5% trypsin in PBS (PAA Laboratories) to detach monolayers. All cell lines were routinely tested for mycoplasma and human cell lines were verified by short tandem repeat profiling (LGC Standards). For long term storage, cells were pelleted by centrifugation, and the cell pellet resuspended in DMEM containing 10% dimethyl sulphoxide (DMSO) and 40% FBS. After overnight storage at -80°C cells were transferred to liquid nitrogen.

The human ovarian cancer cell lines, A2780 and A2780CP, were kindly provided by Dr Aris Eliopoulos (University of Birmingham, UK) and IGROV-1 cells by Dr M Ford (Glaxo Wellcome Research and Development, Stevenage UK). OVCAR4 parental cells were obtained from Dr R. Camalier (NCI-Frederick, MD, USA) and the Bcl2 overexpressing cells (OVCAR4-Bcl2) produced previously within our lab (McNeish, Bell et al. 2003). OVCAR-4 Bcl2 cells were cultured in the presence of 1 mg/ml of G418 antibiotic (Roche). SKOV3ip1 were kindly provided by Dr Janet Price (University of Texas-MD Anderson Cancer Center, Texas) and SKOV3 cells were obtained from Cancer Research UK Cell Services (Clare Hall, South Mimms, Hertfordshire, UK). TOV21G cells were obtained from Prof F Balkwill (Centre for Cancer and Inflammation, Barts Cancer Institute, Queen Mary University of London).

IOSE25 cells, hTERT-immortalised human ovarian surface epithelial cells, were kindly provided by Prof F Balkwill (Centre for Cancer and Inflammation, Barts Cancer Institute, Queen Mary University of London) and were maintained in NOSE-CM medium, supplemented with human epidermal growth factor (10ng/ml), hydrocortisone (0.5µg/ml), insulin (5µg/ml), bovine pituitary extract (4µl/ml), and 15% FBS.

The human lung adenocarcinoma cell line A549 was purchased from ATCC.

Various cell lines were also used for analysis of protein expression levels of decorin but were not cultured. Cells were provided in the form of frozen cell pellets from Centres within the Barts Cancer Institute, Barts and the London School of Medicine and Dentistry, Queen Mary University, London. A panel of pancreatic cell lines; comprising FA6, PT45, Panc1, Aspc1, T3M4, 8988S, 8988T and A8184 were kindly provided by Dr Tatjana Crnogorac-Jurcevic, Centre for Molecular Oncology, after original purchase from CRUK. The breast cancer cell lines T47D and H3396, and MCF10A normal breast cells were provided by Kayi Chan, Centre for Tumour Biology, and the prostate cancer cell lines DU145 and LnCap, and PNT2 normal prostate cells by Ling Shen, Centre for Molecular Oncology.

The African green monkey kidney cell line CV1 was purchased from ATCC and used for virus purification by plaque assay and virus expansion. It was also used to determine viral titres and for titration of samples during $TCID_{50}$ assays.

Murine ovarian surface epithelial cells (MOSEC) were obtained from Kathy Roby, University of Kansas (described in (Roby, Taylor et al. 2000)) and MOVCAR7 from Denise Connolly at the Fox Chase Cancer Center, Philadelphia (described in (Connolly, Bao et al. 2003)). Both cell lines were cultured in DMEM supplemented with 5% FBS, 1x Insulin Transferrin-Selenium (Gibco) and 100 units/ml penicillin and 100μg/ml streptomycin. The murine prostate adenocarcinoma cell line Tramp C1 was purchased from ATCC and the murine pancreatic cancer cell line Panc02 was a kind gift from Dr Thorsten Hagemann, Centre for Cancer and Inflammation, Barts Cancer Institute.

2.2 Cloning techniques

The Lister wild-type vaccinia virus strain (Lister-wt) was bought from ATCC and used as a control for vaccinia behaviour throughout some of this work. It was also used as the backbone for expression of RFP and mDCN to create the Lister-dTK strain and Lister-mDCN respectively.

2.2.1 Cloning strategy for recombination plasmids

In order to create the Lister-dTK strain, a shuttle plasmid termed pDR LARA TK was used, which already existed in our lab. As pDR LARA TK already expresses RFP under control of the vaccinia I1L promoter, no further cloning was required and this plasmid was simply recombined into the Lister strain to create the Lister-dTK virus. Methods for virus production are described in section 2.3.

The pD-LARATK-BNNX shuttle plasmid that also pre-existed in our lab was used for homologous recombination to create the Lister-mDCN virus. The murine decorin gene was cloned into the pD-LARATK-BNNX recombination plasmid together with DsRed2, a red fluorescent protein. The two genes were separated by an internal ribosomal entry site (IRES) sequence that allows translation of both genes from a single dicistronic mRNA. The plasmid containing IRES-DsRed2 (pIRES2-DsRed2) was originally bought from Clontech (CA, USA) and a plasmid containing murine decorin under control of the I1L promoter (pUC57 murine decorin) was designed and then synthesised by Genscript (NJ, USA).

The IRES-DsREd2 sequence was first cloned into the shuttle vector by digestion of both the vector and the IRES-DsRed2 containing plasmid with the restriction endonucleases BamH1 and Not1. Murine decorin was then cloned into this using Sal1 and BamH1 restriction endonucleases to create the final recombination plasmid, pD-LARA TK BNNX-mDCN-IRES-DsRed.

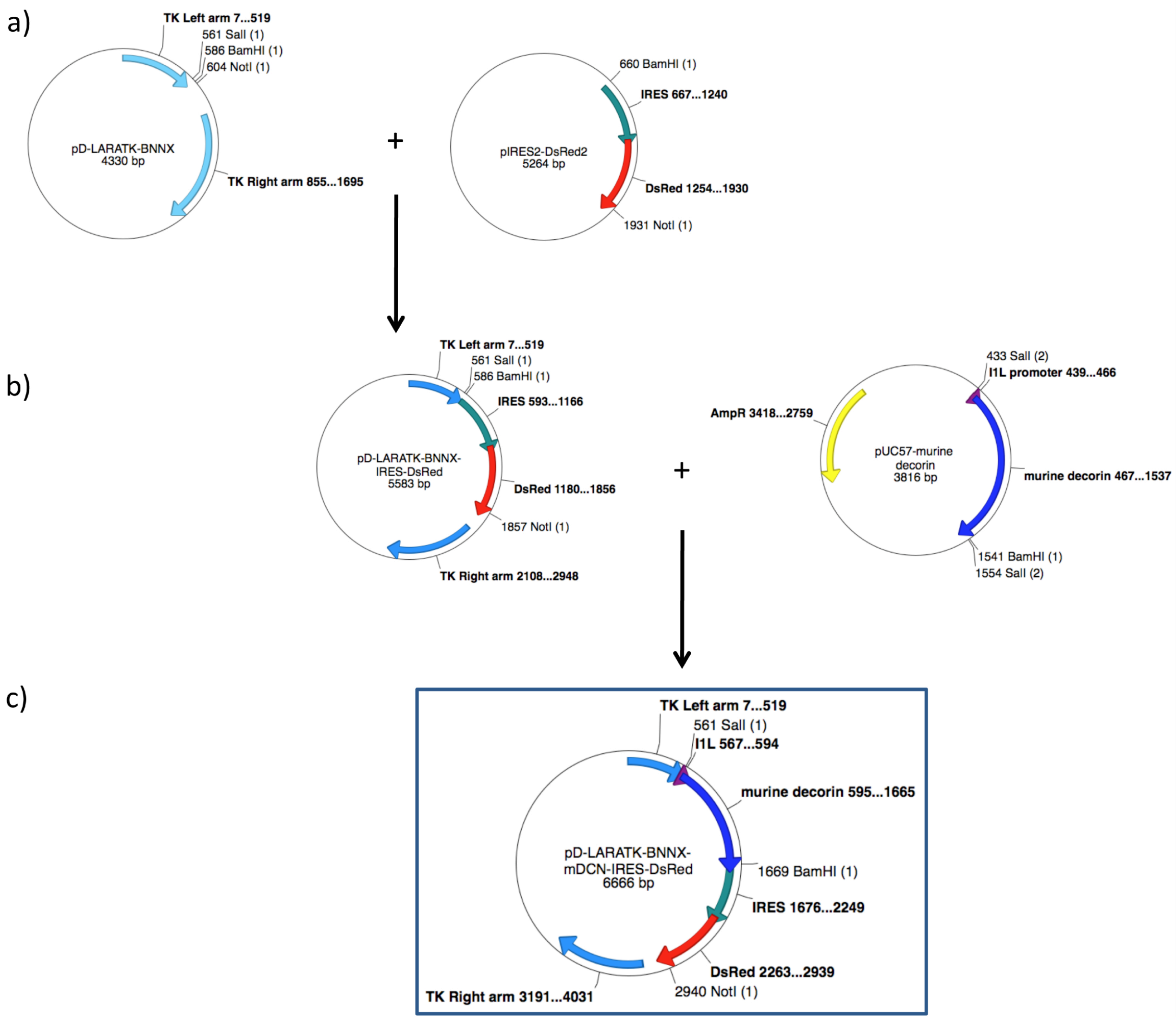

Figure 10: Construction of the recombination plasmid used to create Lister-mDCN virus. a) IRES-DsRed2 was cloned into the pD LARATK-BNNX shuttle plasmid by digestion of both plasmids with BamH1 and Not1 restriction endonucleases and ligation of the IRES-DsRed2 insert into the vector. b) The resulting plasmid was further digested with BamH1 and Sal1. Digestion of the pUC57 plasmid containing murine decorin with the same enzymes allowed ligation to create c) the final plasmid used for homologous recombination with Lister-wt. This created the vaccinia strain Lister-mDCN.

All plasmids were digested in a final volume of 20µl dH$_2$0 containing 1µg DNA, 1ul of each restriction enzyme (New England Biolabs (NEB) MA, USA), and 2µl of NEBuffer 3 (NEB), which was the appropriate buffer for the enzymes used. All digestions took place at 37°C for one hour.

2.2.2 DNA analysis by gel electrophoresis

Gel electrophoresis was used to confirm DNA digestion and successful cloning. All 20µl of digested DNA was run on a 1% (w/v) agarose gel (1g of agarose in 1x Tris-Borate-EDTA (TBE) buffer with 5µl ethidium bromide at 0.5µg/ml) for 1 hr at 100V. Samples were run alongside a 1kb DNA ladder (Invitrogen). Bands were visualised under UV light to ensure that the expected digestion pattern was observed or that inserts were present in the ligated vector. Digested fragments of DNA required for ligation were excised from the gel under UV light with a sterile blade and DNA purified using QIAquick Gel Extraction kit (Qiagen) following the microcentrifuge protocol in the kit insert.

2.2.3 Ligations

Extracted DNA was ligated using Rapid DNA Ligation kit (Roche). The molar ratio of the linearised backbone and the desired insert were calculated from the formula below. Ligation ratios were adjusted to 1:1, 2:1 and 3:1 for insert:vector backbone. Generally, a 3:1 insert:vector ration was found to be sufficient for the majority of ligations.

$$\frac{\text{Length of insert (kb)}}{\text{Length of vector (kb)}} \quad \text{x ng of vector = ng insert required for a 1:1 ratio}$$

Ligation reactions were set up in a 21µl volume using 1µl T4 DNA ligase, 10µl T4 DNA ligation buffer and different ratios of insert to backbone as described above. DNA was diluted in 1xDNA dilution buffer supplied in the kit. A control reaction comprising of backbone only was included to identify re-ligation of the vector and as a comparison for empty vector size against the insert containing vector on subsequent gel electrophoresis. Ligations were carried out at room temperature for 5 minutes prior to transformation into competent *E.coli* bacteria.

2.2.4 Transformations

Chemically competent One Shot® TOP10 *E.coli* were transformed using 2μl of standard ligation reactions. Cells were held on ice for 10 minutes before addition of DNA and a further 20 minutes on ice. Bacteria were subjected to heatshock at 42°C for 45 seconds and transferred immediately to ice for 2 minutes, before resuscitation in 200μl SOC medium (Invitrogen) (2% w/v tryptone, 0.5% w/v yeast extract, 10mM NaCl, 2.5mM KCl, 10mM $MgCl_2$, 10mM $MgSO_4$, 20mM glucose) and incubated at 37°C for 30 minutes. 100μl of culture was then spread onto pre-warmed agar plates selecting for ampicillin resistance (50μg/ml) and plates incubated overnight at 37°C.

2.2.5 Plasmid Screening

Colonies were picked from plates the following day into 7ml of liquid broth (LB) containing 50μg/ml of ampicillin (Roche). These cultures were then incubated overnight on a shaker maintained at 37°C. Subsequent screening of colonies was carried out by restriction enzyme digest, cracking gel or sequencing to ensure successful cloning.

2.2.5.1 Cracking gel

Positive clones were initially screened by cracking gel, which detects positive clones by size, as plasmids containing the inserted gene are larger than the empty vector. This was performed before extraction of DNA from bacterial cultures, and was used in conditions where there were multiple colonies to screen due to high background on the control ligation plate. 1 ml of bacterial culture was spun at 13000rpm for 1 minute and the pellet dissolved in 40μl of distilled water. 40μl of phenol chloroform was added, the sample vortexed and spun at 13000rpm for 2 minutes. 30μl of the top phase supernatant was transferred to a fresh eppendorf tube and any RNA digested by incubation with 6μl of 6X loading dye (30% glycerol, 0.3% bromophenol blue, 0.3% xylene cyanol in distilled water) containing 1μg/μl of RNase for 5 minutes at room temperature. The samples were then run on a 0.7% agarose gel for 1hr at 100V and any positive clones distinguished by size.

2.2.5.2 Restriction enzyme digest

For screening by restriction enzyme digest, DNA was extracted from bacterial cultures using QIAprep Spin Miniprep Kit (Qiagen) according to the manufacturer's protocol. 1ml of the original culture was stored. The concentration of eluted DNA was measured using a Nanodrop® ND-1000 spectrophotometer (Labtech International Ltd, East Sussex, UK). Samples were assessed at 260nm versus a blank control of the elution buffer.

Restriction enzyme screening digests were performed using enzymes and buffers from New England Biolabs (NEB) (MA, USA). Enzymes were selected for their ability to cut at unique sites within the inserted gene, or sites that spanned either side, using A Plasmid Editor (ApE Universal) software. This creates a distinct digestion pattern that differs from the empty vector. Briefly, for enzymes requiring the same digestion buffer, 1μg of DNA was digested at 37°C for 1 hour in a total volume of 20μl containing 2μl of the appropriate 10X buffer and 1μl of each enzyme. Samples were run on a 1% agarose gel at 100V and bands visualised under UV light. For digestions where enzymes showed maximum activity in differing buffers, 1μg of DNA was first digested in a total volume of 10μl in the buffer with the lowest salt concentration for 30 minutes at 37°C. The second buffer and enzyme was then added to a total of 20μl for a further 30 minutes. Samples were then run on a gel and bands visualised as above.

2.2.5.3 Sequencing

All sequencing analysis to check orientation and insertion of transgenes was carried out by the Genome Centre (William Harvey Institute, Queen Mary University of London).

2.2.6 DNA purification

Following screening, positive clones were expanded by adding the 1ml of stored culture to 200ml of LB containing 50μg/ml ampicillin and incubated overnight at 37°C on a shaker. DNA was extracted the following day using QIAGEN Plasmid Maxi Kit (Qiagen) and following the standard protocol. DNA concentration was measured using a Nanodrop® ND-1000 spectrophotometer (Labtech International Ltd, East Sussex, UK) and stored at -20°C.

2.3 Vaccinia Virus Production

2.3.1 Viral DNA Extraction

Extraction of viral DNA for use in the recombination of transgenes into the virus was performed using QIAmp DNA Blood Mini Kit (Qiagen). 20μl of proteinase K (Qiagen) was added to 200μl of virus, followed by 200μl of Buffer AL (supplied with the extraction kit) and then incubated at 56°C for 10 min in a heat block. 200μl of ethanol was added to the sample, mix was pulse-vortexed for 15 seconds, and transferred to a QIAmp spin column in a 2 ml collection tube. After centrifugation for 1 min at 8000rpm, the QIAmp spin column was transferred to a new collection tube. 500μl of Buffer AW1 (supplied) was added and the sample centrifuged again at 8000rpm for 1 min. 500μl of Buffer AW2 (supplied) was added and the column was centrifuged at 13000rpm for 3 min, followed by another 1 minute after transfer to a new collection tube. After placing the column in a sterile Eppendorf tube, 40μl of distilled H_2O was added and the column centrifuged at 8000rpm for 1 min to elute the purified DNA. DNA concentration was again measured using a Nanodrop® ND-1000 spectrophotometer and stored at -20°C.

2.3.2 Recombination

2×10^5 CV1 cells/well were seeded in a 6 well plate in 1.6ml of 10% FBS-DMEM. Cells were infected 24hrs later with the Lister strain of vaccinia virus at 0.05pfu/cell in 1ml serum-free DMEM for 1 hour. Infection medium was removed, cells washed with sterile PBS and 1ml of 2% FBS-DMEM added.

Cells were transfected with 0.3μg viral DNA and 0.5μg DNA of the recombination plasmid/well using FuGeneHD transfection reagent (Roche). 3μl FuGeneHD was added to 100μl serum free medium in a sterile 1.5ml eppendorf tube, mixed by tapping and flicking, and incubated at room temperature for 15 minutes. DNA was diluted in 100μl serum free medium and the transfection medium added dropwise, mixed by tapping, and incubated for a further 45 minutes at room temperature. DNA and transfection reagents were prepared whilst the cells were in the infection medium. After removal and addition of 1ml fresh 2% FBS-DMEM, all 200μl of the transfection complex was added per well in a dropwise manner and cells incubated at 37°C for a further 2 hours. Cells were then topped up with an additional 2ml/well of 2% FBS-DMEM.

Cells were visualised under a fluorescence microscope 48-72hrs after transfection for the presence of fluorescent protein (RFP or DsRed2) expressed from the transfected plasmid. When a high level of fluorescence was observed cells and the supernatant were scraped together using a sterile plastic scraper. Recombinant samples were freeze-thawed three times on dry ice, vortexed each time the sample was thawed at 37°C, and stored at -80°C prior to plaque purification.

2.3.3 Plaque Purification

5×10^5 CV1 cells/well were seeded in a 6 well plate in 1.6ml of 10% FBS-DMEM. Twenty-four hours later, cells were infected with recombinant virus covering a range of 10^{-2} to 10^{-7} dilutions in 1ml serum-free DMEM for 2 hours. Infection medium was then removed and cells washed with PBS. An equal volume of autoclaved 2% bacteriological agar (Sigma, MO, USA) was mixed with 2X DMEM prepared from DMEM powder (SAFC Biosciences, Kansas, USA) and FBS to give a final concentration of 1X 10% FBS-DMEM and 1% agar. 3ml agar mix was added per well and left at room temperature for 10 minutes to allow the agar to set. Cells were then returned to the incubator.

Cells were observed under a fluorescence microscope 48-72hrs after infection for the presence of selection fluorescent proteins, indicating positive recombinant plaques. Two well-isolated positive plaques were picked per recombinant virus using a sterile glass pipette and transferred to individual eppendorf tubes. The plaques were then dissolved in 100µl of Hank's Buffered Salt Solution (HBSS) (Gibco) and subjected to three rounds of freeze thawing (dry ice/37°C).

Viruses were subjected to further rounds of plaque purification following the protocol above until all plaques expressed the marker of interest, when the virus was deemed pure. In this case, the virus was expanded in CV1 cells in one well of a 6 well plate. Cells were infected with the pure plaque dissolved in HBSS for 2 hours in serum free DMEM. This infection medium was then replaced with 2ml 2% FBS-DMEM instead of agar and used as a primary expansion.

2.3.4 Virus Expansion and Purification

A $T175cm^2$ flask with CV1 cells at 80% confluency was infected with 100µl of the primary virus expansion from the 6 well plate by adding it directly to the medium in the flask. The remaining virus was stored at -80°C. Cells were observed for signs of cytopathic effect (CPE) following virus infection and, typically 48-72hrs post-infection, cells detached from the flask surface. The remaining adherent cells were disturbed by agitation of the flask and the cells and supernatant collected in a 50ml Falcon tube and freeze-thawed three times to release virions from the cells. Virus expansion was stored at -80°C prior to large scale propagation and purification.

CV1 cells in 10% FBS-DMEM were seeded in a multi layer cell factory CF-10 (Fisher Scientific, Leicestershire, UK) until 70-80% confluent when the medium was decanted. Cells were infected with 10ml of the primary T175 virus expansion in 1 litre of 2% FBS-DMEM. Infected CV1 cells were harvested when signs of CPE were seen, taken as detachment of cells, which was typically 2-4 days post-infection. Maximum cell detachment was achieved by agitation of the monolayers. Cells and supernatant were transferred to 2 sterile 500ml Sorval bottles and centrifuged at 3500rpm for 15 minutes to collect the cell pellet. Medium was aspirated and the pellet resuspended in 30ml of PBS to wash traces of serum and media away. This was centrifuged at 3500rpm for 15minutes and the pellet resuspended in 14ml of 10mM Tris-HCl pH9.

Virus purification consisted of three cycles of freeze thawing and centrifugation at 900rpm for 5 minutes. The supernatant was collected and the pellet resuspended in 3ml of 10mM Tris-HCl pH9 followed by further centrifugation at 900rpm. The pellet was discarded and supernatants combined in a total volume of 30ml 10mM Tris-HCl pH9 after sonification. This was layered equally onto 4 SW27 ultracentrifuge tubes, each containing 17ml of 36% sucrose diluted in 10mM Tris-HCl pH9 and centrifuged at 13,500rpm for 80 minutes at 4°C. The supernatant was aspirated and the viral pellet resuspended in 1ml of 1mM Tris-HCl pH9. This constituted the purified virus and the titre was determined by $TCID_{50}$ assay.

2.3.5 Virus titration: $TCID_{50}$ assay

The $TCID_{50}$ assay (tissue culture inhibitory dose 50%) is a limiting dilution assay that enables the quantification of any infectious particles in the test sample. It was used to determine the titre of viruses by titrating 10 fold serial dilutions of virus onto CV1 cells in a 96 well plate. Titrations were performed on triplicate plates. A 10 fold serial dilution of virus was prepared in 50μl of 2% FBS-DMEM per well. Dilutions typically started at 10^{-6}. CV1 cells were seeded immediately on top at a density of 25,000 cells/well in 150μl of 2% FBS-DMEM to give a total volume of 200μl per well. Plates were analysed 5 days post-seeding/infection by observation of CPE and the titre in pfu/ml was determined using the calculation described below.

Wells exhibiting CPE were counted per dilution row and used in the following calculation to determine the TCID50 value.

Log TCID50 = A - D (S – 0.5)

A = Log of the highest dilution showing CPE in more than 50% of the wells

D = Log of the dilution factor.

S = summation of the proportion of positive wells in each row.

Quantification of infectious particles was expressed as plaque-forming units per ml (pfu/ml). This was calculated by adjusting the Log TCID50 to the volume used to infect the wells to obtain Log TCID50/ml and multiply this value by the coefficient factor 0.69. According to the Poisson distribution, the proportion (p) of wells not receiving infectious units at a given dose is $e^{-\mu}$, where μ is the concentration of infectious viral particles at that dose. As TCID50 is the dose at which 50% of the wells are infected ($p = 0.5$), meaning that $0.5 = e^{-\mu}$, therefore $\mu = 0.69$.

2.4 Cell Survival assays

2.4.1 Cell Proliferation

To determine the effect of recombinant murine decorin (rmDCN) on TrampC1 proliferation/survival, cells were seeded at a density of 2×10^5 cells/well of a 6 well plate in 10% FBS-DMEM, or media containing 2μg/ml or 10μg/ml rmDCN. Each condition was tested in triplicate. At 24hrs, 48hrs and 72hrs post-seeding, cells were trypsinised and resuspended in total of 1ml DMEM. Cell number was counted using a Beckman Coulter counter, and the average of duplicate counts calculated.

2.4.2 MTS assay

Cell proliferation assays were carried out using the CellTiter 96 AQueous Non-Radioactive Cell Proliferation Assay kit (Promega) that contains the tetrazolium salt 3-(4,5-dimethylthiazol-2-yl)-5-(3-carboxymethoxyphenyl)-2-(4-sulfophenyl)-2H-tetrazolium) known as MTS, used in conjunction with the electron coupling reagent phenazine methosulfate (PMS). Mitochondrial enzymatic activity in viable cells reduces MTS to the water-soluble product formazan, and this reduction is facilitated by PMS. The number of living cells is directly proportional to the concentration of formazan in the sample, determined by the absorbance at 490nm. At the time of analysis, medium was removed from plates by inversion and 21μl of MTS/PMS in a 20:1 ratio added in a final volume of 100μl DMEM per well. Following incubation at 37°C for between 1 and 6 hrs depending on the cell line the plate was read at 490nm using an OpsysMR plate reader (DynexTechnologies Inc, Chantilly, US).

The optical density (OD) of wells with medium alone (background value of MTS reagents in the absence of cells) was subtracted from the OD of those containing untreated cells only. Experimental ODs were expressed as a percentage of those of untreated cells (100% viable cells).

2.4.3 MTT assay

Cell survival was also measured using MTT (3-(4,5-Dimthylthiazol-2-yl)-2,5-diphenyltetrazolium bromide) (Sigma), which is also reduced to formazan in living cells. As MTT is not a water-soluble tetrazole the resulting purple formazan product must be dissolved in dimethyl sulfoxide (DMSO) before analysis.

MTT assays were performed in 24 well tissue culture plates and cells seeded at a density of 10^4/well in 1ml of complete medium. Typically, cells were treated with virus, drug or inhibitor 24hrs post-infection and cell survival measured by adding 100μl/well MTT (final concentration 500μg/ml) and incubating at 37°C for 3hrs. The medium was then aspirated and formazan crystals dissolved in 200-400μl of DMSO depending on the colour intensity of the cystals. In order to compare between conditions, the volume of DMSO was selected based on the highest intensity and all other wells treated in the same manner. Plates were read at 560nm on a Wallac 1420 Multilabel counter plate reader (PerkinElmer Life and Analytical Sciences). Cell survival was normalised for background absorbance and expressed as percentage of untreated cells (100% survival).

2.4.4 Dose response to vaccinia strains

The sensitivity of cells to Lister-wt, Lister-dTK or Lister-mDCN was determined by MTS assay. Briefly, $5x10^3$ cells were seeded per well of a 96 well plate, in 90μl of 2% FBS-DMEM (supplemented as indicated in section 2.1), with the exception of IOSE25 cells where $3x10^4$ cells were seeded per well. Cells were infected 24 hours later with a 10 fold serial dilution of virus in triplicate, typically starting with a highest dose of 1000pfu/cell. The dilution series was prepared in a separate 96 well plate and 10μl of the appropriate dilution added per well direct to the culture media. Cell survival was analysed 72 hrs post-infection unless otherwise indicated. Plates were read as described in section 2.4.2 and dose-response curves constructed using GraphPad Prism version 5.0b for Macintosh (GraphPad Software, San Diego CA, USA). The efficient concentration $(EC)_{50}$ is the dose of virus required to kill 50% of cells, and was calculated from the equations of the sigmoidal curves generated by GraphPad Prism software.

2.4.5 Dose response to cisplatin

The sensitivity of cells to cisplatin was determined by MTS assay. $5x10^3$ cells were seeded per well of a 96 well plate, in 90μl of 2% FBS-DMEM (supplemented as indicated in section 2.1), and cisplatin added 24hrs later. A dilution series of cisplatin, ranging from 100μM to 1pM, was prepared and 10μl of the appropriately diluted drug added per well direct to the culture media, in triplicate. Cell survival was determined 72hrs after addition and the EC50 calculated as described in section 2.4.4.

2.4.6 Toxicity of inhibitors

The toxicity of all inhibitors used throughout the body of this work was first assessed to select appropriate concentrations for combination studies. Toxicity of the pan-caspase inhibitor zVAD-fmk (Calbiochem) was determined by MTT assay. Cells were seeded at a density of 10^4/well in 1ml of complete media and zVAD-fmk added 24hrs, 48hrs and 72hrs later to triplicate wells. Cell survival was analysed 96hrs post-seeding following addition of 25μM zVAD-fmk daily, and 120hrs post-seeding following addition of 10μM and 2.5μM zVAD-fmk daily. Plates were read and cell survival determined as described in section 2.4.3.

Toxicity of the autophagy inhibitors 3-methyladenine (3-MA) (Sigma) and chloroquine (Sigma) was determined by MTS assay. Cells were seeded at a density of $5x10^3$ cells per well of a 96 well plate, in 90μl of 2% FBS-DMEM (supplemented as indicated in section 2.1), and either 3-MA or chloroquine added 24hrs later to triplicate wells. 3-MA was tested at concentrations of 2mM, 1mM and 100μM and chloroquine at 20μM, 10μM, 5μM and 1μM. Cell survival was analysed 72hrs after addition of drug as described in section 2.4.2.

Toxicity of the RIP1 kinase inhibitor necrostatin-1 was assessed by MTT assay using concentrations of 300μM, 100μM, 30μM and 10μM necrostatin-1. Cells were seeded at a density of 10^4/well in 1ml of complete media and necrostatin-1 added 24hrs later to triplicate wells. Cell survival was analysed 72hrs later and cell survival determined as described in section 2.4.3.

2.4.7 Combination assays

In assays where drugs or inhibitors were used in combination with virus, these were added directly to the appropriate wells 2 hours post-infection unless otherwise stated. The equivalent volume of vehicle only was added to control wells ensuring that all cells were maintained in an equal volume of medium and subjected to the same concentration of diluent.

Where cisplatin was used in combination with Lister-dTK, cell survival was analysed by MTS assay. Cells were seeded at a density of $5x10^3$ cells per well of a 96 well plate, in 90μl of 2% FBS-DMEM (supplemented as indicated in section 2.1), and either cisplatin or Lister-dTK added 24hrs later. Dosing schedules consisted of pre-treatment with cisplatin for 24hrs followed by infection with a serial dilution of Lister-dTK ranging from 10^3 - 10^{-6} pfu/cell, or infection with virus followed by addition of cisplatin 2hrs or 24hrs post-infection. Two concentrations of cisplatin were used based on the toxicity of individual cell lines to the drug. These were 10μM and 1μM for A2780CP cells, 3μM and 1μM for Igrov1 and Skov3ip1 cells and 1μM and 0.3μM for A2780 cells. As a control, cells were also infected in the absence of cisplatin. In all dosing schedules, cell survival was analysed 72hrs post-infection and each condition was tested in triplicate wells. Cell survival in wells treated with both Lister-dTK and cisplatin was expressed as a percentage of the survival of cells treated with cisplatin only to normalise to the effect of the drug alone. Dose-response curves were constructed using GraphPad Prism version 5.0b for Macintosh (GraphPad Software, San Diego CA, USA). The efficient concentration $(EC)_{50}$ of Lister-dTK was calculated from the equations of the sigmoidal curves generated by GraphPad Prism software.

Where Lister-dTK was used in combination with the autophagy inhibitors 3-methyladenine (3-MA) or chloroquine (CQ), the pan-caspase inhibitor zVAD-fmk, or the RIP1 kinase inhibitor necrostatin-1, cells were seeded as above and cell survival was determined 72hrs post-infection by MTS assay. Inhibitors were added 2hrs post-infection and cell survival normalized to cells treated with inhibitor alone as above. Where 10μM zVAD-fmk was added daily to cells, cells were seeded at 10^4 cells/well of a 24well plate and infected with 1pfu/cell Lister-dTK 24hrs later. Cell survival was determined 96hrs post-infection by MTT assay.

Where the effect of recombinant murine decorin (rmDCN) on the cytotoxicity of Lister-dTK was studied, rmDCN was added 2hrs post-infection at 2μg/ml or 10μg/ml and cell survival determined 72hrs post-infection by MTS assay.

Where siRNA was used in combination with Lister-dTK, cells were first transfected with siRNA as described in section 2.5.2. The following day, cells were infected with 100pfu/cell, 10pfu/cell or 1 pfu/cell Lister-dTK by adding 50μl appropriately diluted virus directly to culture medium. Cell survival was determined by MTT assay 72hrs post-infection, and expressed as a percentage of uninfected control cells that had been transfected with siRNA.

To assess whether Bcl2 over-expression was able to inhibit apoptosis, the survival of OVCAR4 and OVCAR4-Bcl2 cells in response to 10μM cisplatin was determined by MTT assay 72hrs after addition of drug. Similarly, the ability of zVAD-fmk to inhibit apoptosis was assessed in A2780CP and Igrov1 cells by determining cell survival 48hrs after treatment with 10μM cisplatin in the presence or absence of 10μM zVAD-fmk. Cells were seeded at density of 10^4 cells/well of a 24 well plate and drugs added 24hrs later in both cases.

2.4.8 Sulforhodamine B assay

The sulforhodamine B assay measures total biomass by staining cellular proteins with the sulforhodamine B dye (Acid red 52) (Sigma) and then solubilising the incorporated dye into a tris base solution. The absorbance is then measured spectrophotometrically at 560nM and is relative to the number of cells. Cells were seeded in a 96 well plate and infected with virus alone or virus plus inhibitor as per section 2.4.2. Cell survival was assessed 72hrs post-infection by removing culture medium and fixing cells in 100μl/well of 10% trichloroacetic acid (TCA) for 1 hour at 4°C. Cells were washed with water before staining with 50μl/well of 0.4% w/v sulforhodamine B in 1% acetic acid for 30 minutes at room temperature. Excess dye was removed by repeated washing with 1% acetic acid, plates air dried and then the incorporated dye solubilised in 100μl/well of 10mM tris base solution. Plates were read at 565nM on Wallac 1420 Multilabel counter plate reader (PerkinElmer Life and Analytical Sciences). Cell survival was expressed as a percentage of untreated cells. Dose response curves were constructed as per section 2.4.2.

2.5 Transfections

2.5.1 Transfection of plasmids into cells

During cloning of the mDCN-IRES-DsRed sequence into the final recombination plasmid used during homologous recombination to create the Lister-mDCN strain, CV1 cells were transfected with intermediary plasmids. This was to confirm that plasmids at each stage of the cloning process expressed the appropriate transgenes. Lysates where decorin was expressed also acted as positive controls for subsequent immunodetection of decorin in panels of cancer cell lines.

2 x 10^5 cells were seeded per well of a 6 well plate in 1.6ml of the appropriate growth medium. Cells were transfected with varying amounts of DNA (typically ranging from 0.5μg to 2μg) using FuGeneHD transfection reagent (Roche, Basel, Switzerland). DNA was first diluted in 100μl serum free medium. 3μl FuGeneHD was added per μg of DNA in serum free medium in a separate sterile 1.5ml eppendorf tube containing 100μl serum free medium, mixed by tapping and flicking, and incubated at room temperature for 15 minutes. This transfection medium was then added dropwise to the diluted DNA, mixed by tapping, and incubated for a further 45 minutes. All 200μl of the transfection complex was added to 1ml

2% FBS-DMEM per well in a dropwise manner and cells incubated at 37°C for a further 2 hours. Medium was then aspirated and replaced with 2ml/well of DMEM supplemented with 2% FBS. Where gene expression was under the control of a viral promoter, cells were first infected with 0.1pfu/cell Lister-wt for 1 hr in 1ml serum-free medium, after which medium was removed, cells washed in PBS and then transfected as above.

As a positive lysate for human decorin for detection of decorin in a panel of human pancreatic cancer cell lines, CV1 cells were infected as above and then transfected with 2μg of an intermediary plasmid expressing human decorin, pD-LARATK hDCN (Figure 11), as described above. Cells were harvested 48hrs post-transfection and protein extracted as described in section 2.9.1.

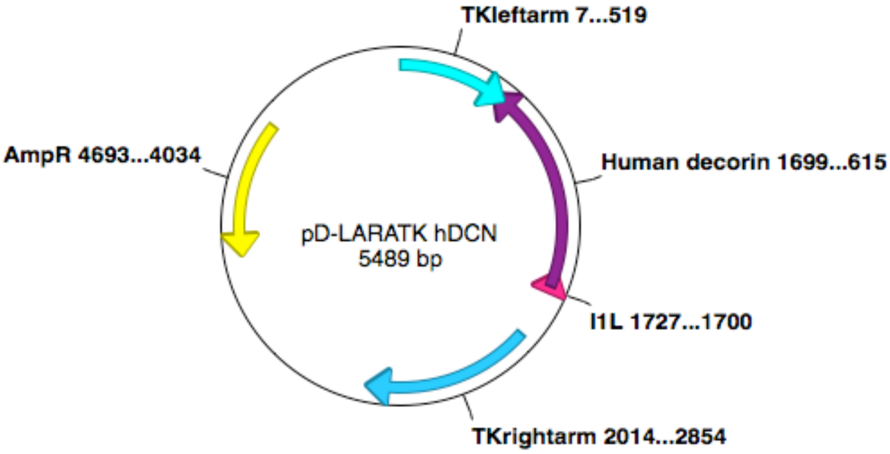

Figure 11: Schematic representation of the pD-LARATK-hDCN plasmid. Human decorin is expressed under control of the intermediate vaccinia virus promoter, I1L.

2.5.2 Transfection of siRNA

Small interference RNA (siRNA) targeted against RIP1 and RIP3 was obtained from Dharmacon in the form of a mixed pool of 4 separate siRNAs (ON-TARGET*plus* SMARTpool). A non-targeting (NT) pool of siRNA was also used (Dharmacon). All cell lines were transfected using DharmaFECT 1 transfection reagent (Dharmacon). Concentration of siRNA was first optimised in all cell lines using concentrations ranging from 1-50nM siRNA. A final concentration of 10nM RIP1 siRNA was used for subsequent transfection of A2780, A2780CP, Skov3ip1 and TOV21G cells, and 5nM for Igrov1 cells. Similarly, 10nM RIP3 siRNA was used for transfection of TOV21G cells.

Cells were seeded at a density of $5x10^4$ cells/well of a 24 well plate in 1ml of complete medium. The following day cells were transfected with siRNA as follows; stock siRNA was prepared to a working stock of 2μM in DMEM. The appropriate amount of siRNA was diluted in 50μl/well of antibiotic-free DMEM in an eppendorf tube, and 0.75μl/well DharmaFECT1 added to 50μl/well of antibiotic-free DMEM in a separate eppendorf. Following a 5 minute incubation at room temperature, siRNA solution and DharmaFECT1 solution were mixed by pipetting and incubated for a further 20 minutes at room temperature. This was then added to 400μl of 10% FBS-DMEM to give a total volume of 500μl/well. Medium was aspirated from cultured cells and replaced with 500μl/well of transfection media as described above.

To confirm knockdown of targeted proteins, cells were harvested between 24hrs and 120hrs post-transfection depending on individual experimental conditions, detailed alongside individual graphs. Protein expression was determined by western blotting.

2.6 Viral replication

2.6.1 TCID50 assay

In human ovarian cancer cell lines and various murine cancer cell lines, viral replication was determined by performing burst assays, followed by limiting dilution tissue culture infectious dose $(TCID)_{50}$ assays in CV1 cells. For the burst assay, cells were seeded at a density of $2x10^5$ cells/well in 6 well plates in 1.6ml complete growth medium. Replication of Lister-dTK in human ovarian cancer cell lines was determined following initial infection with 1 pfu/cell in serum free medium for 2 hrs, after which the infection medium was aspirated and replaced with 2ml of 2% FBS-DMEM/well. Replication of Lister-dTK and Lister-mDCN in murine cell lines was determined following initial infection with 0.1pfu/cell. Where the effect of recombinant murine decorin (rmDCN) on Lister-dTK replication in TrampC1 cells was studied, this was added to the medium 2hrs post-infection. At 24hrs, 48hrs and 72hrs post-infection cells were detached by scraping, and collected together with the supernatant. In addition, the replication of Lister-dTK and Lister-mDCN at early timepoints (9hrs, 12hrs and 18hrs post-infection) was also determined in MOSEC cells. Samples were freeze-thawed three times and assayed by $TCID_{50}$ assay in CV1 cells.

The titre of replicating infectious viral particles in each sample was determined by the limiting dilution TCID50 assay. CV1 cells were seeded at a density of 10^4 cells/well of a 96 well plate in 90μl 2% FBS-DMEM. Serial dilutions of samples were prepared and titrated down the plate 24hrs later by adding 10μl/well. Starting dilutions ranged from 10^{-1} to 10^{-5} depending on the cell line and time of harvest. No virus was added to the first 2 columns as these acted as negative controls for the assay. All samples were titrated on triplicate plates and cells were analysed for the presence of CPE 5 days post-infection.

The pfu/ml was calculated as described in Section 2.3.5 and then adjusted to pfu/cell based on the number of cells seeded (2×10^5) in the original sample. This was to allow easier comparison between different cell lines and assays.

2.6.2 Quantitative PCR

Quantitative PCR (qPCR) was performed on DNA harvested from subcutaneous TrampC1 tumours from athymic mice. Tumours were excised and lysed overnight in a 600μl total volume of lysis buffer (Qiagen), containing proteinase K. DNA was then extracted from a proportion of the tumour lysate calculated to contain 25mg of tissue based on the original tumour mass, using DNeasy Blood and Tissue Kit (Qiagen). qPCR was performed on 40ng extracted DNA using SYBR Green PCR Mastermix (ABI) and the 7500 Real Time PCR System (ABI), in a total reaction volume of 20μl. Primers (SigmaAldrich) were designed to amplify a vaccinia early transcription factor gene and are shown below.

Forward primer:	5' ACAGAAGCGTGTTATTGTTCCATATT
Reverse primer:	5' AGGCGAACAACAAAGCGATT

Programme cycles consisted of 50°C for 2mins, 95°C for 10mins and then 40 cycles of 95°C for 15 seconds, followed by 60°C for 60 seconds. A dissociation curve was also performed at 95°C for 15mins, 60°C for 1 min and then 95°C for 15seconds. A standard curve was prepared using DNA extracted from the Lister-wt virus, as described in section 2.3.1. A 10 fold dilution series of DNA was performed to prepare standards containing $5\text{-}5 \times 10^8$ copies of virus each. The threshold cycle (Ct) value of each sample was then compared against the standard curve to calculate the amount of viral DNA within individual tissue samples. This was then expressed as virus copy number/whole tumour using the following calculation:

$$\frac{\text{Amount of DNA in whole tumour (ng)}}{\text{Sample size of 40ng}} \quad \text{x virus copy number based on Ct value}$$

To enable comparison between tumours this was then expressed as virus copy number/mg tissue by dividing the value calculated above by the original tumour mass in mg. Each sample and standard was tested in triplicate and the mean used for the above calculations.

2.7 Virus spread assays

2.7.1 Organotypic cultures

TrampC1 cells were embedded in a collagen matrix comprising 10% FBS, 10% 10X DMEM (final concentration 1X), cells in 10% volume normal growth media and 70% collagen/matrigel mix. Rat tail Collagen I (Marathon Laboratory Supplies), and matrigel (Scientific Laboratory Supplies) were prepared in a 70:30 ratio. All reagents were kept on ice whilst preparing the collagen matrix. A total of 1ml of collagen matrix containing 5x10^{6} TrampC1 cells was added per well of a 24-well plate and allowed to set at 37°C in a humidified incubator for 1hr. 0.5x10^{6} cells were then added on top in 500μl normal growth medium and infected with 10^{6} pfu of either Lister-dTK or ListermDCN 24hrs later in serum free medium for 2hrs. Infection medium was then aspirated and replaced with 1ml of 2% FBS-DMEM. Gels were gently removed from wells between 24 and 72hrs post-infection and fixed in formol-saline containing 4% formaldehyde (Fisher-Scientific) overnight. Gels were then transferred to 70% ethanol for immunohistochemistry for vaccinia virus proteins.

Organotypics were also set up as described above using MOSEC or Panc02 cells, where the number of cells embedded in the collagen matrix ranged from 0.5x10^{6} to 5x10^{6} cells per gel. All other steps remained the same.

2.7.2 Collagen penetration assay

TrampC1 or MOSEC cells were seeded at a density of $2x10^5$ cells per well of a 24-well plate and infected with 0.1pfu/cell of Lister-dTK or Lister-mDCN 24hrs later for 2hrs in serum free medium. Cells were then washed with PBS and 300µl of a collagen matrix (as described in section 2.7.1) added per well. Following incubation at 37°C for 1hr to allow the gel to set, gels were topped with 500µl of normal growth medium. Medium was harvested 24hrs, 48hrs and 72hrs post-infection and the titre of replicating infectious viral particles determined by the limiting dilution TCID50 assay. With the exception of initial storage at -80°C, samples were not freeze-thawed prior to virus determination. CV1 cells were seeded at a density of 10^4 cells/well of a 96 well plate in 90µl 2% FBS-DMEM and 10µl/well of neat sample added to wells 3-12 of row A of the plate 24hrs later. The sample was then titrated down the plate in a 10-fold serial dilution. Medium only was added to the first 2 columns of wells on the plate, as these acted as negative controls for the assay. All samples were titrated on triplicate plates and cells were analysed for the presence of CPE 5 days post-infection. The pfu/ml was calculated as described in Section 2.3.5.

2.8 Quantification of intracellular ATP

Intracellular adenosine tri-phosphate (ATP) levels were determined in uninfected A2780, A2780CP, Skov3ip1 and TOV21G cells, and following infection with 10pfu/cell of Lister-dTK. Cells were harvested at 0hrs, 8hrs, 24hrs, 48hrs and 72hrs post-infection and protein extracted and quantified as described in section 2.9.1. ATP levels were quantified using a luciferase based ATP determination kit (Invitrogen A22066), which is based on the requirement of ATP for luciferase to convert its substrate D-luciferin into light.

90µl assay reagents (25mM tricine buffer, 5mM $MgSO_4$, 0.1mM EDTA, 0.5mM D-luciferin, 1µM DTT and 1.25µg/ml Firefly luciferase in distilled H_20) were added to 10µl diluted protein/well in triplicate wells, and the plate read immediately at 560nm on a Wallac 1420 Multilabel counter plate reader (PerkinElmer Life and Analytical Sciences). ATP levels in 2µg/well sample protein were quantified using a standard curve of ATP, prepared from the kit, ranging from 1µM to 1nM. The average total intracellular ATP from triplicate samples was then expressed in µmol/gram protein.

2.9 Protein expression levels

2.9.1 Preparation of whole protein lysates

For the preparation of whole protein lysates, cells were collected by trypsinisation and combined with the supernatant. Cell pellets were collected by centrifugation, resuspended in PBS and centrifuged again. The final cell pellet was resuspended and lysed on ice in RIPA buffer (50mM Tris HCl pH 8.0, 150mM NaCl, 1 mM EDTA, 1% Igepal CA-630 (NP-40), 0.1% SDS) containing 1 protease inhibitor tablet (Roche) per 20ml buffer. After centrifugation at 13000rpm for 5 minutes, supernatant was transferred to a clean 1.5ml Eppendorf tube and protein concentration determined using Pierce BCA Protein Assay Kit (Thermo-Scientific). Briefly, bovine serum albumin (BSA) (SIGMA) standards were prepared by diluting in distilled water and 5μl of either standard or sample added per well of a 96 well plate in duplicate. 200μl of working solution (Reagent A:Reagent B in 50:1 ratio) was added per well and incubated at 37°C for 30 minutes before reading at 562nm. A standard curve of absorbance *vs* concentration was constructed for the different concentrations of BSA and the protein concentration in each sample was calculated from this graph.

Lysates were diluted to either 1μg/μl or 0.5μg/μl in RIPA buffer in a total volume of 100μl containing sample loading dye (5% SDS, 20% buffer IIb (0.5M Tris, 0.2M NaH_2PO_4 pH 7.8), 5% β-mercaptoethanol, 50% Glycerol, a few grains of bromophenol blue, 20% distilled water). Samples were denatured at 100°C for 5 minutes and then either used immediately or stored at -20°C.

2.9.2 SDS Gel electrophoresis

Samples were ran on either a NuPAGE 4-12% Bis-Tris precast gel (Invitrogen) or a 10%, 12% or 15% polyacrylamide gel as indicated throughout. Resolving gels were constructed by mixing gel buffer (80ml 1.5M Tris-HCl pH 8.7, 3.2ml 10% SDS, 160μl TEMED in distilled water to a total volume of 200ml) with the appropriate volume of polyacrylamide and 100μl 10% ammoniumpersulfate (APS) in a final volume of 10ml. Gels were constructed and allowed to set in a multiple gel caster system (Amersham Biosciences). Stacking gel was prepared by adding 50μl of APS to 5ml of stock stacking solution (8.3ml 30% acrylamide, 6.25ml IIb solution, 0.5ml 10% SDS, 50μl TEMED in distilled water to 50ml total volume) and added to the top of the gel before inserting a comb and allowing the gel to set at room temperature.

10μg or 20μg of sample protein was loaded per well alongside 5μl of PageRuler Prestained protein ladder (Fermentas UK, York, UK) for separation by electrophoresis using the Mighty Small II mini-vertical electrophoresis system (Amersham Biosciences). Tris-Glycine SDS PAGE Running buffer was used for reducing polyacrylamide gels, or 1X MOPS Buffer (Invitrogen) for precast gels.

Proteins were then transferred onto Hybond-P PVDF membranes (GE Healthcare, Buckinghamshire, UK) using a Trans Blot SD Semi-Dry Transfer Cell (BioRad). Briefly, PVDF membranes were soaked in methanol for 5 minutes followed by a further 5 minutes in transfer buffer (2.9g Tris, 14.5g Glycine, 200ml methanol in distilled water to a total volume of 1 litre). Two pieces of blotting paper (BioRad) and the gel were also soaked in transfer buffer before assembly of the PVDF membrane, topped with the gel, between the two blotting papers. Transfer of proteins from the gel to membrane was performed at 20V for 45 minutes.

Membranes were blocked in 5% (w/v) non-fat milk (Marvel, Dublin, Ireland) in Tris-buffered saline Tween-20 buffer (TBS-T) containing 20mM Tris-Hcl pH 7.4, 500mM NaCl and 0.05% Tween-20 for a minimum of 1 hour at room temperature. Membranes were then rinsed with TBS-T before incubation with the primary antibody. Conditions for each antibody are shown in Table 3. Membranes were incubated with the primary antibody overnight at 4°C with a gentle rocking motion and then washed three times with TBS-T for a minimum of 10 minutes each time. Membranes were incubated with the appropriate secondary antibody (Dako) conjugated to horseradish peroxidase (HRP) in 3% BSA-TBS-T for 1 hour at room temperature followed by a further three washes with TBS-T.

Proteins were detected using ECL Plus Western Blotting Detection Reagents (GE Healthcare, Buckinghamshire, UK) and visualized by exposure of the membrane to Hyperfilm ECL (GE Healthcare, Buckinghamshire, UK) prior to developing in a Curix 60 Developer (Agfa, Middlesex, UK).

For the subsequent detection of other proteins in the same samples, on the same membrane, membranes were first stripped in 20ml buffer (2% SDS, 62.5mM Tris, 100mM β-mercaptoethanol in water) at 50°C for 30 minutes on a shaker. Membranes were then washed in TBS-T and re-blocked in 5% milk-TBST for a minimum of one hour. Following this, proteins were detected using the appropriate primary antibody (Table 3) and protocol as described previously.

Antibody	**Species**	**Conditions**	**Supplier**
Actin	Goat	1:1000 in 2% BSA-TBS-T	Santa Cruz
Bcl2	Mouse	1:1000 in 5% milk TBS-T	Santa Cruz
Caspase 3	Rabbit	1:1000 in 5% milk TBS-T	Cell Signaling
Caspase 8	Mouse	1:1000 in 3% BSA-TBST	BD Pharminogen
Decorin-murine	Rat	1:500 in 2% BSA-TBS-T	R&D Systems
Decorin-human	Mouse	1:300 in 2% BSA-TBS-T	R&D Systems
EGFR	Rabbit	1:1000 in 5% BSA-TBS-T	R&D Systems
pEGFR	Rabbit	1:1000 in 5% BSA-TBS-T	R&D Systems
Erk	Goat	1:500 in 5% BSA-TBST	Santa Cruz
p-Erk	Goat	1:500 in 5% BSA-TBST	Santa Cruz
HMGB1	Rabbit	1:1000 in 5% BSA-TBST	Abcam
Ku70	Goat	1:1000 in 2% BSA-TBS-T	Santa Cruz
LC3B	Rabbit	1:1000 in 5% BSA-TBST	Cell Signaling
p21	Rabbit	1:1000 in 5% BSA-TBST	Santa Cruz
PARP	Mouse	1:500 in 3% BSA-TBST	Santa Cruz
Cleaved PARP	Rabbit	1:1000 in 5% milk TBS-T	Cell Signaling
RIP1	Rabbit	1:1000 in 5% BSA-TBS-T	Cell Signaling
RIP3	Rabbit	1:300 in 5% milk TBS-T	Imgenex
Smad2	Mouse	1:1000 in 5% milk TBS-T	Cell Signaling
Phospho Smad2	Rabbit	1:1000 in 5% milk TBS-T	Cell Signaling
Vaccinia Virus	Rabbit	1:1000 in 3% BSA-TBS-T	AbD Serotec

Table 3: Antibodies used for protein detection by western blotting. Antibody providers are Abcam (Cambridge, UK), AbD Serotec (Oxford, UK), BD Pharminogen (Oxford, UK), Cell Signalling® Technology (MA, USA), Imgenex (San Diego, CA), R&D Systems (Abingdon, UK) and Santa Cruz Biotechnology (CA, USA).

2.9.3 Detection of secreted proteins by immunodetection

The release of HMGB1 from cells infected with vaccinia virus was determined by immunodetection of the protein in the culture media of cells. A2780 cells were mock infected, or infected with 10pfu/cell Lister-dTK. The supernatant and cells were collected separately at 24hrs, 48hrs and 72hrs post-infection. Protein was extracted from the cells and lysates prepared as described in section 2.9.1 for determination of intracellular HMGB1. To detect HMGB1 in the supernatant of cells, the supernatant was first concentrated using centrifugal filter units (Fisher Scientific) by centrifuging at 4300rpm for 30 minutes. An equal volume (30µl) of the concentrated supernatant of each sample was then prepared for western blotting by the addition of sample loading dye (described in section 2.9.1).

2.9.4 Detection of secreted proteins by ELISA

The release of decorin into the supernatant of infected cells was detected by enzyme linked immunosorbent assay (ELISA). MOSEC and TrampC1 cells were seeded at a density of $2x10^5$ cells/well and infected with Lister-dTK and Lister-mDCN at 1pfu/cell and 0.1 pfu/cell 24hrs later. The supernatant of infected cells was collected at 24, 48 and 72hrs post-infection, centrifuged and the supernatant stored at -80°C for analysis by ELISA. All conditions were tested in duplicate.

A 96 well plate was coated with 100µl goat anti-mouse decorin antibody (R&D systems AF1060) at 1µg/ml in PBS overnight at 4°C. Wells were washed three times with 200µl of PBS-T and then blocked with 200µl of 5% w/v non-fat milk for 2hrs. Wells were washed with PBS-T as before and 100µl of each sample added in duplicate per well for 2hrs. As a positive control, and to form a standard curve, recombinant murine decorin (rmDCN) (R&D systems) was also included. PBS was used as a negative control. Wells were washed with PBS-T three times and 100µl of rat anti-mouse decorin antibody (R&D systems MAB1060) added/well at 1µg/ml for three hours. Following washing, 100µl of anti-rat HRP-conjugated secondary antibody was added at a 1:4000 dilution for 2 hrs before further washing. Pre-warmed substrates (R&D systems) were added in 100µl/well comprising a 1:1 ratio of stabilized hydrogen peroxide (substrate A) and stabilized tetramethylbenzidine (substrate B) for 20 mins at room temperature, protected from the light. The reaction was stopped by adding 50µl/well of 2N sulphuric acid (R&D systems) and then read at 450nm with a reference filter of 560nm using an OpsysMR plate reader.

2.9.5 Co-immunoprecipitation

To detect the formation of a RIP1/RIP3/caspase 8 ripoptosome or necrosome-like complex, co-immunoprecipitation was performed using an antibody to immunoprecipitate caspase 8. A2780 and TOV21G cells were seeded at a density of $2x10^6$ cells/$10cm^2$ plate and infected with 10pfu/cell of Lister-dTK in serum-free media for 2hrs, after which infection medium was replaced with normal growth medium. Prior to harvest, cells were treated with 25μM zVAD-fmk overnight and then cells harvested 96hrs post-infection. As a positive control, cells were also treated with 100μM etoposide + 25μM zVADfmk or 25ng/ml TNFα + 25μM zVAD-fmk overnight. Uninfected cells were harvested as a negative control. Cells were scraped into 1ml lysis buffer (30mM Tris pH7.4, 120M NaCl, 2mM EDTA, 2mM KCl, 10% glycerol, 0.2% NP-40) containing protease inhibitors (Roche) and protein extracted on ice for 30 minutes. Protein was quantified by BCA assay; 100μg protein was diluted in 100μl of lysis buffer and denatured at 100°C for 5 minutes in the presence of a reducing sample buffer (5% SDS, 20% buffer IIb (0.5M Tris, 0.2M NaH_2PO_4 pH 7.8), 50% Glycerol, a few grains of bromophenol blue, 20% distilled water) containing 100μM of the reducing agent DTT. These lysates were used as a control for protein input on subsequent SDS-PAGE analysis of co-immunoprecipitated samples. The remaining protein was used in a co-immunoprecipitation assay.

Protein was prepared at 1μg/μl in a total volume of 500μl lysis buffer and 2μg polyclonal goat caspase-8 antibody (Santa Cruz) added. Samples were incubated at 4°C for 2hrs with a gentle rolling motion. Protein G Sepharose 4 fast flow (GE Healthcare) was washed three times with lysis buffer and a 50% slurry prepared by mixing equal volumes of protein G and lysis buffer. 50μl of protein G 50% slurry was added to samples and incubated overnight at 4°C, mixing gently on a roller. The following day, samples were centrifuged at 13,000rpm for 30 seconds and washed in 1ml lysis buffer, followed by a further wash with 1ml 50mM Tris. The supernatant was removed and the final pellet resuspended in 30μl of reducing sample buffer (described above).

SDS gel electrophoresis was perfomed as described in section 2.9.2 to detect caspase 8, RIP1 and RIP3 in 15μl immunoprecipitated sample and 20μg of protein lysates. As both RIP3 and caspase 8 are a similar size to the heavy chain of IgG (55kDa), their detection would be obscured by IgG using a secondary antibody that detects both the heavy and light chains. Anti-mouse and anti-rabbit HRP conjugated secondary antibodies that were specific for the light chain of IgG (Jackson Immuno Research Laboratories Inc.) were therefore used for the detection of caspase 8 and RIP3 respectively.

2.10 Microscopy

2.10.1 Examination of immunostained tissue sections

Analysis of tissue sections was performed using an Axiophot microscope connected to a Zeiss AxioCam camera and using Axiovision software (Zeiss).

2.10.2 Confocal Microscopy to visualise LC3B cellular localisation

The localisation of LC3B following infection with vaccinia virus was monitored with the use of a replication-defective adenovirus expressing LC3B tagged to GFP (Ad-LC3-GFP) that existed within our lab already. A2780CP and Igrov1 were selected for analysis due to their high levels of adenovirus infectability, which were previously determined by other members of Prof. McNeish's research group. Cells were seeded in 8 well chamber slides (Fisher Scientific) at a density of 10^4 cells/well in 400μl 10% FCS-DMEM. The following day cells were co-infected with 1pfu/cell of Lister-dTK and 30 pfu/cell Ad-LC3-GFP in 200μl serum free medium/well for 2 hrs, after which a further 200μl of 4% FCS-DMEM was added/well. Cells were fixed in 200μl 4% paraformaldehyde for 30mins at room temperature 72hrs post-infection and then washed in PBS. Slides were mounted using ProLong Gold antifade reagent with DAPI (Invitrogen) and allowed to set for 30mins at room temperature before storage at 4°C, protected from the light. Cells were viewed using a confocal laser scanning microscope (LSM 510 META, Carl Zeiss, Inc., Germany) with a 63x/1.4 NA Plan-Apochromat oil immersion objective. A Diode 405nm laser, 488nm Argon laser and Helium Neon 543nm laser were used to excite DAPI, GFP and RFP respectively. This allowed merged images to be constructed showing nucleus (DAPI), LC3B (GFP) and vaccinia (RFP) staining. High quality (12 bit, 1024 pixels) images were captured using LSM 5 Software, version 3.2.

2.10.3 Electron microscopy

A2780 cells were seeded onto glass cover slips in a 24 well plate at a density of 3x 10^4 cells/well in 1ml of 10% FBS-DMEM. The following day triplicate cells were infected with a three fold dilution series of Lister-dTK ranging from 10 pfu/cell to 0.1 pfu/cell in 500μl serum free media for 2hrs, after which 500μl of 4% FBS-DMEM was added/well. Three days post-infection cells were washed in PBS and fixed in 1ml 3% glutaraldehyde in PBS per well for 30mins at room temperature. Cells were then washed in PBS and stored in PBS at 4°C. Uninfected cells were also fixed as a control.

Further processing was carried out by Graham McPhail, Nanovision Centre, Queen Mary University of London. After initial fixation in phosphate buffered 4% glutaraldehyde, the cells (on coverslips) were washed in phosphate buffer for a minimum of 2h, then post-fixed for 1h in 1% aqueous osmium tetroxide. After 2 washes in distilled water, they were dehydrated through a graded ethanol series, cleared in propylene oxide and infiltrated with Araldite epoxy resin (Table 4).

The cells were embedded by inverting a "Beem" capsule filled with resin on top of the coverslips and curing for 48h at 60°C. The capsule with attached coverslip was plunged into liquid nitrogen and the capsule "popped-off" leaving the cells embedded in the capsule. Ultrathin sections (60-90nm) were cut and stained with uranyl acetate and lead citrate and examined in a JEOL JEM1230 transmission electron microscope with images being collected on an Olympus "Morada" digital camera.

VIAL NUMBER	REAGENT	TIME	TEMPERATURE
1	BUFFER	1h	4°C
2	OSMIUM TETROXIDE	1h	4°C
3	DE-IONISED WATER	5min	RT
4	DE-IONISED WATER	5min	RT
5	DE-IONISED WATER	5min	RT
6	50% IMS	15min	RT
7	70% IMS	15min	RT
8	90% IMS	15min	RT
9	100% IMS	15min	RT
10	100% IMS	20min	RT
11	100% IMS	20min	RT
12	100% IMS	30min	RT
13	PROPYLENE OXIDE	5min	RT
14	PROPYLENE OXIDE (PO)	5min	RT
15	PROPYLENE OXIDE	5min	RT
16	1:1 PO:ARALDITE	1h	RT
17	1:2 PO:ARALDITE	1h	RT
18	ARALDITE	1h	RT
19	ARALDITE	1h	RT
20	ARALDITE	1h	RT
21	ARALDITE	1h	RT

Table 4: Preparation of cells for electron microscopy. Samples were dehydrated, cleared in propylene oxide and infiltrated with araldite in a series of steps. RT=room temperature.

2.11 Flow Cytometry

2.11.1 Cell cycle analysis

Cells were seeded at a density of $2x10^5$ cells/well of a 6 well plate and infected the next day with 1 pfu or 0.1 pfu/cell virus in serum free medium for 2hrs followed by incubation in 2% FBS-DMEM. Where cisplatin was used this was added in 2% FBS-DMEM 24hrs after seeding. Uninfected cells were used as a control and all conditions were tested in duplicate. Samples were harvested 24hrs, 48hrs and 72hrs post-infection or addition of drug by collecting both supernatant and cells by trypsinisation. Cells were pelleted by centrifugation and resuspended in 1ml ice-cold 70% ethanol whilst vortexing before fixing for a minimum of 24hrs at 4°C. The DNA content of cells was analysed by washing cells with PBS and then incubating with 20μg RNase A (Invitrogen) and 100μg propidium iodide (PI) (Sigma) in a total volume of 300μl of PBS for 30 minutes at 37°C in the dark.

Ten thousand events were acquired by flow cytometry on a FACScalibur cytometer (Becton Dickinson Immunocytometry Systems, Belgium) with CellQuest Pro Software version 4.0.2. A primary gate on forward scatter (FSC) versus side scatter (SSC) was set to exclude cell debris, and a second gate to exclude doublets on a dot plot of pulse width (FL2-W) versus pulse area (FL2-A). PI fluorescence (FL3-H) was then plotted against cell counts on a linear scale to distinguish between the different phases of the cell cycle. Cell populations were quantified by setting the G1 marker around the first peak at 2N DNA, and the G2/M marker at the second peak at 4N DNA content. The S phase marker encompassed all cells between these two peaks and the sub-G1 marker counted cells with <2N DNA. A fifth marker was also set to quantify cells with >4N DNA.

2.11.2 Surface expression levels of epidermal growth factor receptor

An extracellular antibody against EGFR (R&D systems) was used to detect surface expression levels. As this antibody was raised against the human EGFR, its ability to recognise murine EGFR was first confirmed in MOSEC, MOVCAR7 and TrampC1 cells, using the human breast carcinoma line MDA-MB-468 as a positive control.

Levels of EGFR were examined in uninfected cells and cells infected with Lister-dTK or Lister-mDCN. $2x10^5$ cell were seeded per well of a 6 well plate and infected 24hrs later with 1 pfu/cell or 0.1pfu/cell of virus. Cells were collected 72hrs post-infection and prepared at

$4x10^6$ cells/ml in 50µl DMEM in a FACS tube. 50µl of anti-EGFR at 5µg/ml was added per tube for 30mins on ice and cells washed three times with 1ml wash buffer (DMEM containing 0.1% BSA and 0.1% sodium azide)). 50µl anti-goat Alex-488 conjugated secondary antibody was then added at 2µg/ml for 30 mins on ice. Cells were washed a further three times with DMEM 0.1/0.1 before resuspension in 330µl washing buffer for analysis by flow cytometry. Cells that had not been incubated with antibodies were used as a negative control. To control for background fluorescence, cells were incubated with secondary antibody only or with normal goat IgG (R&D Systems) at 5µg/ml instead of the primary antibody.

Flow cytometry was performed on a FACScalibur using the software described in section 2.11.1. Ten thousand events within a gated population on forward scatter (FSC) versus side scatter (SSC) were collected. The percentage of EGFR positive cells within this gated population was quantified on a histogram of green fluorescence (FL1) against cell count, using a marker that encompassed less than 1% control, uninfected cells. As the distribution of positive cells was not symmetrical around the mean, the geometric mean was instead calculated using CellQuest Pro Software and used as a measure of EGFR positivity.

2.11.3 Annexin V detection of phosphatidylserine externalisation

A2780, A2780CP, Igrov1 and Skov3ip1 cells were either mock-infected or infected with 1 pfu/cell of Lister-dTK or Lister-mDCN and harvested 72hrs post-infection. Cells were pelleted by centrifugation and washed in 3ml PBS at 1500rpm for 5mins. The cell pellet was then resuspended in 100µl of annexin V binding buffer (10mM Hepes, 140mM NaCl and 2.5mM $CaCl_2$, ph 7.4 using NaOH), as the binding of annexin V to phosphatidyleserine (PS) is dependent on the presence of calcium. 2.5µl Annexin V FITC-conjugate (Invitrogen) was added for 20mins at room temperature, followed by the addition of 2µM final concentration DAPI (Invitrogen) immediately before analysis by flow cytometry. As PS externalisation precedes the loss of cell membrane integrity (which accompanies the latest stages of cell death resulting from either apoptotic or necrotic processes) the cell impermeable dye DAPI was used to distinguish between viable cells and dead or damaged cells.

Flow cytometry was performed on a Fortessa cytometer using FACS Diva software and cells were initially gated based on forward scatter (FSC) versus side scatter (SSC). Ten thousand events from this population were then collected and apoptotic cells quantified using a quadrant gating system. To enable accurate gating of cell populations the following controls were used on untreated cells; unstained cells, cells stained with annexin V only and cells stained with DAPI only. Viable, non-apoptotic cells were negative for both annexin V staining and DAPI staining. Apoptotic cells were defined as those positive for annexin V and negative for DAPI staining, thus having an intact cell membrane that is impermeable to DAPI. Cells positive for both annexin V and DAPI were not presumed to be apoptotic, as annexin V positivity combined with the loss of cell membrane integrity does not distinguish between late apoptotic cells, and cells that have died from other means such as necrosis.

2.12 In vivo experiments

All *in vivo* experiments were performed within the Biological Services Unit (BSU) at Queen Mary University of London under UK Home Office personal and project license authority.

2.12.1 Intratumoural spread of Lister VV strains

CD1 nude/nude mice were injected subcutaneously with 10^5 TrampC1 prostate cancer cells in 200μl of PBS into the left flank. Mice were separated into two groups of 6 mice to receive a single intratumoural dose of 10^6 pfu of either Lister-mDCN or Lister-dTK-RFP. At days 2, 4 and 6 post-injection 2 mice from each group were killed and tumours excised. Tumours were fixed in formalin (Sigma) for 24 hours before transfer to 70% ethanol. Sections were then cut and stained for vaccinia viral proteins by immunohistochemistry by the Pathology Department (Barts Cancer Institute).

2.12.2 Intratumoural virus replication

CD1 nude/nude mice were injected subcutaneously with $5x10^4$ TrampC1 cells in 200μl of PBS into the left flank. When tumours reached 100-200mm^3 in volume, mice were randomly allocated to receive a single intratumoural dose of 10^8 pfu of either Lister-mDCN (n=6) or Lister-dTK-RFP (n=6) in 30μl PBS. Two mice received PBS only as a negative control. At days 4 and 8 post-injection of virus mice were imaged using the IVIS imaging system, and, at each timepoint, one control mouse and 3 each of Lister-mDCN or Lister-dTK-RFP treated mice killed. Tumours were harvested and snap-frozen in liquid nitrogen for analysis of virus replication by qPCR.

2.12.3 Intratumoural efficacy of Lister VV strains

CD1 nude/nude mice were injected subcutaneously with $5x10^4$ TrampC1 cells in 200μl of PBS into the left flank. Tumours were measured regularly until they reached $100\text{-}200mm^3$ in volume. Mice were then randomly allocated into three cohorts of eight mice each to receive a total of three intratumoural doses of PBS, Lister-mDCN or Lister-dTK-RFP (10^8 pfu), delivered every 2 days in 30μl volume PBS/dose. Mice were monitored for signs of ill health and tumours measured every 2-3 days. On days 8 and 17 following the first dose, surviving mice were anaesthetised (2% isofluorane in O_2 by inhalation) and imaged using a Xenogen In Vivo Imaging System (IVIS) (Xenogen, Alameda, CA) to monitor red fluorescence expressed from both virus strains. Under UK Home Office regulations, mice were killed accordingly when tumours reached the maximum allowed size of $1.4cm^3$, or when there were signs of ulceration.

2.12.4 Intraperitoneal spread of Lister-dTK

CD1 nude/nude mice were injected with $5x10^6$ Skov3ip1 ovarian carcinoma cells intraperitoneally (ip). Mice were monitored daily for signs of health and injected with a single dose of 10^8 pfu of Lister-dTK ip in 400μl PBS or vehicle alone after three months when tumours were estimated to be at an advanced state. Mice were killed 72hrs post-injection and tumour, liver and spleen harvested. Tissue was fixed in formaldehyde after which it was processed, embedded in paraffin, sectioned and stained for vaccinia virus proteins by the Pathology Service, Barts Cancer Institute.

2.12.5 Intraperitoneal efficacy of Lister VV strains

C57BL/6 mice were injected intraperitoneally (ip) with $5x10^6$ MOSEC cells expressing luciferase (MOSEC-luc) in 200μl PBS. Mice were injected with 200μl of sterile 15mg/ml D-luciferin (Xenogen) in PBS on day 18 and imaged using the IVIS system as described in section 2.12.3. Luminescence data from defined regions of interest were analysed with Living Image Software (Xenogen) and are presented as average radiance ($p/s/cm^2/sr$). Mice were randomly allocated, by cage, to receive PBS (n=12), Lister-dTK (n=14) or Lister-mDCN (n=14). Mice were injected intraperitoneally on days 22, 25 and 28 with 10^8 pfu/dose of Lister-dTK or Lister-mDCN in 400μl PBS. A separate cohort was injected with vehicle (PBS) alone. Tumour burden was further monitored by luminescence imaging as described above on days 24, 35, 43 and 63. Mice were assessed regularly for signs of health and none were culled based on Home Office morbidity limits such as approaching 20% body weight loss, presence of significant ascites or poor well being.

Following the transient response observed in the first experiment a second experiment was repeated in C57BL/6 mice with $5x10^6$ MOSEC-luc injected intraperitoneally. Again, mice were randomly allocated to receive PBS (n=10), Lister-dTK (n=15) or Lister-mDCN (n=15). Mice were injected with 200μl of sterile 15mg/ml D-luciferin (Xenogen) in PBS on the morning of day 10 and imaged using the IVIS system as described in section 2.12.3. Luminescence data from defined regions of interest were analysed with Living Image Software (Xenogen) and are presented as average radiance ($p/s/cm^2/sr$). Mice were then injected 7hrs later with the first dose of either PBS or virus, to allow time for recovery after general anaethesia. Mice were injected intraperitoneally on days 10-14 inclusive with 10^8 pfu/dose Lister-dTK or Lister-mDCN in 400μl PBS, or PBS alone. Tumour burden was assessed by luminescence imaging as in the first experiment, and mice were anaesthetised and imaged on days 10, 17, 24, 28, 38, 46, 52 and 59 and 68, when the experiment was terminated.

2.13 Immunohistochemistry

2.13.1 Tissue Preservation and Processing

Harvested organotypics, organs and tissue were prepared for paraffin processing by fixing overnight in formol-saline containing 4% formaldehyde (Fisher Scientific) before transfer to 70% ethanol. Tissue was dehydrated in preparation for paraffin embedding as follows; immersion in 70% ethanol for 1 hour, transfer to 96% ethanol for 1 hr, 96% ethanol for 1 hr, transfer to 96% ethanol overnight followed by immersion in 100% ethanol for 1 hr, 100% ethanol for 1.5hrs, 100% ethanol for 1.5hrs and finally tissue transferred to xylene for 1.5hrs after which it was immersed in paraffin (60°C) for a minimum of 12 hrs. Paraffin-embedded tissue sectioning and Haematoxlin and Eosin (H&E) staining were carried out by Keyur Trivedi and Dr Mohammed Ikram (Pathology Service, Barts Cancer Institute).

2.13.2 Immunostaining on paraffin sections: vaccinia virus

Tumour tissue, murine liver and spleen sections were stained for vaccinia virus proteins using polyclonal rabbit anti-vaccinia antibody (AbD Serotec, Oxford UK) and for decorin using a goat anti-decorin antibody (R&D Systems AF1060, Abingdon UK). Automated immunostaining was performed by the Pathology service, Barts Cancer Institute. Although not shown within this thesis, antibody concentration was optimised and non-specific IgG and background staining controlled for using the appropriate species IgG and secondary-only controls respectively.

2.13.3 Immunostaining on paraffin sections: HMGB1

Staining for HMGB1 was performed on Skov3ip1 tumours that were treated with either PBS or Lister-dTK (see section 2.12.5). Sections were de-waxed and rehydrated by immersion in xylene for 5 minutes, xylene for a further 5 mins, 100% ethanol for 2 mins, 100% ethanol for 2 mins, 80% ethanol for 2mins, 70% ethanol for 2 mins, 50% ethanol for 2 mins and then a final wash in distilled H_2O. To block endogenous peroxidase activity, sections were incubated for 15mins at room temperature in methanol containing 0.45% (v/v) hydrogen peroxide, followed by washing in PBS. Antigen was retrieved by means of heat retrieval using 10mM sodium citrate buffer pH6. Slides were microwaved in buffer for 20 minutes and then cooled to room temperature before washing twice in PBS for 2 mins each time.

As the secondary antibody used for detection of HMGB1 was biotinylated, endogenous biotin was blocked with avidin using the Avidin/Biotin blocking kit (Vector Laboratories, SP-2001), which has a high affinity for biotin, for 10 minutes at room temperature in a humid environment. Sections were then washed in PBS twice before incubation with biotin for a further 10 minutes, followed by washing twice in PBS. As the primary HMGB1 antibody was raised in a rabbit, sections were blocked in 1:1000 dilution of rabbit normal serum for 30 minutes at room temperature. After washing twice in PBS for 2 minutes each time, 1:1000 HMGB1 antibody (Abcam) in 0.1% BSA was added overnight at 4°C. The following day, after washing in PBS, a 1:200 dilution of anti-rabbit biotinylated secondary was added to slides for 30 minutes at room temperature. Sections were washed twice in PBS as before. Using the Elite ABC kit (Vector Laboratories, PK-6102), the avidin-HRP conjugate was added, and sections incubated for 30mins at room temperature. Slides were washed twice in PBS, after which chromogenic DAB substrate (Diamino Benzidine Tetrahydrochloride) was added for a maximum of 5 minutes. Slides were rinsed in running tap water for 1 minute before counterstaining for nuclei using Mayers haematoxlin (Sigma) for 1 minute. Slides were rinsed under running water and then immersed in PBS for 1 minute. Stained sections were dehydrated by performing the initial steps in reverse; immersion in distilled H_20) for 2 mins, 50% ethanol for 2 mins, 70% ethanol for 2 mins, 80% ethanol for 2 mins, 100% ethanol for 2 mins, 100% ethanol for 2 mins, immersion in xylene for 2 mins, and then immersion in xylene for a further 5 mins. Sections were allowed to dry after which coverslips were mounted using DPX mountant for microscopy (VWR International Ltd 360294H).

Chapter 3

Potential of vaccinia virus for use against ovarian cancer

3. Potential of vaccinia virus for use against ovarian cancer

As discussed previously, vaccinia virus has many features that make it suitable for use as an oncolytic agent. Deletion of the thymidine kinase gene is a common modification that confers tumour specificity, and as such was deleted from the Lister strain to create Lister-dTK. The potential of Lister-dTK for treatment of ovarian cancer was determined in a series of preliminary experiments, designed to assess the replication and cytotoxicity of Lister-dTK across a panel of human cell lines. Additionally, as murine cells have previously been shown to support vaccinia replication (Hung, Tsai et al. 2006), the same experiments were performed in two murine ovarian cell lines to determine suitability for subsequent *in vivo* studies. Following demonstration of viral protein expression *in vitro*, a small 'proof-of-principle' *in vivo* study was also performed to demonstrate infection and replication of Lister-dTK in advanced tumours. This also served to confirm tumour selectivity of Lister-dTK. Furthermore, as cisplatin is currently the first line treatment for ovarian cancer, combination studies were performed to determine if Lister-dTK could act synergistically with cisplatin to enhance ovarian cancer cell death.

3.1 Construction of Lister-dTK

A recombinant vaccinia virus derived from the European vaccine Lister strain was constructed that had a deletion of the thymidine kinase (TK) gene to confer tumour selectivity. Red fluorescent protein (RFP) was expressed from the TK site by homologous recombination to allow positive selection of recombinant virus during virus production, and as a tool for future imaging of virus both *in vitro* and *in vivo*. The natural vaccinia virus promoter, I1L, was used to control RFP expression, as it has previously demonstrated exceptionally high activity compared to other natural vaccinia promoters (Liu, Kremer et al. 2004). Expression of β-galactoside under control of the I1L promoter revealed an increase in protein expression until 24hrs post-infection when it reached a plateau, classing it as an intermediate promoter that exhibits activity over ten times stronger than that of other intermediate promoters (Liu, Kremer et al. 2004).

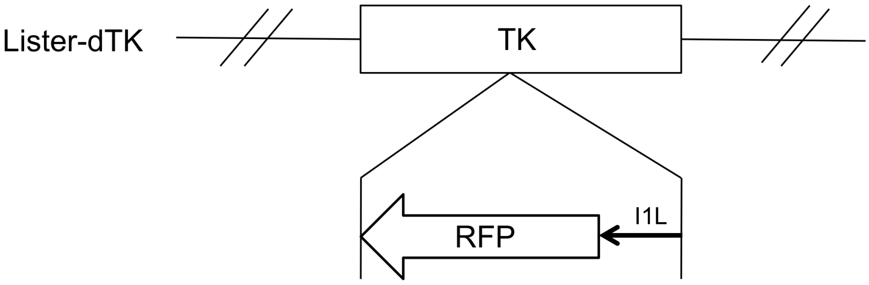

Figure 12: Schematic representation of the genomic structure of the recombinant vaccinia virus Lister-dTK. The thymidine kinase gene was deleted by homologous recombination with a plasmid containing the expression cassette. I1L is a natural vaccinia promoter and controls expression of RFP from the TK locus.

3.2 Lister-dTK is cytotoxic to ovarian cancer cells in vitro

To evaluate the use of a modified vaccinia virus as a potential therapeutic agent for the treatment for ovarian cancer, the ability of Lister-dTK to kill ovarian cancer cell lines *in vitro* was compared to that of the wild-type virus. Previous published literature has focused mainly on the use of modified vaccinia viruses in *in vivo* studies of mice bearing murine ovarian tumours (Hung, Tsai et al. 2006; Chalikonda, Kivlen et al. 2008; Chang, Ma et al. 2009; Zhang, Tsai et al. 2010) and as yet, there appears to be no in depth study of the difference in cytotoxicity between human cell lines.

A panel of human ovarian cancer cells was infected with increasing doses of virus, and cell survival measured by MTS assay 72hrs post-infection (Figure 13). The deletion of thymidine kinase to confer tumour specificity could also attenuate cytotoxicity in tumour cells as well as normal cells, as has been demonstrated with a triple-deleted vaccinia virus (Yang, Guo et al. 2007). However, Lister-dTK was able to kill ovarian cancer cells with comparable, or better, efficacy than the wild-type virus in A2780, their cisplatin resistant counterparts A2780CP, Igrov1, Skov3ip1 and OVCAR4 cells (Figure 13), although the difference in EC50 between the two viruses was not significant in any of the cell lines tested. The sensitivity of ovarian cancer cell lines to Lister-dTK was fairly similar, with the most sensitive Skov3ip1 cells having an EC50 of 1pfu/cell and the least sensitive A2780CP cells just under 7pfu/cell.

One of the limitations of other oncolytic viruses, such as adenoviruses, is their inability to replicate and kill murine cells thus restricting their use in pre-clinical studies. In contrast, vaccinia virus is able to kill both MOSEC and MOVCAR7 cells with great efficiency (Figure 14). The EC50 of Lister-dTK was 0.3pfu/cell and 0.1 pfu/cell in MOSEC and MOVCAR-7 cells respectively, meaning that MOSEC cells are between 3-20 times more sensitive to vaccinia virus than the human cell lines, and MOVCAR7 cells 10-70 times more sensitive.

The wild-type virus also demonstrated enhanced efficacy in murine cells compared to human cell lines although, similar to in human cell lines, it was less efficient than the Lister-dTK strain, albeit not significantly so.

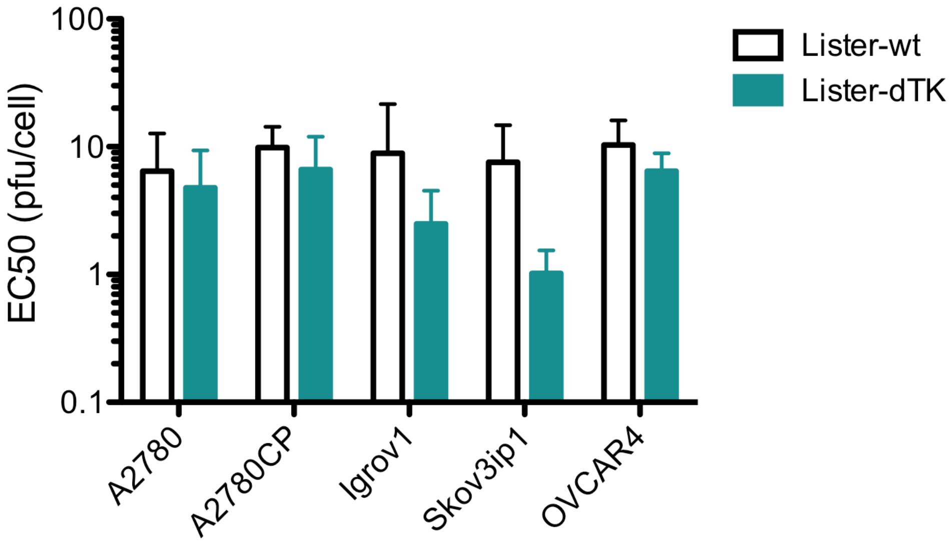

Figure 13: Cytotoxicity of Lister-dTK in human ovarian cancer cell lines. Cells were infected with a serial dilution of virus and cell survival analysed by MTS assay 72hrs post-infection. Cell survival was normalised to that of uninfected cells and the EC50 calculated from dose response curves constructed using Prism software. Data shows the mean EC50 + SD from a minimum of 3 experiments, each performed in triplicate. Differences in the EC50 of Lister-wt and Lister-dTK in each cell line are not significant unless marked.

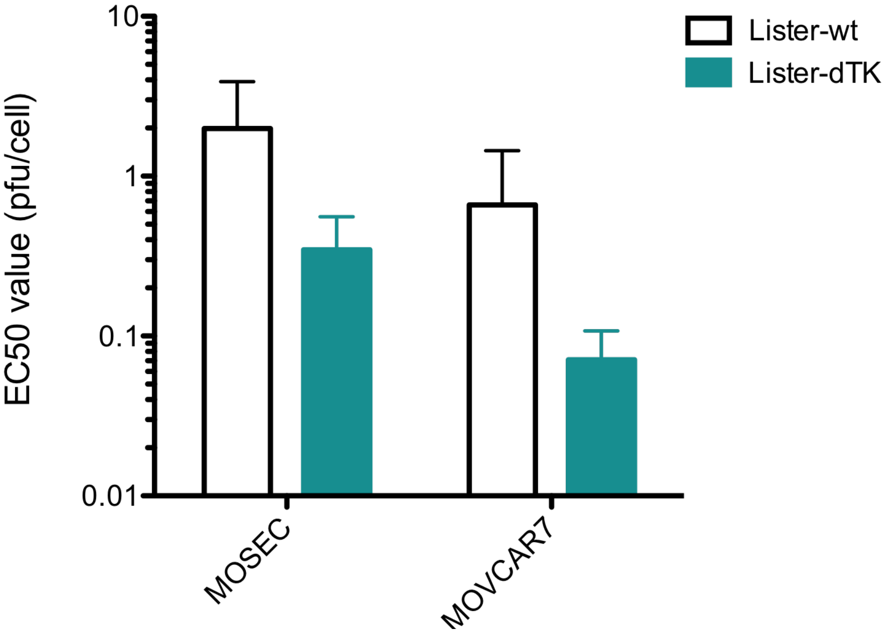

Figure 14: Cytotoxicity of Lister-dTK in murine ovarian cancer cell lines. Cells were infected with a serial dilution of virus and cell survival analysed by MTS assay 72hrs post-infection. Cell survival was normalised to that of uninfected cells and the EC50 calculated from dose response curves constructed using Prism software. Data shows the mean EC50 + SD from 5-6 experiments in triplicate, differences between the EC50 of the wt and dTK virus in each cell line are not significant unless shown.

3.3 *Replication of Lister-dTK*

Having determined that Lister-dTK was able to kill cells at least as effectively as the wild-type virus, the replication kinetics of both viruses were next studied in the same cell lines. Replication over a 72hr time period was analysed by TCID50 in human and murine ovarian cancer cell lines following initial infection with either 0.1 pfu/cell (murine cells) or 1 pfu/cell (human cell lines). Consistent with the similar sensitivity of A2780, A2780CP, Igrov1 and Skov3ip1 cells to Lister-wt (Figure 13), replication was also fairly similar over the course of infection, although the titre of Lister-wt continued to increase steadily in A2780, A2780CP and Igrov1 but peaked at 48hrs in Skov3ip1 cells (Figure 15). Despite a comparable titre at 72hrs post-infection for both Lister-wt and Lister-dTK (between 1000-10,000 pfu/cell depending on the cell line), replication kinetics appear faster in the Lister-dTK virus, perhaps reflecting the increase in cytotoxicity observed in Figure 13. The titre of replicating Lister-dTK peaked at 48hrs in A2780, A278CP and Igrov1 cells, and at 24hrs in Skov3ip1, which again correlates to the increased sensitivity of Skov3ip1cells to Lister-dTK compared to other human cell lines.

In contrast, Lister-wt and Lister-dTK demonstrated very similar profiles of replication in murine cell lines (Figure 17and C), and almost identical titres at 48hrs post-infection (Figure 17C and D). The titre of both viruses peaked at 48hrs in MOSEC and MOVCAR7 cells, after which they reached a plateau, perhaps indicating restriction of further replication due to cell death. Interestingly, although MOVCAR7 cells are more sensitive to both Lister-wt and Lister-dTK, the titre of each virus was at least a log lower at 48hrs and 72hrs post-infection in this cell line compared to MOSEC cells.

Expression of vaccinia virus proteins from infected cells was confirmed in human cell lines at 72hrs post-infection (Figure 16). Levels of protein were highest in Skov3ip1 cells, which corresponds to the lower EC50 and more rapid replication in this cell line. Vaccinia virus proteins were also detected in murine cell lines, and as early as 24hrs and 48hrs post-infection in both human and murine cells, throughout this work.

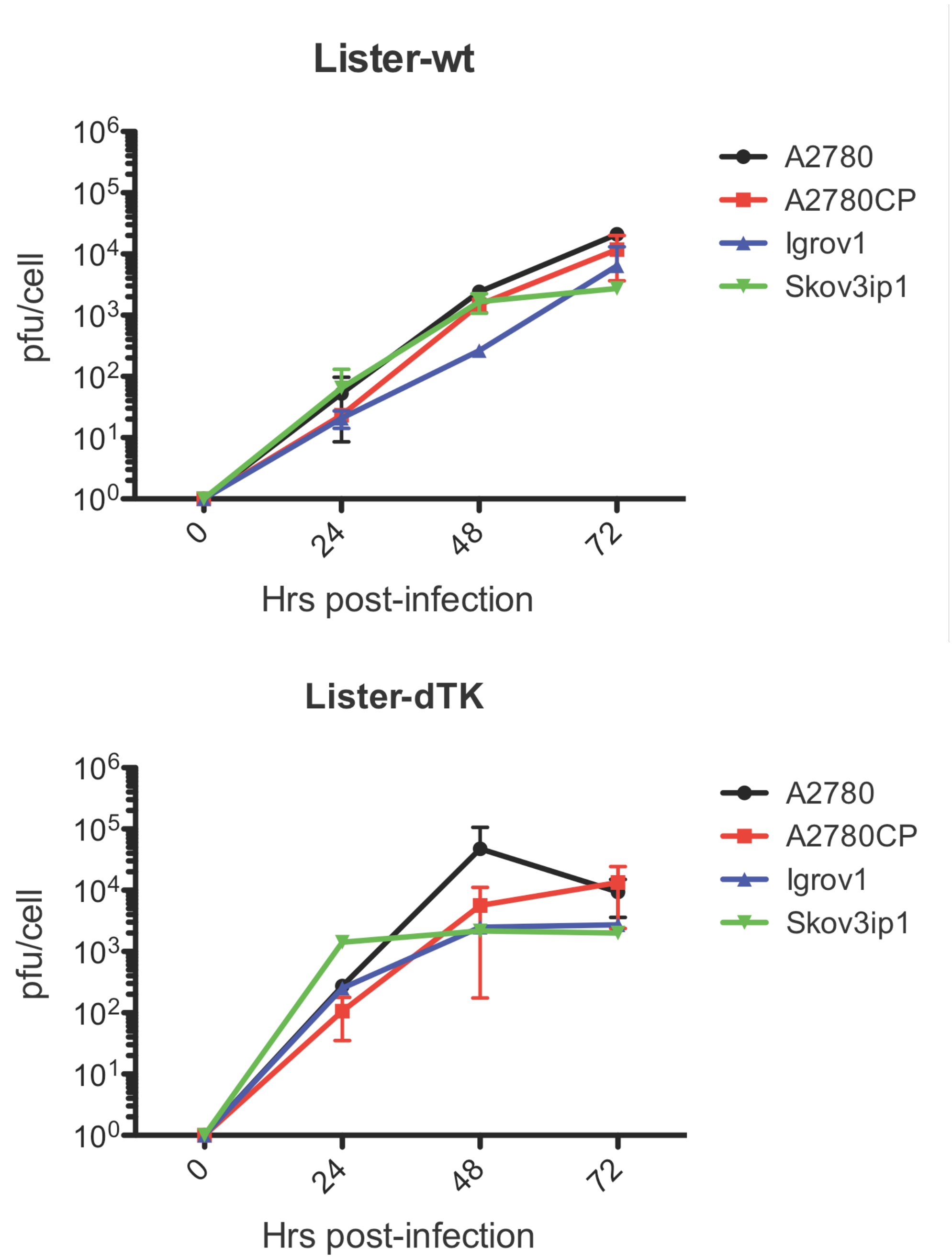

Figure 15: Replication of vaccinia virus in human ovarian cancer cell lines. Cells were infected with 1pfu/cell and harvested at 24, 48 and 72hrs post-infection. The titre of virus was determined by a limiting dilution assay in CV1 cells. Data shows the mean + SD of two experiments performed in triplicate.

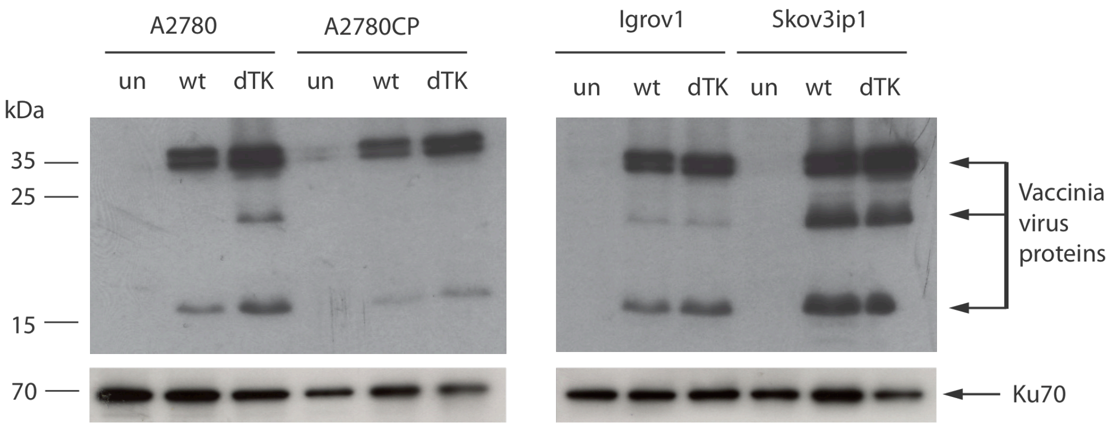

Figure 16: Expression of vaccinia virus proteins in infected human ovarian cancer cell lines. Cells were infected with 1 pfu/cell of Lister-wt or Lister-dTK and vaccinia virus proteins detected 72hrs later in cell lysates.

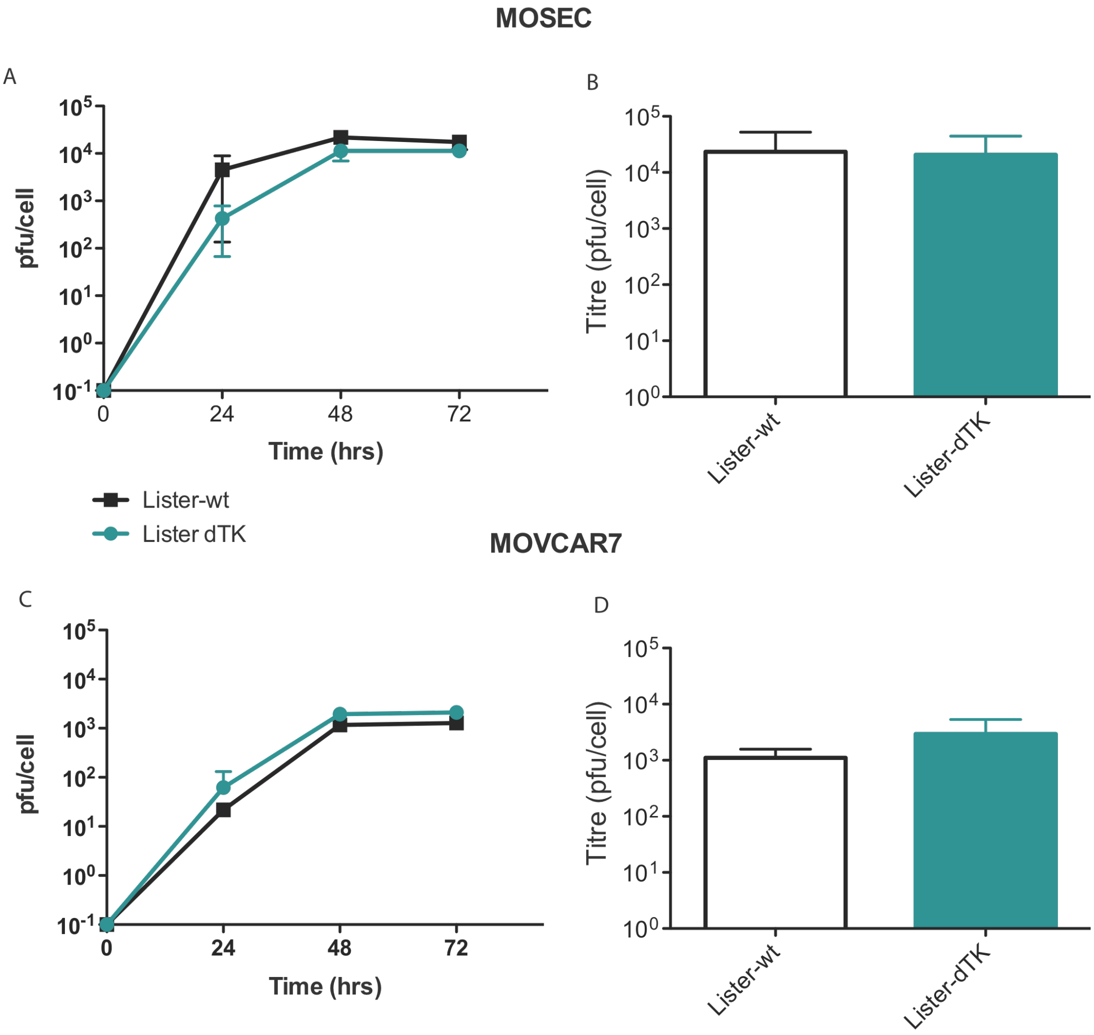

Figure 17: Replication of vaccinia virus in murine ovarian cancer cell lines. MOSEC (A) and MOVCAR7 (C) cells were infected with 0.1pfu/cell and harvested at 24, 48 and 72hrs post-infection to determine the titre. Data shows the mean + SD of a single experiment performed in triplicate. (B and D) Virus titre at 48hrs post-infection. Data shows the mean + SD of three experiments.

3.4 Specificity of Lister-dTK

To confirm the tumour specificity of Lister-dTK, the cytotoxicity of this modified virus was compared to that of the wild-type virus in IOSE25 cells, hTERT-immortalised cells derived from parental non-malignant ovarian surface epithelium. Lister-dTK was attenuated in IOSE25 cells, with an EC50 ten-fold higher than that of Lister-wt (Figure 18). In contrast, human and murine ovarian cancer cell lines were more sensitive to the Lister-dTK virus, which demonstrated equal or enhanced cytotoxicity compared to the wildtype virus.

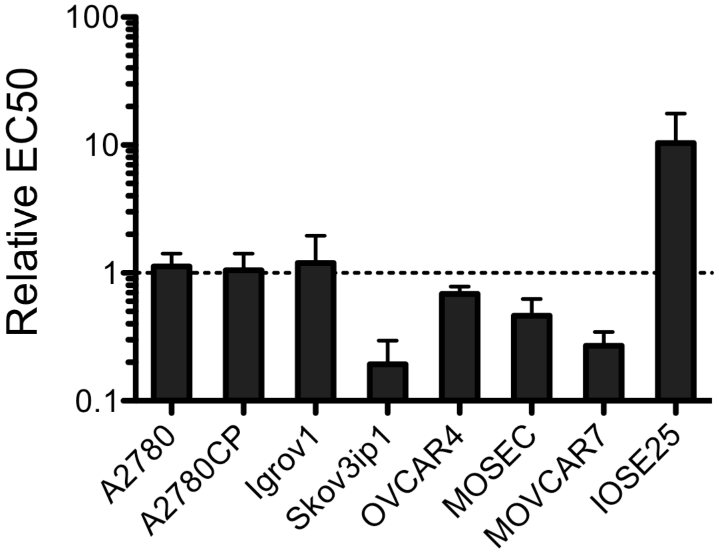

Figure 18: Relative EC50 of Lister-dTK compared to the EC50 of Lister-wt. The EC50 of Lister-dTK relative to the EC50 of Lister-wt was calculated from individual experiments, each performed in triplicate. Bars show the mean + SEM relative EC50 from a minimum of 2 experiments.

To further confirm specificity of Lister-dTK, a preliminary experiment *in vivo* was performed to determine selective replication of Lister-dTK in tumour tissue only. To reflect the clinical presentation and treatment of ovarian cancer, nude female mice bearing advanced intraperitoneal Skov3ip1 tumours were administered with a single dose of Lister-dTK intraperitoneally, as it has been suggested that intraperitoneal delivery of chemotherapeutics may enhance survival compared to intravenous delivery (Armstrong, Bundy et al. 2006). Tumour, liver and spleen were harvested 72hrs post-injection of virus and stained for the presence of vaccinia virus proteins.

Consistent with the clinical presentation of advanced ovarian cancer, whereby small nodules of tumour normally cover the peritoneum and surrounding organs such as the liver, pancreas and gut, mice showed signs of tumour dissemination through the peritoneal cavity upon termination of the experiment. These were often very small in size and covering the surface of organs (Figure 19E-F and Figure 20A-D); as such, it was difficult to obtain pure tumour tissue for analysis by immunohistochemistry. However, where obtained, tumour tissue was positive for vaccinia virus proteins just 72hrs after virus injection and virus infection appeared to start at the tumour periphery spreading inwards (Figure 19A and B). Closer inspection revealed cytoplasmic expression of virus proteins in infected cells (Figure 19D), consistent with the known life cycle of vaccinia. Necrotic tissue, as determined by H&E staining (areas of less intense staining, Figure 19A,) was absent for vaccinia proteins. As expected, mice infected with PBS did not express vaccinia virus proteins either in tumour tissue or in neighbouring normal organs such as the pancreas (Figure 19F).

Tumour burden and dissemination could only be analysed at the experiment endpoint, and thus mice were randomly assigned to receive either PBS or Lister-dTK regardless of the stage of disease. Tumour specific replication of Lister-dTK is demonstrated in Figure 20A-D, where a single dose of virus was administered to a mouse with tumour dissemination to the liver. Replication of Lister-dTK is evident in tissue tissue but there is a lack of virus proteins in adjacent normal liver tissue (Figure 20B and D). In contrast, mice receiving PBS did not show any signs of tumour burden on the liver upon termination of the experiment (Figure 20E). As expected, normal liver tissue in these mice was again absent for vaccinia virus proteins (Figure 20F). No virus proteins were detected in the spleen of either PBS or Lister-dTK treated animals (data not shown).

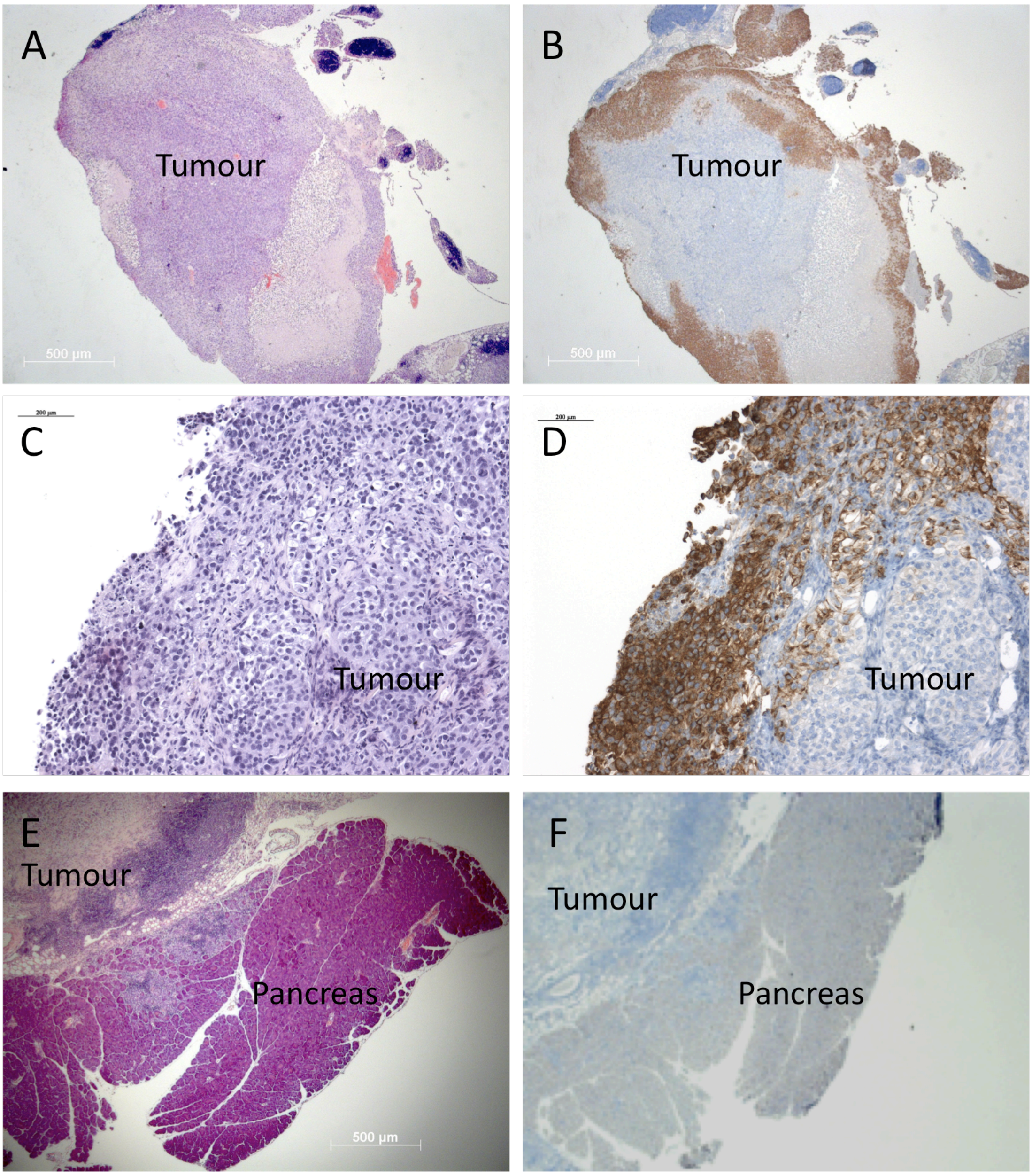

Figure 19: Infection and replication of Lister-dTK in ovarian cancer tumour tissue *in vivo*. Mice bearing advanced intraperitoneal Skov3ip1 tumours received either a single dose of 10^8 pfu Lister-dTK (A-D) or PBS (E-F) and organs harvested for immunohistochemistry 72hrs later. (A, C, E) H&E staining (B, D, F) Vaccinia virus staining.

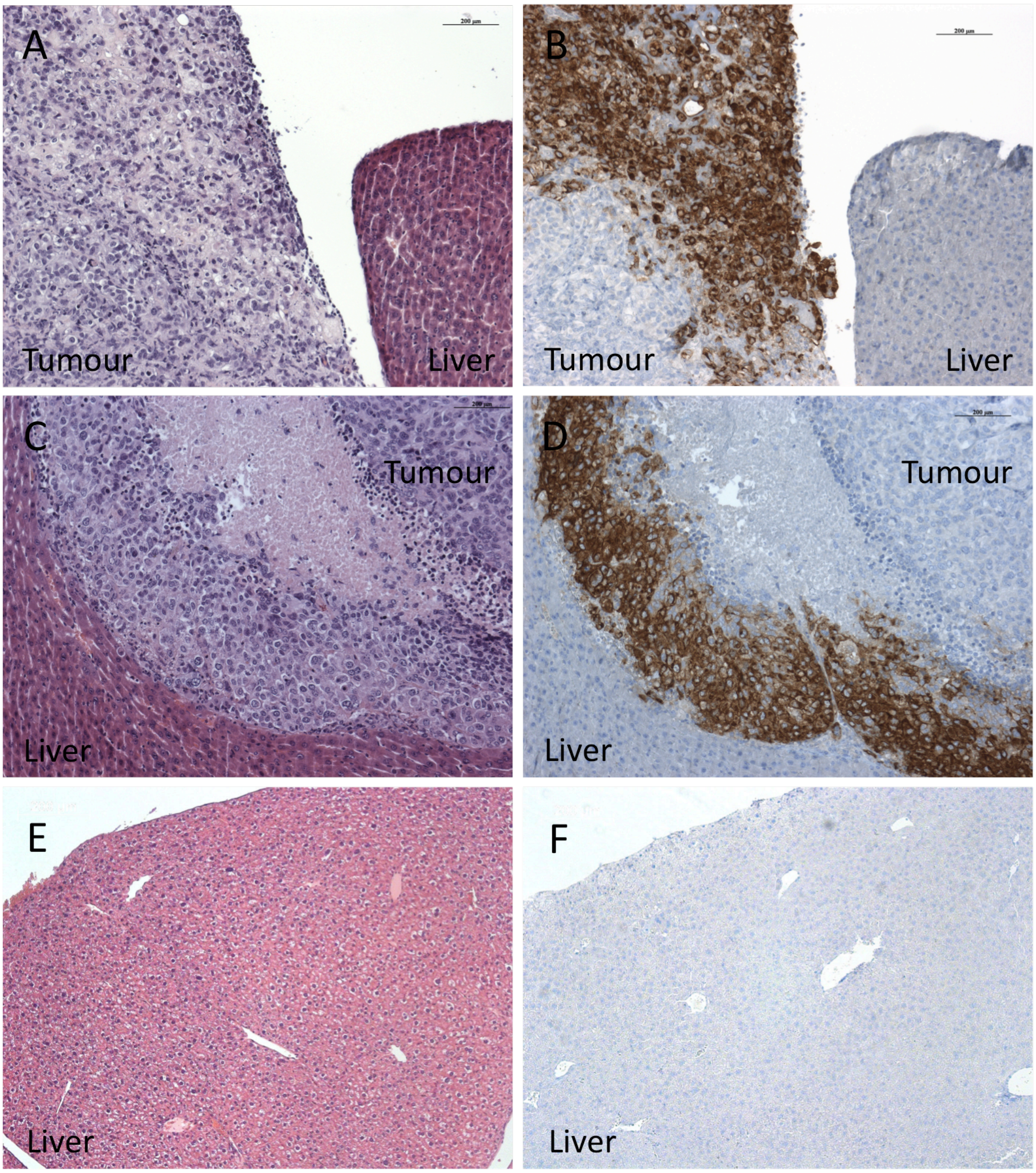

Figure 20: Selective replication of Lister-dTK in a liver metastase. Mice bearing advanced intraperitoneal Skov3ip1 tumours received either a single dose of 10^8 pfu Lister-dTK (A-D) or PBS (E-F) and organs harvested for immunohistochemistry 72hrs later. (A, C, E) H&E staining (B, D, F) Vaccinia virus staining.

3.5 Lister-dTK does not show synergy with cisplatin in ovarian cancer cell lines in vitro

Oncolytic adenovirus has previously shown synergy with paclitaxel in ovarian cancer (Ingemarsdotter, Baird et al. 2010) and recently, oncolytic vaccinia virus has also demonstrated synergy with paclitaxel in ovarian cancer, albeit in only one cell line (Huang, Sikorski et al. 2011). As cisplatin is currently the chemotherapy of choice for ovarian cancer, cell survival assays using Lister-dTK and cisplatin were performed to determine if combination therapy could enhance overall cell death.

The sensitivity of four cell lines to cisplatin alone was determined by MTS assay (Figure 21). A2780 cells were the most sensitive with an EC50 of 1.7μM; their cisplatin resistant counterparts, A2780CP, were over 20 times less sensitive with an EC50 of 37.5μM. Igrov1 and Skov3ip1 cells demonstrated intermediate levels of sensitivity to cisplatin, with EC50s of 8.1μM and 6.0μM respectively. Based on these EC50s, two concentrations of cisplatin were selected for use in combination assays. These were 1μM/0.3μM for A2780 cells, 10μM/3μM for A2780CP cells and 3μM/1μM for Igrov1 and Skov3ip1 cells.

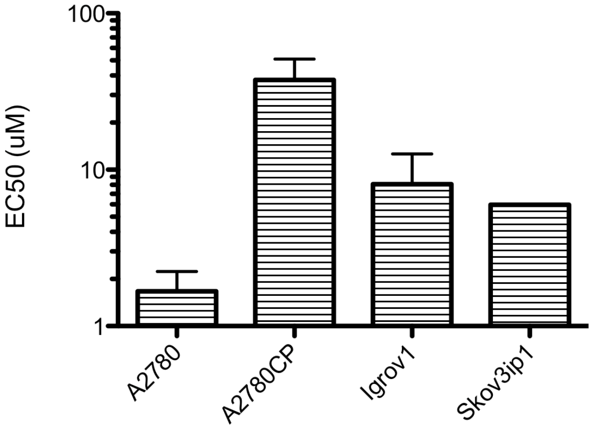

Figure 21: Sensitivity of ovarian cancer cell lines to cisplatin. Cells were infected with a serial dilution of cisplatin ranging from 100μM to 1pM and cell survival measured 72hrs later. Dose response curves were constructed to calculate the EC50. Data shows the mean + SD from 2-4 experiments, with the exception of Skov3ip1 cells in which the experiment was only performed once.

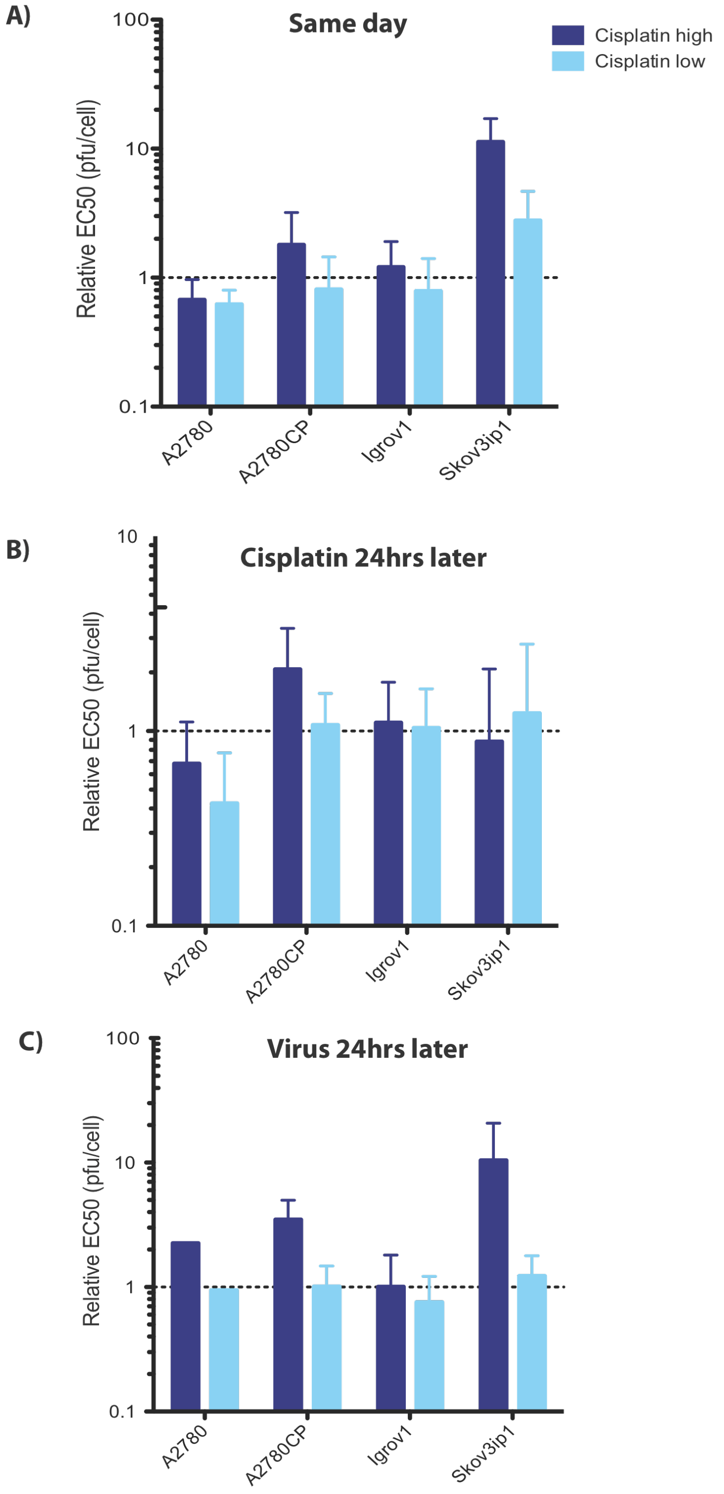

Figure 22: Combination studies with Lister-dTK and cisplatin. Cells were infected with a serial dilution of Lister-dTK followed by A) cisplatin 2 hrs post-infection or B) 24hrs post-infection. C) Cells were infected with Lister-dTK after 24hrs pre-treatment with cisplatin. Doses of cisplatin were 1μM (A2780), 10μM (A2780CP) and 3μM (Igrov1 and Skov3ip1) for high doses and 0.3μM (A2780), 3μM (A2780CP) and 1μM (Igrov1 and Skov3ip1) for low doses. Cell survival was measured 72hrs post-infection by MTS assay and normalised to the survival of either untreated cells or cisplatin only-treated cells. The EC50 of combination groups is expressed relative to the EC50 of Lister-dTK alone. Data represents the mean+SD of a minimum of 2 experiments, each performed in triplicate.

Combination of Lister-dTK with cisplatin did not enhance cell death once survival had been normalised to the effect of cisplatin alone (Figure 22); this was true irrespective of the dosing schedule. Cisplatin was added 2hrs post-infection to minimise interference of virus entry but did not alter the efficacy of Lister-dTK, either in a positive or negative manner, in A2780, A2780CP or Igrov1 cells (Figure 22A). In Skov3ip1 cells there was an attenuation of Lister-dTK, reflected by the increase in EC50, although this was not significant. Similarly, the addition of cisplatin 24hrs post-infection did not alter the EC50 of Lister-dTK in any of the cell lines tested (Figure 22B). As it was possible that cisplatin could lead to changes in the cell cycle that could enhance either virus infection or replication, cells were also pre-treated with cisplatin for 24hrs before infection with virus (Figure 22C). It has previously been reported that vaccinia infection results in a decrease in cells in G1 and an increase in cells in S phase or G2/M (Wali and Strayer 1999) and hypothesised that this may enhance replication. More recently, it has also been demonstrated that vaccinia preferentially infects cells in either S or G2/M phase (Huang, Sikorski et al. 2010) and that an increase in this population by treatment with paclitaxel doubled the percentage of infected cells after 2hr exposure to virus.

Overnight treatment with cisplatin led to a modest increase in cells in S phase of the cell cycle. The percentage of untreated cells in S phase varied between cell lines but was fairly constant at 16-19%. This rose to 19-24% following treatment with the higher dose of cisplatin (Figure 23). Similarly, the percentage of cells in G2 ranged from 16-23% in untreated cells and this number increased by approximately to 22%, 26% and 25% in A2780, Igrov1 and Skov3ip1 cells respectively. A2780CP cells, which had been treated with the highest concentration of cisplatin at 10μM, had a G2 population that increased from 22% in untreated cells to over 40% in cells treated with cisplatin. Interestingly, there was a higher increase following treatment with 3μM cisplatin (54%) compared to with 10μM (42%). Despite this increase in A2780CP cells in the G2 phase of the cell cycle, and perhaps therefore an increase in cells susceptible to initial infection, there was no corresponding decrease in EC50 of Lister-dTK when cells were pre-treated with cisplatin (Figure 22C). There was also no overall increase in efficacy of Lister-dTK following pre-treatment with cisplatin in A2780, Igrov1 and Skov3ip1 cells (Figure 22C).

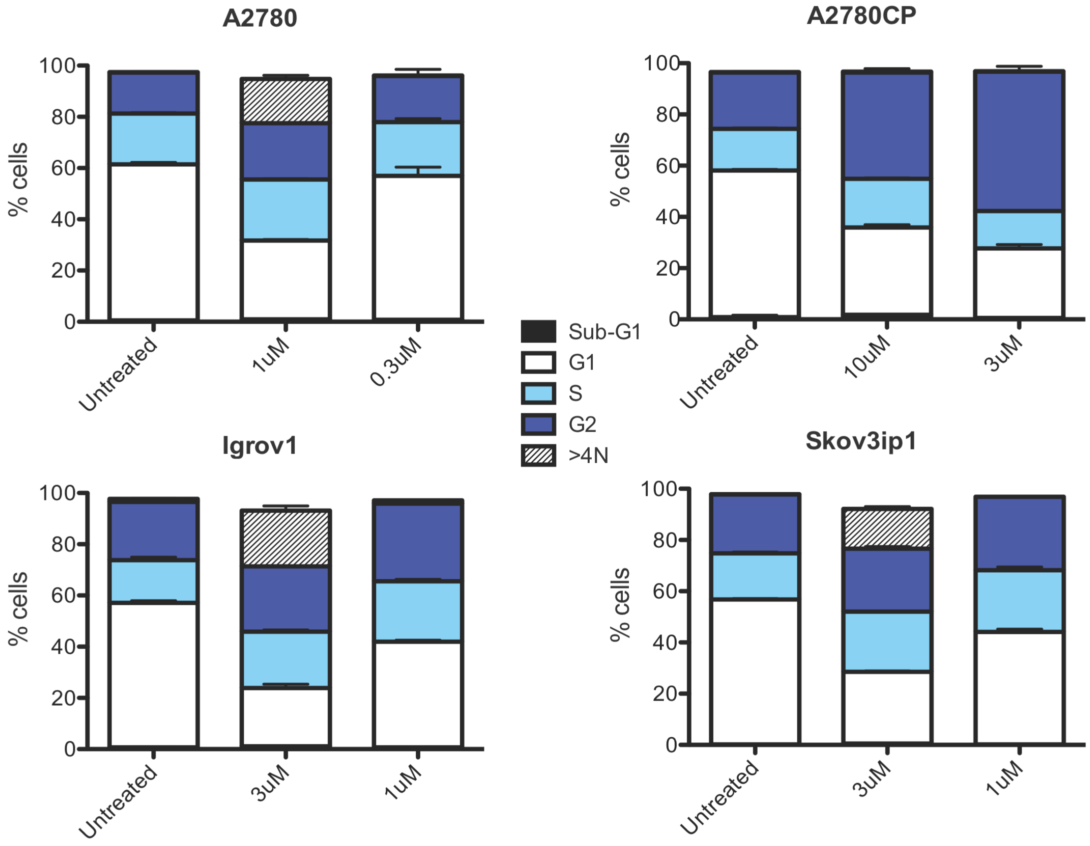

Figure 23: Effect of cisplatin on cell cycle. Cells were treated with cisplatin overnight and stained with propidium iodide to determine populations of cells within the cell cycle. Bars indicate the % of cells within each stage from one experiment performed in duplicate.

3.6 *Discussion*

Whilst vaccinia virus has been used successfully to treat several cancers in pre-clinical models including breast (Zhang, Yu et al. 2007), pancreatic (Yu, Galanis et al. 2009), prostate (Gentschev, Donat et al. 2010), mesothelioma (Kelly, Woo et al. 2008) and liver cancer (Kim, Oh et al. 2006), its use in ovarian cancer is less well studied. It has previously been demonstrated that a hyperattenuated recombinant virus derived from the Lister strain was able to infect human ovarian ES3 cells preferentially *in vivo*, although this was in nude mice and virus was delivered just one day after tumour cell injection (Hung, Tsai et al. 2006). Furthermore, virus clearance was rapid and only the wild type virus was used in immunocompetent mice, which has no application in clinical use. Another group demonstrated some therapeutic effect in an established intraperitoneal model of mouse ovarian cancer in immunocompetent mice, although this was not as effective as delivery of virus at a very early stage of disease (simultaneous injection with tumour cells) (Chalikonda, Kivlen et al. 2008).

As ovarian cancer is restricted to the peritoneal cavity it may be a good target for oncolytic vaccinia virus, which can be delivered locally to the intraperitoneal cavity. This route may be preferential over intravenous delivery as it allows higher local concentrations of virus, and there is evidence that the same applies for the delivery of chemotherapy, as intraperitoneal delivery improves survival compared to intravenous delivery (Markman, Bundy et al. 2001; Armstrong, Bundy et al. 2006). In order to determine the suitability of oncolytic vaccinia virus for ovarian cancer, it is necessary to study its effects in a variety of cell lines and under conditions that best reflect potential clinical application. In this respect, a tumour selective virus termed Lister-dTK was constructed that is deleted in the thymidine kinase gene and its efficiency in a panel of ovarian cancer cell lines tested. Additionally, as the majority of patients present with metastatic disease, we chose to determine specificity *in vivo* in mice bearing advanced intraperitoneal tumours. Furthermore, the current treatment for ovarian cancer after debulking surgery is a platinum-based drug, although resistance commonly develops and tumour regrowth is a frequent occurrence. Despite this, it is likely that initial use of oncolytic vaccinia would be with current approved therapies. To determine whether the addition of Lister-dTK might provide an advantage over cisplatin alone, a series of experiments were performed to investigate synergistic activity *in vitro*.

Comparison of a number of ovarian cancer cell lines revealed that all were sensitive to Lister-dTK *in vitro* and that there was little variation between cell lines. The EC50 value of Lister-dTK in individual human cell lines ranged from 1-7pfu/cell at 72hrs post-infection, in contrast to other oncolytic viruses such as adenovirus, which demonstrate over 100-fold differences in sensitivity (Flak, Connell et al. 2010). This implies that vaccinia virus may be of better use clinically and has the potential to infect and destroy a wide range of cells. In addition, results here demonstrate that Lister-dTK is capable of infecting and killing two murine ovarian cancer cell lines *in vitro.* Thus there is the potential for further investigation in pre-clinical *in vivo* models.

Interestingly, whilst the EC50 of Lister-dTK was similar across all five human ovarian cancer cell lines tested, there were differences in replication and virus protein expression between cell lines. With the exception of A2780CP cells, virus titre peaked at 48hrs post-infection in all other cell lines. In the most sensitive Skov3ip1 cells, virus titre peaked at 24hrs post-infection and virus protein expression in these cells was also the strongest out of four human cell lines. Although the reasons behind this seemingly more rapid replication are not known it is presumed that this contributes to the increased sensitivity of Skov3ip1 to Lister-dTK. As there is no known receptor for vaccinia virus and it is able to infect virtually almost all cells, the binding and entry of virus into cancer cells is not thought to be a limiting factor in the treatment of ovarian cancer. Furthermore, the cytoplasmic life-cycle of vaccinia virus means that it is less reliant on host cell proteins and therefore, in theory, should replicate to a similar degree in all cancer cell lines, widening its potential use in the treatment of ovarian cancer. There were similarities between replication and sensitivity to Lister-dTK, although A2780 cells had a viral titre over 10 times higher than that in Skov3ip1 cells at 48hrs post-infection, yet were less sensitive. Similarly, MOVCAR7 cells were more sensitive to Lister-dTK than MOSEC cells yet viral titre at 24, 48 and 72hrs post-infection was almost 10 times lower.

Although the aim of these preliminary experiments was to establish whether Lister-dTK could replicate in and kill a range of ovarian cancer cell lines, and not to determine what causes sensitivity, these results do suggest that cell lysis does not just occur when a critical threshold of virus particles is reached, as more cell death was observed in cells with a lower virus yield. The definitive mechanism of cell death by vaccinia virus is not known and was attributed to cell lysis in ES2 ovarian cancer cells in a previous study (Hung, Tsai et al. 2006). Attempts to determine the pathways responsible for cell death were addressed in future work within this thesis.

Consistent with other studies that show tumour specificity of vaccinia virus deleted in thymidine kinase in other cancers (Puhlmann, Brown et al. 2000; Yu, Galanis et al. 2009), Lister-dTK demonstrated tumour specificity both *in vitro* and *in vivo* in these preliminary results. In all seven human and mouse ovarian cancer cell lines tested, Lister-dTK exhibited comparable or better cytotoxicity compared to the wild-type strain. In contrast, IOSE25 hTERT immortalised ovarian surface epithelial cells (non-cancerous control) were 10 times more sensitive to Lister-wt than Lister-dTK. Furthermore, analysis by immunohistochemistry showed specific expression of virus proteins exclusively in tumour tissue. No evidence of virus could be seen in either the liver or spleen 72hrs post-infection. In addition, even when tumour tissue was immediately adjacent to normal liver tissue (as is common in ovarian cancer where tumour nodules can grow on the surface of organs), specific replication in tumour tissue but not in normal tissue was observed. Together, these results confirm what has been observed in other cancers following delivery of tumour-selective vaccinia strains; that replication and expression of virus proteins culminates in tumour cell death in a dose-dependent manner *in vitro*. In addition, mimicking a potential clinical scenario, Lister-dTK was delivered to metastatic disease and tumour specificity demonstrated. While a full biodistribution study was not performed, this has been shown previously using a TK deleted Western Reserve strain, which is considered to be more potent than the Lister strain. Even with this potentially more toxic strain, replication in tumour tissue far exceeded that in healthy tissue (Puhlmann, Brown et al. 2000).

Treatment with both cisplatin and Lister-dTK did not enhance cell death in any of the four human ovarian cell lines tested when cell survival was normalised to the effect of cisplatin alone. This was the case irrespective if cells were treated with virus or cisplatin first, or if the two treatments were administered simultaneously. It was noted that pre-treatment of cells with cisplatin for 24hrs led to an increase in cells in G2 of the cell cycle at the time of infection, particularly in A2780CP cells. Although it has been described that vaccinia virus not only induces cell cycle progression but preferentially infects cells in either S-phase or G2 (Huang, Sikorski et al. 2010), this does not correspond to increased efficacy of Lister-dTK in A2780CP cells. This may reflect efficient infection regardless of the stage cells are at in the cell cycle in this model (although this was not tested), or that any advantage conferred by increased infectivity is negated by the reduced pool of viable cells for replication to proceed in due to cell death caused by the drug.

It is worth noting here that these experiments were designed to see if cisplatin could augment the oncolytic activity of Lister-dTK *in vitro*, similar to the synergy observed between a Western Reserve double-deleted virus and paclitaxel (Huang, Sikorski et al. 2010), another treatment of choice for ovarian cancer. In this study, synergy was observed in one ovarian cancer cell line (UCI-101) tested *in vitro*, whereby it was demonstrated that increased cell death was not merely an additive effect, although the *in vivo* model used here was colorectal and not ovarian cancer (Huang, Sikorski et al. 2010). Although no synergistic effect between Lister-dTK and cisplatin was observed in the work presented in this chapter, it may well be that the combined treatments result in improved control of tumour growth *in vivo*, as has been described elsewhere for pancreatic cancer (Yu, Galanis et al. 2009). This was not tested here, but the lack of positive results *in vitro* do not exclude the potential for combination therapy that may have an additive, albeit not synergistic, effect to improve survival or slow tumour growth.

The results presented in this chapter suggest that Lister-dTK may have potential in the treatment or control of tumour growth, as it shows activity in 5 human ovarian cancer cell lines and two murine cell lines. These proof-of-principle experiments show the ability of Lister-dTK to infect, replicate in and kill cells *in vitro*, although cytotoxicity was not enhanced by combination therapy with cisplatin. A single dose of Lister-dTK delivered intraperitoneally to nude mice bearing advanced Skov3ip1 tumours showed that Lister-dTK could infect and replicate in primary tissue bulk and metastases, and crucially that this replication was tumour specific. Having confirmed that Lister-dTK possesses these key features- specificity and efficacy, (*in vitro* at least), a number of questions naturally arise.

Can Lister-dTK eradicate or control tumour growth, and can this be achieved using clinically relevant models encompassing advanced intraperitoneal disease and appropriate viral delivery methods? Given that the majority of oncolytic viruses are armed with genes to promote overall anti-tumour activity, through stimulation of the immune system, improving virus dissemination or inhiting angiogenesis, can the introduction of such a gene enhance the ability of Lister-dTK to destroy ovarian cancer tumours? And finally, what are the mechanisms and pathways that contribute to tumour cell death? It is well known that even advanced tumours initially respond to cisplatin before resistance occurs and recently it has been demonstrated for the first time that tumours can also require resistance to an oncolytic herpes simplex virus (Song, Haddad et al. 2012). This resistance is associated with changes in expression of several genes, including those that produce proteins that interact with apoptotic pathways. Will deciphering the mechanisms that oncolytic vaccinia virus kills tumour cells lead to novel ways of manipulating the process to optimise cell death, and to prevent acquired resistance? Attempts to address these issues were made in the following two chapters with the expression of decorin, an extracellular matrix protein from Lister-dTK, and investigation into which cell death pathways are involved in Lister-dTK induced ovarian cancer cell death.

Chapter 4

A novel oncolytic vaccinia virus expressing decorin

4. A novel oncolytic vaccinia virus expressing decorin

The role of decorin in inhibiting tumour growth and progression has been under scrutiny for several years, and as further mechanisms are uncovered it is becoming a novel therapeutic possibility. It has a defined role in ECM modulation, inhibition of several tyrosine kinase receptor signalling pathways and inhibition of tumour promoting growth factors such as TGFβ. Decorin has also been shown to inhibit tumour growth in prostate cancer by interactions with the androgen receptor (Hu, Sun et al. 2009), indicating that there are perhaps other as yet undiscovered mechanisms. Recently, an oncolytic adenovirus expressing decorin was delivered intra-tumourally to glioma cells and shown to exhibit inhibitory effects on both tumour growth and metastasis (Choi, Lee et al. 2010). Interestingly, penetration and viral spread of the virus throughout the tumour was increased compared to the control virus and this was shown to be collagen binding dependent. The multiple mechanisms of decorin in inhibiting tumour progression, coupled with its apparent ability to enhance viral delivery and spread, make it a promising transgene of choice for expression from a replication-selective oncolytic vaccinia virus.

4.1 Expression of decorin in cancer

Loss of decorin has been demonstrated as permissive for both tumour development (Iozzo, Chakrani et al. 1999) and metastatic spread, which can be inhibited by either stable transfection or delivery of decorin to tumour cells (Reed, Waterhouse et al. 2005; Goldoni, Seidler et al. 2008; Shintani, Matsumine et al. 2008). As decorin has also been described to inhibit cell growth through induction of p21 (De Luca, Santra et al. 1996) and to trigger apoptosis through caspase-3 activation (Seidler, Goldoni et al. 2006) it is possible that this protein may be downregulated in cancer. A panel of ovarian, pancreatic and prostate cancer cell lines were screened to first determine the expression of decorin in these cancers.

Consistent with work showing the absence of decorin in ovarian cancer cell lines and human tumours (Nash, Deavers et al. 2002), decorin was not detected in six ovarian cancer cell lines by western blotting (Figure 24A). Similarly, decorin was also undetectable in a panel of pancreatic cancer cell lines (Figure 24B), consistent with a previous study (Koninger, Giese et al. 2004). Naturally occurring decorin proteoglycan has a molecular mass of approximately 100kDa (compared to the 40kDa protein core detected by the antibody) and a band was detected at this size in T3M4, 8988S and 8988T cells. To ensure that the absence of decorin in pancreatic cancer cell lines was not due to glycosylation obscuring the antigenic site, cell lysates were also treated with the deglycosylating enzyme PNGase F overnight, which removes N-linked oligosaccahrides. Following treatment with PNGase F, decorin remained undetectable in pancreatic cancer cell lines. The expression of decorin was further determined in two prostate cancer cell lines and in the immortalised normal prostate cell line, PNT2 (Figure 24D). Decorin was detected in PNT2 cells and to a lesser degree in DU145 and LnCap cells, indicating potential downregulation of decorin in these two prostate cancer cell lines.

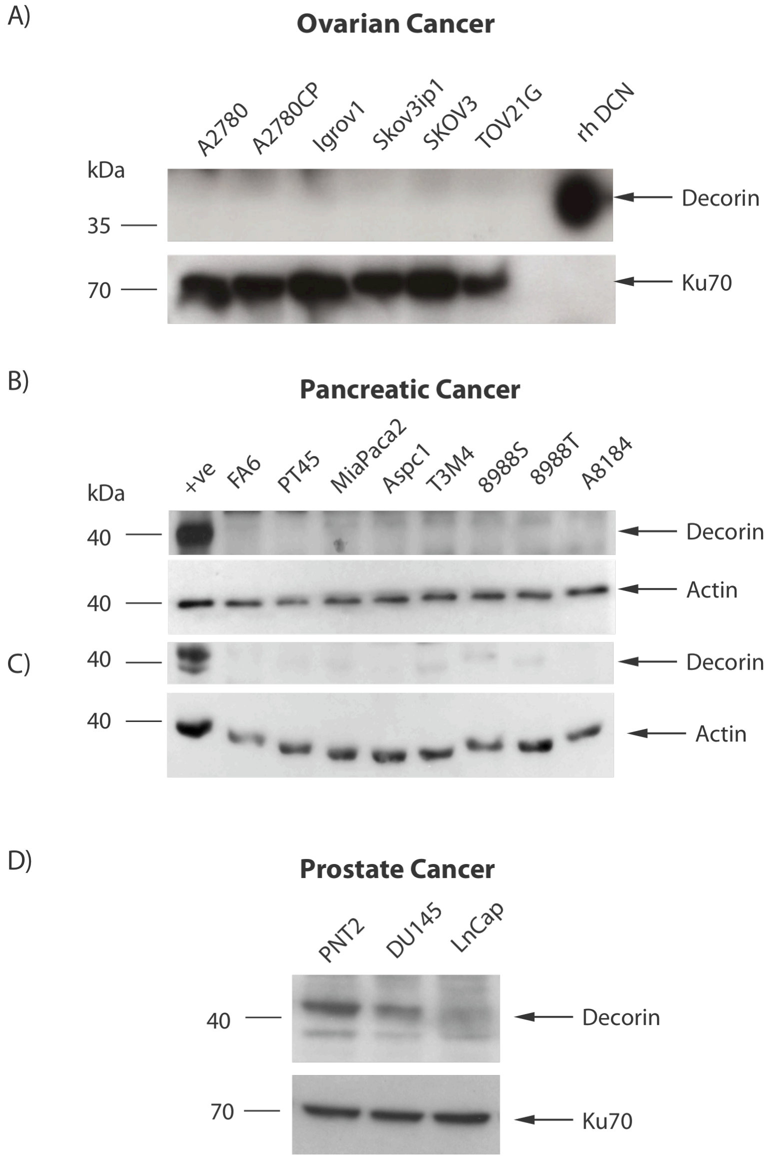

Figure 24: Expression of decorin in human cancer cell lines. Panels of A) ovarian, B and C) pancreatic and D) prostate cell lines were tested for the expression of decorin protein by western blotting. The presence of decorin following treatment with a deglycosylating enzyme overnight (PNGase F) was also determined in pancreatic cancer cell lines (C). Positive controls included recombinant human decorin protein (A) and CV1 cells transfected with a plasmid encoding decorin (B and C).

4.2 Recombinant decorin does not inhibit virus replication or cytotoxicity

Having confirmed that decorin was not present in a panel of ovarian and pancreatic cancer cell lines, and was decreased in two prostate cancer cell lines compared to normal prostate cells, the effect of recombinant decorin on vaccinia virus replication and cytotoxicity was next established. This was to ensure that, upon insertion into the viral genome, the expression of decorin would not interfere with the virus life cycle to attenuate virus efficacy.

A cell viability assay was carried out to determine the survival of TrampC1 cells in response to either Lister-dTK alone, or Lister-dTK in the presence of recombinant decorin (Figure 25A). Decorin at a concentration of either 2μg/ml or 10μg/ml did not attenuate the cytotoxicity of Lister-dTK. Similarly, the presence of decorin did not attenuate replication of Lister-dTK (Figure 25C) and in fact virus titre at 72hrs post-infection was increased in the presence of 2μg/ml recombinant decorin, although this may reflect variability of the assay, as the TCID50 assay is not very precise at calculating titres within one log of each other.

Decorin has been described as having growth-inhibitory effects on tumour cells, and a decrease in proliferation may attenuate vaccinia virus, which partly relies on the high nucleotide pool in replicating host cells for efficient virus replication. Additionally, it has been suggested that vaccinia virus preferentially infects cells in either S phase or G2 phase of the cell cycle (Huang, Sikorski et al. 2010). To determine the role of decorin on the proliferation of TrampC1 cells, cells were cultured in the absence or presence of recombinant decorin for 72hrs, and cell number counted daily. There was no significant decrease in proliferation at 2μg/ml decorin; although a concentration of 10μg/ml decorin led to a decrease in cell proliferation of 15% at 24hrs and 48hrs, this only reached significance at 72hrs when there was a decrease of 22% (Figure 25B). As proliferation was not monitored in the presence of a similar control protein, such as biglycan, it cannot be ascertained whether this decrease in proliferation is specifically due to the action of decorin. Although the replication and cytoxicity of Lister-dTK in the presence of decorin was not determined at timepoints past 72hrs post-infection, it appears that the decrease in proliferation observed does not negatively affect either replication or virus-induced cell death.

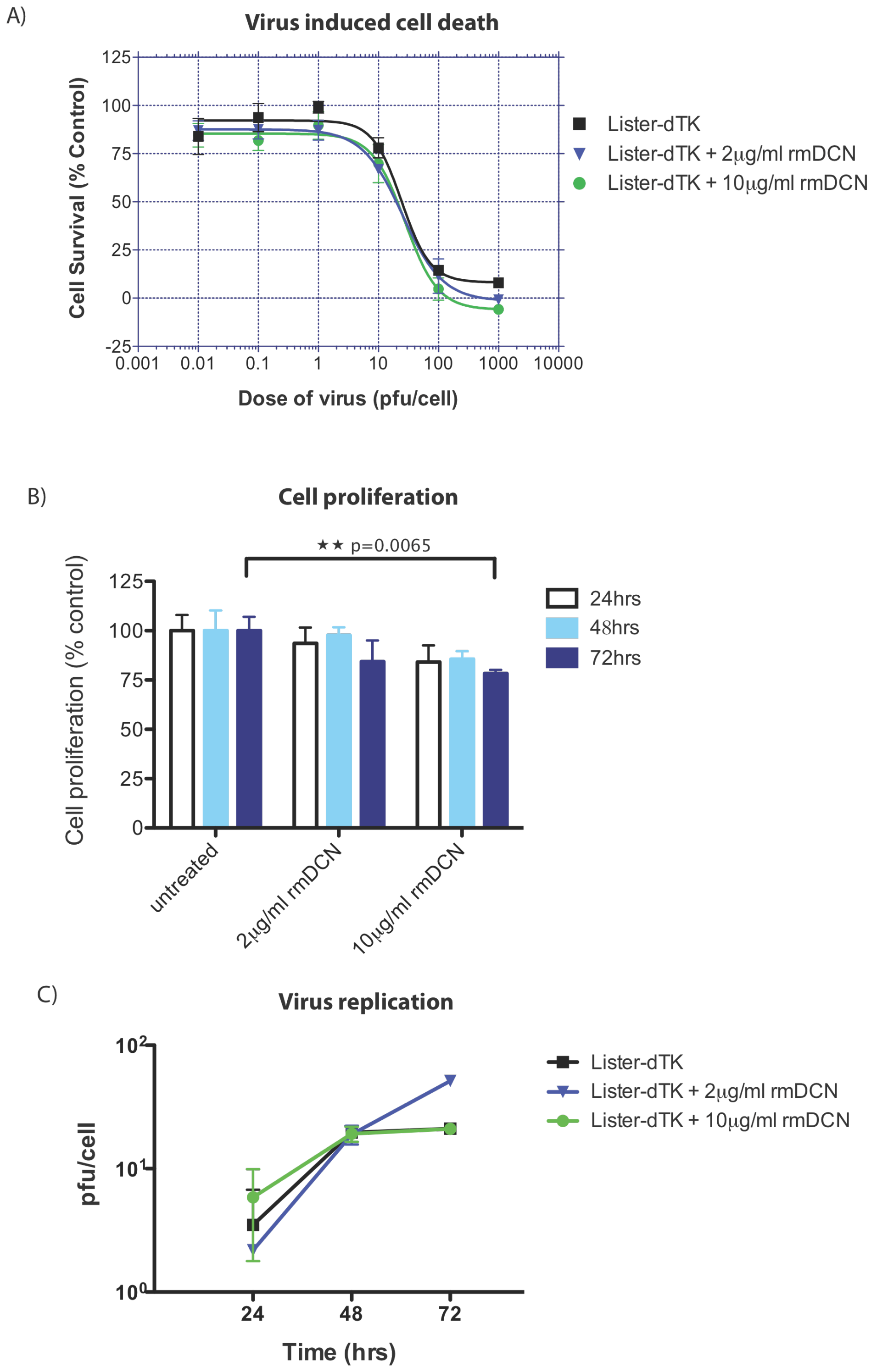

Figure 25: Effect of recombinant murine decorin on A) virus-induced cell death B) cell proliferation and C) virus replication. A) TrampC1 cells were infected with increasing doses of Lister-dTK for 2 hrs and then cultured either in normal growth media or in the presence of recombinant murine decorin. Cells survival was determined 72hrs post-infection by MTS assay. B) TrampC1 cells were grown in the presence or absence of decorin. After trypsinisation, cell number was determined daily and is expressed as a percentage of the number of untreated cells at each timepoint. The graph represents a single experiment performed in triplicate wells. C) TrampC1 cells were infected with an initial dose of 0.1pfu/cell for 2hrs and then cultured in the presence or absence of decorin for three days. Virus titre was determined 24hrs, 48hrs and 72hrs post-infection by TCID50 assay. Results represent the mean+SD titre from 2 experiments, each performed in triplicate.

4.3 Construction of a novel oncolytic vaccinia virus: Lister-mDCN

To date, the effects of re-expression of decorin in tumour cells have been studied mainly through treatment with recombinant decorin protein (Koninger, Giese et al. 2004; Goldoni, Seidler et al. 2008; Hu, Sun et al. 2009), stable transfection (Grant, Yenisey et al. 2002; Shintani, Matsumine et al. 2008) or delivery by replication-defective adenoviral vectors (Reed, Gauldie et al. 2002; Reed, Waterhouse et al. 2005). Recently, an oncolytic adenovirus expressing decorin was delivered intra-tumourally to glioma cells and shown to retain its growth and metastasis inhibitory effects (Choi, Lee et al. 2010). Having determined, albeit in a small set of experiments in one cell line, that recombinant decorin did not negatively effect either replication or cytotoxicity of the oncolytic vaccinia virus Lister-dTK a novel virus expressing decorin was constructed. As vaccinia virus is able to replicate in murine cells lines, and as decorin is proposed to interact with the host tumour microenvironment, it was decided to take advantage of these features by constructing a virus expressing murine decorin to enable future studies in immunocompetent models. This virus was termed Lister-mDCN.

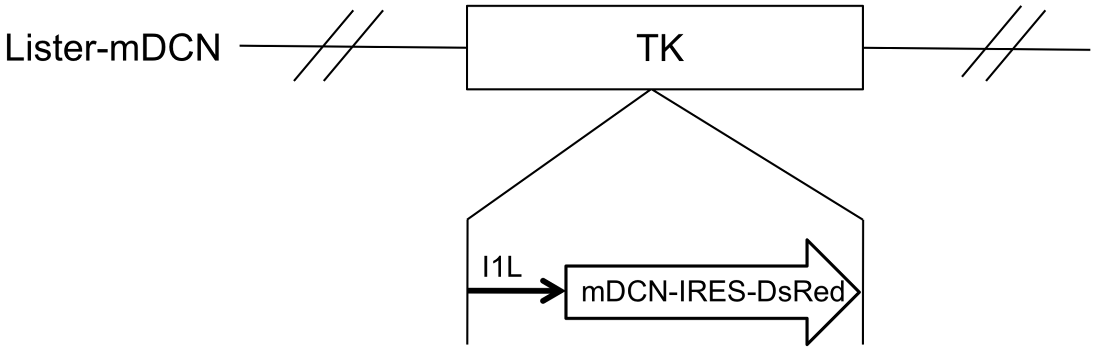

Figure 26: Schematic representation of Lister-mDCN. A recombination plasmid encoding both murine decorin and DsRed, separated by an IRES sequence, under control of the I1L promoter was cloned as described in the Materials and Methods. This sequence was flanked by sequences homologous to regions of the vaccinia thymidine kinase gene, allowing homologous recombination into the Lister-wt virus to create Lister-dTK.

The thymidine kinase gene was deleted from the Lister strain of vaccinia virus to retain tumour specificity and replaced with a cassette encoding decorin. The fluorescent protein DsRed was also included to enable selection of positive plaques and for future imaging of the virus. The two sequences were separated by an internal ribosomal entry site (IRES) sequence to allow translation of both genes from a single dicistronic mRNA, and thus avoiding any potential promoter interference from two individual promoters in close proximity.

4.4 Characterisation of Lister-mDCN

A series of experiments was performed to confirm expression of decorin from the newly constructed Lister-mDCN, and to evaluate its replication potential and cytotoxicity relative to that of a control virus, Lister-dTK. In addition to characterisation in two murine ovarian cancer cell lines (MOSEC and MOVCAR7), Lister-mDCN efficacy was also determined in a murine pancreatic cancer cell line (Panc02) and a murine prostate cancer cell line (TrampC1).

4.4.1 Expression and release of decorin from infected cells

Expression of decorin protein core (approx. 40kDa) was evident in Lister-mDCN infected MOSEC cells, Panc02 cells and TrampC1 cells (Figure 27). In contrast, both uninfected and Lister-dTK infected cells did not demonstrate expression of decorin in any of the cell lines tested. As expected, the amount of decorin present in Lister-mDCN infected cells was dose-dependent, with higher amounts expressed following initial infection with 1pfu/cell compared to 0.1pfu/cell in MOSEC and TrampC1 cells (Figure 27). Panc02 cells appeared less permissive to virus infection as decorin was only expressed at the higher dose of virus, which correlated to decreased vaccinia virus protein expression in this cell line compared to both MOSEC and TrampC1 cells.

As decorin is proposed to have effects on the extracellular tumour microenvironment via its interaction with ECM components, growth factors and their receptors, the secretion of decorin from infected cells was also confirmed by ELISA. Decorin was detected in the supernatant of Lister-mDCN infected MOSEC and TrampC1 cells in increasing quantities as infection progressed (Figure 28). Release of decorin was also dose-dependent as infection with 1pfu/cell resulted in higher detectable concentrations than infection with 0.1pfu/cell. Decorin could be detected at low levels in the supernatant 24hrs post-infection with 1pfu/cell in TrampC1 cells, and to a lesser degree in MOSEC cells. Interestingly, this release of decorin appears to precede cell death as cell lysis is not likely to be significant at 24hrs post-infection, suggesting that decorin may be actively secreted out of the cell before membrane rupture and the release of cellular content. As infection progressed the concentration of decorin in the supernatant increased steadily to 78ng/ml and 57ng/ml at 48hrs post-infection in MOSEC and

TrampC1 cells respectively, reaching 187ng/ml and 162ng/ml at 72hrs post-infection. Decorin was undetectable in the supernatant of both uninfected and Lister-dTK infected cells.

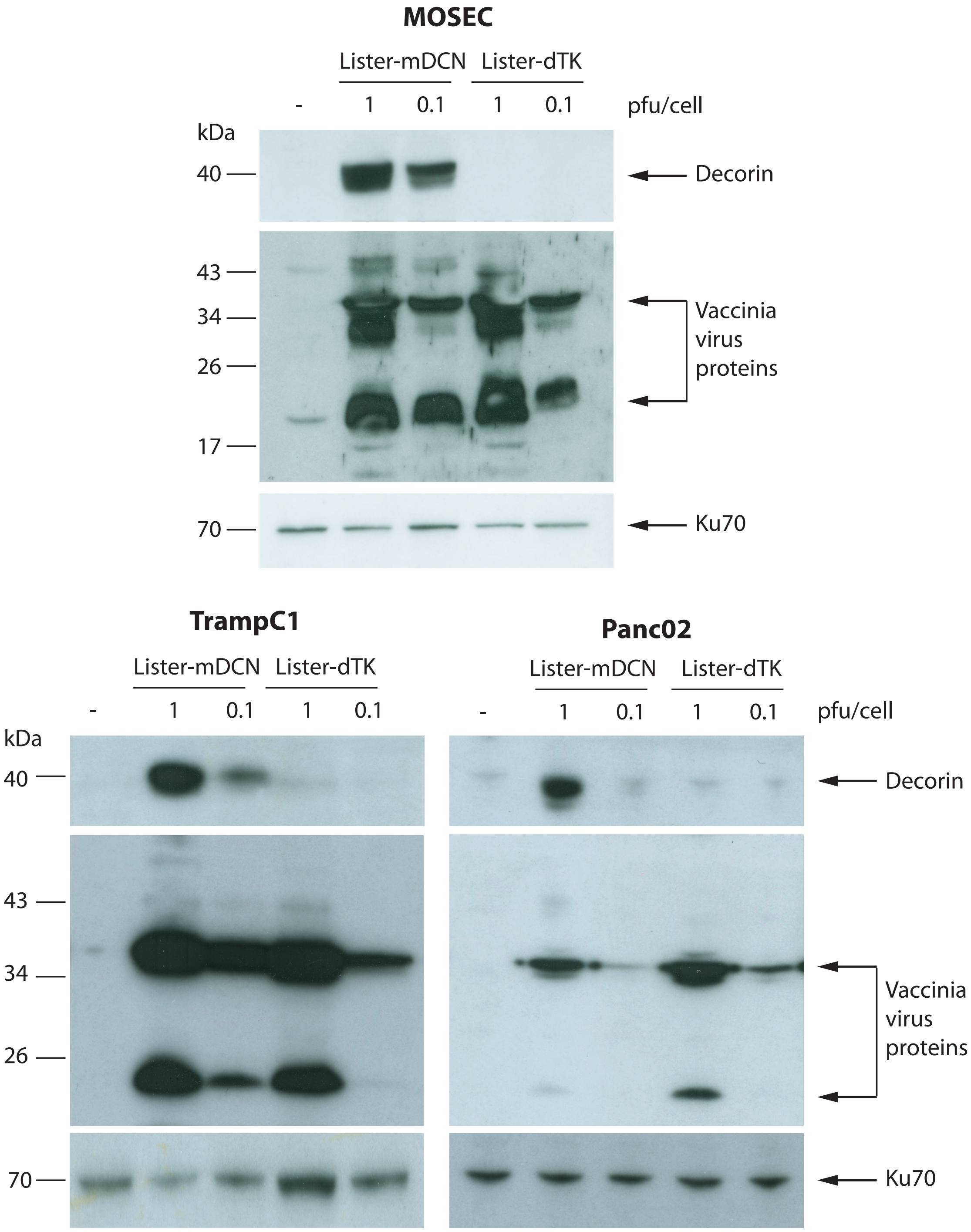

Figure 27: Expression of decorin protein in Lister-mDCN infected cells. Cells were infected with virus and cell lysates harvested 72hrs post-infection. Expression of decorin in infected cells was confirmed by western blotting.

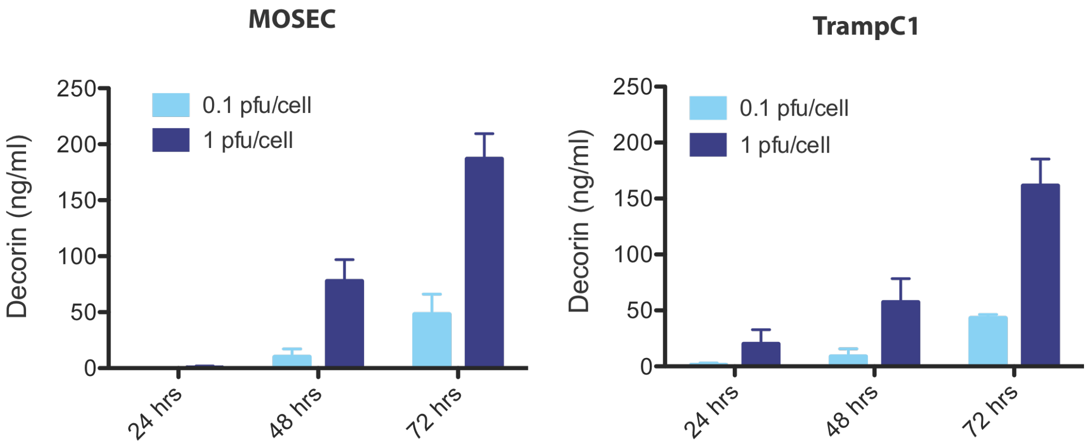

Figure 28: Release of decorin from infected cells. The supernatant of Lister-mDCN infected cells was collected over a 72hr timecourse post-infection and the amount of decorin present in the supernatant quantified by ELISA.

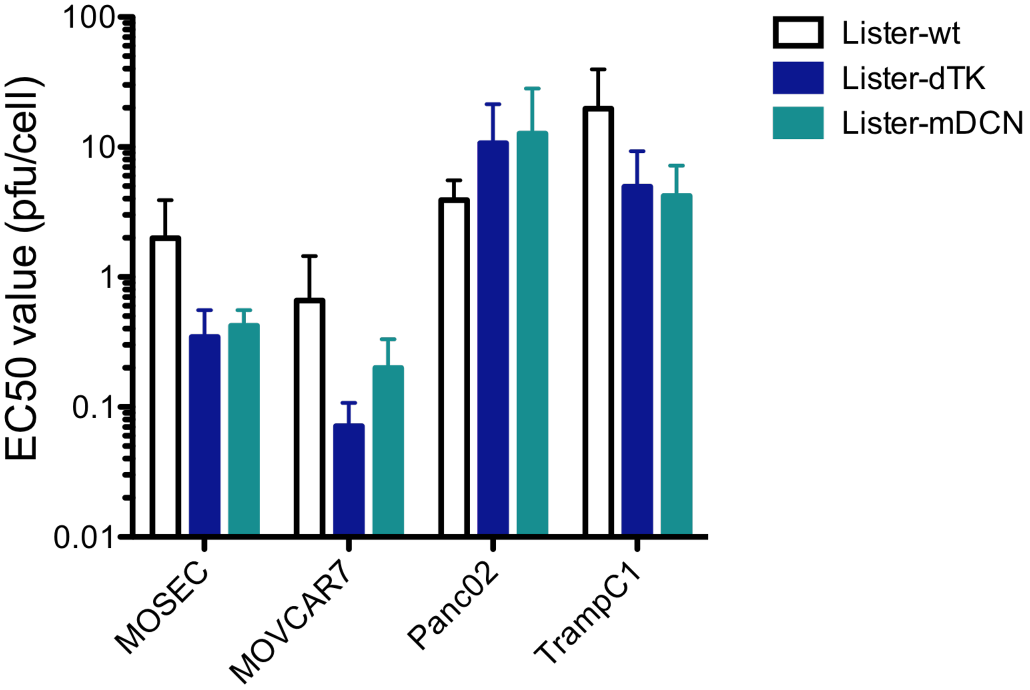

Figure 29: Cytotoxicity of Lister-mDCN compared to Lister-dTK in murine cancer cell lines. Cells were infected with increasing doses of virus and cell survival analysed by MTS assay 72hrs post-infection. The EC50 was calculated from dose response curves created using Prism software. Data show the mean+SD EC50 from a minimum of three experiments, each performed in triplcate.

4.4.2 Cytoxicity of Lister-mDCN

To determine if Lister-mDCN retained the cytotoxicity of the control Lister-dTK virus, cell survival was measured 72hrs post-infection using a cell viability assay. In addition, the cytotoxicity of both viruses was compared to the wild-type virus, Lister-wt. With the exception of Panc02 cells, Lister-dTK and Lister-mDCN demonstrated enhanced cytotoxicity in three of the four murine cell lines tested (Figure 29). Both Lister-dTK and Lister-mDCN had an EC50 at least 4 times lower than that of that the wild-type virus in MOSEC, MOVCAR7 and TrampC1 cells. In contrast, these viruses were attenuated in Panc02 cells and the EC50s were three times higher than the EC50 of Lister-wt.

There was no statistically significant difference in the cytotoxicity of Lister-mDCN compared to that of Lister-dTK in MOSEC, MOVCAR7, Panc02, or TrampC1 cells (Figure 29). The ovarian cancer cell lines MOSEC and MOVCAR7 were remarkably sensitive to Lister-mDCN with an EC50 value of 0.4pfu/cell and 0.2pfu/cell respectively. In contrast, TrampC1 and Panc02 cells were less sensitive with an EC50 of 4.2pfu/cell and 12.7pfu/cell respectively. In all four cell lines, the EC50 of Lister-mDCN was comparable to that of Lister-dTK. This suggests that, whilst Lister-mDCN does not demonstrate superior efficacy over Lister-dTK *in vitro*, neither does expression of decorin detrimentally affect cytotoxicity. As the effects of decorin are largely proposed to be mediated through receptor signalling within the tumour microenvironment and direct interaction with ECM structural components, it is perhaps not surprising that *in vitro* cell survival assays revealed no significant advantage of Lister-mDCN over Lister-dTK. This is consistent with preliminary data that showed that recombinant decorin did not attenuate either virus replication or cytotoxicity (Figure 25).

4.4.3 Replication of Lister-mDCN

To further confirm that expression of decorin from Lister-mDCN did not result in attenuation of the virus, the replication efficiency of Lister-mDCN was compared to that of Lister-dTK and Lister-wt in MOSEC, MOVCAR7, Panc02 and TrampC1 cells. Cells were infected with an initial dose of 0.1pfu/cell and virus titre firstly determined over 72hrs of infection to study the kinetics of replication, and then in subsequent experiments at 48hrs post-infection to generate sufficient numbers for statistical analysis.

Over a 72hr timecourse of infection Lister-mDCN replicated to a similar, or greater, level than both Lister-wt and Lister-dTK in MOSEC, MOVCAR7 and TrampC1 cells (Figure 30).

Replication of Lister-mDCN appeared attenuated in Panc02 cells compared to Lister-dTK over a timecourse of infection, although this difference was not apparent upon further analysis of virus titre at 48hrs post-infection (Figure 30C). At 48hrs post-infection, there was no significant difference in titre between Lister-mDCN and Lister-dTK in MOSEC, MOVCAR7 or Panc02 cells. There was however, a significant increase in recoverable virus of Lister-mDCN compared to Lister-dTK at 48hrs post-infection in TrampC1 cells.

Consistent with the greater sensitivity of MOSEC and MOVCAR7 cells to Lister-mDCN compared to Panc02 or TrampC1 cells (Figure 29), enhanced replication was also observed in these ovarian cancer cell lines (Figure 30). Replication of Lister-mDCN was particularly rapid in MOSEC cells, with a recoverable virus titre of over 1000pfu/cell after initial infection with just 0.1 pfu/cell. In both MOSEC and MOVCAR7 cells, virus titre peaked at 48hrs and then reached a plateau; presumably as virus-induced cell death limited the amount of cells available for virus infection and subsequent replication. Again, consistent with the reduced cytotoxicity of vaccinia virus in Panc02 and TrampC1 cells, lower virus titres were recoverable from these cell lines (Figure 30), particularly in Panc02 cells which also had the highest EC50 of Lister-dTK and Lister-mDCN (Figure 29). Over a 72hr timecourse, the titres of Lister-wt, Lister-dTK and Lister-mDCN continued to rise in TrampC1 cells; this is in contrast to the plateau observed in MOSEC and MOVCAR7 cells. It is therefore possible that, had it been measured over a longer time period, both replication and cytotoxicity of Lister-mDCN (or vaccinia virus in general) in TrampC1 cells might reach levels comparable to that observed in MOSEC and MOVCAR7 cells.

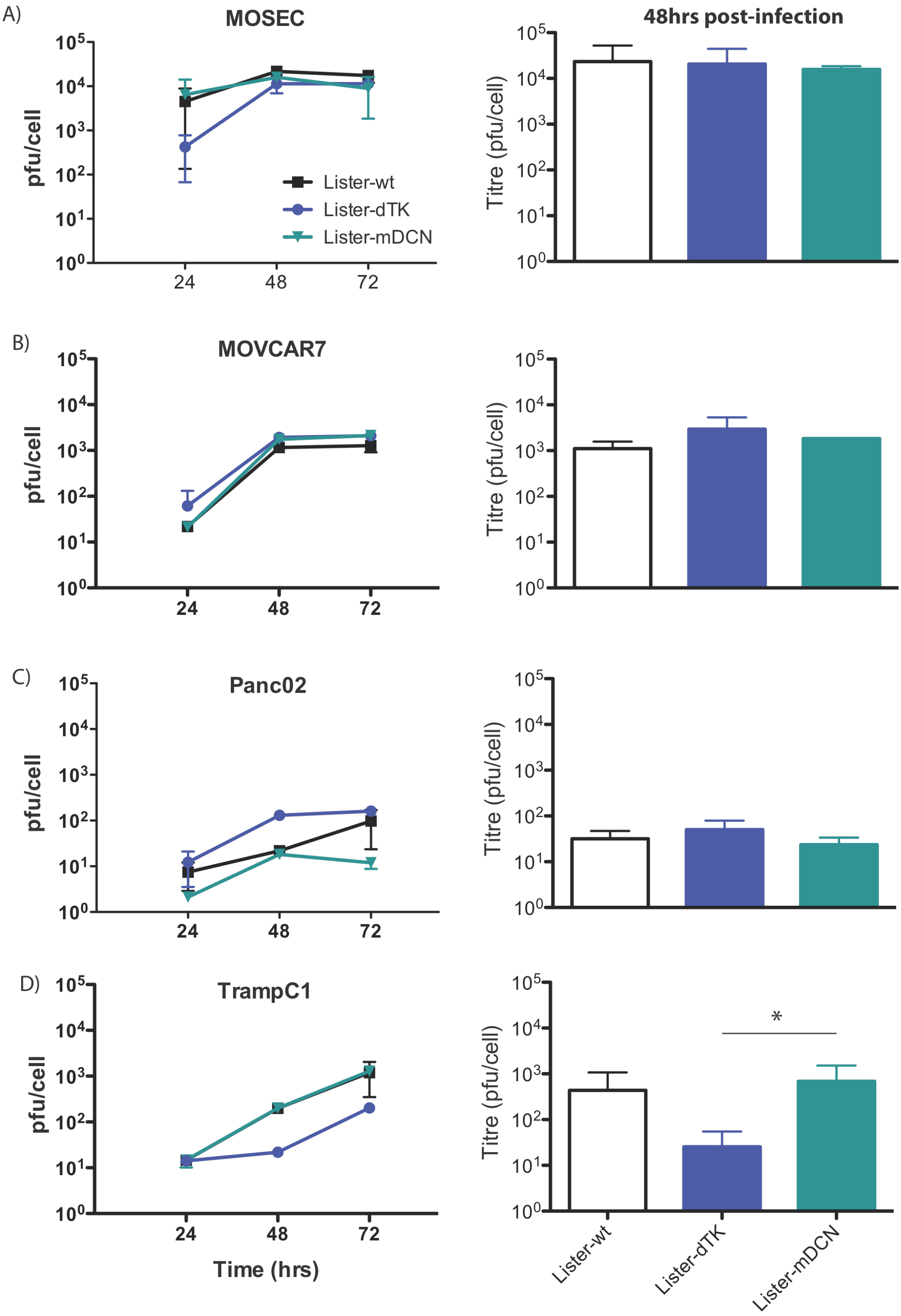

Figure 30: Replication of Lister-mDCN in murine cancer cell lines. Cells were infected with 0.1pfu/cell of virus and virus titre determined by TCID50 assay over a 72hr timecourse (n=1 in triplicate). Recoverable virus at 48hrs post-infection was titred in a further two experiments (n=3 in triplicate). *=p<0.05

4.5 Spread of Lister-mDCN

Previously, an adenovirus expressing decorin was reported to have improved efficacy and intratumoural spread over a control virus in a model of glioma (Choi, Lee et al. 2010). In order to investigate the ability of Lister-mDCN to penetrate a collagen matrix *in vitro*, and to replicate and spread throughout subcutaneous tumours *in vivo*, TCID50 assays and expression of viral DNA and proteins were assessed and compared to Lister-dTK.

4.5.1 In vitro spread through a collagen matrix

To assess the spread of Lister-mDCN *in vitro*, organotypic cultures were set up which comprised of tumour cells embedded in a collagen/matrigel matrix and an overlaying monolayer of cells. Following infection of the cell monolayer with vaccinia virus, the gels were harvested at various timepoints post-infection, fixed, sectioned and stained for the presence of vaccinia virus proteins. It was hoped that this would enable quantification of virus spread *in vitro*. However, whilst there was some evidence of virus replication and protein expression in the monolayer of Lister-dTK or Lister-mDCN infected TrampC1 cells, this did not extend to cells in the matrix below (Figure 31). Uninfected cells were absent of vaccinia virus proteins as expected. This experiment was also performed using Panc02 and MOSEC cells at various timepoints, and with varying numbers of cells embedded within the matrix. Vaccinia virus proteins were not detected in embedded cells on any occasion (data not shown).

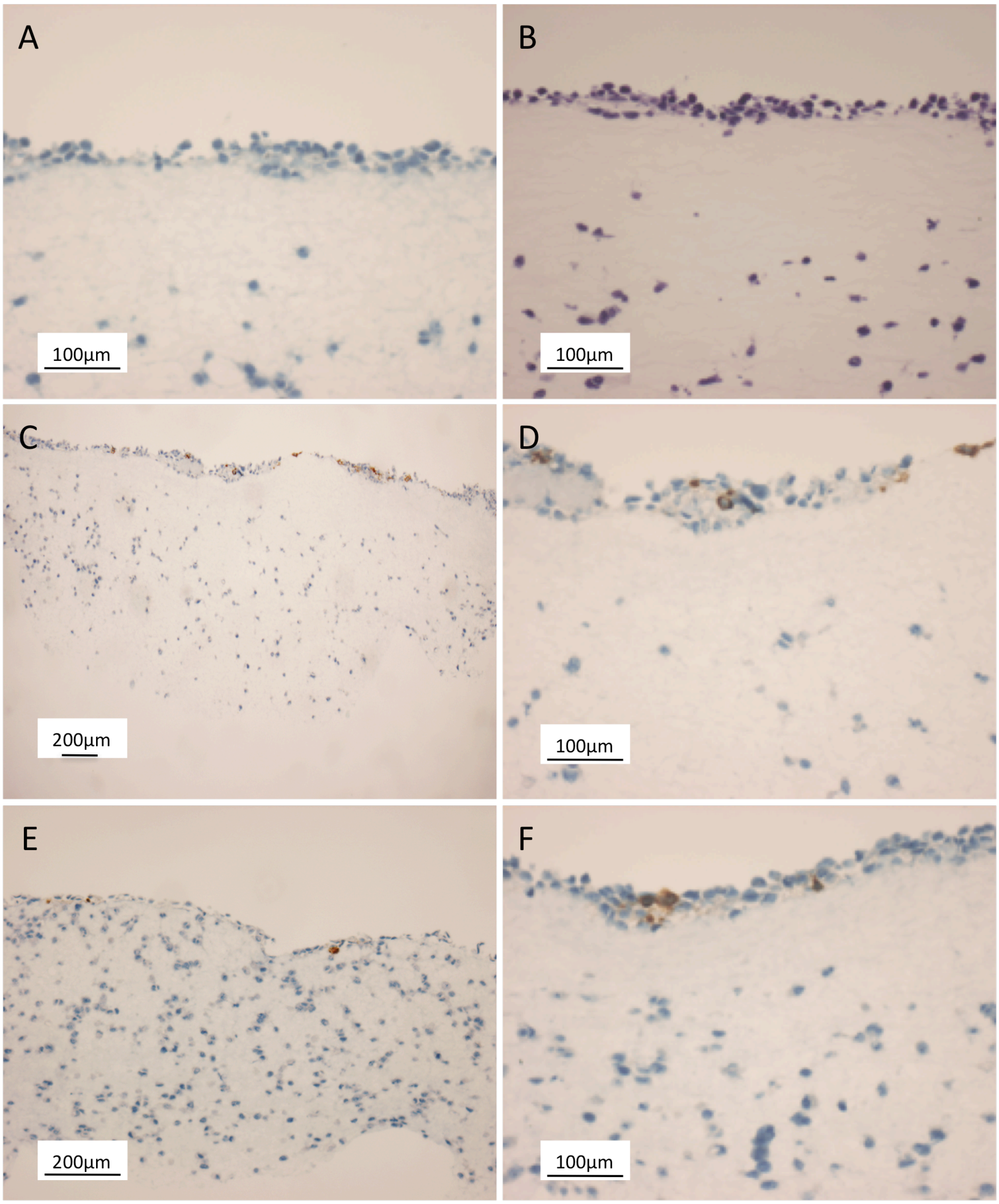

Figure 31: Virus spread in TrampC1 organotypics. $5x10^6$ cells were embedded in a 70:30 collagen/matrigel matrix and overlaid with $0.5x10^6$ cells in normal growth media. Cells were (A and B) mock-infected, (C and D) infected with 1pfu/cell Lister-dTK or (E and F) infected with 1 pfu/cell Lister-mDCN. Gels were harvested 24hrs post-infection and fixed in formalin for analysis by immunohistochemistry. Sections were stained for the presence of vaccinia virus proteins (A, C-F) and with H&E (B). Representative images from triplicate wells are shown here.

A second experiment was then performed which looked at the spread of virus through a thinner collagen matrix that did not contain any cells. A monolayer of cells was infected with 0.1pfu/cell of Lister-dTK or Lister-mDCN and then overlaid with a thin gel comprising 70% collagen and 30% matrigel, topped with normal growth medium (Figure 32). This medium was harvested at 24hrs, 48hrs and 72hrs post-infection and virus titre determined by TCID50 assay. Before determining virus titre, the supernatant was spun to ensure that no migrating cells were present. Gels were also harvested, fixed and stained with H&E to confirm that cells were not migrating through the collagen matrix.

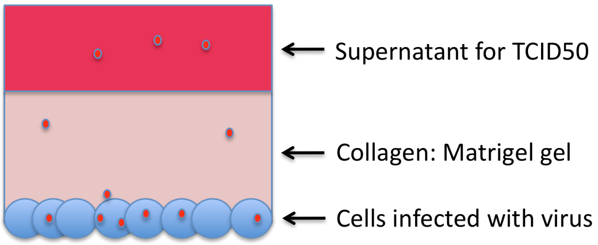

Figure 32: Schematic diagram of assay used to detect virus spread through a collagen matrix.

Consistent with the lower replication of Lister strains in TrampC1 cells compared to MOSEC (Figure 30) the spread of virus through a collagen matrix following infection of TrampC1 cells was also reduced compared to that of MOSEC cells (Figure 33). At 24hrs post-infection, virus could be detected in the overlaying medium of TrampC1 cells infected with Lister-dTK. In contrast, virus was undetectable in cells infected with Lister-mDCN, suggesting inhibition of virus spread through a collagen matrix. However, this cannot be explained by differences in replication of the two strains, as Lister-mDCN demonstrates enhanced replication compared to Lister-dTK in TrampC1 cells (Figure 30D). Increased spread of Lister-dTK through the collagen matrix was also observed at 48hrs and 72hrs post-infection in TrampC1 cells (Figure 33B). Similarly, virus titre was between 1-2 logs higher in Lister-dTK infected MOSEC cells compared to Lister-mDCN infected cells at every timepoint tested (Figure 33A). This was surprising, and the opposite of what had been expected given the hypothesised interactions of decorin with the collagen matrix that were proposed to enhance virus spread.

It is worth noting that the titre of virus in the supernatant, presumably having spread through the collagen matrix from infected cells below, represents only a small proportion of the initial infectious dose. TrampC1 cells were initially infected with 0.1 pfu/cell, of which <0.003pfu/cell was detected in the medium overlaying a collagen matrix at 24hrs post-infection with Lister-dTK, <0.03pfu/cell at 48hrs post-infection and 4pfu/cell at 72hrs post-infection. This corresponded to titres of $1.3x10^3$ pfu/ml, $1.2x10^4$ pfu/ml and $1.7x10^6$ pfu/ml respectively (Figure 33B). The proportion of virus in the medium of Lister-mDCN infected cells was even lower, with 0.0002pfu/cell detected at 48hrs post-infection and just 0.1pfu/cell at 72hrs post-infection. Titres of both viruses were higher in MOSEC infected cells.

It is possible that the titres obtained here reflect production and spread of the extracellular enveloped (EEV) form of vaccinia rather than spread of the more common mature virions that are released upon cell lysis, particularly as virus was detected at early timepoints and in low quantities, consistent with what is known about EEV production. This was studied briefly, by quantifying the amount of virus in the supernatant of infected MOSEC cells at early timepoints post-infection, before cell lysis was likely to occur (Figure 34). Whilst replication of intracellular Lister-mDCN was slower than that of Lister-dTK, titres were comparable at 18hrs post-infection (Figure 34A). In contrast, the titre of virus in the supernatant of infected Lister-mDCN cells (presumed to be EEV), was considerably lower than that of Lister-dTK cells at 12hrs and 18hrs post-infection, and was undetectable at 9hrs post-infection (Figure 34B).

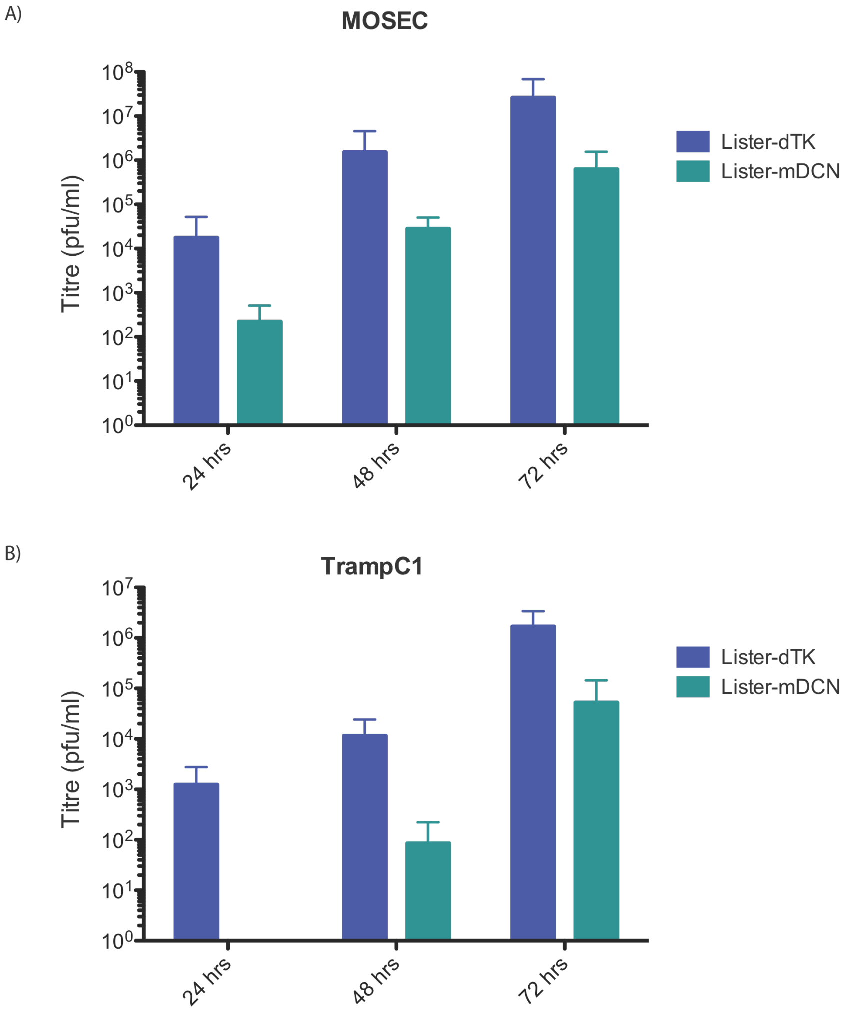

Figure 33: Spread of vaccinia virus through a collagen matrix. $2x10^5$ cells were infected with 0.1 pfu/cell of Lister-dTK or Lister-mDCN for 2 hrs and then overlaid with a 70:30 collagen matrix, which was allowed to set for one hr. Gels were then topped with normal growth media which was harvested at 24, 48 and 72hrs post-infection and titred by TCID50 assay. Data show the mean+SD of virus titre from a single experiment performed in triplicate (TrampC1) or two experiments in triplicate (MOSEC).

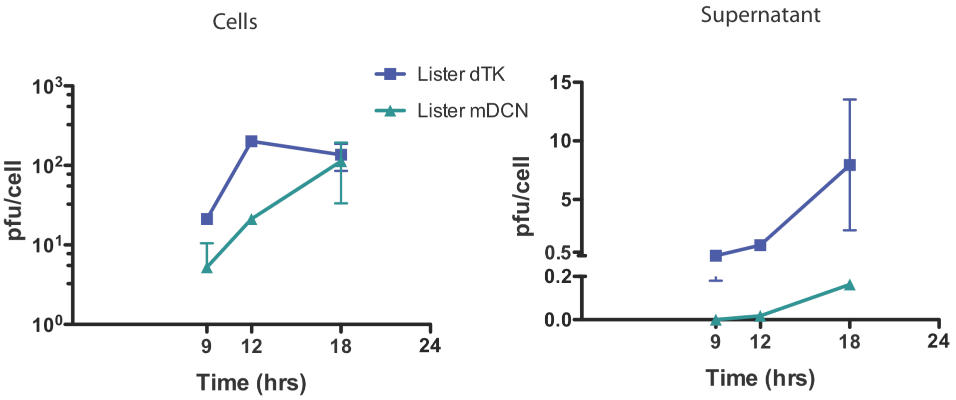

Figure 34: Early replication of Lister strains in MOSEC cells. Cells were infected with 0.1 pfu/cell and virus titre determined in both the cells (A) and the supernatant of infected cells (B) by TCID50 assay. Data show the mean+SD of triplicate wells, each titred in triplicate.

4.5.2 In vivo spread of Lister-mDCN

In order to further investigate the spread of Lister-mDCN *in vivo*, CD1 nu/nu mice bearing subcutaneous TrampC1 tumours were injected with a single dose of virus and the amount of viral DNA and viral proteins present within the tumour determined by quantitative PCR and immunohistochemistry at various timepoints after virus delivery.

4.5.2.1 Quantification of viral DNA after intratumoural delivery of Lister-mDCN

Mice were injected with a single intratumoural dose of 10^8 pfu of Lister-dTK or Lister-mDCN when tumours reached 100-200mm^3 in size. At days 4 and 8 post-injection of virus, four mice from each treatment group were culled and tumours excised. Extracted whole tumours were lysed overnight and DNA extracted from a volume of lysate corresponding to 25mg tissue. Viral DNA was amplified by qPCR using primers targeting an early vaccinia transcription factor, and normalised to the input tumour mass as individual tumour weights ranged from 103-201mg at day 4 to 309-520mg at day 8, with a mean weight of 165mg and 415mg respectively.

Viral DNA was lower in Lister-mDCN treated tumours compared to Lister-dTK treated tumours at both day 4 and day 8 following virus injection (Figure 35), although the decrease was not significant. Four days after virus injection, the mean viral load was 9.7×10^6 virus copies per mg tissue in mice treated with Lister-mDCN and 8.0×10^7 in those treated with Lister-dTK. Virus copy number increased eight days post-infection, although not as much as perhaps expected, to 2.4×10^7 virus copies per mg tissue in Lister-mDCN treated tumours and 1.7×10^8 in Lister-dTK treated tumours. This attenuation of Lister-mDCN replication *in vivo* did not correspond to a decrease in replication *in vitro,* as Lister-mDCN replication was significantly higher than that of Lister-dTK (Figure 30d). Mice treated with PBS demonstrated very low levels of virus copy number; however, this was at a similar level to that detected in water samples (non template control (NTC)) and likely represents non-specific amplification.

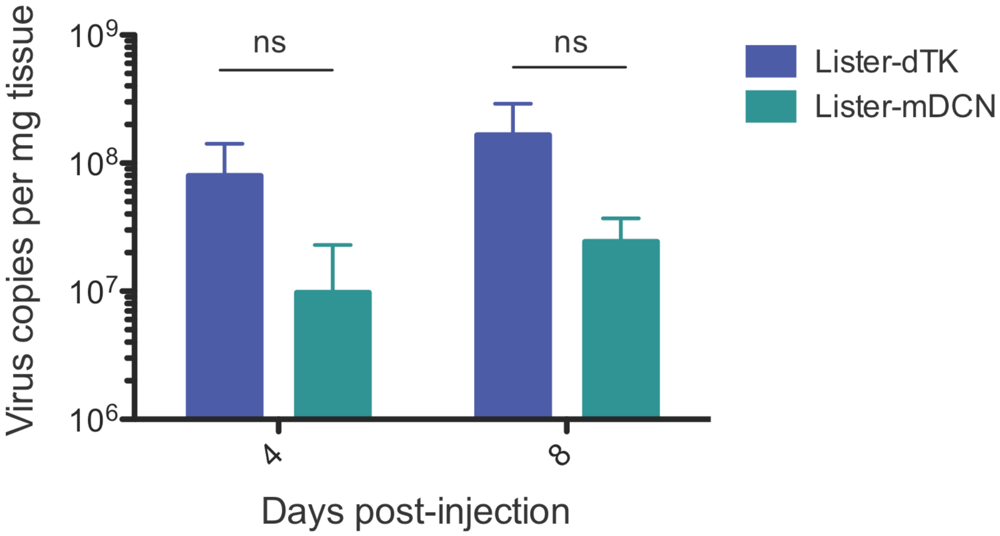

Figure 35: Replication of viral DNA in subcutaneous TrampC1 tumours. CD1 nu/nu mice were injected subcutaneously with 5x10^4 TrampC1 cells. When tumour size reached 100-200mm^3, a single dose of 10^8 pfu Lister-dTK or Lister-mDCN was injected intra-tumourally. Tumours were harvested 4 days and 8 days post-infection and DNA extracted from 25mg tumour tissue for quantification of virus copies by qPCR. Virus copies per mg tissue were determined using a standard curve of Lister-wt DNA. Data show the mean+SD virus copies/mg of four tumours per group.

4.5.2.2 Viral protein expression after intratumoural delivery of Lister-mDCN

To visualise virus dispersion throughout the tumour mass as opposed to quantification of viral DNA, 12 x CD1nu/nu mice bearing subcutaneous TrampC1 tumours were again injected intratumourally with a single dose of 10^6 pfu of either Lister-dTK or Lister-mDCN. On days 2, 4 and 6 post-injection two mice in each treatment group were culled, tumours excised and subsequent tumour sections stained for the presence of vaccinia virus proteins by immunohistochemistry. Expression of vaccinia virus proteins was evident from 2 days post-infection (Figure 36), which was the earliest timepoint tested, and there were no obvious differences between Lister-dTK and Lister-mDCN treated tumours. Vaccinia infected cells were dispersed throughout the tissue mass; furthermore there was no clear indicator of the site of injection and therefore virus spread from the initial site could not be determined. This was also the case at day 4 post-infection, although there was evidence of greater virus infection at this stage. Interestingly, no viral proteins could be detected at day 6 in tumour tissue taken from animals treated with Lister-dTK, although there was some evidence of infection in Lister-mDCN treated tumours (Figure 36).

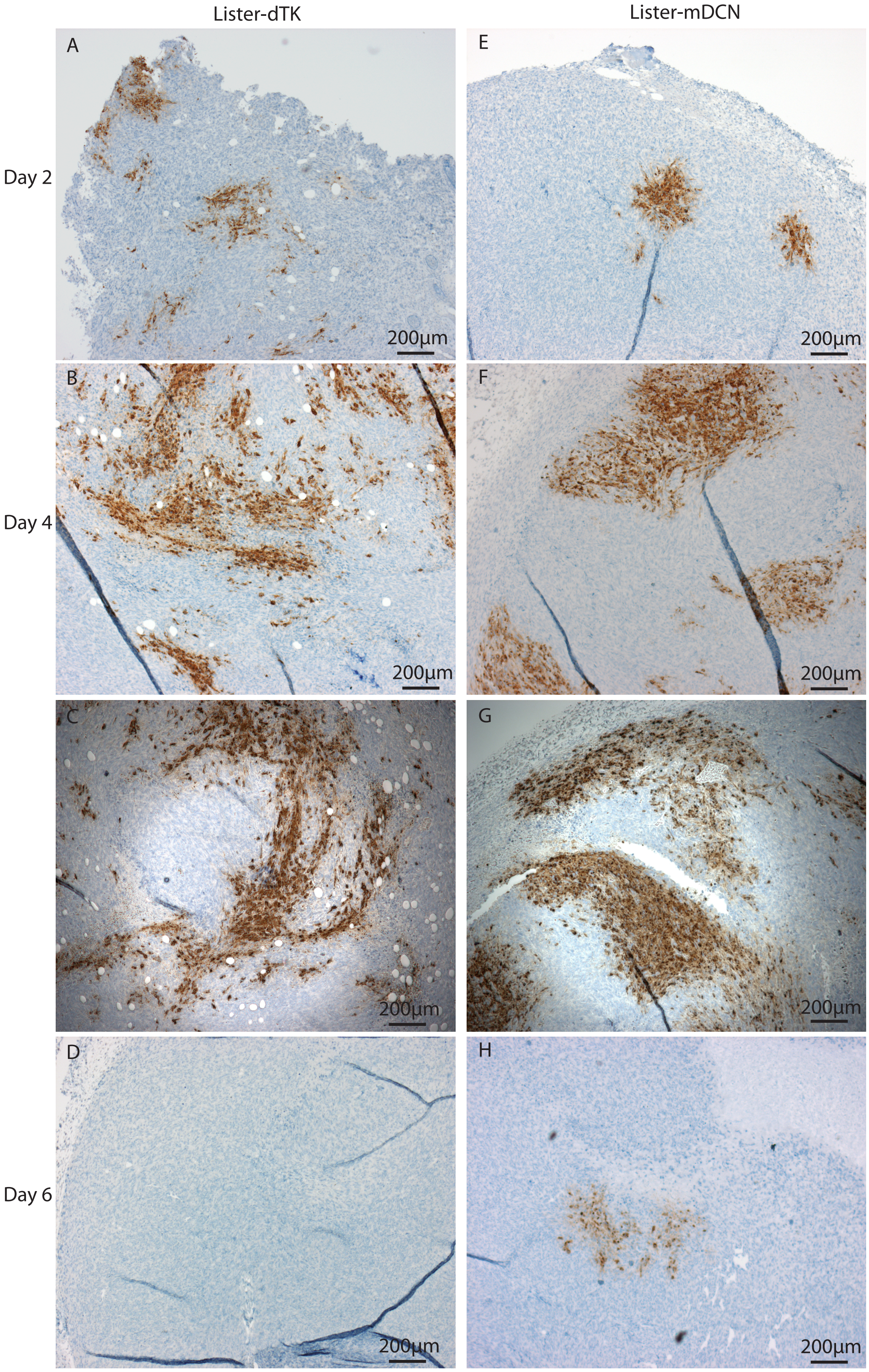

Figure 36: Intratumoural spread of Lister-mDCN. CD1 nu/nu mice were injected with a single dose of 10^6 pfu Lister-dTK (Panels A-D) or Lister-mDCN (panels E-H) and tumours harvested 2, 4 and 6 days post-infection (n=2 per group). Sections were stained for vaccinia virus proteins.

4.6 Functional assays

The interactions of decorin with various biological pathways may exert multiple anti-tumourigenic effects, including cellular growth arrest of numerous cancer cell lines by induction of p21 (De Luca, Santra et al. 1996; Santra, Mann et al. 1997) and downregulation of the EGFR (Csordas, Santra et al. 2000; Santra, Eichstetter et al. 2000; Seidler, Goldoni et al. 2006; Hu, Sun et al. 2009), induction of apoptosis (Seidler, Goldoni et al. 2006; Wu, Wang et al. 2008) and sequesteration of TGFβ (Schonherr, Broszat et al. 1998; Droguett, Cabello-Verrugio et al. 2006).

To determine if expression of decorin from a replicating vaccinia virus, Lister-mDCN, was also able to demonstrate such activity in MOSEC ovarian cancer cells and TrampC1 prostate cancer cells, a number of assays were employed. These included analysis of cell cycle by flow cytometry, and of levels of EGFR and downstream signalling proteins by immunodetection. In addition, potential inhibition of the TGFβ signalling pathway was studied.

4.6.1 Cell cycle analysis

Typically, decorin has been shown to decrease proliferation by arresting cells in G0/G1 of the cell cycle (De Luca, Santra et al. 1996; Santra, Mann et al. 1997; Wu, Wang et al. 2008). To determine the effect of Lister-mDCN on cell cycle, MOSEC cells were infected with 1pfu/cell of Lister-mDCN and cell cycle analysis performed by flow cytometry using the DNA-binding dye propidium iodide to determine cellular DNA content (Figure 37). This also allowed crude analysis of apoptotic induction by quantification of cells with subG1 levels of DNA. At 48hrs post-infection with either Lister-mDCN or the control Lister-dTK virus, there was no significant increase in the percentage of cells with subG1 DNA compared to untreated cells. At 72hrs, there was a small but significant increase from 0.7% to 2.0% following infection with Lister-mDCN; however, this was significantly less than the 4.6% observed following infection with Lister-dTK. This suggests that expression of decorin from Lister-mDCN decreases rather than enhances the induction of apoptosis in infected cells.

In contrast to published studies, which report G1 arrest as a consequence of p21 induction by decorin (De Luca, Santra et al. 1996; Santra, Mann et al. 1997), the percentage of cells in G1 was significantly lower at 48hrs and 72hrs post-infection with Lister-mDCN compared to untreated cells, with a reduction from 51% to 41%, and 70% to 46% respectively. This is perhaps not surprising given that vaccinia is proposed to drive cells through the cell cycle, and infection with Lister-dTK also resulted in a decrease of cells in G1. However, at 72hrs post-infection, the percentage of cells in G1 after infection with Lister-dTK was significantly lower (38%) compared to infection with Lister-mDCN (46%), suggesting that expression of decorin may have some modest effect on cell cycle arrest despite the fact that vaccinia virus induces progression through the cell cycle.

Infection with either virus had no effect on the percentage of cells in S phase compared to untreated cells at 48hrs post-infection, although there was a significant increase at 72hrs post-infection from 11% in untreated cells to 24% in Lister-dTK treated cells. Whilst there was a small increase to 15% in Lister-mDCN treated cells this was not significant compared to uninfected control cells, and was significantly lower than that of Lister-dTK treated cells. Again, this may suggest that while the presence of decorin cannot override the growth-stimulatory effect of vaccinia to inhibit cell proliferation overall, it can partially compensate to reduce the percentage of cells in S phase to that nearer those found in uninfected cells. This reduction in cell proliferation does not appear to negatively impact on the cytotoxicity (Figure 29) or replication (Figure 30) of Lister-mDCN compared to Lister-dTK.

Interestingly, infection with Lister-mDCN also leads to a significant increase in the percentage of cells in G2 compared to both untreated cells and cells infected with Lister-dTK (Figure 37). At 48hrs post-infection there was an increase from 20% in untreated cells to 28% following infection with Lister-mDCN and, at 72hrs post-infection this nearly doubled from 14% to 27%.

Overall, there were significant differences in each population of cells following infection with either Lister-dTK or Lister-mDCN at 72hrs post-infection. These leaned towards an attempt at cell cycle arrest, as G1 and G2 populations were significantly increased in Lister-mDCN treated cells compared to Lister-dTK treated cells, and in fact the G2 population was even higher than that of uninfected cells, implying G2/M arrest. This did not correspond to an increase in apoptotic cell death however, as the proportion of cells with subG1 DNA was lower following infection with Lister-mDCN compared to Lister-dTK. The increase in G1 and G2 populations in Lister-mDCN treated cells was at the expense of cells in S phase, which were significantly lower than that of cells treated with Lister-dTK and comparable to that of uninfected cells.

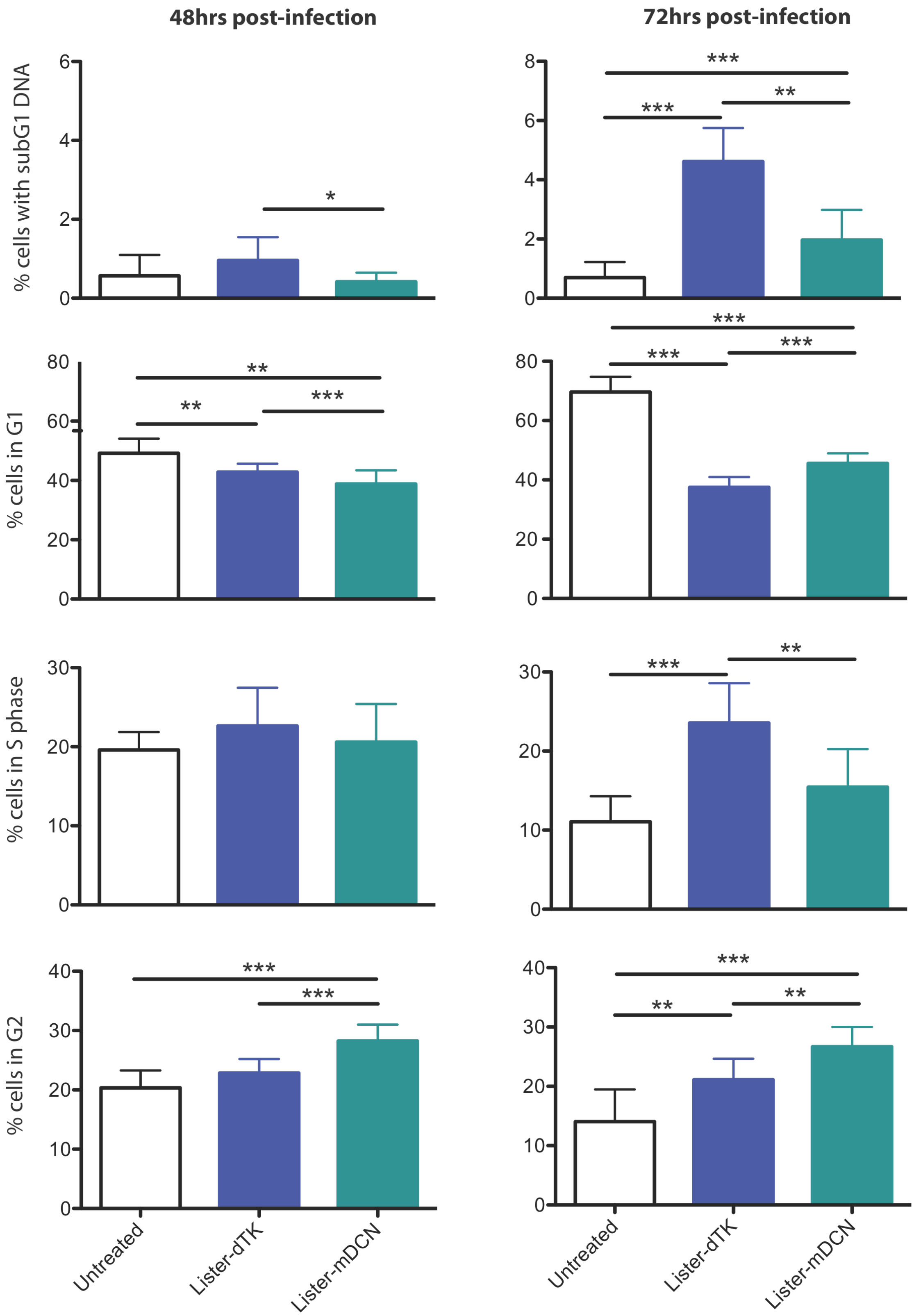

Figure 37: Effect of Lister-mDCN on the cell cycle. MOSEC cells were infected with 1 pfu/cell of Lister-dTK or Lister-mDCN and harvested 48hrs and 72hrs post-infection for analysis of cell cycle by flow cytometry. Data show the mean+SD of cells gated from three separate experiments, each perfomed in triplicate.

4.6.2 Downregulation of EGFR

As decorin has been reported to bind to the EGFR (Santra, Reed et al. 2002) and downregulate its expression and phosphorylation (Csordas, Santra et al. 2000; Santra, Eichstetter et al. 2000), levels of EGFR and the downstream signalling proteins Erk1/2 were determined in MOSEC and TrampC1 cells following infection with Lister-mDCN.

Surprisingly, given the role of the vaccinia growth factor (VGF) in stimulating cellular proliferation via interaction with the EGFR (Buller, Chakrabarti et al. 1988; Buller, Chakrabarti et al. 1988; Andrade, Silva et al. 2004; Vermeer, McHugh et al. 2007; Postigo, Martin et al. 2009), levels of total EGFR were decreased in MOSEC cells following infection with both Lister-dTK and Lister-mDCN (Figure 38). This was evident at 48hrs post-infection and, even more surprisingly, there was a greater decrease in total EGFR in Lister-dTK infected cells compared to Lister-mDCN infected cells. This was despite comparable replication (Figure 30) and cytotoxic effects (Figure 29) of the two viruses at 48hrs post-infection. At 72hrs post-infection, EGFR was undetectable in both Lister-dTK and Lister-mDCN infected cells. The decrease in total EGFR corresponded to a decrease in phosphorylated EGFR (Figure 38). Although total EGFR levels were relatively unchanged at 24hrs post-infection, a reduction in phosphorylated EGFR was observed at this timepoint. Conversely, the reduction was greater in Lister-mDCN infected cells than in Lister-dTKinfected cells, despite higher overall EGFR expression. Whilst phosphorylated EGFR was observed in uninfected cells at 48hrs and 72hrs, none could be detected in Lister-dTK or Lister-mDCN infected cells at these timepoints post-infection (Figure 38).

To determine if the decrease in EGFR expression and activation corresponded to abrogation of downstream signalling pathways, the expression of Erk1/2 was determined in the same samples. Levels of Erk1 remained unchanged following infection with Lister-dTK and Lister-mDCN at 24hrs, 48hrs and 72hrs post-infection (Figure 38). Expression of total Erk2 appeared to decrease marginally in infected cells at 48hrs post-infection, and this decrease was more apparent at 72hrs post-infection. Consistent with the relatively similar levels of Erk1 in uninfected and infected cells, levels of phosphorylated Erk1 were also similar. Interestingly, there appeared to be a decrease in Erk2 phosphorylation (second lower band) at 72hrs post-infection with Lister-dTK but not with Lister-mDCN (Figure 38). However, as the antibody used to detect phosphorylated Erk was raised against a short amino acid containing phosphorylated Tyr204 of Erk, and as only Erk1 and not Erk2, is phosphorylated at the Tyr204 site, it is presumed that the band observed at 42kDa (assumed to be Erk2) is non-specific.

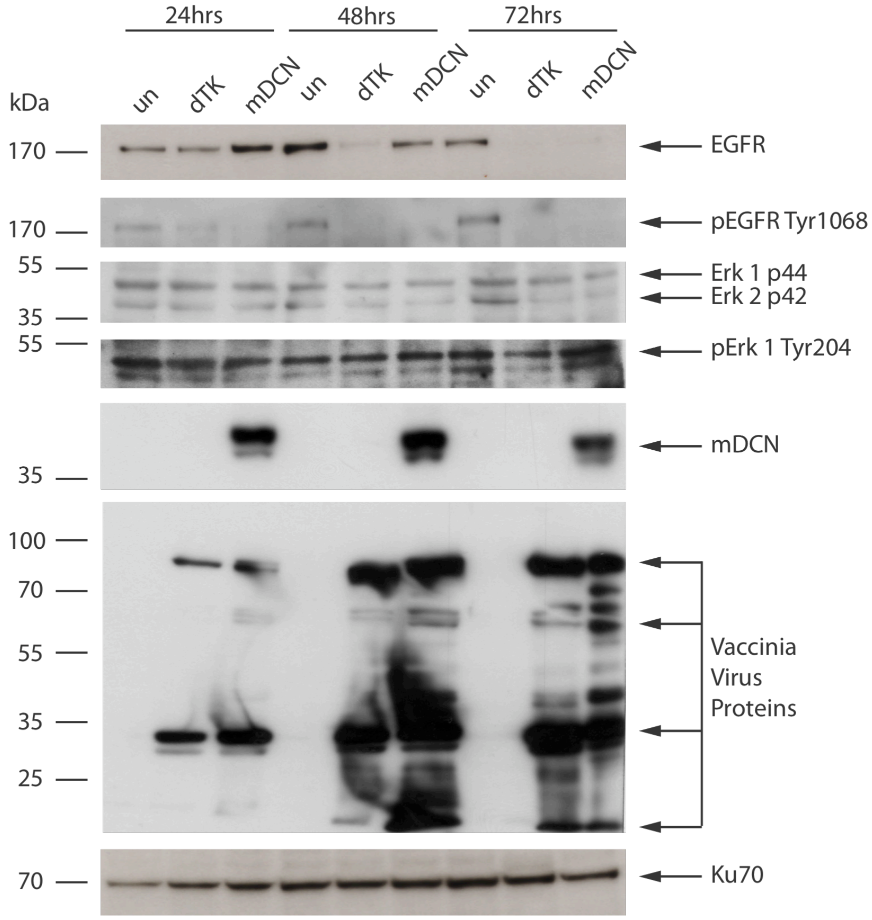

Figure 38: Expression of EGFR, pEGFR and downstream signalling following infection with vaccinia virus. MOSEC cells were infected with 1pfu/cell Lister-dTK or Lister-mDCN and harvested 24hrs, 48hrs and 72hrs post-infection. Total levels of EGFR, pEGFR Tyr1068, Erk1, Erk2, pErk1 Tyr204 and pErk2 Tyr204 were determined by western blotting.

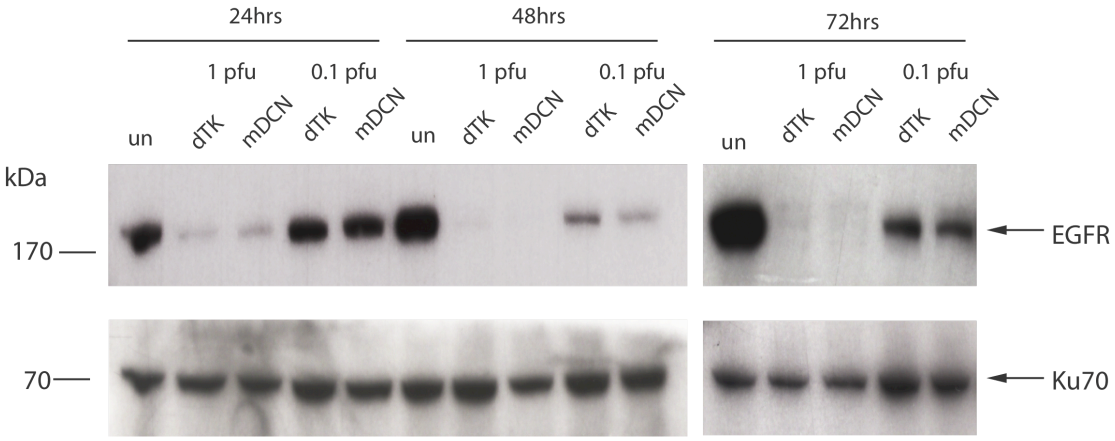

Figure 39: Vaccinia virus decreases total levels of EGFR. TrampC1 cells were infected with 0.1pfu/cell and 1pfu/cell of virus and lysates collected at 24hrs, 48hrs and 72hrs post-infection. EGFR was detected from total cell lysates by western blotting. Representative blot of 2 experiments shown.

Downregulation of EGFR was also observed in TrampC1 cells infected with Lister-mDCN (Figure 39) although, again, this was also observed in cells infected with Lister-dTK as well, suggesting that it is a result of vaccinia virus infection and not interaction between decorin and the EGFR. At 24hrs post-infection with 1 pfu/cell Lister-dTK or Lister-mDCN, EGFR expression was decreased compared to uninfected cells, and was undetectable at 48hrs and 72hrs post-infection. This decrease in EGFR was dose-dependent, as cells infected with a lower dose (0.1pfu/cell) had levels of EGFR similar to that of uninfected cells at 24hrs. A decrease was observed at 48hrs and 72hrs post-infection, although this was less than cells infected with 1pfu/cell.

The surface expression of EGFR was also analysed in TrampC1 cells by flow cytometry (Figure 40). Consistent with the decrease in total EGFR observed by western blotting (Figure 39), a decrease in EGFR at the cell membrane surface was also apparent. At 72hrs post-infection with 0.1pfu/cell of Lister-dTK or Lister-mDCN, levels of EGFR decreased by 45% and 42% respectively. This decrease was again dose-dependent as infection with 1pfu/cell Lister-dTK or Lister-mDCN resulted in a reduction of surface levels of EGFR of 58% and 50% respectively.

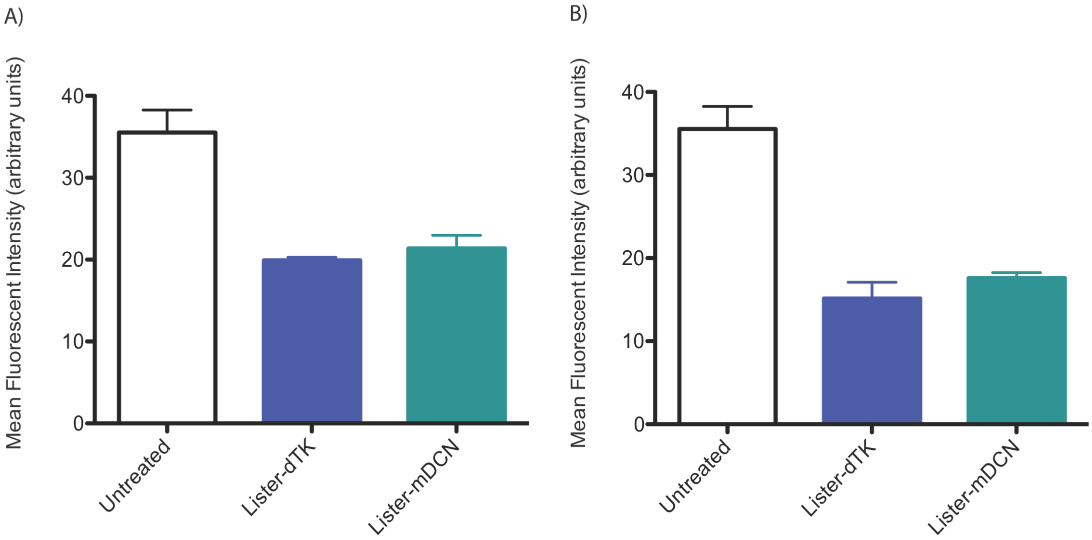

Figure 40: Vaccinia virus decreases surface levels of EGFR. TrampC1 cells were infected with A) 0.1 pfu/cell or B) 1 pfu/cell of virus and harvested 72hrs post-infection. Mean Fluorescent Intensity (MFI) represents levels of EGFR as determined by flow cytometry. Bars show the mean+SD MFI of triplicate wells.

4.6.3 Effect of decorin on TGFβ signalling

Decorin has been show to bind to TGFβ and preventing interaction with its receptor (Droguett, Cabello-Verrugio et al. 2006). The effect of mDCN expressed from Lister-mDCN on TGFβ signalling was therefore investigated in MOSEC cells. MOSEC cells infected with Lister mDCN showed no change in phosphorylation levels of Smad2, a signalling molecule phosphorylated upon TGFβ receptor activation, following addition of TGFβ compared to either uninfected or Lister-dTK infected cells (Figure 41a). In fact, infection with 1pfu/cell Lister-mDCN appeared to increase levels of phospho-Smad2 even in the absence of TGFβ stimulation in comparison to uninfected or Lister-dTK infected cells. Cells cultured in the presence of recombinant mDCN also failed to show a decrease in levels of phosphorylated Smad2.

Although human TGFβ shares 99% homology with murine TGFβ (and thus murine decorin might be expected to bind to the recombinant human TGFβ), in order to exclude the possibility that the absence of signalling inhibition by mDCN was due to an inability to bind human TGFβ, a further experiment was performed using human cells and the recombinant human decorin protein. A549 lung carcinoma cells were cultured in the presence of decorin for 48 hours and human TGFβ added before cells were harvested to assess levels of Smad2 phosphorylation (Figure 41b). The presence of 100nM and 10nM decorin had no effect on Smad2 phosphorylation, whereas treatment with 1nM decorin for 48 hours led to a small decrease, which also corresponded with a decrease in total Smad2 levels.

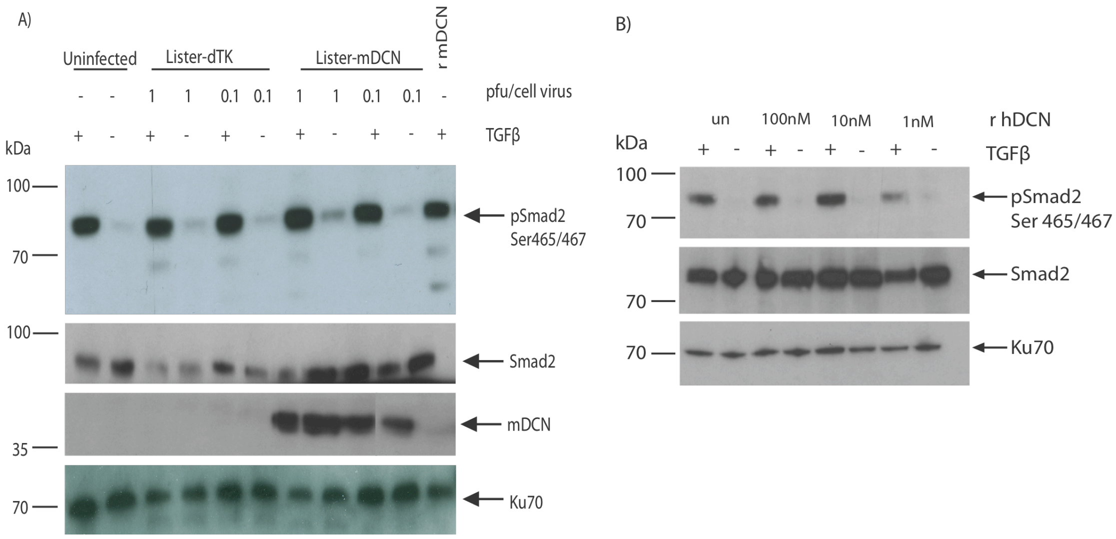

Figure 41: Effect of decorin on TGFβ signalling. Lister-mDCN does not inhibit phosphorylation of Smad2 in response to TGFβ. A) MOSEC cells were infected with Lister-dTK or Lister-mDCN at 1pfu/cell or 0.1pfu/cell and collected 48hrs later, after stimulation with 5ng/ml recombinant human TGFβ for 90 minutes prior to harvest. As a control for decorin interaction in the absence of virus, cells were also cultured in the presence of 100nM recombinant murine decorin (rmDCN). The line in the blot detecting mDCN shows where adjacent lanes were brought together. B) A549 human lung carcinoma cells were cultured in the presence of recombinant human decorin (rhDCN) for 48hrs before the addition of 5ng/ml recombinant human TGFβ for 90 minutes. Levels of total Smad2 and phosphorylated Smad2 (Ser465/467) were analysed by western blotting.

4.7 Anti-tumour efficacy of Lister-mDCN in vivo

To determine if Lister-dTK had any anti-tumour efficacy *in vivo*, and if Lister-mDCN demonstrated any advantage over this control virus, viruses were delivered either intratumourally to TrampC1 tumours growing subcutaneously (sc), or intraperitoneally (ip) to MOSEC tumours also growing ip. Tumour burden was monitored by either external measurement of sc tumours, or by *in vivo* bioluminescent imaging respectively.

4.7.1 Intratumoural delivery

Nude mice bearing subcutaneous TrampC1 tumours were injected intratumourally with PBS, or 10^8 pfu/dose of either Lister-dTK or Lister-mDCN on days 16, 18 and 20 after tumour cell implantation, for a total of three doses. Several mice showed signs of tumour ulceration on day 24, 8 days after the first intratumoural injection, and thus had to be culled under UK Home Office license regulations. This ulceration was not virus-specific as several mice that had received PBS also had ulcerating tumours, and was believed to be an effect of rapidly growing tumours. As a result, the experiment was terminated on day 24, with the exception of four mice, two of which had received PBS and two of which Lister-mDCN. Whilst treatment with Lister-mDCN did not result in tumour regression, or a stable tumour volume, the rate of tumour growth was significantly reduced compared to that of mice receiving PBS (Figure 42A and Figure 42B). Treatment with Lister-mDCN also resulted in a significant difference in end tumour volume compared to that of mice treated with Lister-dTK (Figure 42A). In contrast, Lister-dTK failed to have any significant effect on either overall tumour volume (Figure 42A), or tumour growth relative to individual tumour size at the time of the first injection (Figure 42B), although there was a trend towards a reduction in relative tumour growth which may have been more evident if the experiment had progressed beyond 24 days.

Two mice each in both the PBS and the Lister-mDCN treatment group were healthy at day 24 and showed no signs of tumour ulceration. These four mice were allowed to progress until the maximum tumour volume was reached in one mouse in the PBS group; this aimed to provide preliminary *in vivo* data that might indicate tumour efficacy had the entire experiment been continued until completion. Although the numbers were small, there was a significant reduction in tumour growth in mice treated with Lister-mDCN compared to PBS (Figure 42C) and tumour volume did not reach the maximum permitted volume when the experiment was terminated completely.

Upon termination of the experiment at either day 24 or day 33, tumours were excised and fixed for immunohistochemistry for the detection of vaccinia virus proteins, indicating virus replication *in vivo*. Tumour sections were also stained for decorin to demonstrate *in vivo* expression of the protein from Lister-mDCN. As expected, mice treated with PBS had tumours absent of vaccinia virus proteins (Figure 44B); there was some evidence of positive staining for decorin, although this was weak and constrained to the stroma (Figure 43B). In contrast, mice treated with Lister-mDCN demonstrated clear expression of decorin in the tumour (Figure 43C and D), which overlapped with expression of vaccinia virus protein expression (Figure 43E and F). Staining for decorin was weaker than that of vaccinia proteins, although this does not necessarily imply reduced expression as it may reflect different sensitivities of the antibodies to their respective target antigens. The presence of decorin was particularly strong in the cytoplasm of infected cells, although there was also evidence of staining in the extracellular matrix (Figure 43D). This may represent release of decorin from infected cells, either by active secretion or cell lysis, which is consistent with the detection of decorin in the supernatant of infected cells *in vitro* (Figure 28). Whereas the tumours of mice treated with Lister-dTK demonstrated large areas of virus infection (Figure 44E and F), there was no evidence of decorin expression (Figure 44C and D).

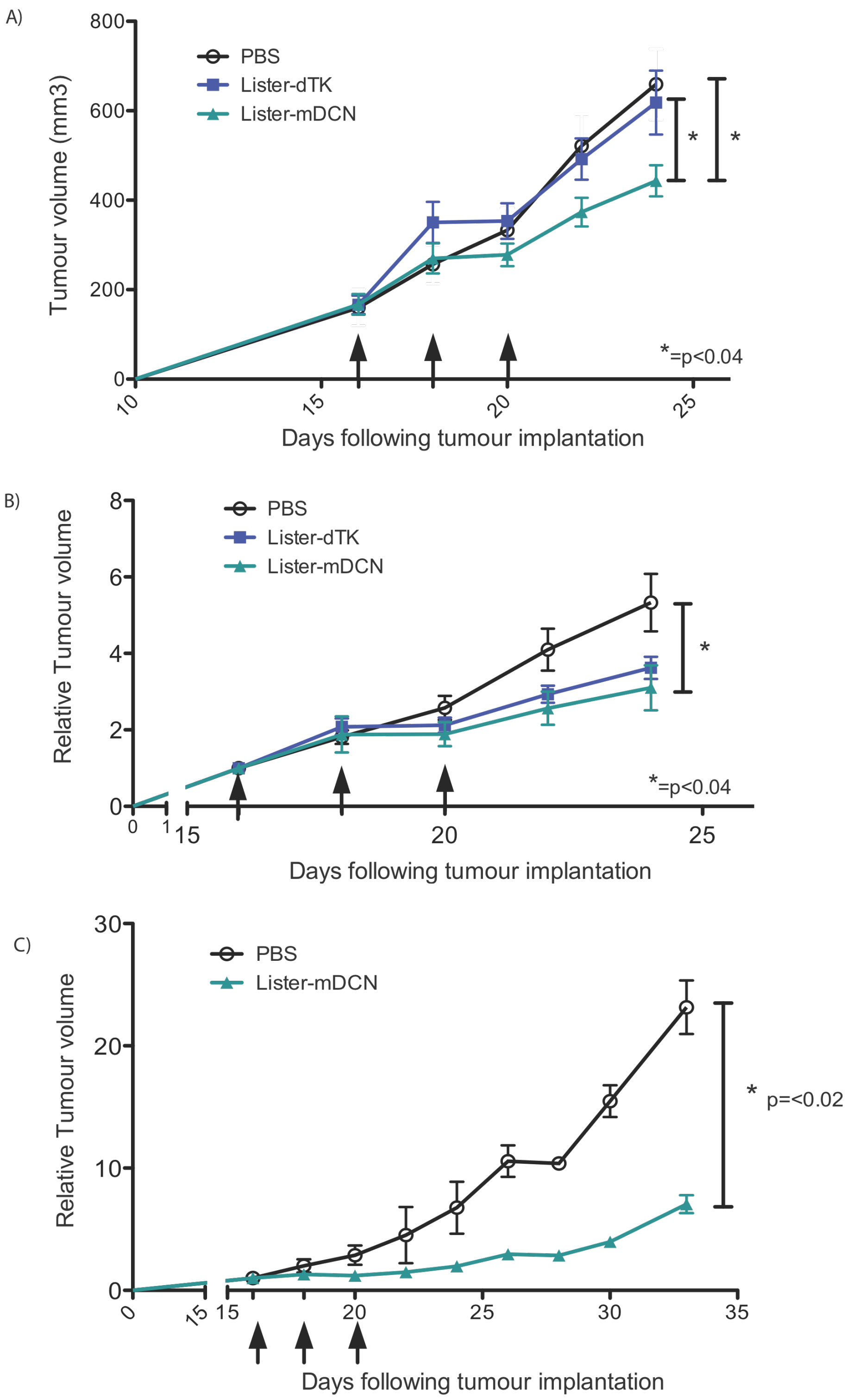

Figure 42: Growth of subcutaneous TrampC1 tumours in nude mice following intratumoural delivery of Lister-mDCN. CD1 nude/nude mice were injected subcutaneously with 5x10^4 TrampC1 cells. PBS, Lister-dTK or Lister-mDCN (10^8 pfu) was delivered intratumourally on days 16, 18 and 20 following tumour implantation, when tumours were approximately 100-200mm^3. Tumour size was measured at regular intervals and data shows the mean+SEM of each treatment group). A) Tumour volume (n=8 per group. B) Tumour growth relative to individual starting volume at the time of first dose (n=8 per group). C) Relative tumour growth (n=2 per group).

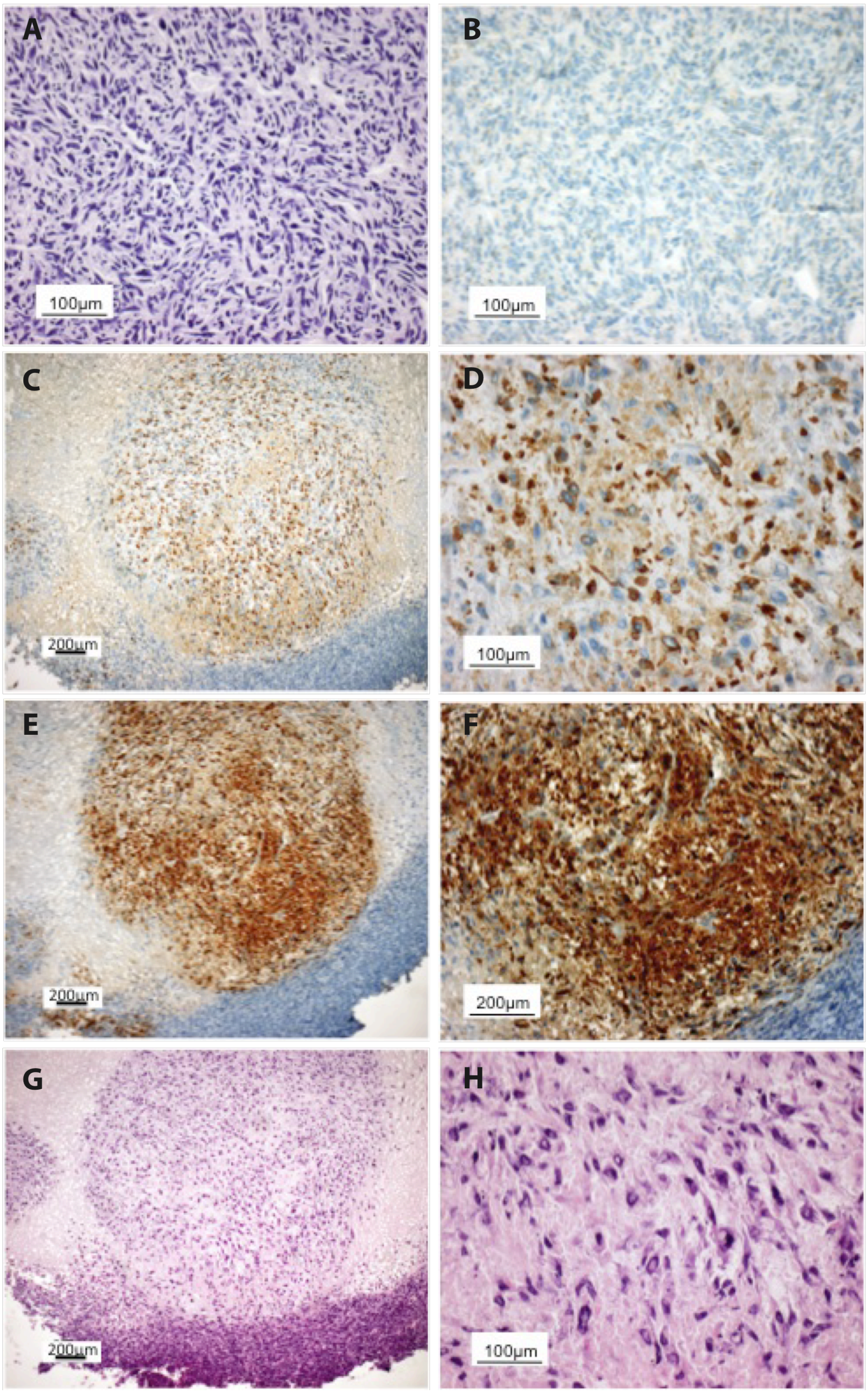

Figure 43: Immunohistochemistry of TrampC1 tumours treated with (A and B) PBS or (C-H) three doses of 10^8 pfu Lister-mDCN. Tumours were sectioned and stained for the presence of decorin (B-D) or vaccinia virus proteins (E-F), parallel sections were stained with H&E (A, G and H).

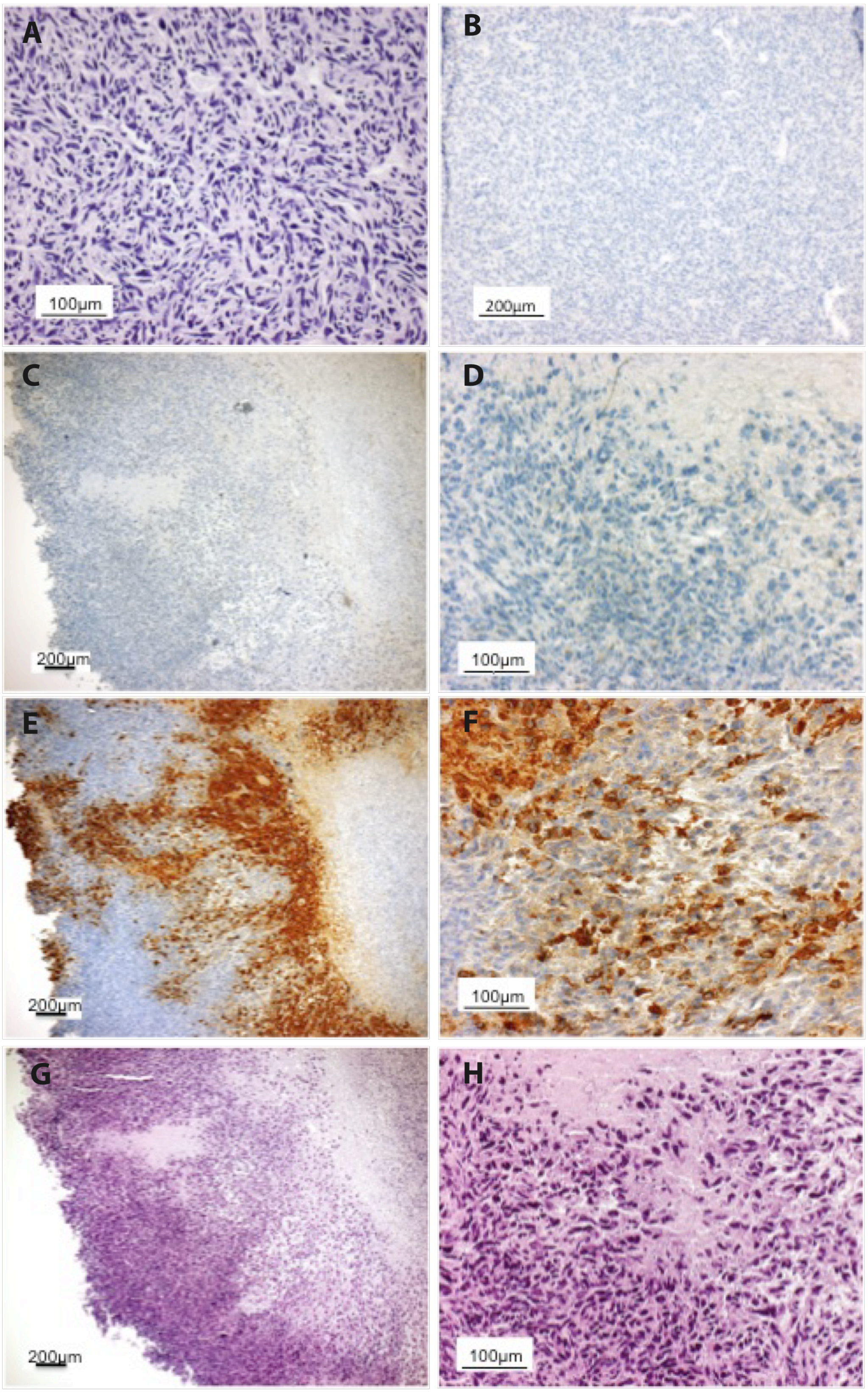

Figure 44: Immunohistochemistry of TrampC1 tumours treated with (A and B) PBS or (C-H) three doses of 10^8 pfu Lister-dTK. Tumours were sectioned and stained for the presence of decorin (C-D) or vaccinia virus proteins (B, E-F), parallel sections were stained with H&E (A, G and H).

4.7.2 Intraperitoneal delivery

In order to determine the effect of Lister-mDCN on the growth of ovarian tumours, an intraperitoneal model of ovarian cancer was used in immunocompetent female mice. Previously, it was demonstrated that intraperitoneal (ip) delivery of vaccinia virus was able to replicate specifically in primary and metastatic tumour tissue in nude mice bearing ip Skov3ip1 tumours. To expand on this work, and as decorin is proposed to have an effect on the tumour microenvironment and potentially the immune response, the effect of Lister-mDCN and Lister-dTK on controlling tumour growth in immunocompetent mice was studied. $5x10^6$ MOSEC cells expressing luciferase were injected into the peritoneal cavity of immunocompetent C57BL/6 mice and tumour burden monitored at regular intervals using bioluminescence imaging.

4.7.2.1 MOSEC ip tumours treated with three doses of Lister-mDCN

Mice were randomly assigned to receive PBS, Lister-dTK or Lister-mDCN (10^8 pfu/dose) in three doses ip on days 22, 25 and 28 following injection of tumour cells. Tumour burden was quantified by measuring luminescence and normalising photon flux from a defined region covering the entire abdominal area.

Following three doses of Lister-mDCN, a decrease in mean luminescence ($p/s/cm^2/sr$) was observed from $3.0x10^5$ on day 18 to $7.6x10^4$ on day 35 (Figure 45A). When the individual tumour burden at day 35 was normalised to that on day 18, 12 out of 14 mice treated with Lister-mDCN showed signs of initial tumour regression, with an overall mean decrease in tumour burden of over 70% (Figure 45B). Over the same period a decrease in tumour burden was also observed in mice treated with Lister-dTK and PBS; although this may highlight experimental variation in measurements taken on different days, these decreases were smaller than that in the Lister-mDCN treated group, suggesting potential therapeutic activity of Lister-mDCN.

Response to Lister-mDCN was transient however, and the mean tumour burden was comparable in all three groups at day 46 (Figure 45A and Figure 45B). Despite rapid growth of MOSEC-luc cells *in vitro*, tumour growth is relatively slow *in vivo* and although an increase in tumour burden was observed between days 18 and 46 this was relatively small. There was a 2.3 fold increase in tumour burden in mice treated with PBS, which was only just higher than that of mice treated with either Lister-dTK or Lister-mDCN where both groups showed a 2.1 fold increase in tumour burden. Between days 46 and 63, when the experiment was terminated, tumour burden continued to increase in all three groups, with the final tumour burden in mice treated with Lister-dTK exceeding that of mice treated with PBS (Figure 45). Mice treated with Lister-mDCN had an overall reduced tumour burden compared to mice treated with either Lister-dTK or PBS (Figure 45A) and, although tumours still progressed, this was slower with a 6-fold increase in tumour burden compared to a 17-fold increase and a 29-fold increase in PBS and Lister-dTK treated mice respectively (Figure 45B). Tumour burden at day 63 was significantly lower in Lister-mDCN treated mice compared to Lister-dTK treated, although treatment with either virus did not significantly reduce tumour growth compared to the PBS control treatment group.

Interestingly, these differences in tumour growth were only apparent at day 63, as tumour burden was very similar at the approximate time that angiogenesis is initiated (day 45) in MOSEC tumours growing ip (personal communication, Iain McNeish, BCI, Queen Mary). Therefore, the slower tumour growth rate in mice treated with Lister-mDCN after this time may be a result of interactions of decorin with factors involved in angiogenesis, as has been described previously (Grant, Yenisey et al. 2002; Fiedler and Eble 2009), although this was not investigated further. Upon termination of the experiment, tumour burden was low in all mice examined and insufficient tissue was obtained for pathological review.

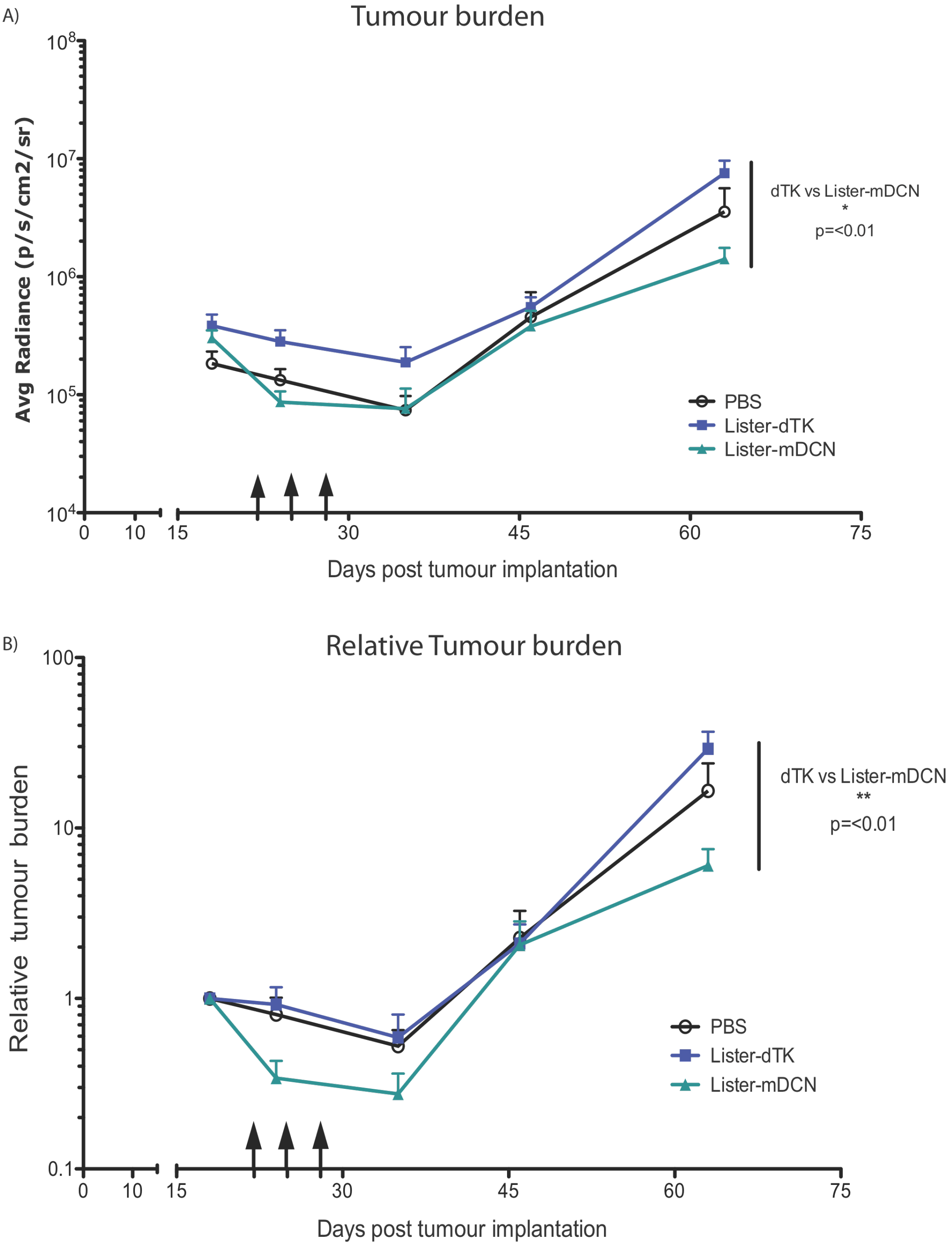

Figure 45: Growth of MOSEC intraperitoneal tumours following intraperitoneal delivery of Lister-mDCN. Mice were injected with 5x10^6 MOSEC-luc cells followed by ip delivery of PBS, Lister-dTK or Lister-mDCN (10^{8}pfu) on days 22, 25 and 28 (indicated by solid arrows on x axis). A) Data shows the mean+SEM of luminescence in photons/second/cm^2/steradian (p/s/cm^2/sr). B) Tumour burden was normalised relative to the individual starting tumour burden determined on day 18. Data shows the mean+SEM relative growth per group. n=14 (Lister-dTK and Lister-mDCN) and n=12 (PBS).

4.7.2.2 MOSEC ip tumours treated with 5 consecutive doses of Lister-mDCN

As partial tumour regression, albeit transient, was observed following intraperitoneal delivery of Lister-mDCN a second experiment was performed that aimed to improve upon this by earlier treatment, coupled with a higher dose delivered more frequently. As before, $5x10^6$ MOSEC cells expressing luciferase were injected into the peritoneal cavity of C57BL/6 immunocompetent mice and tumour burden monitored by bioluminescence imaging. Mice were injected intraperitoneally with PBS, Lister-dTK or Lister-mDCN (10^8 pfu) on 5 consecutive days, starting on day 10 after tumour cell injection. Tumour cell burden was measured on day 10 prior to the first dose and at regular intervals thereafter. Four mice in the PBS group, two in the Lister-dTK treated group and one in the Lister-mDCN group had a mean luminescence of $<10^4$ p/s/cm^2/sr on day 10 compared to the mean group average of $8x10^4$, $6.4x10^4$ and $8.9x10^4$ respectively. These mice had a 30-420 fold increase in luminescence upon the next assessment of tumour burden on day 17 (compared to an average of 1.5-2.4 fold increase), and as such were excluded from future analysis. In addition, one mouse in the PBS group was culled on day 13 due to ill health.

Tumour burden was monitored in the remaining mice until day 67 and treatment with either Lister-dTK or Lister-mDCN did not demonstrate anti-tumour efficacy compared to PBS treated mice (Figure 46). Tumour burden, as determined by bioluminescence imaging, increased steadily over the timecourse of the experiment with a 47-fold, 64-fold and 50-fold increase in luminescence in PBS, Lister-dTK and Lister-mDCN treated mice respectively (Figure 46B). In contrast to the first experiment, when transient regression of tumours was observed shortly after virus delivery (Figure 45) there was no such regression of tumour in this experiment (Figure 46).

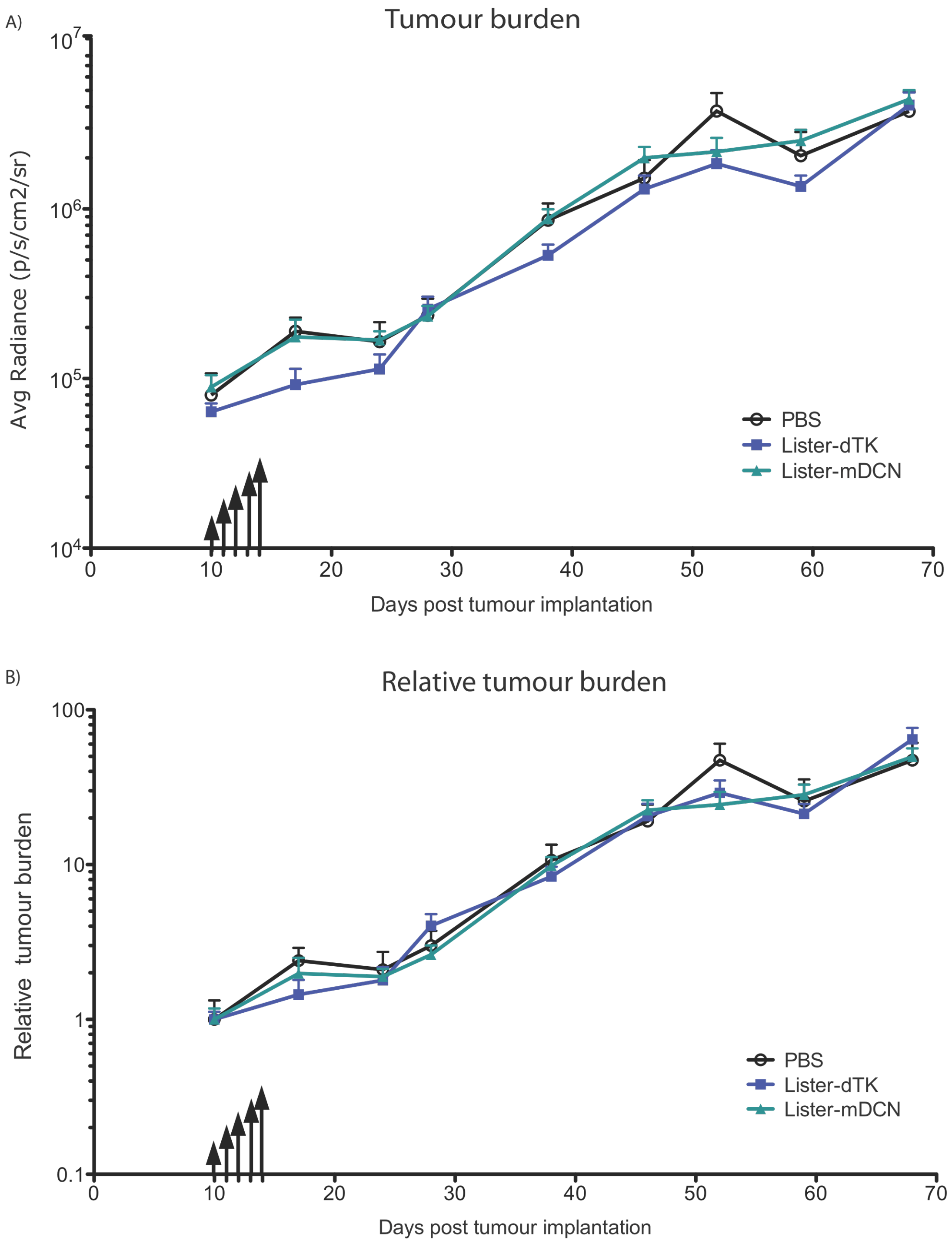

Figure 46: Growth of MOSEC tumours ip following delivery of Lister-mDCN daily. C57BL/6 mice were injected with $5x10^6$ MOSEC-luc cells followed by 5 doses of PBS, Lister-dTK or Lister-mDCN (10^8pfu) ip on days 10-14 (indicated by solid arrows on x axis). A) Data show the mean+SEM of luminescence in photons/second/cm^2/steradian (p/s/cm^2/sr). B) Tumour burden was normalised relative to the individual starting tumour burden determined on day 18. Data show the mean+SEM relative growth per group. n=14 (Lister-mDCN), n=13 (Lister-dTK) and n=5 (PBS).

4.8 Discussion

A novel vaccinia virus, Lister-mDCN, was constructed to express the extracellular matrix protein decorin and its efficacy compared to that of a control virus, Lister-dTK. Decorin has a growth inhibitory effect on tumour cells (Nash, Loercher et al. 1999; Koninger, Giese et al. 2004; Hu, Sun et al. 2009; Bi, Pohl et al. 2012), and interactions with both the EGF receptor (Moscatello, Santra et al. 1998; Csordas, Santra et al. 2000; Hu, Sun et al. 2009) and c-met receptor (Goldoni, Humphries et al. 2009). Furthermore, its expression from a replicating adenovirus may enhance viral spread (Choi, Lee et al. 2010). Unfortunately, despite expression and release of decorin from Lister-mDCN infected cells, no demonstrable effect of decorin could be shown. Furthermore, replication and cytoxicity of both viruses were comparable and Lister-mDCN failed to exhibit enhanced spread or *in vivo* activity compared to the control virus.

Initial findings demonstrated that addition of recombinant decorin did not detrimentally affect *in vitro* replication or cytotoxicity of vaccinia virus. Previously, recombinant decorin has been shown to inhibit the proliferation of ovarian (Nash, Loercher et al. 1999), pancreatic (Koninger, Giese et al. 2004), colon (Bi, Pohl et al. 2012) and prostate (Hu, Sun et al. 2009) cancer cells in culture. Here, treatment of TrampC1 prostate cancer cells with 10µg/ml recombinant decorin for 72hrs decreased cell number by 22%, suggesting that decorin may have some growth inhibitory effect. Whilst this would need to be repeated in several more cell lines, and using a similar protein as a negative control, to draw a meaningful conclusion, this is consistent with data from other studies. Treatment of the colon cancer cell line HCT116 with 3µg/ml recombinant protein core for 24hrs also inhibited proliferation by 22% (Bi, Pohl et al. 2012). Other studies have shown a better response but these have used a concentration of decorin up to ten times in excess of that used here (Nash, Loercher et al. 1999; Koninger, Giese et al. 2004).

Interestingly, the ability of decorin to inhibit cell growth appears to rely on interactions with components of the ECM for some cell lines, as pancreatic cancer cell growth was only inhibited by decorin when cultured on collagen coated surfaces (Koninger, Giese et al. 2004). In contrast, proliferation of the ovarian cancer cells SKOV3 and 2774 was inhibited by decorin, but this was not apparent when cells were grown on Matrigel basement membrane protein coated surfaces (Nash, Loercher et al. 1999). Regardless of culture conditions, growth inhibition by decorin has been attributed to a p21-mediated arrest in G1 of the cell cycle (Nash, Loercher et al. 1999; Koninger, Giese et al. 2004). Whilst the effect of recombinant decorin on cell cycle was not studied here, comparison of the cell cycle of MOSEC cells grown on plastic and infected with either Lister-dTK or Lister-mDCN, showed a significantly higher percentage of cells in G1 in Lister-mDCN infected cells. Interestingly, infection with Lister-mDCN also led to an increase in cells in G2 compared to both untreated and Lister-dTK infected cells, an effect which has not previously been documented. It is important to note that the differences in cell cycle observed here cannot definitely be attributed directly to the actions of decorin however, as it is possible that differences between individual constructs, their replication and cytotoxicity may also affect both cell proliferation and cell death.

Lister-mDCN failed to demonstrate enhanced replication or cytotoxicity *in vitro* in murine ovarian, pancreatic and prostate cancer cell lines, with the exception of an increase in recoverable virus at one timepoint in TrampC1 prostate cancer cells. As this was not a primary expectation, this was not in itself disappointing. The actions of decorin were not proposed to directly enhance virus replication or cell death. Rather, it was a concern that the reported growth inhibition and downregulation of EGFR by decorin might adversely affect virus efficacy. Thus, these experiments were designed to address this concern, and duly showed that insertion of decorin into Lister-dTK did not attenuate the virus.

Further analysis of Lister-mDCN infected cells demonstrated that decorin protein was expressed in a dose dependent manner and, consistent with previous data (Nash, Deavers et al. 2002), uninfected ovarian cancer cells were devoid of decorin. Crucially however, levels of decorin in the supernatant of infected cells were far lower than the effective concentrations used to demonstrate growth-inhibitory activity, or downregulation of EGFR activity, elsewhere in previous studies. Levels of decorin reached 162ng/ml and 187ng/ml 72hrs post-infection in TrampC1 and MOSEC cells respectively. In contrast, growth inhibitory effects on tumour cell growth were observed at concentrations in excess of 75μg/ml (Nash, Loercher et al. 1999; Koninger, Giese et al. 2004; Hu, Sun et al. 2009), far exceeding that which was achieved by expressing decorin from vaccinia virus here.

Similarly, the concentration at which decorin has been shown effectively to decrease phosphorylation of EGFR in prostate cancer and squamous cell carcinoma cells ranges from 50-100μg/ml (Moscatello, Santra et al. 1998; Hu, Sun et al. 2009). Where decorin has been shown to attenuate EGF-induced EGFR phosphorylation, this has also been at a concentration hugely in excess of that of the natural ligand, 80 μg/ml compared to 100ng/ml of EGF (Hu, Sun et al. 2009). Whilst it can be argued that these high concentrations are not physiologically relevant (normal serum level of decorin in healthy people is reported at 1.8 ± 0.09 ng/ml (Bolton, Segal et al. 2008) and 7.8 ± 3.1ng/ml (Wu, Wu et al. 2010) in two separate studies), it remains that treatment with 10mg/kg protein *in vivo* results in reduced tumour growth, a decrease in proliferation, and an increase in apoptotic tumour cell death (Seidler, Goldoni et al. 2006; Hu, Sun et al. 2009), without any adverse side effects. Furthermore, stable expression of decorin, or expression from vectors that are not likely to achieve such high expression levels, exert similar anti-tumour effects (Csordas, Santra et al. 2000). Nonetheless, the levels of decorin produced by vaccinia infected cells in this work are certainly lower than those achieved elsewhere, and may offer some explanation as to the lack of activity observed.

The EGFR receptor is well characterised for its role in cell proliferation and is a target for a number of therapeutic strategies in the clinic, including monoclonal antibodies and tyrosine kinase inhibitors. Whilst these have shown therapeutic benefit in a subset of patients with breast cancer, and in other cancers, their use against ovarian cancer has been limited to date and they are not approved therapies (Zeineldin, Muller et al. 2010), although the results of a large scale Phase III trial of chemotherapy with erlotinib are due to report in 2013. However, tumour cell dependency on the EGFR is not restricted to its kinase activity and role in proliferation; EGFR has also been shown to stabilise levels of another cell membrane protein, sodium/glucose co transporter (SGLT1), which is essential for the transport of glucose into the cell (Weihua, Tsan et al. 2008). Thus, attempts to target the EGFR by means that do not directly target kinase activity, such as decorin, may still yield results in ovarian cancer. Conversely, it was feared that inhibition of EGFR might attenuate vaccinia replication and spread. However, infection with Lister-mDCN did not reduce either total EGFR expression or levels of phosphorylated EGFR when compared to the control virus, Lister-dTK. Rather, and to our surprise given that vaccinia is widely reported to exploit the EGFR pathway to maximise replication and spread (Buller, Chakrabarti et al. 1988; Andrade, Silva et al. 2004), both Lister-dTK and Lister-mDCN infection led to a marked decrease in levels of both total and phosphorylated EGFR. This effect was dose-dependent in TrampC1 prostate cancer cells and evident as early as 24hrs post-infection, which was the earliest timepoint tested. Levels of total EGFR and phosphorylated EGFR were also undetectable at 72hrs and 48hrs post-infection respectively in MOSEC ovarian cancer cells. However, phosphorylated Erk1, downstream of EGFR activation, was evident and remained consistent between uninfected and infected cells at all timepoints.

Vaccinia-induced downregulation of EGFR has not previously been described, to the best of my knowledge. Whilst VGF has homology to EGF, its mitogenic effects and the observed sustained activation of Erk1/2 have not been directly linked to EGFR signalling, and other viral factors are believed to be involved (Schweneker, Lukassen et al. 2011). However, inhibition of EGFR by either a monoclonal antibody or the receptor tyrosine kinase inhibitor gefitinib have been described as inhibiting virus spread (Buller, Chakrabarti et al. 1988; Langhammer, Koban et al. 2011). It is possible here that vaccinia-induced cell proliferation takes place at earlier timepoints, and that by 24hrs post-infection the receptor is already internalised or host protein synthesis has shut down. This is speculative however, as this was not a primary concern of the project and downregulation of the EGFR by vaccinia was not investigated further. Regardless, replication of both virus strains continued to proceed in TrampC1 cells (Figure 30) despite downregulation of the EGF receptor, and it does not appear to be critical to virus propagation in this cell line.

It was hypothesised that expression of decorin from vaccinia might exert an inhibitory effect on TGFβ signalling, which is proposed to contribute to the immunosuppressive environment induced in ovarian cancer (Yigit, Massuger et al. 2010) and to enhance metastatic potential by inducing epithelial-mesenchymal transition (Do, Kubba et al. 2008). Furthermore, it was recently shown that inhibition of the TGBβ signalling pathway increased survival in a mouse model of ovarian cancer (Yamamura, Matsumura et al. 2012). Upon stimulation with recombinant TGFβ, MOSEC cells demonstrated activated Smad2 as expected and Lister-mDCN failed to reduce these levels. Whilst the level of decorin released from infected cells was low (<100ng/ml), treatment with up to 4μg/ml recombinant decorin also failed to inhibit TGFβ signalling. This is in contrast to reports that show that a region within the protein core of decorin can bind and sequester TGFβ in the ECM to modulate availability with its receptors (Schonherr, Broszat et al. 1998; Droguett, Cabello-Verrugio et al. 2006). Interestingly, whilst extracellular decorin can affect TGFβ signalling, it is proposed that intracellular decorin is also partly required for a TGFβ response. Decorin-null myoblasts show a diminished response to TGFβ compared to wild-type cells and, whilst re-expression of decorin using an adenovirus vector restores activity, this is independent of changes in the Smad pathway (Cabello-Verrugio and Brandan 2007). It has already been shown that the release of decorin from Lister-mDCN infected cells is low compared to intracellular levels, suggesting that sequestration of TGFβ by decorin and therefore inhibition of the signalling pathway may not be achievable. Levels of intracellular decorin in infected cells may influence TGFβ signalling, although it is possible that this assay looking at phosphorylation of Smad2 in response to TGFβ would not reflect any changes.

Overall, hopes that the release of decorin from infected cells might exert anti-tumour activity on neighbouring cells through its interactions with the EGF receptor and the TGFβ signalling pathway were unfounded. However, these were considered secondary to the primary aim, which was to improve the spread of oncolytic vaccinia and thus overall efficacy compared to the control virus. Given the associated problems of trying to quantify virus spread *in vivo,* experiments were first performed on cultured cells *in vitro*. As decorin is proposed to enhance spread through its interactions within the ECM, a 3D model was utilised rather than traditional plaque assays. Cells were embedded in a collagen/matrigel matrix and a cell monolayer infected with a fixed dose of virus, with the view of quantifying virus spread by immunohistochemical detection of vaccinia virus proteins in infected cells within the matrix. However, whilst there was evident infection of the overlaying monolayer, infected cells could not be detected within the matrix and so quantifiable analysis could not be performed. Given that vaccinia is naturally evolved for rapid cell to cell spread and for long range dissemination (reviewed by (Roberts and Smith 2008)), these results were surprising and disappointing, and may reflect the need for further optimisation of the technique. The high percentage of collagen in the matrix (2.4mg/ml), whilst providing the rigidity required for matrix processing for IHC, may have contributed to the lack of dissemination by creating a tight lattice through which the virus could not penetrate. Further optimisation of matrix composition, dosing and cell density may lead to more positive findings.

As an alternative to the 3D model above, the dissemination of virus through a thinner collagen/matrigel matrix into overlaying supernatant was quantified by TCID50 assay. Surprisingly, recoverable virus from the supernatant of Lister-mDCN infected cells was lower than that from Lister-dTK infected cells at all timepoints tested in both MOSEC and TrampC1 cells. Virus titres were far lower than those obtained from traditional replication assays however; the titre in the supernatant of MOSEC cells following presumed diffusion through the matrix was the same as the infectious dose given three days earlier (0.1 pfu/cell). This was in sharp contrast to the 10,000pfu/cell recovered 72hrs post-infection in a TCID50 assay where virus was released directly into the media and did not have to travel through a collagen matrix. This prompted the question of whether the virus detected having migrated through the gel was the EEV form of vaccinia, as this is known to be responsible for distant spread and is produced in small amounts compared to the IMV form. Whilst an effort was made to investigate this by looking at early release (<18hrs post-infection) of virus from infected cells, it was only speculated that these might be the EEV form, as the use of a neutralising antibody against IMV was not used to exclude these virions. These experiments did however reveal that far fewer infectious virions were released early on following Lister-mDCN infection compared to Lister-dTK. Two possibilities arise from these data; the first that expression of decorin from vaccinia somehow inhibits early replication or EEV production- unlikely as it is cloned into the thymidine kinase site (approx. 83kbp within the virus genome), well away from genes encoding EEV proteins (approx. 146kbp). The second is that decorin may influence the collagen matrix in such a way that virus spread is inhibited rather than enhanced.

Attempts to examine the spread of Lister-mDCN *in vivo*, by immunohistochemistry, were difficult. Whilst tumours were injected subcutaneously with virus, there was no visible needle track, or origin of infection. Rather, there were pockets of virus infection spread diffusely throughout the tumour mass, with areas of uninfected tissue in between. There was no obvious difference between the number or size of areas positive for vaccinia-infected cells in Lister-dTK or Lister-mDCN treated tumours, although it was not possible to quantify this for statistical analysis. Quantification of the amount of viral DNA in whole excised tumours revealed a lower amount to be present following delivery of Lister-mDCN compared to Lister-dTK, partially supporting the *in vitro* observation of fewer viral particles penetrating through a collagen matrix. This is in contrast to a paper describing increased spread of an adenovirus expressing decorin (Ad-ΔE1B-DCNG), whereby increased expression and penetration was observed in both tumour spheroids derived from a patient with glioma and in xenograft models when compared to a control virus (Choi, Lee et al. 2010). Ad-ΔE1B-DCNG also led to increased survival and reduced tumour burden compared to treatment with the control virus. In contrast, whilst there was some hint of improved efficacy of Lister-mDCN in mice bearing subcutaneous prostate cancer xenografts here, this work could not be continued due to ulceration at the tumour site. Furthermore, Lister-mDCN had limited activity in an intraperitoneal model of ovarian cancer, although it is worth noting that so too did Lister-dTK.

Efficacy of vaccinia virus against ovarian cancer *in vivo* has been demonstrated previously, with the caveat that the best results are seen when treatment is administered early (one day post tumour inoculation) (Hung, Tsai et al. 2006; Chalikonda, Kivlen et al. 2008) and in nude mice (Hung, Tsai et al. 2006). In addition, virus clearance, particularly in immunocompetent hosts, is rapid and virus cannot be detected either 5 days or 8 days post-delivery (Hung, Tsai et al. 2006; Chalikonda, Kivlen et al. 2008). Here, an immunocompetent, intraperitoneal model using MOSEC cells expressing luciferase was used, as this cell line leads to a highly malignant neoplasm comprising both epithelial and connective tissue (sarcomatous) elements and production of ascitic fluid, mimicking the disease seen in patients with late-stage disease. Tumour burden was measured here by quantifiable bioluminescent imaging, in contrast to previous studies that have relied on visually monitoring animals for ascitic burden and poor health (Yang, Guo et al. 2007; Chalikonda, Kivlen et al. 2008). Based on these criteria, all control mice were deemed to be at the limit of acceptable health and culled by day 57 (Yang, Guo et al. 2007) or day 86 (Chalikonda, Kivlen et al. 2008), whereas in the work presented within this thesis mice were healthy with no sign of ascites at the experimental endpoint of days 63 and 67 in two separate experiments. In addition, mice had a very low tumour burden upon pathological inspection at the experiment endpoint and perhaps could have tolerated a higher initial dose of cells. Where a response was observed in this model elsewhere, survival was extended from 86 days to 120 days, bar one living mouse, in the vaccinia treated group

(Chalikonda, Kivlen et al. 2008) and from 57 days to 123 days in another study (Yang, Guo et al. 2007). Although survival was not measured in this thesis, tumour burden did not differ significantly between control mice and those treated with either Lister-dTK or Lister-mDCN, although there was an indication that Lister-mDCN might perform better than Lister-dTK in one experiment. As there were no signs of toxicity at the doses used, it is possible that a higher dose of virus could have been used to overcome the immunocompetent nature of these animals, in line with that used elsewhere (Yang, Guo et al. 2007).

Overall, the effects of inserting decorin into oncolytic vaccinia were disappointing, but there are a number of reasons that may explain why this strategy did not live up to expectations. The concentration of decorin produced by vaccinia-infected cells was low compared to that which has been used previously and may explain the lack of activity in functional assays such as that involving the EGF receptor, cell cycle and TGFβ signalling. Crucially, the effect of decorin on enhancing the spread of adenovirus was deemed collagen-binding dependent, as constructs with point mutations within the region which binds to collagen fibrils did not demonstrate enhanced activity (Choi, Lee et al. 2010). In addition, tumours treated with an adenovirus expressing decorin were devoid of collagen in comparison to control tumours (Choi, Lee et al. 2010), suggesting degradation by decorin. Collagen, which increases in content from the superficial tumour tissue into deeper tissue (>2mm), is thought to inhibit the spread of large molecules by forming a dense network, and its degradation improved the spread of oncolytic herpes simplex virus in melanoma xenografts (McKee, Grandi et al. 2006). Given that collagen I is the preferred substrate for ovarian cancer cell attachment (Moser, Pizzo et al. 1996), and that the collagen binding integrin $\alpha2\beta1$ is implicated in mediation of peritoneal metastasis (Fishman, Kearns et al. 1998; Shield, Riley et al. 2007), interactions between collagen and decorin might have been anticipated to affect more than proposed viral spread. Decorin binds to collagen via the leucine rich repeats within the protein core (Kalamajski, Aspberg et al. 2007) and is also believed to mask the $\alpha2\beta1$ binding site on collagen (Bhide, Laschinger et al. 2005). Although this interaction involves the protein core, which was expressed from oncolytic vaccinia here, it is possible that the full length protein consisting of additional glycosaminoglycan chain is necessary for some of the anti-tumour activity of decorin (Nash, Deavers et al. 2002; Merline, Moreth et al. 2011) although the native full length form is not believed essential for collagen interactions (Bhide, Laschinger et al. 2005).

Finally, the optimal choice of transgene to express from oncolytic vaccinia is one open to much debate; what enhances the activity of one virus may not work with another, and this also applies across strains of the same virus. Whilst expression of relaxin, another protein capable of ECM remodelling, improved efficacy of adenovirus 5 (Ad5) it did not further improve the activity of a fiber chimeric Ad5/35, which is targeted towards the abundant CD46 receptor on tumour cells rather than the natural coxsackievirus-adenovirus receptor (CAR) (Ganesh, Gonzalez Edick et al. 2007). This implies that where overall virus uptake and potency is high already, expression of a transgene may not promote anti-tumour activity further. Vaccinia virus can already infect a huge range of cells and is not limited by specific receptors for entry. In addition, the replication cycle is rapid leading to more effective infection and destruction of neighbouring cells compared to other oncolytic viruses. Furthermore, vaccinia virus is naturally evolved for long range spread due to the production of EEV. On investigating the feasibility of expressing a pro-drug converting enzyme from vaccinia, it was noted that the system provided minimal benefit over oncolytic vaccinia alone and the authors concluded that it would be difficult to difficult to imagine any such system providing "exceptional synergism within the context of oncolytic vaccinia virus" (Chalikonda, Kivlen et al. 2008). This was attributed to the superior kinetics of oncolytic vaccinia and the fact that ovarian tumour cells are widely distributed through the peritoneal cavity already, making it difficult to achieve bystander effects. The same reasoning can be applied to expression of decorin from vaccinia, whose effects on the ECM and receptors on neighbouring cells may not be apparent in the window before infection by virions released from neighbouring cells.

Inhibition of c-met, a receptor involved in metastasis, by decorin is possible at lower concentrations of decorin (Goldoni, Humphries et al. 2009) and this may be of some therapeutic benefit if decorin is expressed from oncolytic agents. Anti-metastatic activity by decorin has already been shown in several tumour models (Reed, Waterhouse et al. 2005; Goldoni, Seidler et al. 2008; Shintani, Matsumine et al. 2008) although this was not investigated in this work on ovarian cancer, primarily due to the absence of advanced disease in the model used and the fact that numerous tumour nodules are apparent throughout the peritoneal cavity anyway.

It is concluded that expression of decorin from oncolytic vaccinia offered no advantage over a control virus in the ovarian cancer cell lines tested here, and in an immunocompetent, intraperitoneal model of ovarian cancer. Whilst the *in vivo* dosing schedule may require further optimisation in order to demonstrate significant anti-tumour of oncolytic vaccinia alone, it is not anticipated that decorin would demonstrate a significant advantage in this context, based on *in vitro* findings. It may however be appropriate in tumour models where virus spread throughout a larger, single tumour mass is a barrier to effective therapy, or as a transgene from less potent oncolytic viruses.

Chapter 5

Mechanisms of vaccinia-induced ovarian cancer cell death

5. Mechanisms of vaccinia-induced ovarian cancer cell death

5.1 Apoptosis

Vaccinia virus encodes numerous inhibitors of apoptosis but nonetheless has been reported to induce apoptosis in some cells lines. The Western Reserve (WR) strain has been reported to induce apoptosis of infected HeLa G cells but not an alternative epithelial cell line, BSC-40 (Liskova, Knitlova et al. 2011). Similarly, both the WR and non-replicative Ankara strain have been shown to induce apoptosis in melanoma cells (Greiner, Humrich et al. 2006). Vaccinia virus has also been reported to induce apoptosis in infected macrophages (Humlova, Vokurka et al. 2002) and Chinese hamster ovary cells (Ramsey-Ewing and Moss 1998; Greiner, Humrich et al. 2006). The role of apoptosis in cell death of ovarian cancer cells following infection with both the wild type Lister strain and the modified Lister-dTK strain was therefore investigated.

5.1.1 Markers of apoptosis

Apoptosis is not only accompanied by specific morphological changes but also specific and highly regulated biochemical changes, which can be used as markers of apoptosis. These include loss of mitochondrial membrane potential, exposure of phosphatidylserine (PS) on the outer surface of the cell membrane, caspase-3 cleavage and subsequent cleavage of downstream targets, and DNA fragmentation. As apoptosis can occur independently of caspase-3 cleavage, and as an “apoptosis-like programmed cell death” and “necrosis-like programmed cell death” (Leist and Jaattela 2001) have also been described which share some of the hallmarks of apoptosis, it is generally necessary to study multiple markers of apoptosis. To investigate if vaccinia virus induces apoptosis in ovarian cancer cell lines, the following assays were used: western blotting to detect cleaved PARP and caspase-3, and flow cytometry to detect PS externalisation and levels of subG1 DNA.

5.1.1.1 PARP cleavage and caspase-3 cleavage

Apoptosis involves the cleavage of multiple cysteine proteases (caspases); caspase-3 is an effector caspase that is activated downstream of initiator caspases which are closely coupled to apoptotic signals. As caspase-3 is activated upon initiation of either the extrinsic (death receptor) or intrinsic signalling pathways, it therefore acts as a good marker of apoptosis as it cleaves downstream targets irreversibly, committing the cell to apoptotic fate. During apoptosis, poly(ADP-ribose) polymerase (PARP), a 116kDa nuclear protein that is involved in DNA damage detection and repair, is cleaved by caspase-3 to yield an 89kDa fragment. This cleavage contributes to apoptosis by preventing the participation of PARP in DNA repair.

The presence of cleaved PARP and caspase 3 activation were studied in A2780, A270CP, Igrov1 and Skov3ip1 cells following infection with either Lister-wt or Lister-dTK. Staurosporine was used as a stimulant for apoptosis and the ability of all cell lines to undergo apoptosis upon overnight treatment was confirmed by western blotting for PARP and caspase-3 cleavage (data not shown). Cleaved PARP was detected in all of the four cell lines tested as early as 48hrs post-infection (data not shown) and was particularly evident at 72hrs p.i (Figure 47). Caspase-3 cleavage was, largely, undetectable in vaccinia-infected cells although A2780 and A2780CP cells did show evidence of caspase-3 activation in one experiment upon long exposure (Figure 47). This was surprising considering that PARP cleavage is downstream of caspase-3 cleavage, although it is worth noting that PARP can be cleaved by other substrates besides caspase 3.

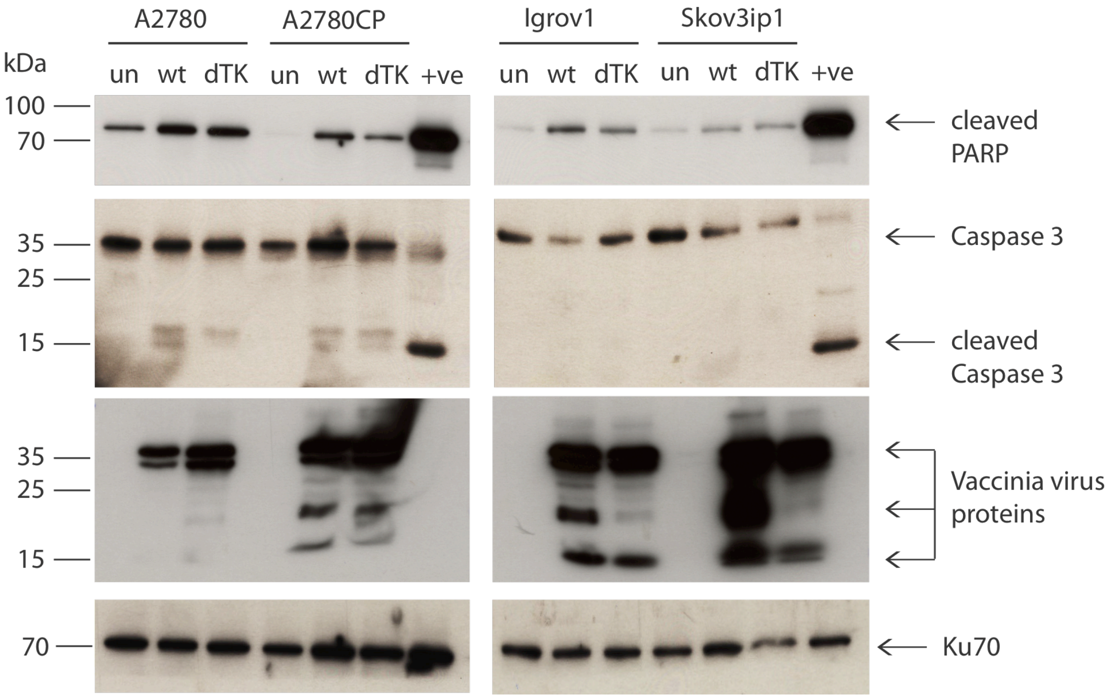

Figure 47: PARP cleavage and caspase 3 cleavage in vaccinia-infected cells. Cells were infected with 1 pfu/cell of virus and harvested 72hrs post-infection. A2780 cells treated with 2μM staurosporine overnight were used as a positive control. Blots are representative of a minimum of three independent experiments.

5.1.1.2 Externalisation of phosphatidylserine

The externalisation of phosphatidylserine (PS) on the outer leaflet of the plasma membrane acts as a recognition signal for the removal of apoptotic cells by phagocytes. This translocation of PS from the cytosolic inner membrane to the outer surface enables it to be detected indirectly by staining with Annexin V, which is membrane impermeable and has a high affinity for PS.

A2780, A2780CP, Igrov1 and Skov3ip1 cells were infected with 1pfu/cell and co-stained with Annexin V (to label PS positive cells) and the membrane impermeable dye DAPI (to distinguish between live and dead cells) 72hrs post-infection. Cells that were annexin V positive and DAPI positive were assumed to have compromised membranes, indicating either late apoptotic or necrotic cell death, and so these were excluded during analysis by flow cytometry (Figure 48b).

A background level of between 1.9% and 3.2% of untreated cells were positive for annexin V; this may represent an apoptotic population as cells were confluent at the time of harvest, or be a result of gating during FACS analysis. A significant increase in annexin V positive cells was observed in A2780, A2780CP and Skov3ip1 cells 72hrs post-infection with Lister-dTK

(Figure 48a); the same trend was observed in Igrov1 cells although this was not statistically significant. The total number of viable annexin V positive cells increased from 2.3% to 10.0% in A2780 cells, 3.2% to 20.0% and 2.7% to 24.7% in Skov3ip1 cells. Infection with Lister-wt resulted in a similar pattern although to a lesser degree, and significant increases in annexin V staining were seen in A2780CP and Skov3ip1 cells only. Analysis 48hrs post-infection revealed no significant increase in annexin V in any of the four cell lines tested (data not shown). Similarly, no increase at 96hrs post-infection was observed (data not shown) as the majority of annexin V positive cells were also DAPI positive and thus could not be counted as early apoptotic.

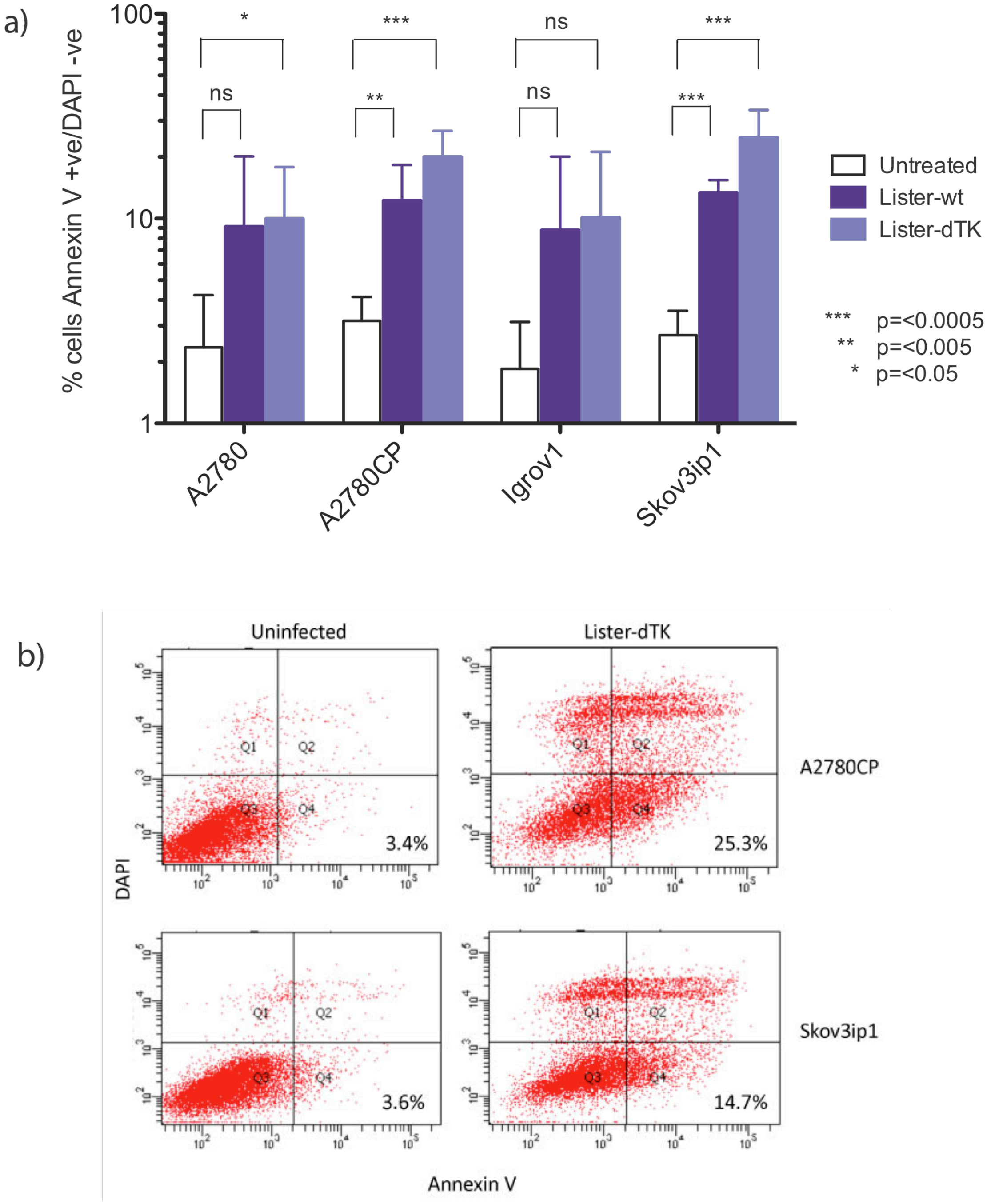

Figure 48: Externalisation of phosphatidylserine on the cell membrane following Lister-dTK infection. Cells were infected with 1 pfu/cell and stained with annexin V and DAPI to distinguish between live and dead cells 72hrs post-infection a) Mean + SD of viable cells staining positive for phosphatidylserine from three experiments performed in duplicate b) Gating for A2780CP and Skov3ip1 untreated and infected cells showing the percentage of viable cells positive for phosphatidylserine in the lower right quadrant (Q4). Data shows one representative replicate.

5.1.1.3 DNA fragmentation

DNA fragmentation is a secondary consequence of apoptosis and can be considered a marker of apoptosis in combination with other detection methods. Caspase activated DNase (CAD) normally exists in a complex with inhibitor of CAD (iCAD). During apoptosis, caspases cleave iCAD to dissociate CAD from the complex; this leads to the cleavage of chromosomal DNA into characteristic 180-200 bp fragments that can be visualised using gel electrophoresis. Alternatively, DNA fragmentation can be measured by flow cytometry as, upon permeabilisation with ethanol, these DNA fragments leak out of the cell resulting in reduced cellular DNA. The percentage of cells in various stages of the cell cycle can be quantified by staining with the DNA binding dye propidium iodide. This can determine the number of cells that have lost sufficient DNA and so appear as a sub-Gl population, presumed to be late apoptotic cells.

A2780, A2780CP, Igrov1 and Skov3ip1 cells were infected with either the wild type virus or Lister-dTK and harvested 48hrs and 96hrs post-infection. Cells were gated as depicted in Figure 49b and the number of cells with sub-G1 DNA quantified. At 48hrs there was no increase in subG1 DNA (data not shown) although by 96hrs Lister-dTK infection resulted in significant increases (Figure 49a). Consistent with the reduced cytotoxicity of the wild type virus compared to Lister-dTK this increase was less marked in Lister-wt infected cells, and only significantly increased in Igrov1 and Skov3ip1 cells. Baseline levels of cells with subG1 DNA were below 3% in A2780, A2780CP, Igrov1 and Skov3ip1 cells; this increased to 8.9%, 10.0%, 16.6% and 10.6% of cells respectively 96hrs post-infection with Lister-dTK.

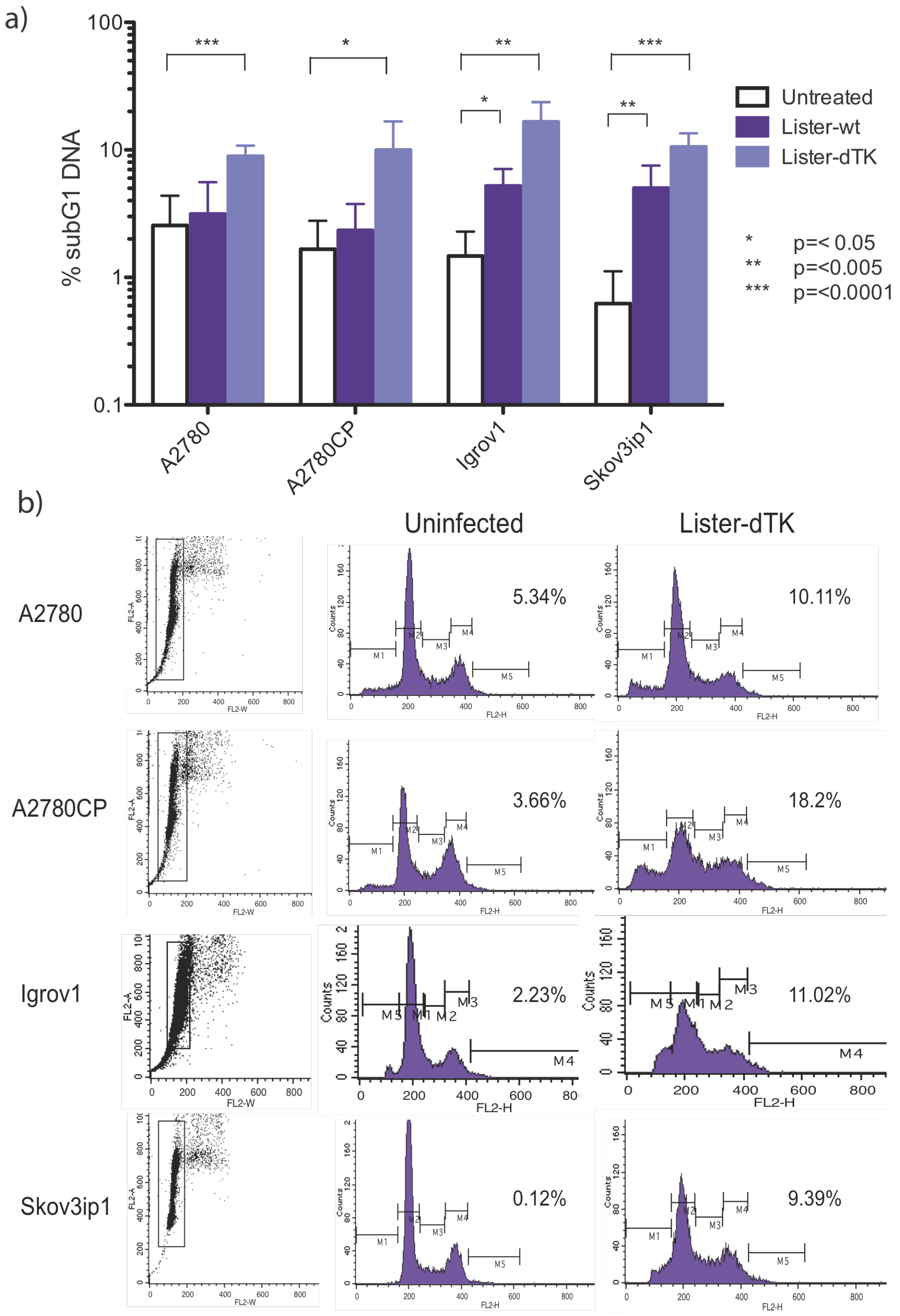

Figure 49: DNA fragmentation following infection with vaccinia virus. Cells were infected with 1pfu/cell and harvested and fixed 96hrs later for analysis by flow cytometry. Cells were stained with propidium iodide and cell populations gated using CellQuest. a) Mean +SD of the percentage of cells with subG1 DNA from 2-4 experiments, each performed in duplicate b) Representative plots of cell populations showing the percentage of cells with subG1 DNA. Data shows % of cells from one sample only and does not depict the mean values from all experiments combined in Figure 49a.

5.1.2 Inhibition of apoptosis

Having observed PARP cleavage and an increase in sub-G1 DNA in A2780, A2780CP, Igrov1 and Skov3ip1 cells following infection with Lister-dTK, as well as an increase in PS externalisation in A2780, A2780CP and Skov3ip1 cells, the contribution of apoptosis to vaccinia-induced cell death was next evaluated by inhibiting key steps of the apoptotic pathway and determining sensitivity to virus following these interventions. As mentioned previously, vaccinia virus encodes multiple inhibitors of apoptosis such as secreted viroceptor proteins that bind host cell cytokines or chemokines, virokines that act as agonistic or antagonistic ligands for host receptors, and proteins that act directly to modulate apoptosis within the host cell. In order to study the effect of apoptosis inhibition on ovarian cancer cell death *in vitro*, two strategies were used: overexpression of the anti-apoptotic protein Bcl2 and inhibition of caspase activity using the pan-caspase inhibitor zVAD-fmk.

5.1.2.1 Overexpression of the anti-apoptotic protein Bcl2

Apoptosis is tightly regulated and Bcl2 is a pro-survival member of the Bcl2 family that inhibits apoptosis (amongst other mechanisms) by binding to the BH3 region of Bak and Bax, two pro-apoptotic proteins. This binding prevents dimerisation of Bak and Bax and blocks the subsequent release of cytochrome c from the mitochondria, which would otherwise interact with Apaf1 to lead to the formation of the apoptosome and induction of apoptosis. Overexpression of Bcl2 has been shown to inhibit apoptosis resulting from various stimuli and many viruses express Bcl2 homologs to prevent premature cell death which would otherwise result in termination of virus replication. Vaccinia virus encodes several known Bcl2 like proteins including F1L, which binds and inhibits Bak to prevent cytochrome c release (Wasilenko, Banadyga et al. 2005), and N1, which is a conserved protein involved in virulence (Cooray, Bahar et al. 2007). Engineeered mutants that lack the N1 gene are attenuated and demonstrate enhanced natural killer cell activation in the host in response to viral infection (Jacobs, Bartlett et al. 2008). Given that inhibitors of apoptosis are evolutionarily conserved in the vaccinia genome, it would suggest that impairment of this pathway is advantageous to virus replication. However, markers of apoptosis were observed following infection with vaccinia virus suggesting that execution of the apoptotic pathway might still commence. The effect of Bcl2 overexpression on sensitivity to vaccinia virus was therefore studied by comparing the EC50 of OVCAR4-Bcl2 overexpressing cells to the parental cell line OVCAR4.

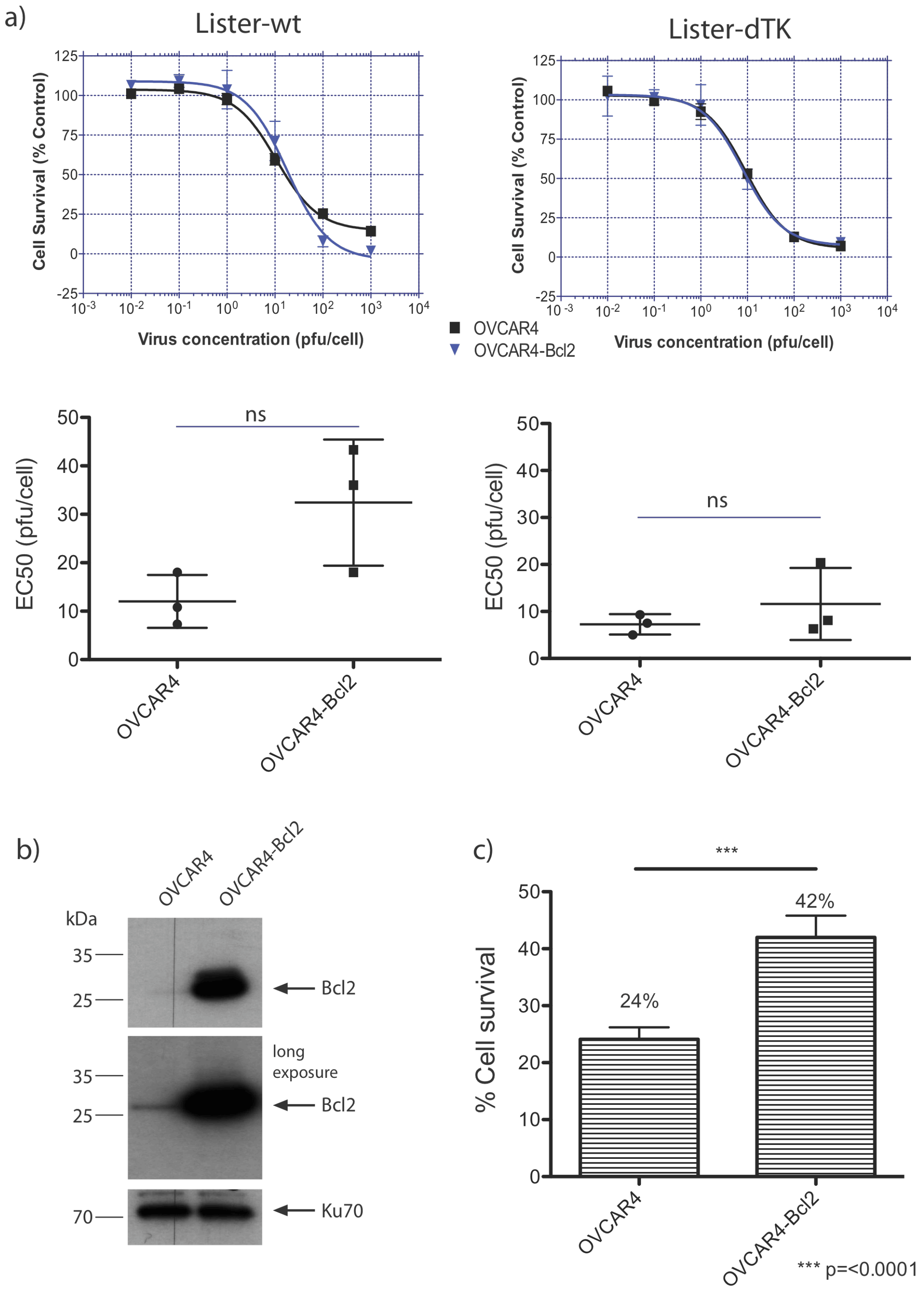

Figure 50: Overexpression of the anti-apoptotic protein Bcl2 in OVCAR-4 cells does not inhibit vaccinia-induced cell death a) *Top:* Representative dose response curves to Lister-wt and Lister-dTK. OVCAR4 and OVCAR4-Bcl2 cells were infected with increasing doses of virus and cell survival determined by MTS assay 72hrs later. *Bottom:* The mean EC50 and SD of three independent experiments, each performed in triplicate. b) Confirmation of Bcl2 overexpression in OVCAR4-Bcl2 cells compared to the parental cell line OVCAR4. c) Bcl2 overexpression inhibits cisplatin induced cell death. Cells were treated with 10μM cisplatin and cell survival determined by MTT assay 72hrs later. Data shows the mean and SD of three experiments, each with 6 replicates.

OVCAR4 cells were generated to overexpress Bcl2 as described previously (McNeish, Bell et al. 2003) and protein levels of Bcl2 were confirmed by western blotting (Figure 50b). Overexpression of Bcl2 significantly inhibited cisplatin-induced cell death, where cell survival increased from 24% in OVCAR4 cells to 42% in OVCAR4-Bcl2 cells following 72hrs treatment with 10μM cisplatin (Figure 50c); however, no such inhibition of cell death was observed following infection with virus. Parental OVCAR4 cells and OVCAR4-Bcl2 cells were infected with increasing doses of Lister-wt and Lister-dTK and cell survival determined 72hrs post-infection by MTS assay. There was no significant increase in EC50 of either Lister-wt or Lister-dTK following overexpression of Bcl2 (Figure 50a), suggesting that regulation of apoptosis by this protein does not contribute to virus cytotoxicity. Given that vaccinia virus strains themselves encode inhibitors of apoptosis and Bcl2 homologs, it may also have been hypothesised that further inhibition of apoptosis could in fact increase virus-induced cell death. However, there was no significant attenuation or enhancement of Lister-wt or Lister-dTK in OVCAR4-Bcl2 cells compared to the parental cell line (Figure 50a).

5.1.2.2 Inhibition of caspase activity

As caspase-3 cleavage was not evident in Igrov1 and Skov3ip1 cells following infection with vaccinia virus, and only on one occasion in A2780 and A2780CP cells (Figure 47a), it was decided to use a pan-caspase inhibitor to inhibit apoptosis, as the activity of caspase-3 during infection with either Lister-wt or Lister-dTK could not be conclusively shown. zVAD-fmk is an irreversible inhibitor of apoptosis that functions by binding to the catalytic sites of caspases.

The toxicity of zVAD was determined in A2780, A2780CP, Igrov1 and Skov3ip1 cells and a single dose at 25μM found not to effect cell proliferation. Although the binding of zVAD to caspases is irreversible it is sometimes advised to add the inhibitor at the same time that apoptosis is induced for optimal activity. As different markers of apoptosis have been evident at varying timepoints following infection with vaccinia virus, the exact kinetics of apoptotic induction in ovarian cancer cell lines are unknown. To this extent, the toxicity of zVAD-fmk when added daily to culture medium was also determined (Figure 51).

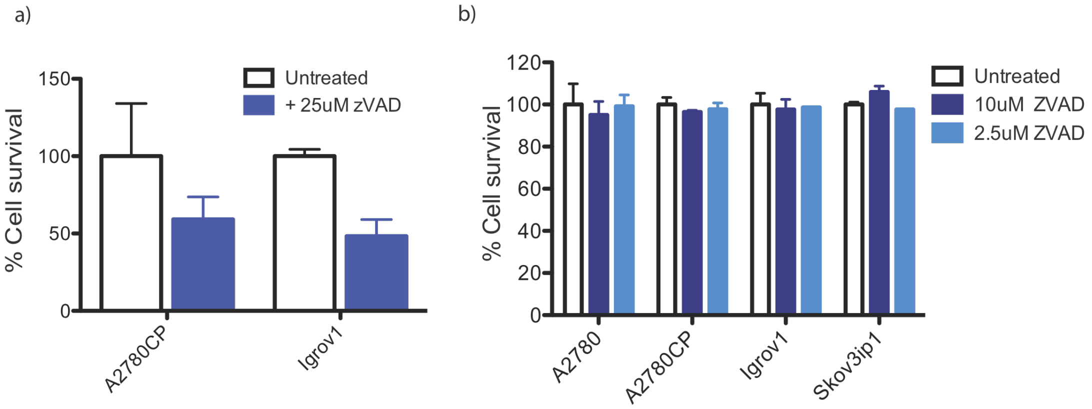

Figure 51: Toxicity of zVAD-fmk added daily to ovarian cancer cell lines at a) 25µM daily and b) 10µM and 2.5µM daily. Cell survival was measured a) 96hrs later and b) 120hrs later by MTT assay. Data shows the mean + SD of a single experiment, performed in triplicate.

When zVAD-fmk was added daily at 25µM over 40% and 50% cell death was observed in A2780CP and Igrov1 cells respectively (Figure 51a); these conditions were not tested in either A2780 or Skov3ip1 cells. At lower concentrations, 10µM and 2.5µM daily, no significant toxicity was observed in any of the cell lines tested (Figure 51b). A concentration of 10µM was thus chosen for cell survival assays where zVAD-fmk was added daily.

The effect of pan-caspase inhibition on cytotoxicity to Lister-dTK was determined by infecting cells with increasing doses of virus, followed by addition of either vehicle alone (DMSO) or 25µM zVAD-fmk 2hrs post-infection. Cell survival was analysed 72hrs post-infection by MTS assay. There was no significant increase in the EC50 value of Lister-dTK in the presence of zVAD-fmk based on the mean EC50 of three independent experiments (table in Figure 52a). However, the EC50 of Lister-dTK alone can vary slightly between experiments based on cell passage number or minor discrepancies in virus dilution, increasing the standard deviation of the mean and therefore limiting subsequent statistical analysis. To compare more accurately any subtle changes in sensitivity to Lister-dTK upon caspase inhibition, the EC50 of cells treated with zVAD-fmk was normalised to the EC50 of cells infected with Lister-dTK alone for each experiment. There was a small (less than 2-fold) but significant increase in the EC50 of Lister-dTK in A2780 and Skov3ip1 cells treated with a single dose of zVAD-fmk (Figure 52a). No significant inhibition of Lister-dTK was observed in A2780CP or Igrov1 cells.

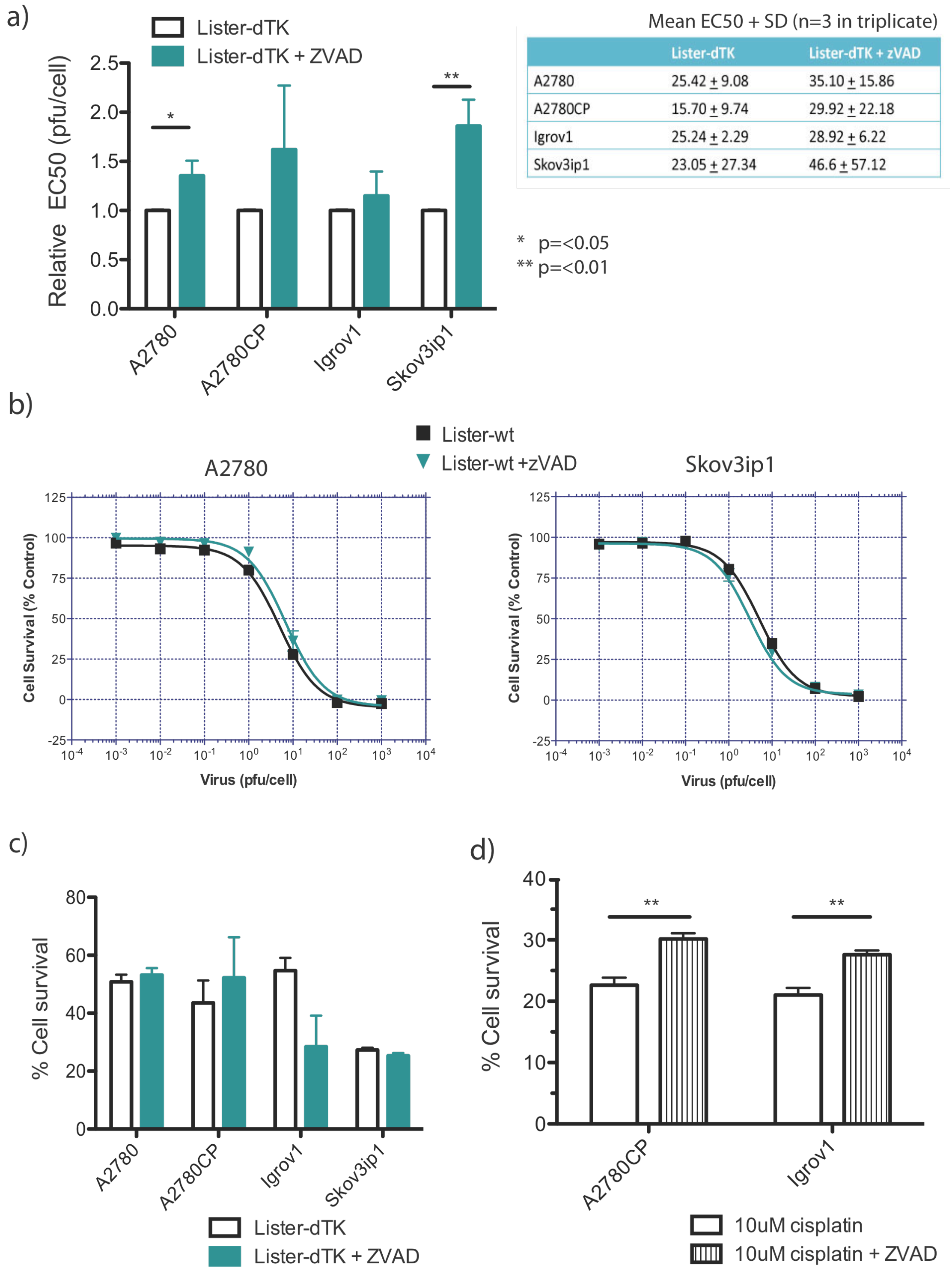

Mean EC50 + SD (n=3 in triplicate)

	Lister-dTK	Lister-dTK + zVAD
A2780	25.42 ± 9.08	35.10 ± 15.86
A2780CP	15.70 ± 9.74	29.92 ± 22.18
Igrov1	25.24 ± 2.29	28.92 ± 6.22
Skov3ip1	23.05 ± 27.34	46.6 ± 57.12

Figure 52: Effect of the pan-caspase inhibitor, zVAD-fmk, on vaccinia induced cell death in ovarian cancer cell lines. a) Cells were infected with increasing doses of Lister-dTK in the presence or absence of 25µM zVAD-fmk, and cell survival determined by MTS assay 72hrs post-infection. *Table:* The mean EC50+SD from three experiments, each performed in triplicate, is shown in the table. *Graph:* The EC50 of Lister-dTK in the presence of zVAD-fmk was normalised to the EC50 of Lister-dTK alone for each experiment. The graph shows the mean and SD of these relative EC50's. b) The effect of zVAD-fmk on the EC50 of Lister-wt. Cells were treated as above. c) The effect of adding 10µM daily to cells infected with 1pfu/cell of Lister-dTK. Cell survival was analysed 96hrs post-infection. D) Inhibition of cisplatin-induced cell death by zVAD-fmk. Cells were co-treated with 10µM cisplatin and 10µM zVAD-fmk, and cell survival measured by MTT assay 48hrs later.

The same experiment was also performed using the wild-type virus (Figure 52b). Again, only minor changes in the EC50 of Lister-wt were observed and treatment with zVAD-fmk had conflicting results, resulting in a modest decrease in sensitivity in A2780 cells and a modest increase in Skov3ip1. Statistical analysis was not performed on these results as the experiment was only performed once using the Lister-wt virus.

In the above experiments, zVAD-fmk was added 2hrs post-infection. As it is unlikely that vaccinia virus induces apoptosis this early in the infectious cycle based on the kinetics of PARP cleavage, PS externalisation and DNA fragmentation observed so far (Figure 47, Figure 48 and Figure 49), and because it may be necessary to add zVAD-fmk at the time of induction of apoptosis for maximum effect, zVAD-fmk was then added daily to infected cells in a separate experiment. Cells were infected with 1pfu/cell of Lister-dTK and10μM zVAD was added daily directly to the cell culture medium based on toxicity studies conducted previously (Figure 51). No significant inhibition of Lister-dTK at 96hrs post-infection was observed upon daily addition of zVAD-fmk (Figure 52c). In contrast, a single dose of 10μM zVAD-fmk was able to inhibit cisplatin-induced cell death 48hrs after administration of drug (Figure 52d). Interestingly, an increase in cell death was observed in Igrov1 cells in the presence of zVAD-fmk (Figure 52c). It has recently been suggested that inhibition of apoptosis by zVAD-fmk can induce programmed necrosis following stimulation with TNFα, and indeed this combination is used as a positive control for the formation of complexes involved in this pathway (Cho, Challa et al. 2009). Inhibition of caspase-8 can lead to a switch from apoptotic cell death to programmed necrosis (Vandenabeele, Galluzzi et al. 2010) and inhibition of caspase-8 by zVAD-fmk, combined with the high levels of TNFα that are known to be released from Igrov1 cells (Kulbe, Thompson et al. 2007), may explain the increase in cell death observed here, although this was not investigated further.

5.2 Autophagy

There is some controversy for the requirement of autophagy for virus replication. There is evidence to suggest that autophagy induction aids replication, and inhibition of autophagy decreases release of infectious enterovirus (Zhang, Xi et al. 2011) and replication of hepatitis B virus in the liver following liver specific knockout of the autophagy protein Atg5 (Tian, Sir et al. 2011). Studies on adenovirus, a virus frequently used in gene therapy of cancer, also conflict on the role of autophagy, with some groups showing induction of autophagy that is involved in viral structural protein expression, virus replication and induction of cell death (Rodriguez-Rocha, Gomez-Gutierrez et al. 2011). In contrast, others demonstrate that autophagy is a cell survival mechanism in response to adenovirus and in fact cell death is enhanced when this pathway is inhibited (Baird, Aerts et al. 2007).

While there is an argument that some viruses utilise aggresomes and autophagy for virus replication (reviewed in (Wileman 2006)), there is little information on the role of autophagy in vaccinia-induced cell death. Whilst it has been shown that the vaccinia virus strain NCYBH does not require cellular autophagy machinery for virion formation, and is able to replicate in autophagy-deficient cell lines (Zhang, Monken et al. 2006), a protective or destructive role of autophagy in cell death induced by a tumour specific modified vaccinia virus has not yet been identified. This is particularly important in a tumour setting as ovarian cancer cells have shown decreased levels of the autophagy proteins Beclin-1 and LC3 (Shen, Li et al. 2008), and the ability to induce autophagy as a protective mechanism against necrosis caused by some therapeutics (Zhang, Qi et al. 2010). The ability of Lister-dTK to induce autophagy, and the role of this process in vaccinia-induced cell death was thus determined in ovarian cancer cell lines.

5.2.1 Markers of autophagy

5.2.1.1 Cleavage of LC3B

Light chain 3 (LC3) exists in three isoforms, of which LC3B is cleaved immediately following synthesis to form LC3B-I (18kDa). During autophagy, LC3B-I is further cleaved to LC3B-II (16kDa) and moves from the cytoplasm to become an essential part of the autophagosome membrane.

Levels of LC3B cleavage following infection with vaccinia virus were determined 72hrs post-infection (Figure 53). Very low levels of LC3B-II were detected in uninfected cells (Figure 53a) although LC3B-I was also difficult to detect as this is less sensitive to detection by the antibody used compared to LC3B-II. It is interesting to note that basal levels of LC3B-II in uninfected cells also varied between experiments, with LC3B-II detected in uninfected cells (Figure 54a and subsequent repeats of data in Figure 53a), suggesting that autophagy is induced under normal cell culture conditions (2% FCS-DMEM) in ovarian cancer cell lines. Infection with both Lister-wt and Lister-dTK resulted in a marked increase in levels of LC3B-II in A2780, A2780CP, Igrov1 and Skov3ip1 cells (Figure 53a). Quantification of LC3B cleavage was performed by calculating the ratio of LC3B-II to LC3B-I and then adjusting this to levels of Ku70, used as a marker of equal loading. LC3B cleavage was then expressed relative to baseline levels in uninfected cells for each cell line. A significant increase in LC3B cleavage was observed in Igrov1 and Skov3ip1 cells following infection with both Lister-wt and Lister-dTK (Figure 53b); in addition, Lister-wt induced a significant increase in LC3B cleavage in A2780CP cells.

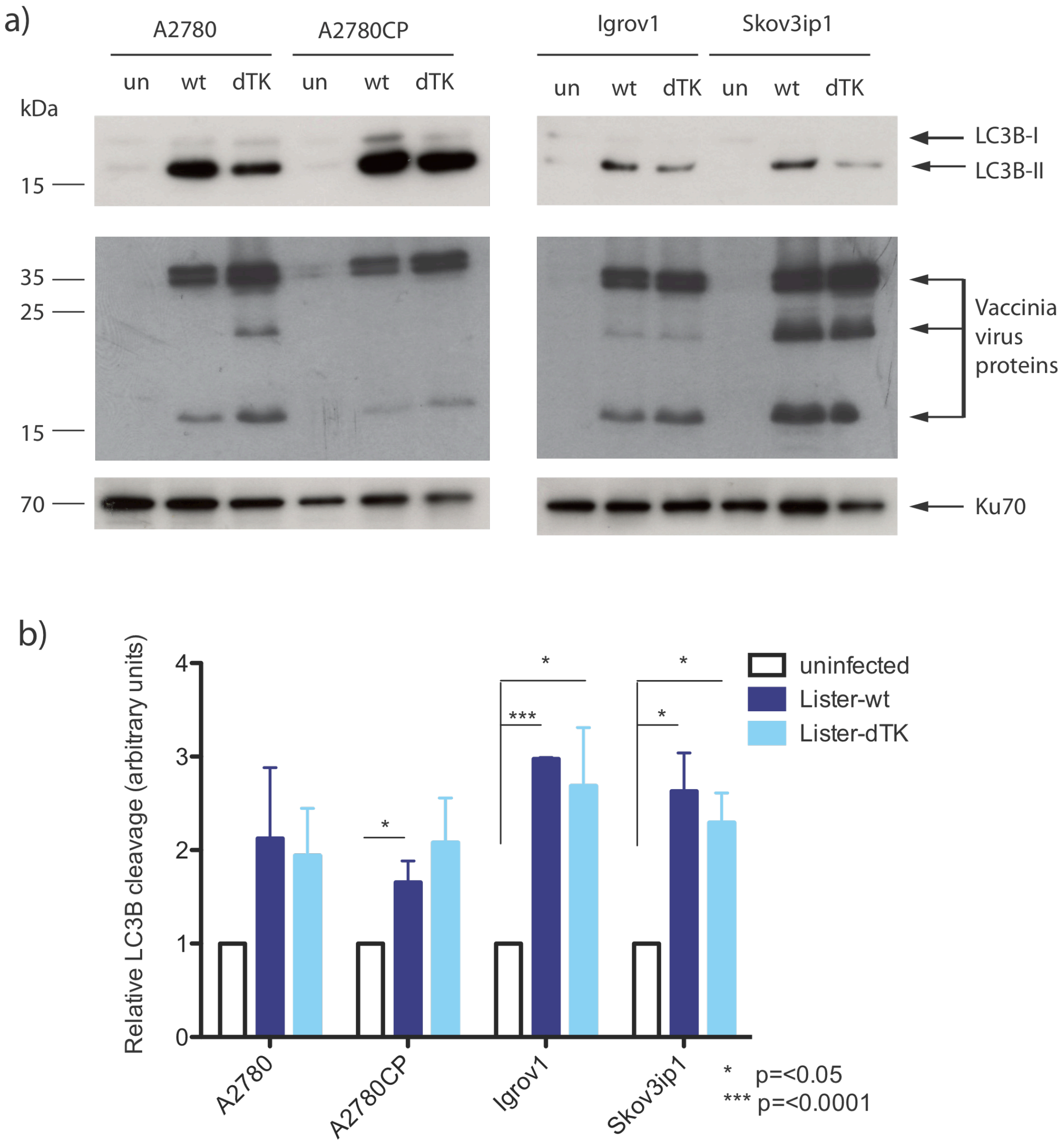

Figure 53: Cleavage of LC3B by vaccinia virus. Cells were infected with 1 pfu/cell of Lister-wt or Lister-dTK and protein extracted 72hrs post-infection for a) detection of LC3B proteins by western blotting. Representative blot of three is shown. B) Quantification of LC3B cleavage relative to uninfected cells. Data shows the mean+SEM of three independent experiments.

However, an increase in LC3B-II as detected by western blotting does not necessarily mean induction of autophagy. The conversion of LC3B-I to LC3B-II during autophagy allows LC3B-II to form part of both the outer and inner membrane of autophagosomes. Therefore, whilst LC3B-II increases during autophagy, any LC3B-II present in the inner membrane is also degraded (along with the contents of autophagosomes) upon fusion of the autophagosome with lysosomes. An increase in LC3B-II levels can therefore represent induction of autophagy or inhibition of this final fusion step of autophagy. Rapamycin is an inducer of autophagy that functions by inactivating mTOR, a negative regulator of autophagy. Induction of autophagy by rapamycin or serum starvation leads to an increase in LC3B-II levels in A2780CP cells (Figure 54c). Similarly, inhibition of autophagy by chloroquine, which blocks autophagosome and lysosome fusion, also results in dose-dependent accumulation of LC3B-II in A2780 cells (Figure 54d). We thus sought to determine whether the observed increase in LC3B-II levels following infection with vaccinia virus (Figure 53) was due to autophagy induction or inhibition of autophagosome/lysosome fusion using the lysosomal inhibitors Pepstatin A and E64d. These inhibit lysosomal turnover of LC3B-II by blocking the activity of lysosome hydrolases such as cathepsins B and L.

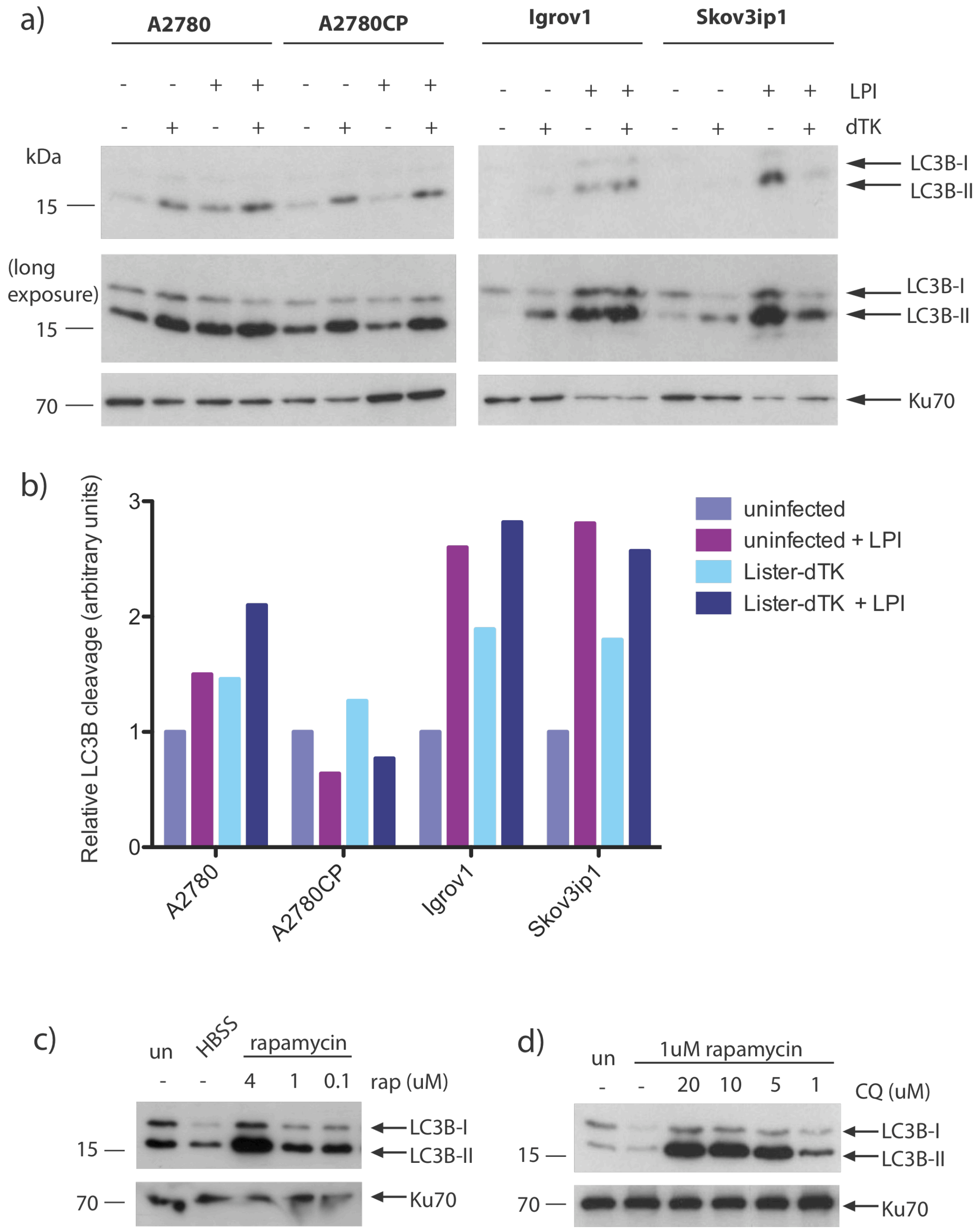

Figure 54: a) Cleavage of LC3B in the presence of the lysosomal protease inhibitors (LPI) E64d and Pepstatin A. Cells were mock-infected or infected with Lister-dTK at 1 pfu/cell in the presence or absence of 10µg/ml pepstatin-A and 10µg/ml E64d. Protein was harvested 72hrs post-infection and LC3B detected by western blotting b) Quantification of LC3B cleavage relative to uninfected cells in the absence of LPI c) Induction of LC3B cleavage in A2780CP cells following either 24hrs of serum starvation (lane 2) or treatment with rapamycin d) Accumulation of LC3B in A2780 cells following treatment with the autophagy inhibitor chloroquine. Autophagy was induced with 1µM rapamycin in the absence or presence of chloroquine.

In the presence of both Pepstatin A and E64d, levels of LC3B-II increased in uninfected A2780, Igrov1 and Skov3ip1 cells (Figure 54a (compare lanes 1 and 3, and lanes 5 and 7 in each blot), quantified in Figure 54b). The largest increase was seen in Igrov1 and Skov3ip1 cells, suggesting that under normal conditions these cells have rapid lysosomal turnover of endogenous LC3B-II. Similarly, levels of LC3B-II also increased in Lister-dTK infected A2780, Igrov1 and Skov3ip1 cells in the presence of lysosomal inhibitors (compare lanes 2 and 4, and lanes 6 and 8, Figure 54a), although to a lesser degree compared to uninfected cells. Interestingly, in both uninfected and infected A2780CP cells levels of LC3B decreased in the presence of inhibitors, although the difference was subtle and the experiment would need to be repeated to draw any conclusions.

Levels of LC3B cleavage in uninfected cells and Lister-dTK infected cells, under conditions of lysosomal inhibition, were very similar (Figure 54b), with only A2780 cells showing a modest increase in the amount of LC3B in infected cells compared to uninfected. This implies that infection with vaccinia virus may not in fact induce autophagy, but instead may affect the rate of lysosomal degradation of LC3B produced during autophagy that occurs normally in ovarian cancer cell lines. Igrov1 and Skov3ip1 cells in particular clearly undergo autophagy under normal cell culture conditions, which can only be detected when pepstatin-A and E64d are used to block the rapid lysosomal degradation of LC3B-II (Figure 54a). If vaccinia virus slows, or partially prevents this degradation, this may explain the increase in LC3B observed following infection (Figure 53).

5.2.1.2 Cellular localisation of LC3B

To further investigate potential induction of autophagy in vaccinia-infected cells, localisation of LC3B within infected cells was studied. During autophagy, LC3B is cleaved and moves from the cytoplasm into the autophagosome membrane. Infection with a non-replicating adenovirus expressing LC3B tagged to GFP (Ad-GFP-LC3) allows visualisation of either diffuse cytoplasmic GFP expression or distinct foci that represent aggregation of LC3B within the autophagosome.

Co-infection with either Lister-wt or Lister-dTK and Ad-GFP-LC3 revealed the presence of aggregates of GFP expression in A2780CP cells (Figure 55) and Igrov1 cells (Figure 56). Localisation of LC3B was not studied in A2780 or Skov3ip1 cells as these have previously demonstrated low infectivity with adenovirus within our lab. Despite a strong increase in LC3B cleavage following infection with vaccinia virus (Figure 53), there were few infected cells expressing LC3B aggregates detected by confocal microscopy. Furthermore, this phenotype was also observed in uninfected control cells, albeit less frequently. As Lister-wt does not express any fluorescent marker, the appearance of green foci in Lister-wt/Ad-GFP-LC3 co-infected cells could not be correlated with virus infection. Expression of RFP from Lister-dTK allowed identification of infected cells and although some vaccinia-infected cells showed the presence of GFP aggregates (Figure 55C and Figure 56C and D), there were many that did not. In addition, expression of diffuse GFP was higher in A2780CP cells that had been co-infected with vaccinia virus, particularly the more potent Lister-dTK, compared to uninfected cells (Figure 55). This suggests that transgene expression from Ad-GFP-LC3 may be enhanced by the presence of vaccinia, thus exaggerating LC3B expression in these cells.

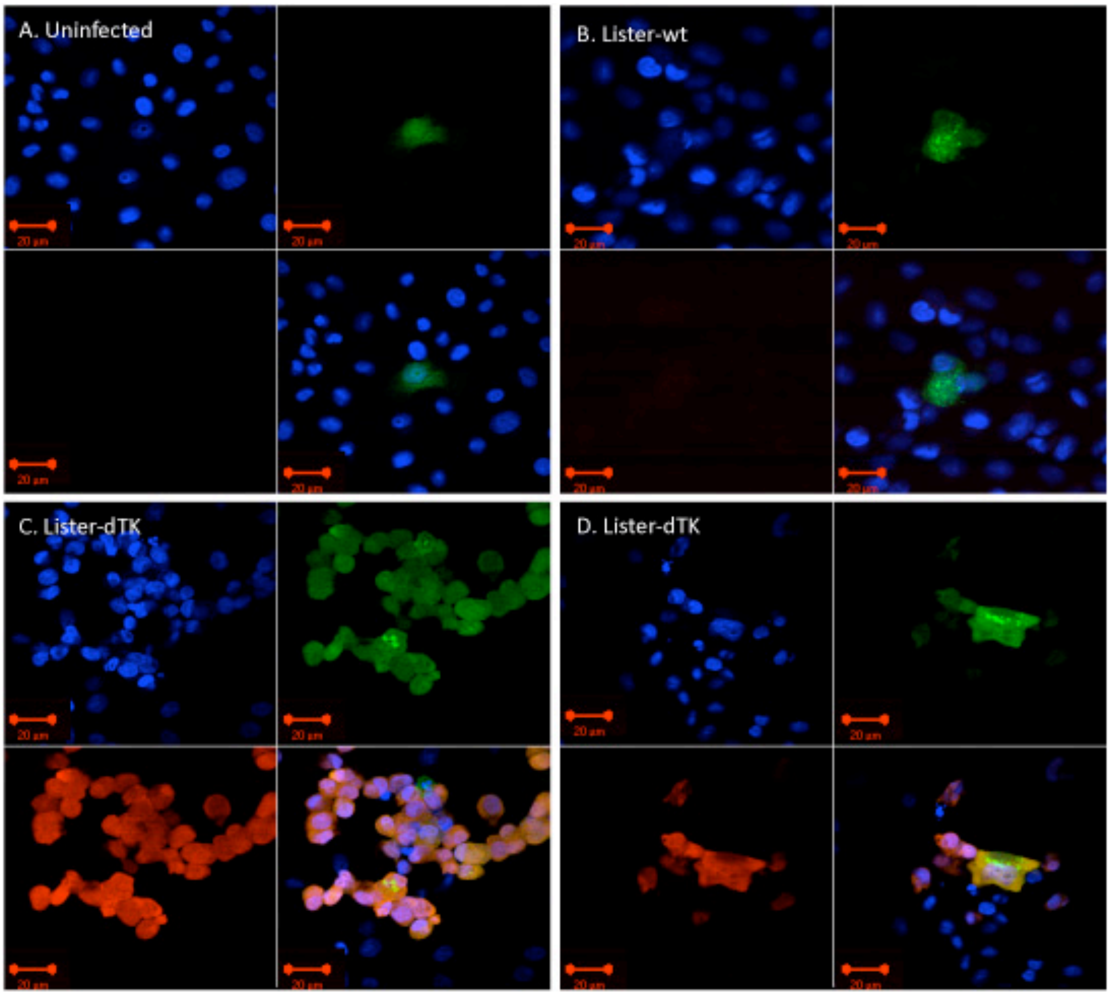

Figure 55: LC3B localisation in A2780CP cells infected with vaccinia virus. Cells were infected with A) Ad-GFP-LC3 alone, B) Ad-GFP-LC3 and Lister-wt or C and D) Ad-GFP-LC3 and Lister-dTK. Ad-GFP-LC3 was used at 30pfu/cell and Lister-wt or Lister-dTK at 1pfu/cell. Cells were fixed for confocal microscopy 72hrs post-infection. Blue staining=DAPI, green staining=LC3B, red staining=RFP expressed from Lister-dTK. Bottom right of each quadrant represents the merged image. Fields depict representative images of duplicate wells.

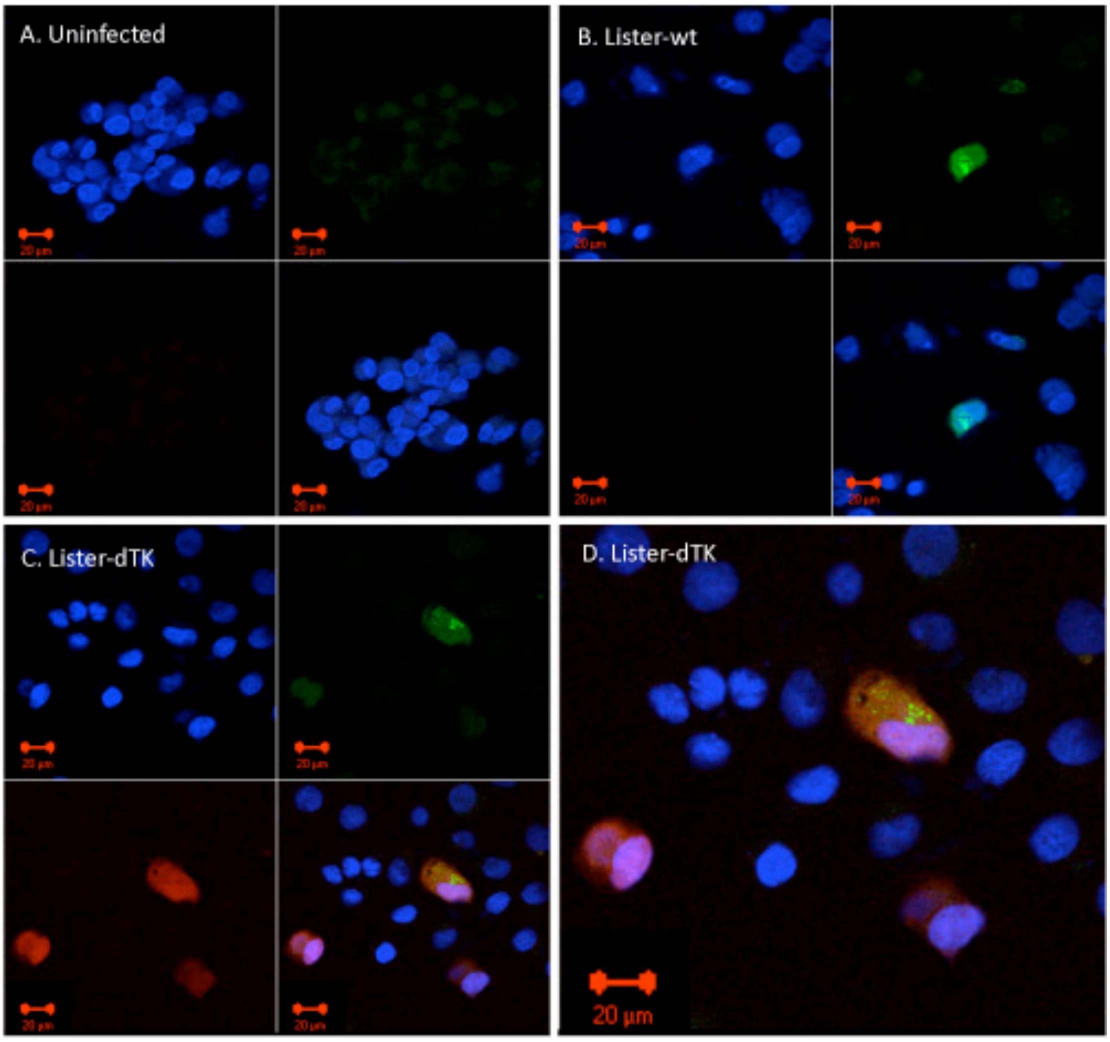

Figure 56: Localisation of LC3B in Igrov1 cells infected with vaccinia virus. Cells were infected with A) Ad-GFP-LC3 alone, B) Ad-GFP-LC3 and Lister-wt or C and D) Ad-GFP-LC3 and Lister-dTK. Ad-GFP-LC3 was used at 30pfu/cell and Lister-wt or Lister-dTK at 1pfu/cell. Cells were fixed for confocal microscopy 72hrs post-infection. Blue staining=DAPI, green staining=LC3B, red staining=RFP expressed from Lister-dTK. Bottom right of each quadrant represents the merged image. Fields depict representative images of duplicate wells.

5.2.2 Inhibition of autophagy

Cleavage of LC3B and the formation of LC3B aggregates following infection with vaccinia suggest that Lister strains induce, or at least modify the rate of, autophagy in ovarian cancer cell lines. To evaluate the role of autophagy, as either a cell survival mechanism or as a mode of cell death, we next sought to inhibit this pathway and evaluate the effect on vaccinia cytotoxicity in ovarian cancer. Three methods of autophagy inhibition were used in conjunction with MTS cell viability assays.

Beclin-1, together with class III PI3K, forms a complex that is involved in the localisation of autophagic proteins to a pre-autophagosomal structure. As well as its role in inhibiting apoptosis, Bcl2 can also inhibit autophagy by binding to the BH3 region of Beclin-1 to prevent formation of this complex (Pattingre, Tassa et al. 2005). Similarly, 3-methyladenine (3-MA) inhibits the activity of class III PI3K (Seglen and Gordon 1982), thus also inhibiting autophagy. As Bcl2 and 3-MA are both early inhibitors of autophagy, a third late inhibitor (chloroquine) was used which acts by raising lysosomal pH to inhibit autophagosome and lysosome fusion. As well as acting as a late inhibitor of autophagy chloroquine can also inhibit beclin-1 independent autophagy, which although uncommon, has been described (Scarlatti, Maffei et al. 2008; Tian, Lin et al. 2010).

5.2.2.1 Overexpression of Bcl2

Overexpression of Bcl2 in OVCAR4-Bcl2 cells decreased LC3B cleavage following infection with both Lister-wt and Lister-dTK to approximately one third of that observed in parental OVCAR4 cells (Figure 57a). As shown previously, and again here in Figure 57c, this inhibition of autophagy does not cause significant attenuation of either Lister-wt or Lister-dTK cell death.

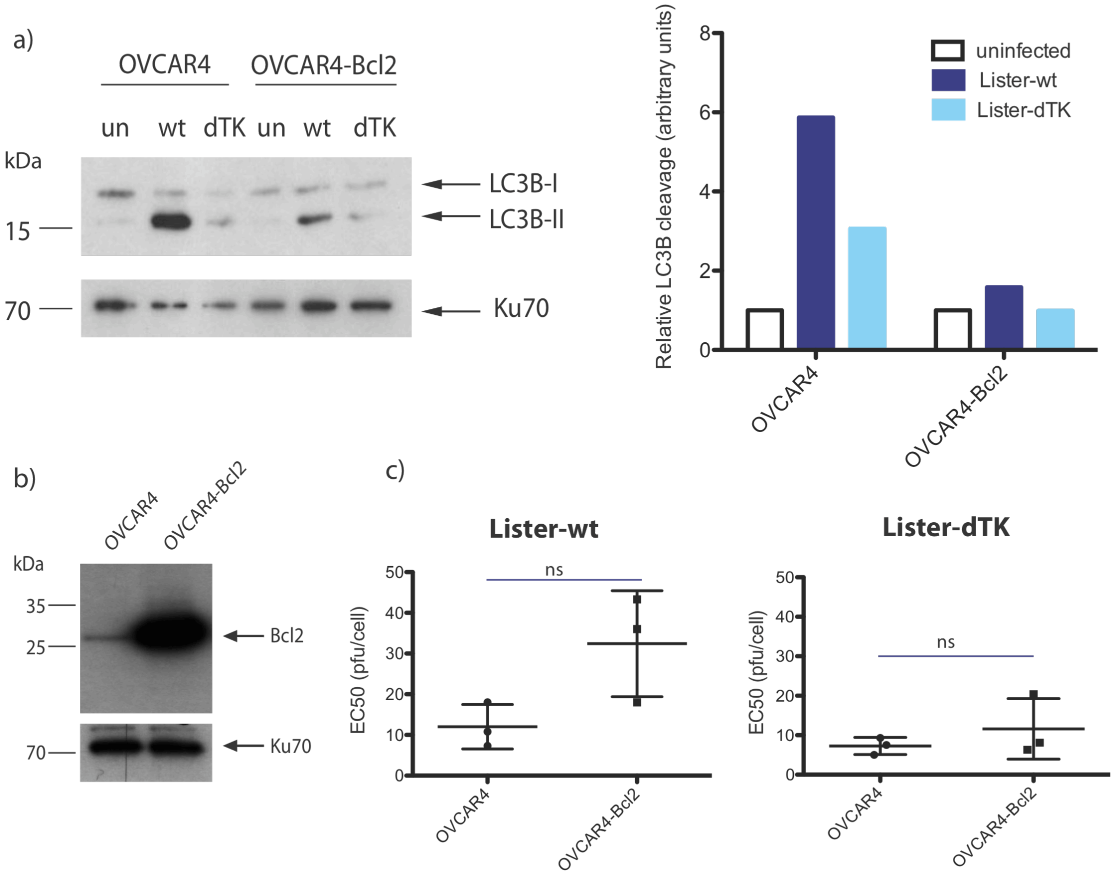

Figure 57: Overexpression of Bcl2 inhibits vaccinia-induced LC3B cleavage but does not affect cytotoxicity. a) Inhibition of LC3B cleavage by Bcl2. Cells were infected with 1pfu/cell of virus and levels of LC3B determined 72hrs post-infection by western blotting. Quantification of LC3B cleavage relative to uninfected cells. b) Confirmation of Bcl2 overexpression in OVCAR4-Bcl2 cells compared to the parental OVCAR4 cells c) Comparison of the sensitivity of OVCAR4 and OVCAR4-Bcl2 cells to vaccinia virus. Data show the mean ± SD of three experiments, each performed in triplicate.

5.2.2.2 Inhibition of autophagy by 3-methyladenine and chloroquine

Next, the effect of the early autophagy inhibitor 3-methyladenine (3-MA) and the late inhibitor chloroquine (CQ) on the cytotoxicity of Lister-dTK were assessed using a cell viability assay in A2780, A2780CP and Igrov1 cells. Toxicity studies showed that concentrations of up to 2mM 3-MA were relatively non-toxic in A2780CP and Igrov1 cells, although A2780 cells were more sensitive to 3-MA, with 88% and 69% viability at 1mM and 2mM 3-MA respectively (Figure 58). Chloroquine was non-toxic at low concentrations (1μM and 5μM) in A2780CP and Igrov1 cells, although some cell death was observed at higher concentrations (Figure 59). A2780 cells were far more sensitive to the effects of chloroquine with 5μM causing 38% cell death, rising to 75% at 20μM.

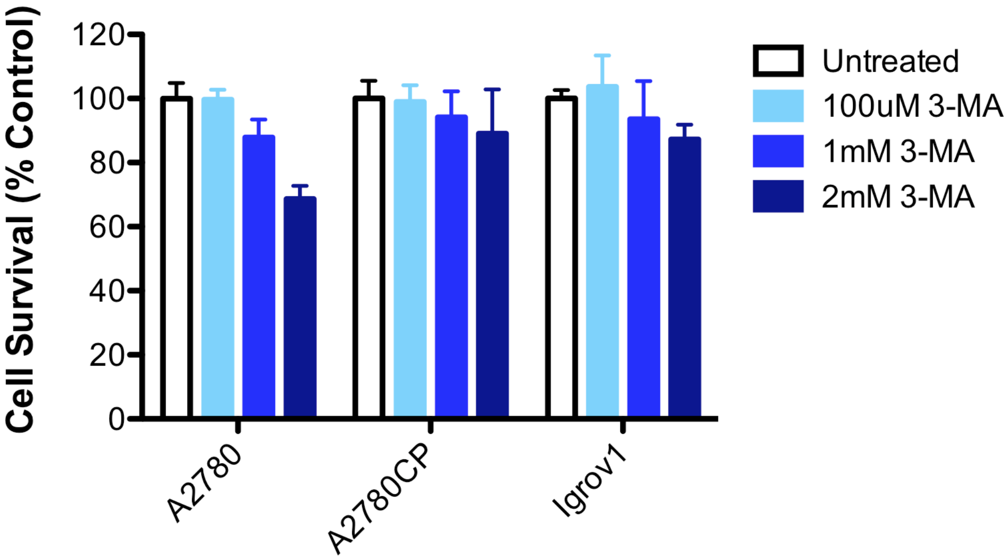

Figure 58: Toxicity of 3-MA in ovarian cancer cell lines. Cells were grown in the presence of varying concentrations of 3-MA and cell survival determined by MTS assay three days later. Data show the mean+SD survival from 2-5 experiments, each performed in triplicate.

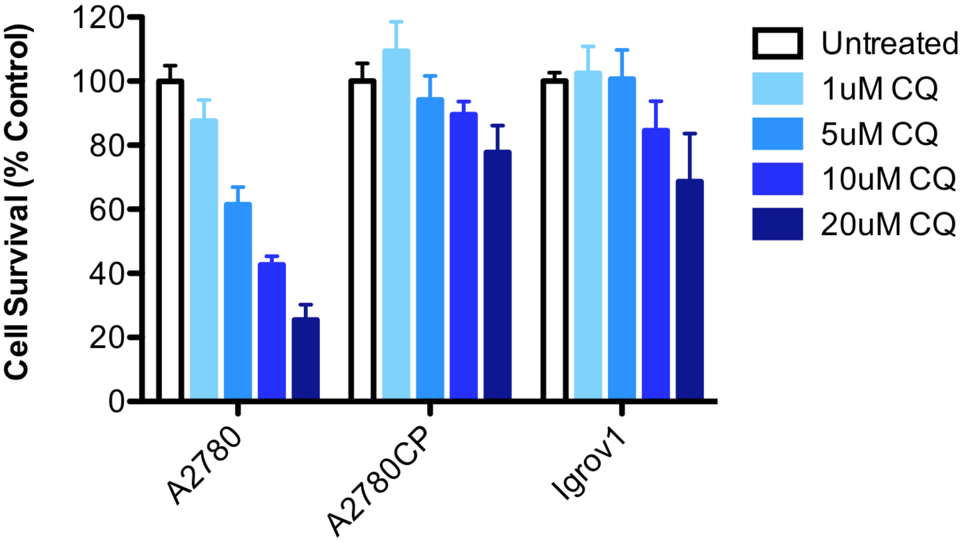

Figure 59: Toxicity of CQ in ovarian cancer cell lines. Cells were grown in the presence of varying concentrations of CQ and cell survival determined by MTS assay three days later. Data show the mean+SD survival from 3-4 experiments, each performed in triplicate.

To avoid interfering with viral entry, 3-MA or CQ was added to cells 2 hrs post-infection with Lister-dTK and cell survival measured 72hrs post-infection. In wells infected with Lister-dTK and either 3-MA or CQ, cell survival was normalised each time to the effect of 3-MA or chloroquine alone. The EC50 of Lister-dTK in the presence of these inhibitors was then expressed relative to the EC50 of Lister-dTK alone for each experiment.

Consistent with inhibition of autophagy by Bcl2, inhibition using an alternative inhibitor, 3-MA, did not attenuate Lister-dTK cytotoxicity in A2780, A2780CP or Igrov1 cells (Figure 60). This suggests that autophagy does not significantly contribute to vaccinia-induced cell death in ovarian cancer cell lines. It also appears to offer no survival advantage, as impairment of autophagy by 3-MA does not render cells more susceptible to death.

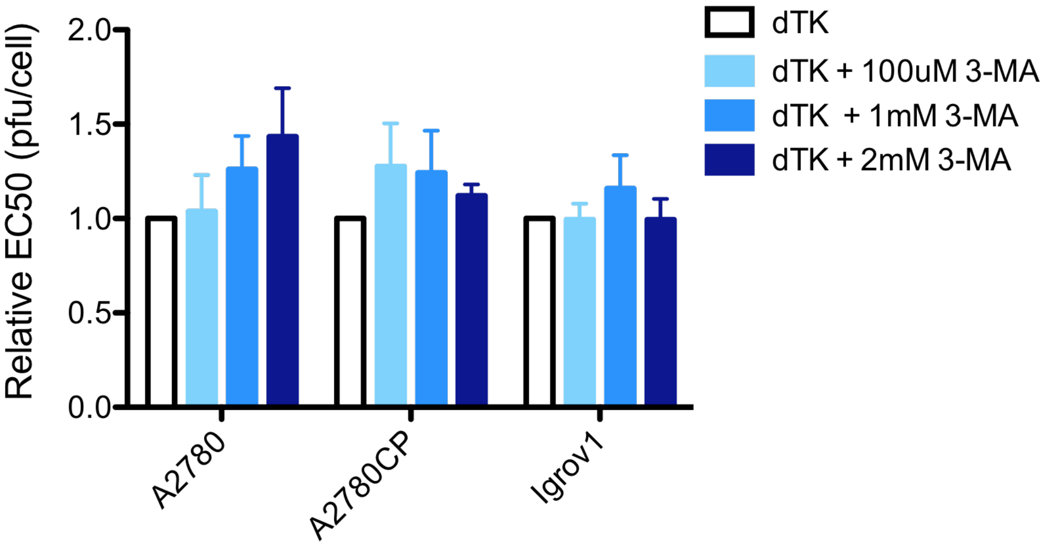

Figure 60: Inhibition of autophagy using 3-methyladenine (3-MA) does not affect vaccinia-induced cell death. Cells were infected with increasing doses of Lister-dTK followed by the addition of either 3-MA or vehicle alone 2 hrs later. Cell survival was measured by MTS assay 72hrs post-infection. The EC50 of Lister-dTK in the presence of 3-MA was normalised to the EC50 of Lister-dTK alone for each experiment. Data show the mean+SD of the relative EC50 from 2-5 experiments, each performed in triplicate.

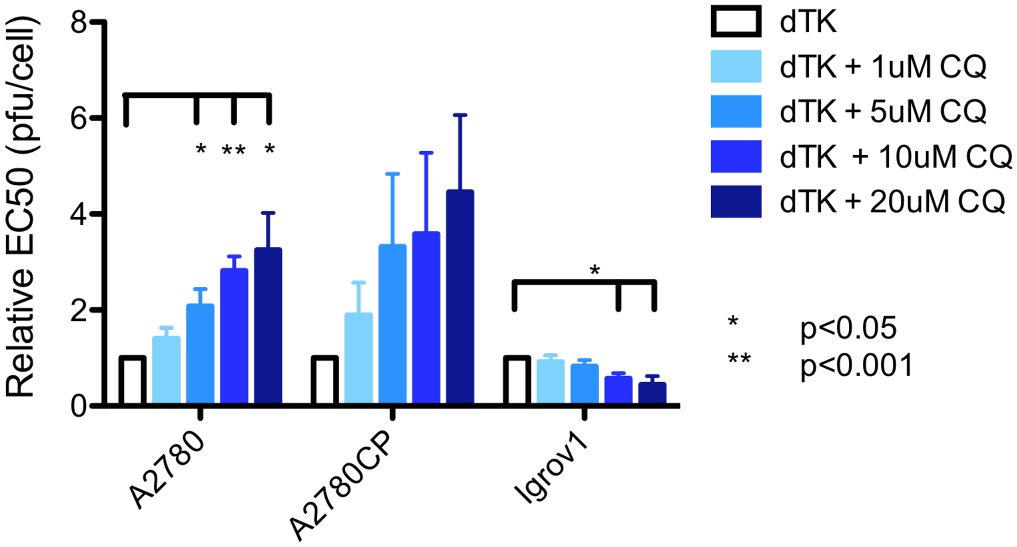

Figure 61: Inhibition of autophagy by chloroquine (CQ) does not affect vaccinia-induced cell death. Cells were infected with increasing doses of Lister-dTK followed by the addition of either CQ or vehicle alone 2 hrs later. Cell survival was measured by MTS assay 72hrs post-infection. The EC50 of Lister-dTK in the presence of CQ was normalised to the EC50 of Lister-dTK alone for each experiment. Data show the mean+SD of the relative EC50 from 3-4 experiments, each performed in triplicate.

Inhibition of autophagy by chloroquine did not significantly increase the EC50 of Lister-dTK in A2780CP cells at any of the concentrations used, although there was a trend for the EC50 to increase with increasing dose of CQ (Figure 61). This same trend was observed in A2780 cells, with a significant 2-fold or 3-fold increase in the EC50 of Lister-dTK in the presence of 5μM, 10μM and 20μM chloroquine. However, at these concentrations between 40% and 75% cell death occurred due to the presence of chloroquine alone (Figure 59), which is likely to have effected the kinetics of vaccinia virus replication. Interestingly, high doses of chloroquine (10μM and 20μM) had the opposite effect on EC50 in Igrov1 cells, and significantly decreased the EC50 of Lister-dTK by approximately 50%. As Igrov1 cells are already sensitive to Lister-dTK however, this corresponded to a reduction in EC50 from 4.6pfu/cell to 2.5pfu/cell and 1.8pfu/cell in the presence of 10μM or 20μM CQ respectively. The physiological relevance of this relatively minor decrease in EC50 of Lister-dTK may be small.

5.3 Necrosis

5.3.1 Markers of necrosis induced by Lister-dTK

Historically, the description of necrosis has leaned towards a negative definition characterised by the absence of apoptotic or autophagic events. Recently, much progress has been made to define necrosis in a positive manner and to describe a series of markers, events and molecular mechanisms that can characterise necrosis. However, a common biochemical denominator and the chronological order of necrotic events are yet to be fully elucidated and necrosis is typically defined by morphological changes, a loss of ATP and release of cellular content as the cell membrane ruptures. In this section, the induction of necrosis by vaccinia virus Lister-dTK is studied by identifying these markers of necrosis in infected cells.

5.3.1.1 Loss of intracellular ATP

It is widely believed that apoptosis is an energy-dependent process whereby ATP is required for various steps of the apoptotic pathway such as formation of the Apaf-1-cytochrome c complex (the apoptosome) and as a phosphoryl donor during phosphorylation of key proteins involved in apoptosis. These include the anti-apoptotic protein Bcl-2, which is inactivated by phosphorylation, and the pro-apoptotic proteins Bad, Bim and Bmf, which are activated by phosphorylation (reviewed in (Skulachev 2006)). In contrast, necrosis is generally considered to be energy independent and is characterised by a loss of intracellular ATP leading to cell death.

Infection with Lister-dTK resulted in a steady decline in the levels of intracellular ATP, which were significantly decreased at 48hrs and 72hrs post-infection in A2780, A2780CP, Skov3ip1 and TOV21G cells (Figure 62a and Figure 62c). Loss of ATP correlated with a decrease in cell survival as virus infection progressed over time but appeared to precede it. At 48hrs p.i, cell survival ranged from 66%-93% with Skov3ip1 cells the most sensitive to Lister-dTK and TOV21G the least sensitive (Figure 62b). Cell death was further increased at 72hrs p.i as infection progressed and cell survival was just 29%-68% of untreated cells, depending on the cell line. A2780CP and Skov3ip1 demonstrated the most cell death at 72hrs p.i with 29% and 43% cell survival respectively. These cell lines also showed the highest decrease in intracellular ATP with levels just 9% and 17% of untreated cells.

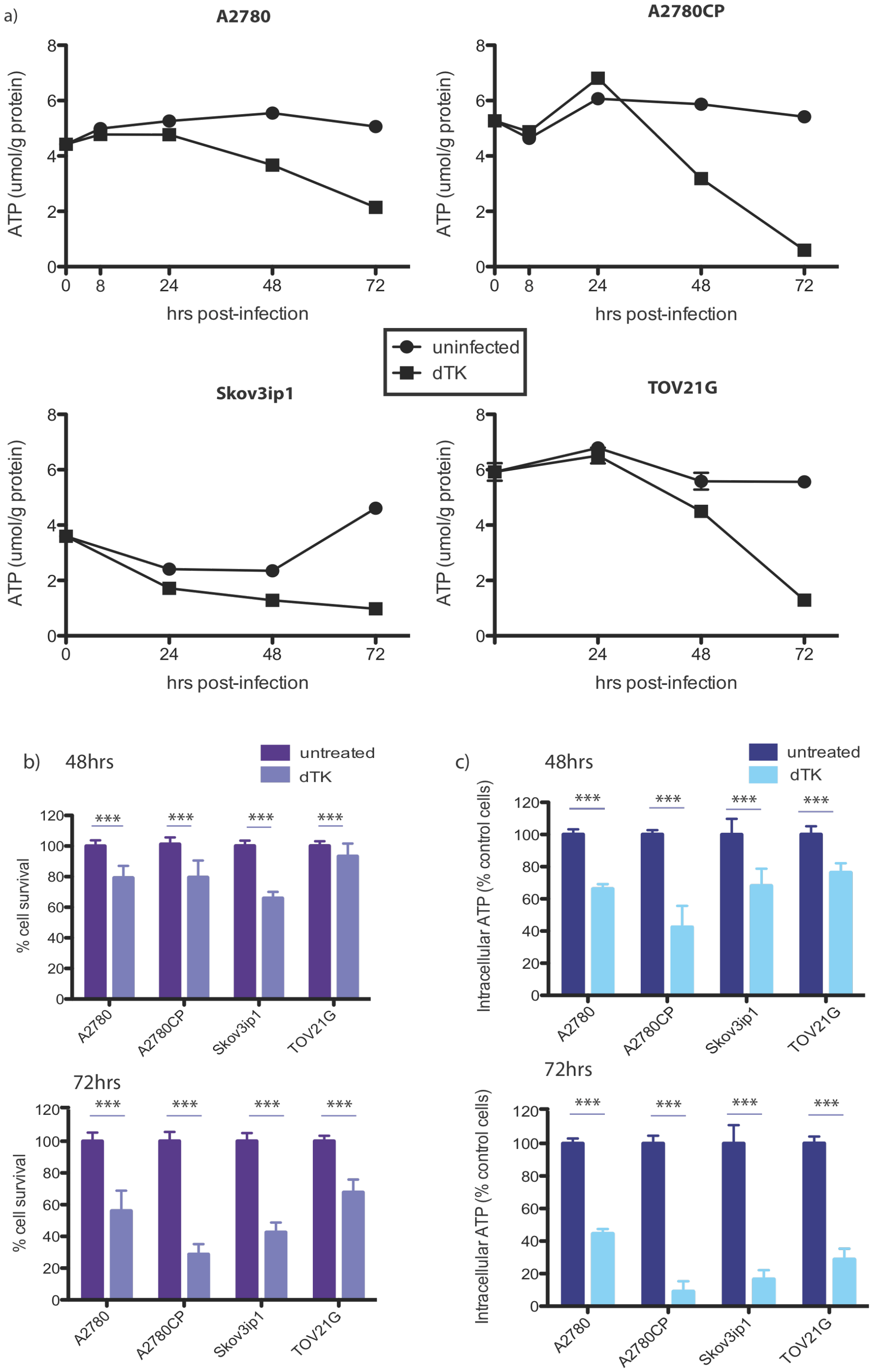

Figure 62: Infection with Lister-dTK leads to loss of intracellular ATP a) Cells were infected with 10 pfu/cell of Lister-dTK and harvested over a timecourse of 72hrs. Intracellular ATP levels were quantified from extracted protein using a luciferase based ATP assay. Data show the mean + SD of a single representative experiment performed in triplicate b) Cell survival following infection with 10 pfu/cell Lister-dTK at 48hrs post-infection (top) and 72hrs post-infection (bottom) Data show the mean + SD of three experiments each performed on 6 replicates c) loss of intracellular ATP 48hrs (top) and 72hrs (bottom) post-infection. Data show the mean + SD of 2-4 experiments, each performed in triplicate. ***p=<0.0001

5.3.1.2 Release of high mobility group box protein 1

High mobility group box protein 1 (HMGB1) is a nuclear protein that is passively released during necrosis but not apoptosis, where chromatin binding prevents its release (Raucci, Palumbo et al. 2007). HMGB1 binds to RAGE to mediate inflammation, and its release triggers the release of pro-inflammatory cytokines (Scaffidi, Misteli et al. 2002). Although there are some data to suggest that HMGB1 release can also occur during apoptotic cell death (Bell, Jiang et al. 2006), release is generally considered to be a marker of necrosis.

Infection with Lister-dTK in A2780 cells resulted in release of HMGB1 into the supernatant at 72hrs post-infection; earlier timepoints did not reveal evidence of protein release (Figure 63). Although there was also some HMGB1 present in the supernatant of uninfected cells at 72hrs this increased two-fold following infection with Lister-dTK.

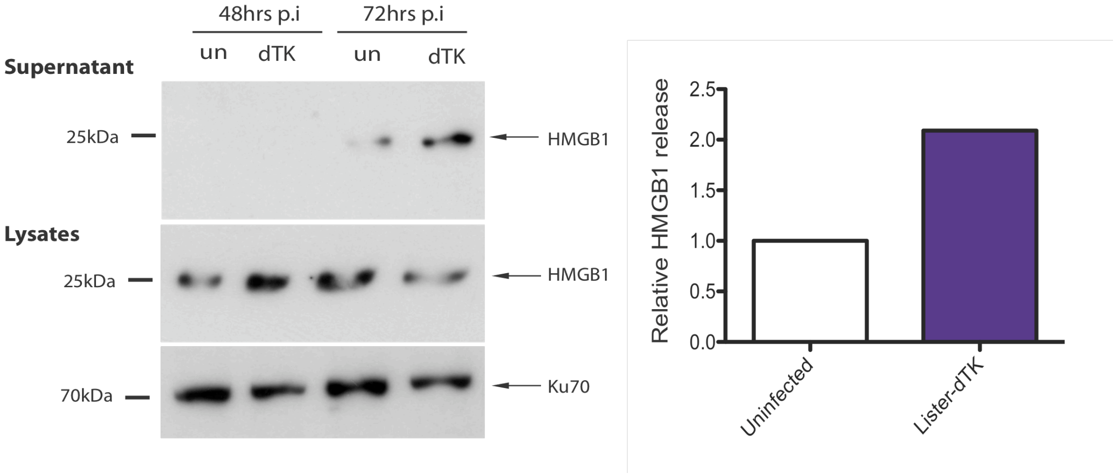

Figure 63: Release of HMGB1 from infected cells. A2780 cells were infected with 10pfu/cell of Lister-dTK and both supernatant and cell lysates collected 72hrs post-infection. HMGB1 was detected by western blotting. Quantification shows the amount of HMGB1 released into the supernatant of infected cells relative to uninfected control cells.

The release of HMGB1 *in vivo* was also determined by immunohistochemistry on excised Skov3ip1 tumours that had been growing intraperitoneally in nude mice. Consistent with published data that describes strong to moderate nuclear expression of HMGB1 in ovarian cancer (Uhlen M 2010), HMGB1 was clearly visible in the nucleus of viable, uninfected Skov3ip1 cells (Figure 64C and D). In contrast, there was more diffuse staining in necrotic tissue, which may represent extracellular HMGB1 that has been released from dying cells. Lister-dTK infected cells did not show obvious differences in HMGB1 localisation compared to their uninfected counterparts (Figure 64B and C), and in both case nuclear HMGB1 was observed.

Similarly, nuclear HMGB1 could be observed in normal mouse liver cells (Figure 65B), although there was also fairly strong cytoplasmic staining that does not corroborate previous findings (Uhlen M 2010) and may be background staining. Whilst there was some evidence of HMGB1 in the nucleus of Lister-dTK infected tumour cells growing on the surface of the liver (compare staining for vaccinia virus proteins in Figure 65A with HMGB1 expression in Figure 65B), the majority of infected cells were devoid of nuclear expression. Due to the presumed high level of background staining, it was difficult to determine if HMGB1 protein was instead present extracellularly around infected cells. However, there does appear to be an association between vaccinia infection and reduction in nuclear HMGB1 expression.

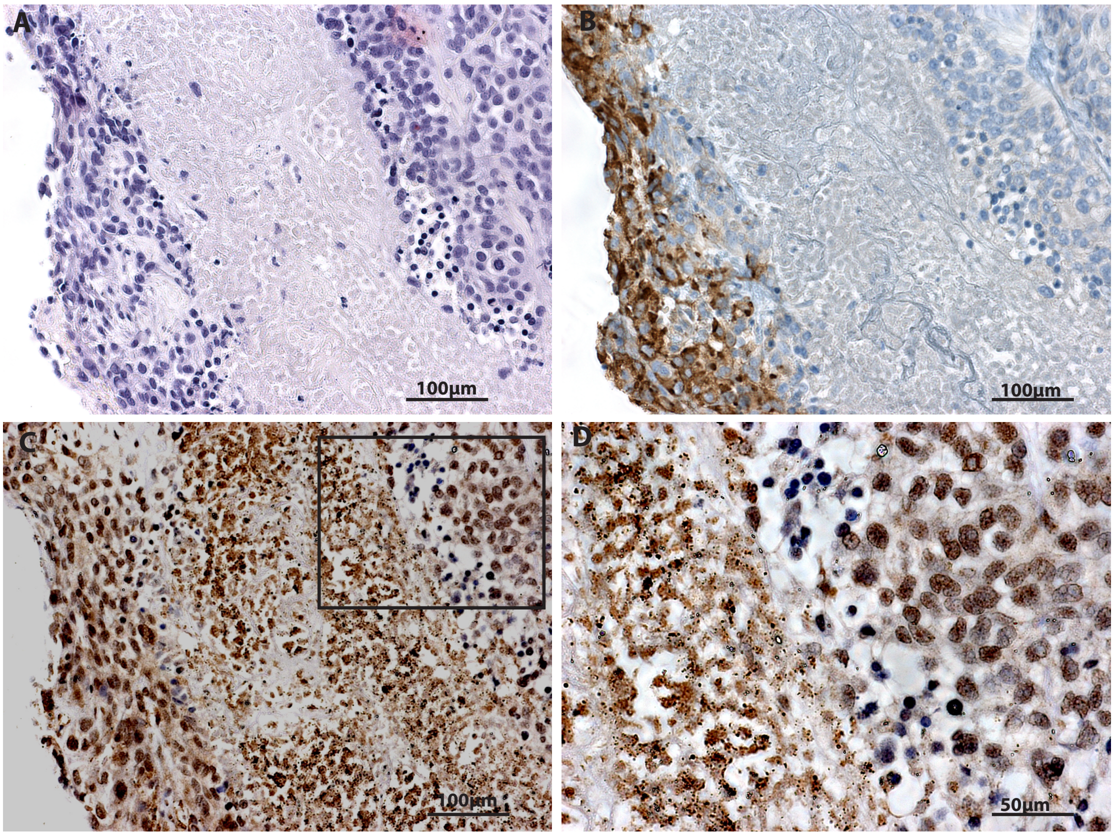

Figure 64: Release of HMGB1 is associated with necrotic tissue *in vivo*. Skov3ip1 intraperitoneal tumours growing in CD1 nu/nu mice were excised following injection with a single intraperitoneal dose of 10^8 pfu Lister-dTK and stained for B) vaccinia virus proteins or C and D) HMGB1. The image in panel D represents a higher magnification of the boxed area in panel C. A) H&E staining was performed on a consecutive tissue section.

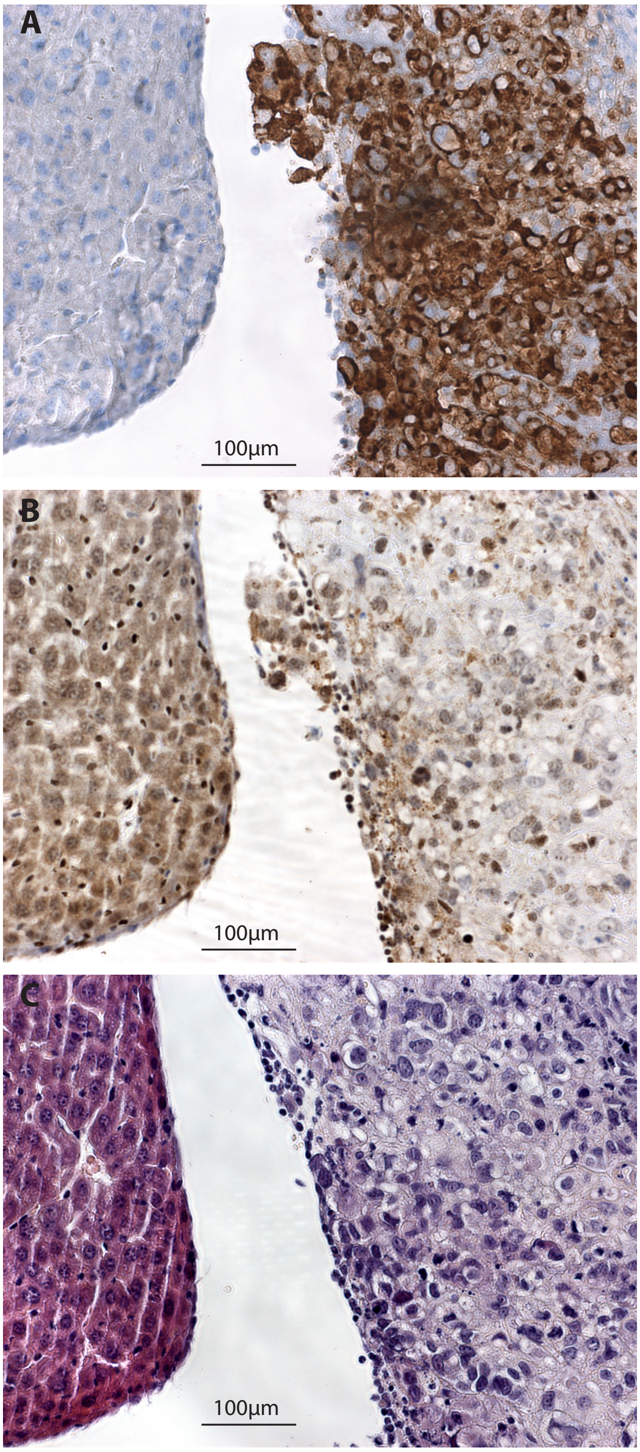

Figure 65: Localisation of HMGB1 in Lister-dTK infected Skov3ip1 tumours. Normal liver and associated tumour was harvested from CD1 nu/nu mice bearing intraperitoneal Skov3ip1 tumours, 72hrs post-infection with a single dose of 10^8 Lister-dTK intraperitoneally. Tissue was stained for A) expression of vaccinia virus proteins and B) HMGB1. Panel C shows specimen histology by staining with H&E.

5.3.1.3 Morphological changes

Unlike apoptosis, which is characterised by cell shrinkage, chromatin condensation and the formation of membrane-enclosed apoptotic bodies, necrotic cells typically have swollen organelles, accompanied by nuclear and cell membrane rupture. The morphology of Lister-dTK infected A2780 cells at 72hrs post-infection was studied by electron microscopy and compared to that of uninfected cells.

Cells in various stages of the infectious cycle could be seen within the same field of view, illustrating the replicative nature of vaccinia as it spreads from cell to cell (Figure 66B). Infected cells ranged from those in the early stages of infection, where virus factories and the formation of immature virions were just occurring, to cells that were in the late stages of infection and burdened with a huge viral load. In addition, there was clear evidence of cell death and resulting cell debris, which was often still associated with virus (Figure 66B).

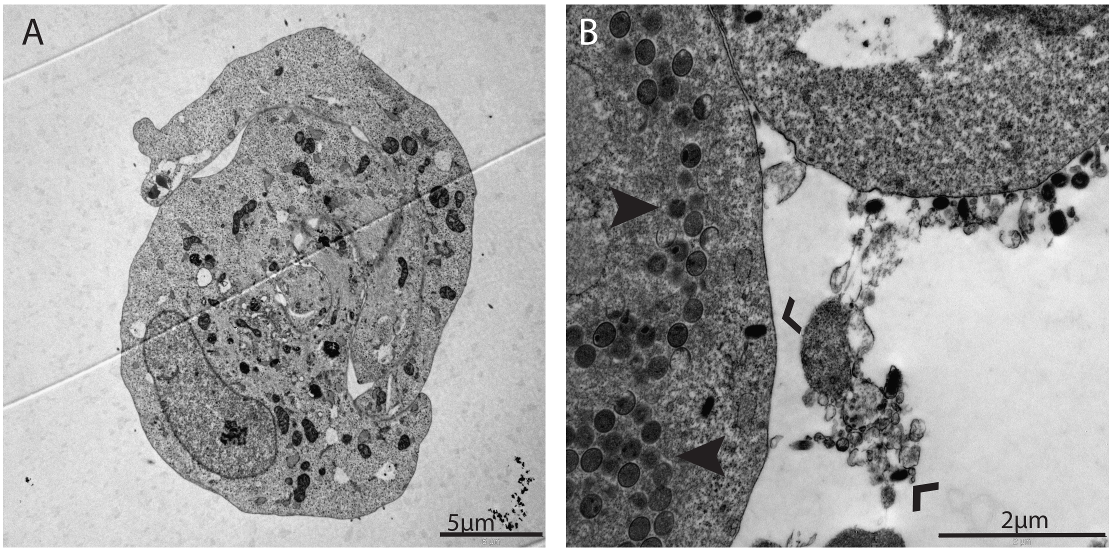

Figure 66: Electron microscopy of infectious vaccinia virions. A) Uninfected A2780 cell B) A2780 cells infected with 10pfu/cell Lister-dTK for 72hrs. A cell in early stage of infection can be seen with immature (closed arrowheads) and intracellular mature virions (IMVs) (open arrowheads). Cell debris from a dead cell can also be seen, still associated with mature virions (open arrowhead), which congregate at the cell surface of a neighbouring cell.

Infected/dying cells typically demonstrated a necrotic morphology. There was evidence of enlarged swollen nuclei in infected cells (Figure 67D) and rupture of both nuclear and cytoplasmic cell membranes (Figure 67C and D). In addition, vacuolar structures, which have occasionally been described as a feature of necrosis, were observed in infected cells (Figure 67B and Figure 67C and D). As vaccinia infection leads to a decrease in levels of intracellular ATP (Figure 62) and encodes proteins that interfere with the mitochondrial route to apoptosis

(Wasilenko, Meyers et al. 2001; Wasilenko, Banadyga et al. 2005), it was proposed that dysregulated mitochondrial activity may result from infection, and that this might be evident in the morphology of mitochondria in infected cells. Although differences were subtle there was evidence of enlarged mitochondria following infection with Lister-dTK (Figure 68D), consistent with the swollen organelles associated with necrosis (Kroemer, Galluzzi et al. 2009).

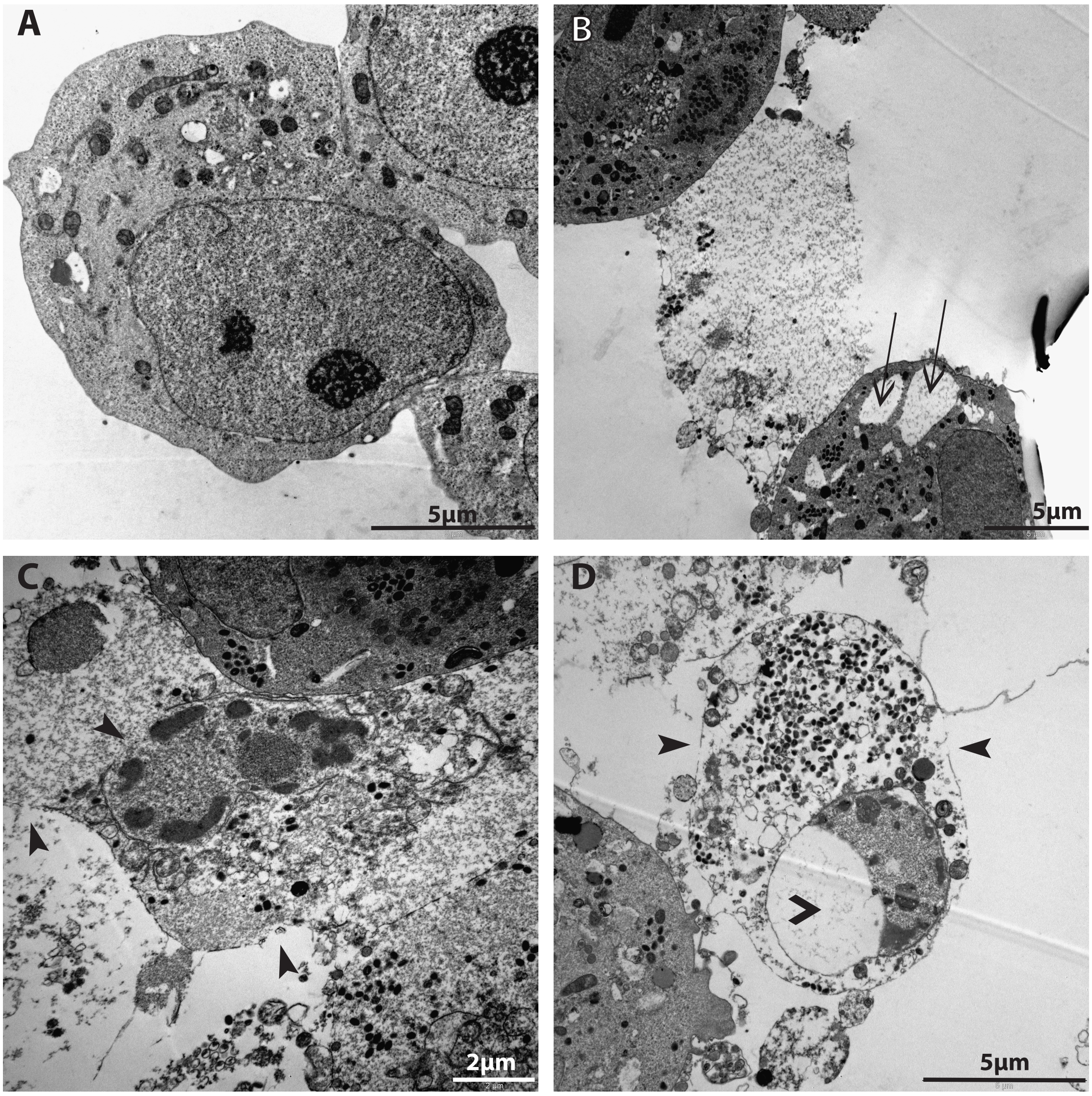

Figure 67: Membrane rupture following infection with Lister-dTK. A2780 cells were infected with 10pfu/cell for 72hrs and cell morphology analysed by electron microscopy. A) Uninfected control cell. B-D) Infected cells. Lister-dTK led to the formation of cytoplasmic vacuoles (arrows), nuclear and cytoplasmic membrane rupture (closed arrowheads) and swollen nuclei (open arrowhead).

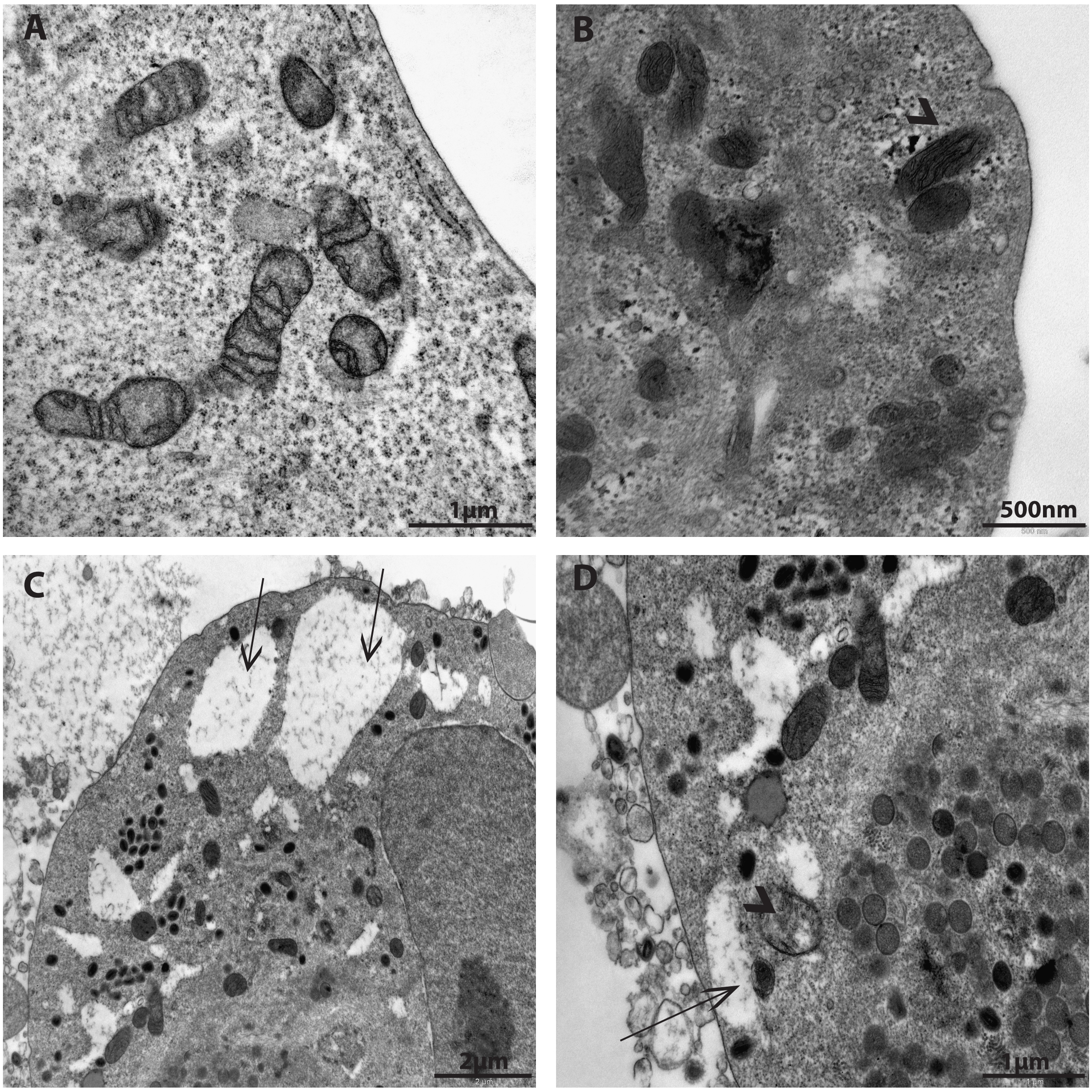

Figure 68: Formation of cytoplasmic vacuoles, and changes in mitochondrial morphology in response to Lister-dTK infection. A2780 cells were infected with 10pfu/cell for 72hrs and cell morphology analysed by electron microscopy. A) Uninfected control cell. B-D) Infected cells. Lister-dTK led to the formation of cytoplasmic vacuoles (arrows), and dense mitochondria (open arrowheads).

5.3.2 Programmed necrosis

The term 'programmed necrosis' has emerged from recent research showing that, in contrast to previously held beliefs that necrosis was an uncontrolled and unregulated affair, it can also occur in a regulated manner in response to various stimuli, including virus infection. Most widely studied is the induction of programmed necrosis via the TNFR pathway, which can result in either apoptosis or necrosis depending on cellular caspase 8 activity. Caspase 8 normally triggers apoptosis and can also cleave, and thus inactivate, two proteins critical to programmed necrosis, RIP1 and RIP3. In the absence or inhibition of caspase 8, signalling pathways can switch from an apoptotic route to an as yet undefined programmed necrosis pathway (Vandenabeele, Galluzzi et al. 2010). As viruses, including vaccinia, encode inhibitors of caspase 8 this pathway may be initiated as an alternative to apoptosis in infected cells.

The pro-necrotic RIP1/RIP3 complex has been detected in the liver of wild-type mice within 24hrs of infection with vaccinia virus (Cho, Challa et al. 2009). Comparison of infection in wild-type and RIP3$^{-/-}$ mice showed significantly reduced inflammation in RIP3$^{-/-}$ which corresponded to increased viral titres in the liver and spleen (Cho, Challa et al. 2009). Similarly, cell death in RIP3$^{-/-}$ T cells *in vitro* was significantly lower than that of the wild-type counterparts. In a review on programmed necrosis in response to infection with murine cytomegalovirus (MCMV), it was also suggested that levels of RIP3 determine sensitivity of the cell to programmed necrosis (Brune 2011), and that the MCMV protein M45 could block RIP1 mediated signalling and an inflammatory response (Mack, Sickmann et al. 2008). It has also been shown that M45 can block RIP3-dependent necrosis in the absence of RIP1 (Upton, Kaiser et al. 2010), suggesting multiple roles of viral inhibitors of programmed necrosis and that the molecular pathway of virus-induced programmed necrosis may differ from that of the TNFα-induced route often described, in which RIP1 is a critical component.

We aimed to investigate the role of programmed necrosis in the sensitivity of ovarian cancer cell lines to vaccinia virus. This centred on detection of individual key proteins involved in this pathway, detection of a pro-necrotic molecular complex termed the necrosome or ripoptosome and investigation into levels of key proteins following infection with virus. Secondly, programmed necrosis was inhibited through use of both a commercial RIP1 inhibitor, necrostatin-1, and by knocking down both RIP1 and RIP3 using siRNA to determine which, if any, of these proteins is most critical in sensitivity to vaccinia-induced cell death.

5.3.2.1 Endogenous levels of RIP1 and RIP3 in ovarian cancer

As RIP1 and RIP3 are key proteins involved in the control and execution of programmed necrosis, endogenous levels of these proteins were examined in a panel of ovarian cancer cell lines (Figure 69). Whilst RIP1 was expressed at a similar level in all of the six cell lines tested, the levels of RIP3 varied considerably between cell lines; levels were fairly similar in A2780, A2780CP, Skov3ip1 and OVCAR4 cells but there was a huge increase in expression in TOV21G cells.

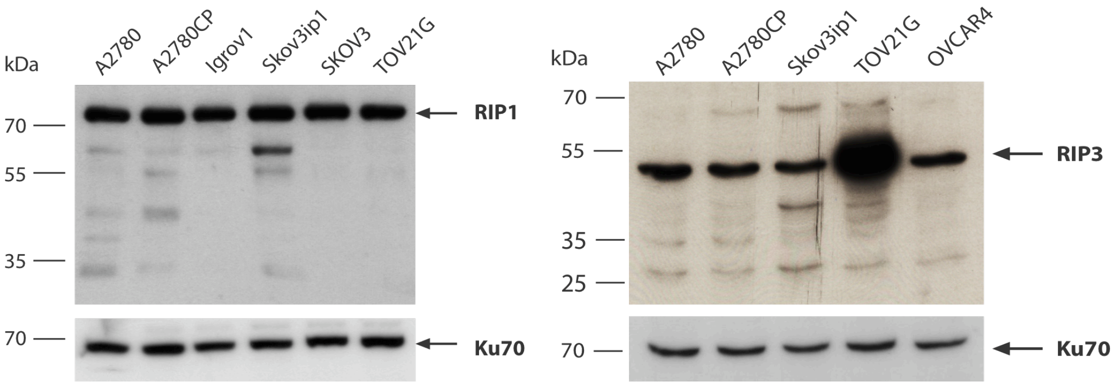

Figure 69: Expression of RIP1 and RIP3 proteins in ovarian cancer cell lines.

5.3.2.2 Levels of RIP1 and RIP3 following infection with vaccinia

Although a RIP1/RIP3 complex has been described following infection with vaccinia, modification of RIP1 and RIP3 expression as a result of infection has yet to be described. To determine if levels of RIP1 and RIP3 were altered in ovarian cancer cell lines following infection with Lister-dTK, protein in uninfected and infected cells was detected by western blotting. As caspase 8 can cleave both RIP1 (Lin, Devin et al. 1999) and RIP3 (Feng, Yang et al. 2007) levels of caspase 8 were also determined. To further understand changes in protein expression, cells were incubated in the presence or absence of a proteasome inhibitor, MG132, for 5hrs prior to harvest, to determine whether a reduction in protein levels was due to proteasomal degradation.

Levels of RIP1 protein were decreased in A2780, A2780CP, Skov3ip1 and TOV21G cells at 72hrs post-infection with 10pfu/cell of Lister-dTK (Figure 70). RIP3 expression varied between cell lines even in uninfected cells, with high expression in TOV21G and very little in Skov3ip1 cells. A demonstrable reduction in RIP3 expression post-infection was observed in TOV21G cells, and to a lesser degree in A2780 and A2780CP cells, although protein loading was unequal between uninfected and infected A2780CP samples which may account for this apparent decrease in expression. As Skov3ip1 cells express very little RIP3 it was difficult to detect any further decrease post-infection in this cell line. Similarly, levels of caspase 8 were reduced in A2780CP, Skov3ip1 and TOV21G cells 72hrs after infection with Lister-dTK.

Incubation with the proteasome inhibitor, MG132, did not reverse the observed decrease in expression of RIP1, RIP3 or caspase 8 (Figure 70). This suggests that vaccinia virus does not decrease expression of RIP1, RIP3 or caspase 8 proteins by proteasomal degradation. In contrast, MG132 was able to increase levels of p21 in both uninfected and infected A2780 cells (Figure 70), and in uninfected A2780CP and TOV21G cells, showing the efficacy of MG132 as a proteasome inhibitor.

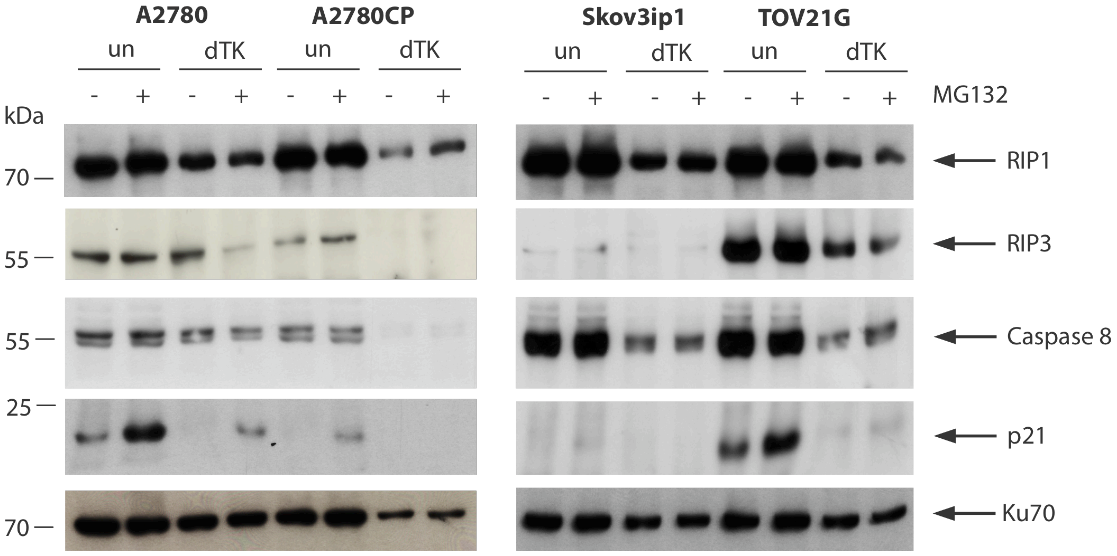

Figure 70: Decreases in RIP1, RIP3 and caspase 8 proteins following infection with Lister-dTK are not due to proteasomal degradation. Cells were infected with 10 pfu/cell Lister-dTK and lysates harvested 72hrs post-infection for detection of proteins by western blotting. Where appropriate, the proteasome inhibitor MG132 was added at 10μM 5hrs before harvest.

5.3.2.3 Formation of a cell death-inducing platform in response to vaccinia

The formation of a cell death-inducing platform, termed the ripoptosome, in response to genotoxic stress has been described which comprises RIP1, FADD and caspase-8 (Tenev, Bianchi et al. 2011). In addition, the recruitment of caspase 10 and caspase inhibitor cFLIP isoforms to this complex has also been described (Feoktistova, Geserick et al. 2011). In contrast to another cell death-inducing platform, the necroptosome, which consists of caspase-8, TRADD, FADD, RIP1 and RIP3 (Vandenabeele, Galluzzi et al. 2010), the ripoptosome forms independent of TNF or death receptor activation. Just as the necroptosome can lead to either apoptotic or necroptotic death depending on the activity of caspase-8, the ripoptosome is regulated by FLIP, cIAP1, cIAP2 and XIAP, which inactivate or target components of the complex for ubiqutylation (Feoktistova, Geserick et al. 2011; Tenev, Bianchi et al. 2011). As a RIP1/RIP3 complex has been identified in vaccinia infected mouse embryonic fibroblasts in the presence of TNFα, and in infected liver cells *in vivo* (Cho, Challa et al. 2009), and as vaccinia virus encodes inhibitors of caspase 8 (Tewari and Dixit 1995; Dobbelstein and Shenk 1996; Kettle, Alcami et al. 1997; Zhou, Snipas et al. 1997; Li and Beg 2000) and poxvirus viral FLIPs have also been described that may be involved in the regulation of cell death pathways (Hu, Vincenz et al. 1997; Thome, Schneider et al. 1997), the formation of cell-death inducing platforms was investigated in Lister-dTK infected ovarian cancer cells.

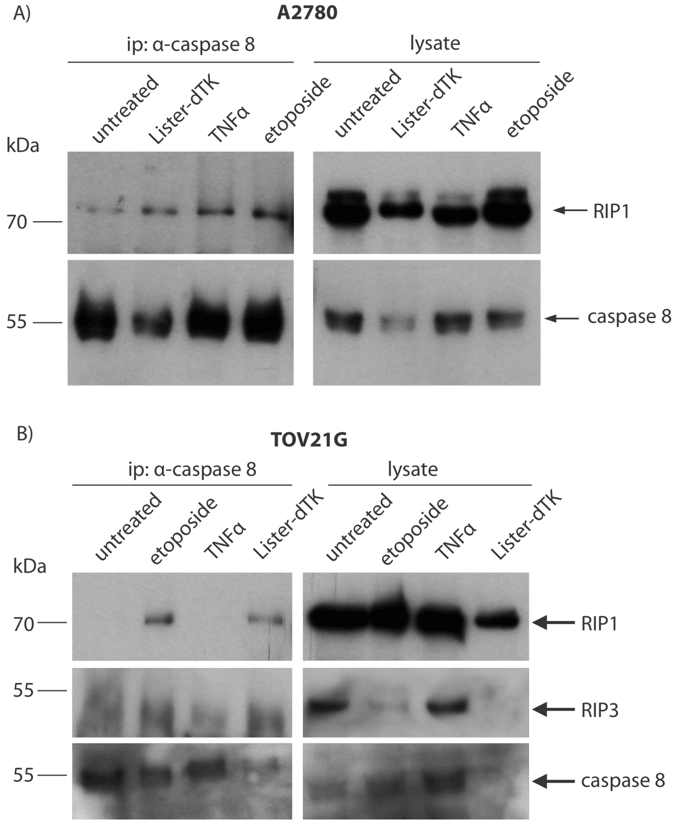

Figure 71: Vaccinia infection stimulates the association of RIP1 to caspase 8 in ovarian cancer cells. A2780 and TOV21G cells were infected with 10pfu/cell Lister-dTK and harvested 96hrs post-infection. Cells were also treated with 100µM etoposide or 25ng/ml TNFα overnight. All samples were incubated in the presence of 25µM zVAD-fmk overnight prior to harvest, as this stabilises caspase-8 containing complexes (Micheau and Tschopp 2003). Caspase-8 was immunoprecipitated (ip), and the presence of RIP1, RIP3 and caspase-8 was assayed by immunoblotting.

Infection with Lister-dTK led to the formation of a RIP1/caspase-8 complex at 96hrs post-infection in A2780 (Figure 71A) and TOV21G cells (Figure 71B). As etoposide (Tenev, Bianchi et al. 2011) and TNFα in the presence of zVAD-fmk (Chan, Shisler et al. 2003; Cho, Challa et al. 2009; Zhang, Shao et al. 2009) have been reported to lead to the formation of the ripoptosome and necroptosome respectively, cells were also treated with 100µM etoposide or 25ng/ml TNFα as potential positive controls. Lister-dTK, etoposide and TNFα initiated RIP1/caspase 8 complex formation in A2780 cells (Figure 71A); interestingly, RIP1 bound to caspase-8 could also be detected in untreated cells. However, as apoptosis can occur downstream of RIP1 and caspase 8 containing complexes, this may represent the apoptotic demise of over confluent cells. Lister-dTK and etoposide also resulted in a RIP1/caspase-8 complex in TOV21G cells, which was not evident in untreated or TNFα treated cells (Figure 71B).

Infection with Lister-dTK led to a reduction of both RIP1 and caspase-8 in A2780 and TOV21G cell lysates (Figure 71, right hand side panels) to the extent that caspase 8 was virtually undetectable in TOV21G infected cells. This reduction in RIP1 and caspase-8 following vaccinia infection was determined in previous experiments (Figure 70) and was more pronounced in TOV21G cells than in A2780, consistent with the data presented here. The reduction in caspase-8 in the total cell lysate led to a lower amount being precipitated in both A2780 and TOV21G Lister-dTK treated samples. Despite this lower input, RIP1 was found complexed to caspase-8 at higher levels in Lister-dTK infected A2780 cells compared to untreated cells. Similarly, complex formation was exclusive to Lister-dTK and etoposide treated TOV21G cells despite a huge decrease in caspase-8 immunoprecipitation in Lister-dTK infected cells.

RIP3 levels were undetectable in infected TOV21G lysates (Figure 70) and in all A2780 lysates (data not shown) although this may represent the limit of detection in this single experiment as previously, whilst RIP3 levels were reduced following vaccinia infection (Figure 70), they were still apparent. A band at the approximate expected size of RIP3 was detected in caspase-8 immunoprecipitated samples, which appeared highest in Lister-dTK and etoposide treated cells (Figure 71B, left panel), although it was difficult to conclusively show that this was specific as there was a high level of background and non-specific bands.

5.3.2.4 Inhibition of RIP1 kinase activity by necrostatin-1

To determine the role of RIP1 kinase activity in vaccinia-induced cell death, A2780, A2780CP, Igrov1 and Skov3ip1 cells were infected with increasing doses of Lister-dTK in the presence or absence of the inhibitor necrostatin-1. Necrostatin 1 specifically inhibits RIP1, and not its family members RIP2 and RIP3, by acting on the kinase domain (KD) to stabilise the closed conformation of the activation segment. The Ser161 autophosphorylation site within this activation segment is thought to be a specific target of necrostatin 1, as mutations in this site conferring either a permanently active conformation (Ser161→Glu) or reduced kinase activity (Ser161→Ala) are insensitive to inhibition by necrostatin-1 (Vandenabeele, Declercq et al. 2008). Whilst other kinase inhibitors of RIP1 exist, such as necrostatin-3 and necrostatin-5, these are believed to act indirectly on RIP1 and so necrostatin-1 was selected for use in cell survival assays.

The toxicity of necrostatin-1 was assessed in four ovarian cancer cell lines (Figure 72) and a concentration of 100µM selected for use in cell survival assays in combination with Lister-dTK based on these results. This is consistent with other studies where necrostatin-1 has been used in the µM range (Cho, McQuade et al. 2011; Feoktistova, Geserick et al. 2011; Tenev, Bianchi et al. 2011). Typically, 100µM Nec-1 resulted in <20% cell death although Igrov1 cells were more sensitive to the effects of this inhibitor (Figure 72).

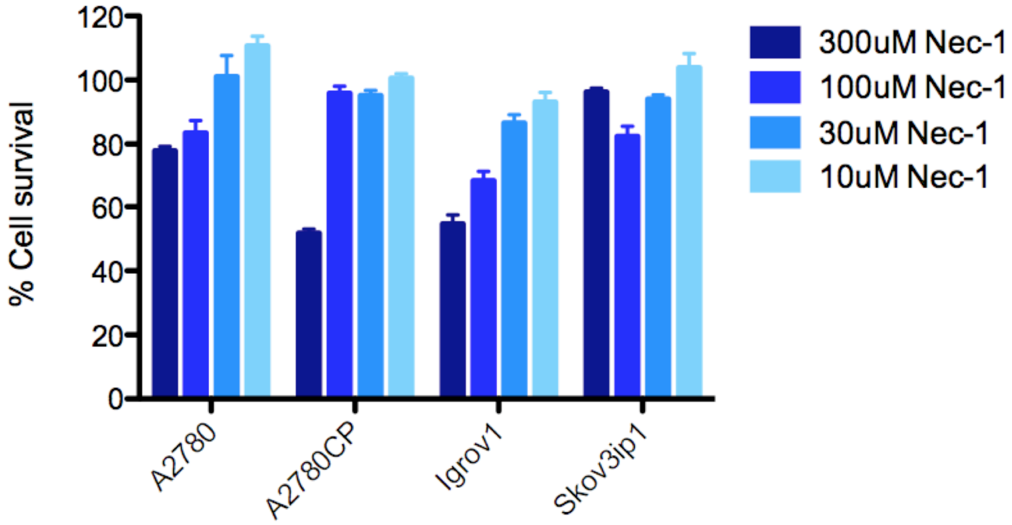

Figure 72: Toxicity of necrostatin-1 to ovarian cancer cell lines. Cell survival was measured by MTT assay 72hrs after addition of necrostatin-1 and is expressed as a % of untreated cells.

To determine whether RIP1 kinase activity is involved in sensitivity to vaccinia virus, cells were infected with a serial dilution of Lister-dTK and either vehicle alone (DMSO), 100µM necrostatin-1, 25µM of the pan-caspase inhibitor zVAD-fmk or both (Figure 73). Inhibitors were added direct to the cell culture medium 2 hrs post-infection to minimise any potential interference with virus entry. Cell survival was analysed 72hrs post-infection by MTS assay and normalised to uninfected cells treated with the same/combination of inhibitors. The presence of necrostatin-1 significantly attenuated the cytotoxicity of Lister-dTK in A2780CP, Igrov1 and Skov3ip1 cells as observed by an increase in the EC_{50}, the amount of virus required to achieve 50% cell death. Inhibition of virus induced cell death was further increased by the addition of zVAD-fmk where a significant attenuation was observed in A2780, A2780CP and Igrov1 cells; the same trend was observed in Skov3ip1 cells although this difference was not significant. However, the experiment was only performed twice in this cell line. As zVAD-fmk alone had a modest, although insignificant, inhibitory effect on cell death, it is not clear if this is simply an additive effect or if caspase inhibition works in synergy with necrostatin-1 to inhibit vaccinia virus cell death.

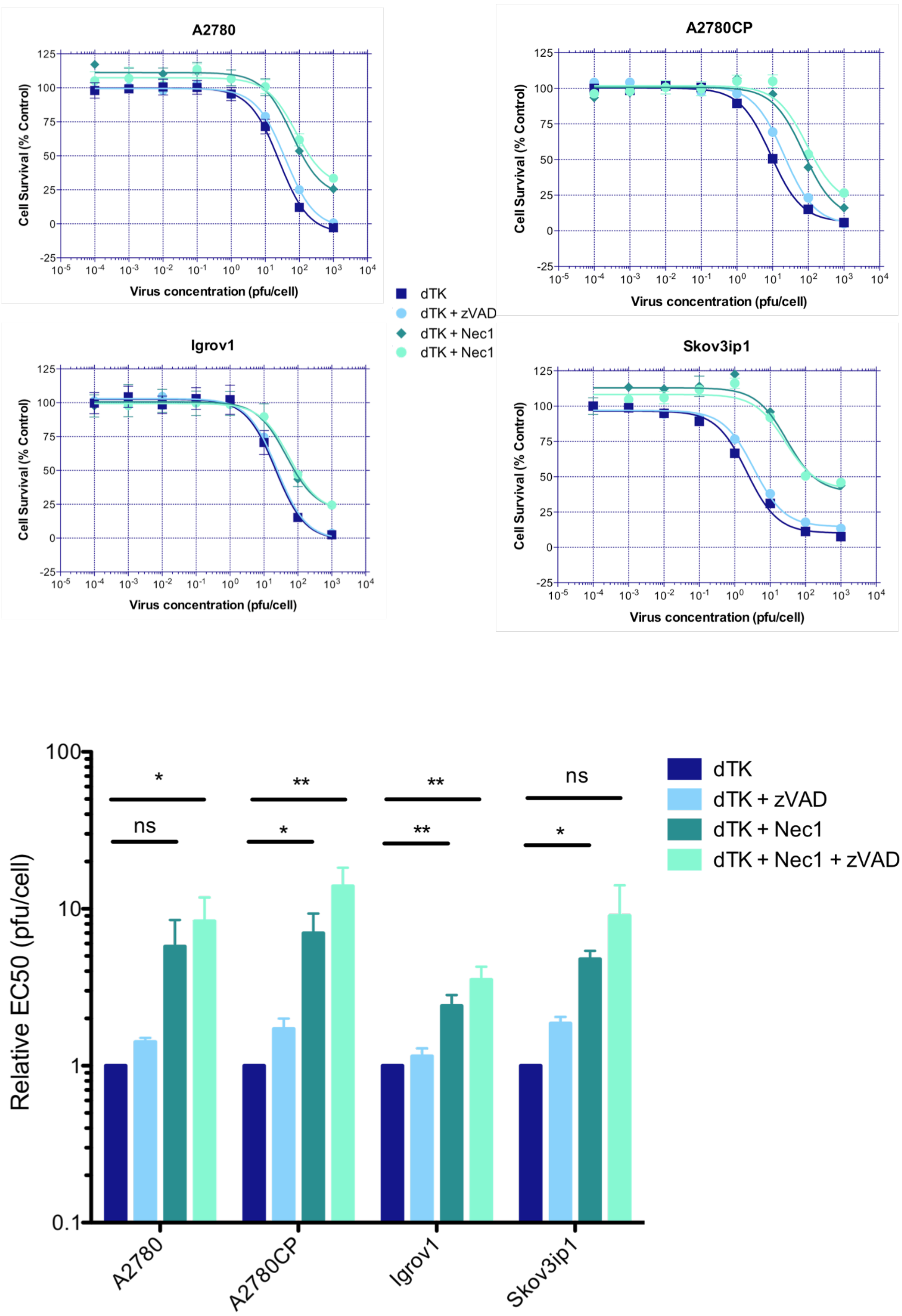

Figure 73: Effect of necrostatin-1 on vaccinia-induced cell death. Top and middle: Cells were infected with a serial dilution of Lister-dTK in the presence or absence of 25µM zVAD-fmk and/or 100µM necrostatin-1. Cell survival was measured by MTS assay 72hrs post-infection and normalised to uninfected cells treated with the same combination of inhibitors. Dose response curves were constructed to determine the EC_{50}. Graphs show the mean+SEM of a representative single experiment performed in triplicate. Bottom: Data showing the mean EC_{50} +SEM of 2-5 experiments, each performed in triplicate. The EC_{50} of combination groups is expressed relative to the EC_{50} of Lister-dTK alone.

Interestingly, necrostatin-1 appeared to exert the most dramatic inhibition of cell death at high concentrations of Lister-dTK (Figure 73). Following initial infection with 1000pfu/cell of Lister-dTK no cells survived 72hrs post-infection. In the presence of necrostatin-1, the surviving cell population increased to 25-40%, suggesting that RIP1 kinase activity may be important in cell death occurring as a result of initial high dose infection. However, upon visual inspection using a light microscope, there was no apparent visual increase in cell number between Lister-dTK infected cells and infected cells in combination with necrostatin-1. This led to some doubt whether the MTS assay used, which measures the reductase activity of mitochondria, was an appropriate assay to use for determining cell death that may result from programmed necrosis, as this pathway is associated with changes in metabolic activity which may effect the outcome. To determine whether the observed attenuation of Lister-dTK upon treatment with necrostatin-1 could be attributed to inhibition of programmed necrosis or was merely an artefact of the assay used, another cell proliferation assay was employed that uses sulforhodamine B to stain cellular protein. The intensity of the incorporated dye can be measured spectrophotometrically and correlates with the total biomass (number of cells).

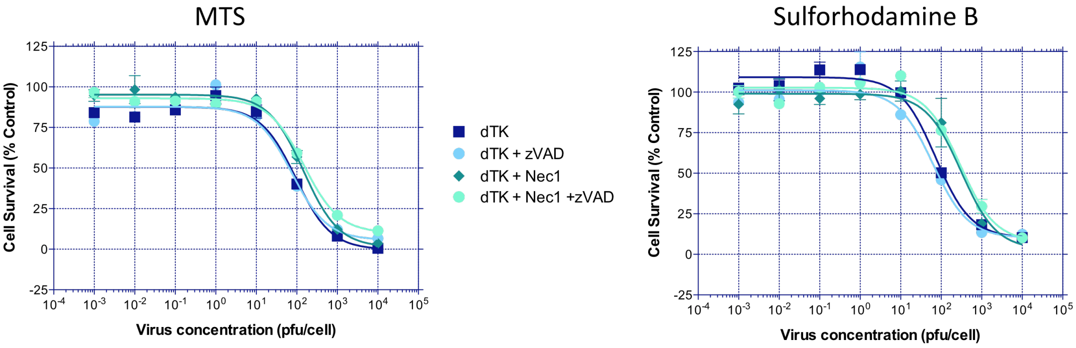

Figure 74: Comparison of MTS assay and sulforhodamine-B assay to evaluate the effect of necrostatin-1 on Lister-dTK induced cell death. A2780CP cells were seeded on duplicate plates and infected with increasing doses of Lister-dTK in the presence or absence of 25μM zVAD-fmk and/or 100μM necrostatin-1. Cell survival was measured 72hrs post-infection by either MTS assay or sulforhodamine B assay. Data points on the graph show the mean+SEM of one representative experiment performed in triplicate.

A comparison between MTS assay and sulforhodamine B assay to measure cell survival revealed a similar EC_{50} for Lister-dTK infected cells (Figure 74), suggesting that the choice of assay does not greatly affect the result. Similarly, the trend towards increased cell survival following treatment with either necrostatin-1 alone or in combination with zVAD-fmk was observed using both assays. Interestingly, at high doses of virus (1000 or 10000 pfu/cell) there were fewer surviving cells in the necrostatin-1/zVAD combination group when analysed by the sulforhodamine B assay compared to the MTS assay. This suggests that measuring mitochondrial activity as opposed to total biomass may not be a true reflection of cell survival, and is one of the limitations of this assay in studying cell death pathways. However, attenuation of Lister-dTK following RIP1 kinase activity inhibition by necrostatin-1 was demonstrated by an increase in EC_{50} using both assays, implying that RIP1 has a role in vaccinia virus induced cell death.

5.3.2.5 Targeting RIP1 and RIP3 using siRNA

To evaluate the role of RIP1 and RIP3 in Lister-dTK cytotoxicity, the sensitivity of ovarian cancer cell lines to Lister-dTK was determined following the use of siRNA to knock down RIP1 and/or RIP3. The optimal concentration of siRNA was evaluated using escalating doses of siRNA and studying the degree of RIP1 protein knockdown 48hrs later; compared to higher concentrations, enhanced knockdown was observed with 10nM siRNA, although this was not improved any further by using concentrations lower than 10nM (Figure 75). Optimisation of siRNA concentration was performed in A2780CP and Skov3ip1 cells (Figure 75) and also in A2780 and Igrov1 cells, with a similar result (data not shown). A concentration of 10nM siRNA was selected for use in A2780, A2780CP and Skov3ip1 cells and 5nM for Igrov1 cells; a timecourse assay to determine the duration of knockdown was also performed in Igrov1 cells (Figure 76). Similarly, the concentration of RIP3 siRNA was optimised in TOV21G cells (Figure 77) as these expressed the highest level of RIP3 protein among the ovarian cancer cell lines tested (Figure 69). 10nM siRNA was selected for use in combination assays with Lister-dTK.

At 24hrs post-transfection, there was a small decrease in RIP1 levels in Igrov1 cells, whereas almost full knockdown of RIP1 protein was observed by 48hrs (Figure 76). This knockdown persisted until 120hrs when there was evidence of re-expression of RIP1 protein. To determine the effect of knocking down RIP1 on sensitivity to vaccinia virus, cells were infected with Lister-dTK 24hrs post-transfection with siRNA and cell survival measured 72hrs post-infection (96hrs post-transfection). At this timepoint, knockdown was still evident, as demonstrated in Figure 76 and subsequent analyses of protein expression that accompanied each cell survival assay.

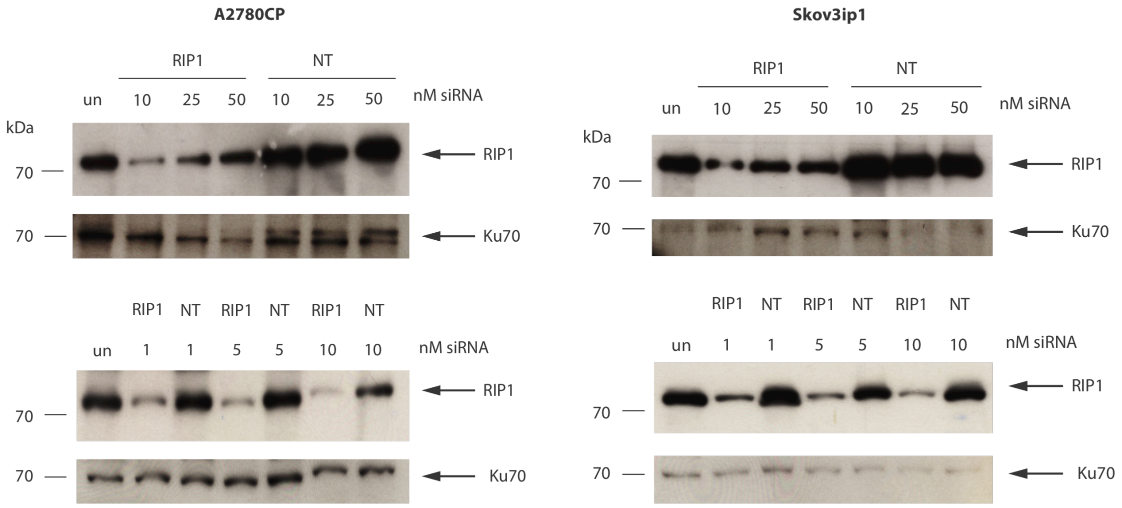

Figure 75: Optimisation of RIP1 siRNA concentration. Cells were transfected with varying concentrations of RIP1 or control non-targeting siRNA and protein expression levels determined by western blotting 48hrs later. Knockdown in A2780CP and Skov3ip1 cells is shown, the same experiment was performed in A2780 and Igrov1 cells with a similar result (data not shown).

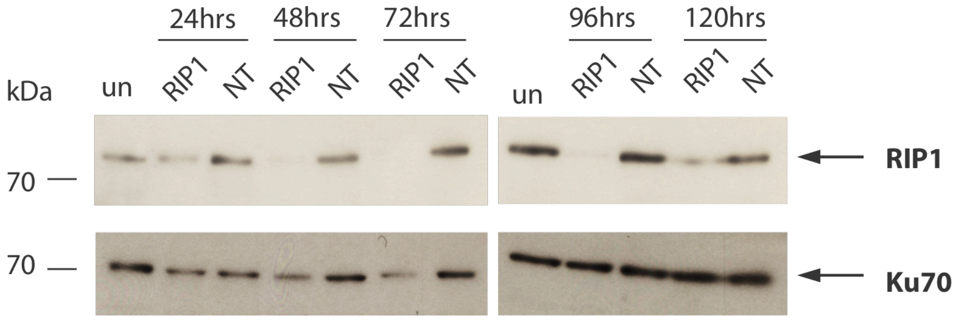

Figure 76: Timecourse of RIP1 knockdown using siRNA. Igrov1 cells were transfected with 5nM siRNA and levels of RIP1 protein determined every 24hrs post-transfection by western blotting.

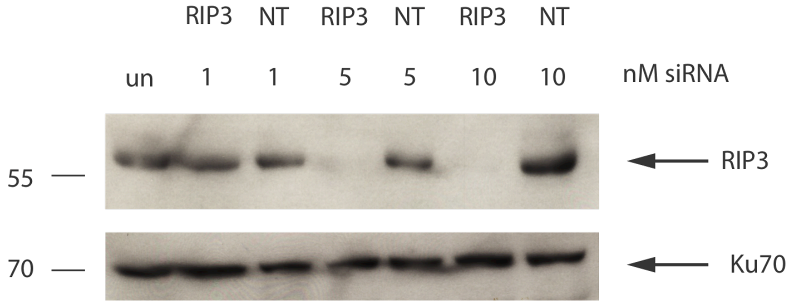

Figure 77: Optimisation of concentration of RIP3 siRNA. TOV21G cells were transfected with either NT or RIP3 siRNA at 1nM, 5nM and 10nM and protein expression determined by western blotting 48hrs later.

5.3.2.6 Knockdown of RIP1 or RIP3 and sensitivity to Lister-dTK

Knockdown of RIP1 had a modest inhibitory effect on Lister-dTK cytotoxicity in Skov3ip1 cells but this effect was not seen in A2780, A2780CP or Igrov1 cells (Figure 78). Similarly, knockdown of RIP3 did not inhibit Lister-dTK induced cell death in TOV21G cells (Figure 79a). Analysis of protein expression demonstrated that, although knockdown of either RIP1 or RIP3 was achieved at a high efficiency by 96hrs, there was still evidence of protein expression at 24hrs, the time of infection (Figure 78 and Figure 79a). (Note: although Igrov1 cells were infected 24hrs post-infection, the earliest analysis of protein expression was at 48hrs post-transfection in this cell line). The highest degree of RIP1 knockdown at 24hrs was observed in A2780 cells and the least in Skov3ip1 cells, which had shown a modest reduction in Lister-dTK induced cell death following knockdown. This made it unlikely that inhibition of Lister-dTK was dependent on a high degree of knockdown at the time of infection: however, to rule out this theory, TOV21G were infected with Lister-dTK 48hrs post-transfection when almost complete knockdown was achieved (Figure 79b). Cell survival was then measured 48hrs post-infection instead of 72hrs to exclude the possibility of protein re-expression during the assay. Despite almost 100% RIP3 knockdown throughout the time of infection, sensitivity to Lister-dTK in TOV21G cells was not affected (Figure 79b). The toxicity of either NT or RIP3 siRNA alone were comparable (data not shown) implying that, although cells were infected directly in the well following transfection, the cell number should have been similar and therefore the infectious dose did not vary between conditions.

As has been described elsewhere for other proteins, knockdown of one protein can lead to a compensatory increase in expression of a protein in the same family. To determine whether it was necessary to knockdown both RIP1 and RIP3 to see an inhibition in Lister-dTK cytotoxicity, cells were transfected simultaneously with both RIP1 and RIP3 siRNA. Simultaneous knockdown of both RIP1 and RIP3 in TOV21G cells did not inhibit Lister-dTK cytotoxicity (Figure 80); other cell lines were not tested due to low levels of endogenous RIP3 protein.

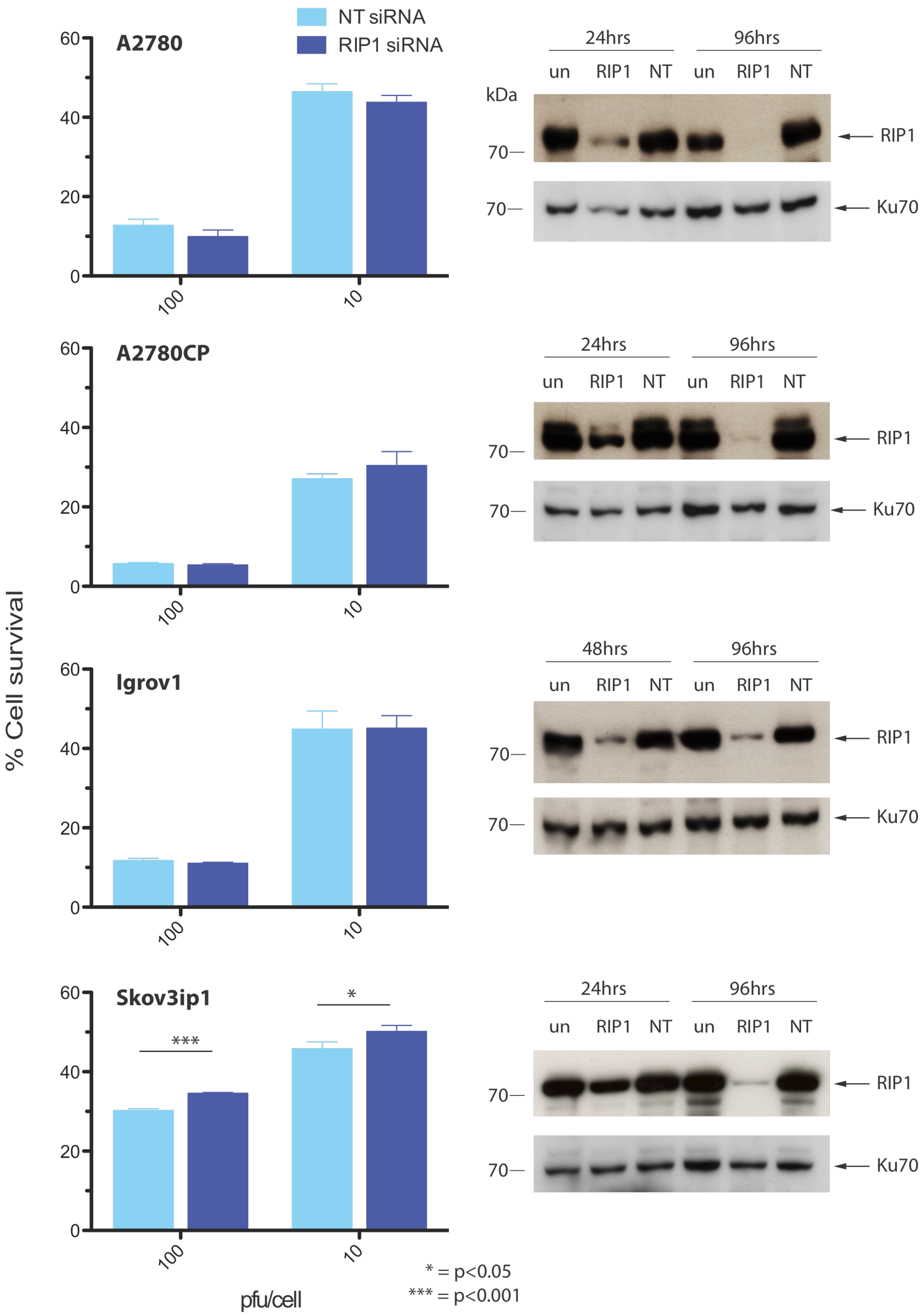

Figure 78: Effect of knocking down RIP1 on sensitivity to Lister-dTK. Cells were transfected with either 5nM (Igrov1) or 10nM (A2780, A2780CP, Skov3ip1) non-targeting (NT) siRNA or RIP1 siRNA and infected with Lister-dTK 24hrs later. Cell survival was measured by MTT assay 72hrs post-infection and expressed as a percentage of uninfected control cells (100% survival) that had been transfected with siRNA. Data shows the mean+SD of a single experiment performed in triplicate. The degree of knockdown at the time of infection (24hrs) and at the assay endpoint (96hrs) was determined by western blotting in a parallel experiment.

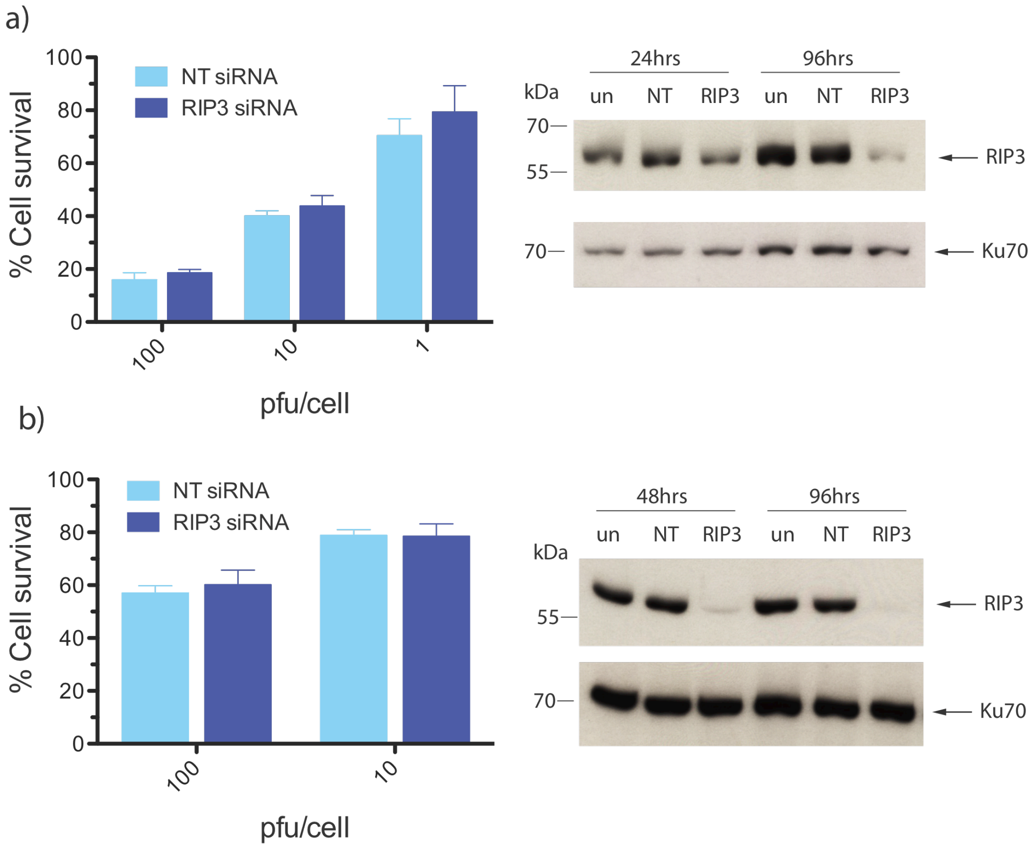

Figure 79: Effect of knocking down RIP3 on sensitivity to Lister-dTK in TOV21G cells. a) Cells were infected 24hrs post-transfection and cell survival analysed by MTT assay 72hrs post-infection. Cell survival is expressed as a percentage of uninfected control cells (100% survival) that had been transfected with siRNA. Data shows the mean cell survival+SD of two experiments, each performed in triplicate b) Cells were infected 48hrs post-transfection and cell survival analysed 48hrs post-infection.

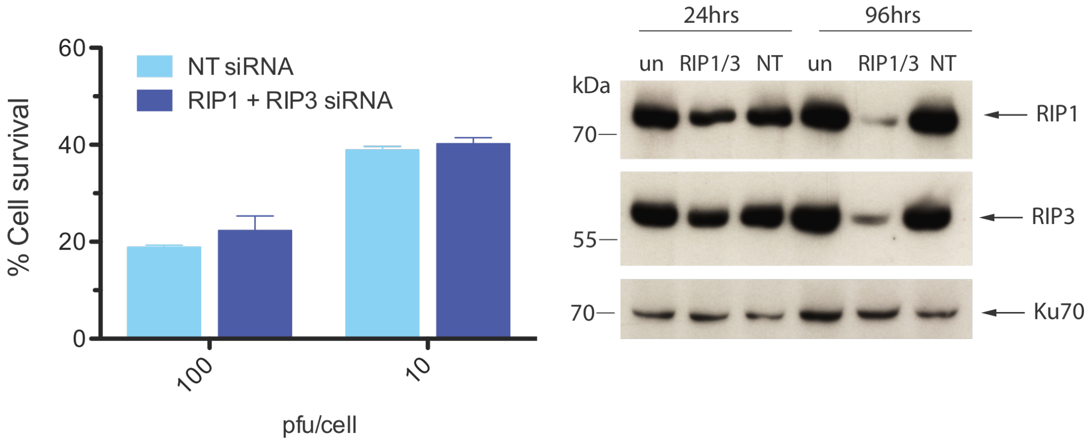

Figure 80: Simultaneous knockdown of RIP1 and RIP3 in TOV21G cells and sensitivity to Lister-dTK. Cells were transfected with 10nM NT siRNA or 10nM each of RIP1 and RIP3 siRNA, and infected with Lister-dTK 24hrs later. Cell survival was measured by MTT assay 72hrs post-infection and expressed as a percentage of uninfected control cells (100% survival) that had been transfected with siRNA. Data shows the mean+SD of a single experiment, performed in triplicate.

Further investigation showed that there was not a compensatory increase in either RIP1 or RIP3 protein expression following knockdown of RIP3 in TOV21G cells or RIP1 in A2780, A2780CP and Skov3ip1 cells respectively (Figure 81). As caspase 8 can cleave and inhibit RIP1 kinase activity, protein expression levels of this protein were also determined and found to remain at a steady level following knockdown of either RIP1 or RIP3.

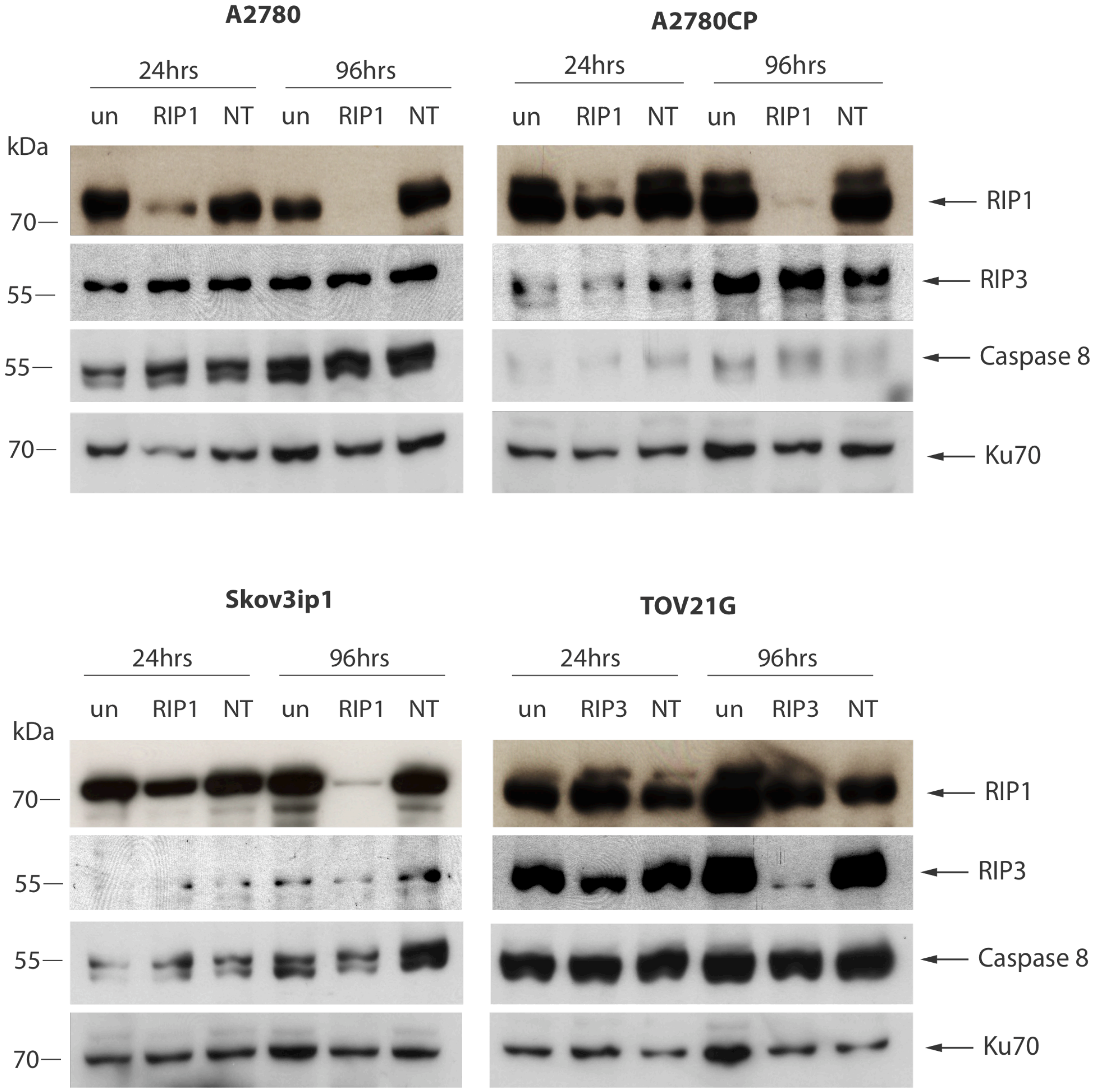

Figure 81: Knockdown of either RIP1 or RIP3 does not lead to compensatory increases in protein expression of RIP3 or RIP1 respectively. A2780, A2780CP and Skov3ip1 cells were transfected with 10nM RIP1 siRNA and TOV21G cells with 10nM RIP3 siRNA. Protein was harvested 24hrs and 96hrs post-transfection and expression of RIP1, RIP3 and caspase-8 determined by western blotting.

5.4 Discussion

The mechanism by which oncolytic vaccinia kills cancer cells, which are likely to have resistance to some death pathways, is unclear. Although tumour regression is the ultimate therapeutic goal, understanding the mechanism of tumour cell death may lead to carefully selected combination therapies that have complementary modes of action, and knowledge of the reasons behind both *de novo* and acquired resistance to viral therapy.

Here, the mechanisms behind Lister-dTK induced cell death in ovarian cancer cell lines were explored, namely apoptosis, autophagy and necrosis. No one pathway emerged as a sole mode of cell death. Rather, features of each were evident and it is likely that the individual pathways, as well as vaccinia-encoded modulators of these, interact with each other. Multiple markers of necrosis were evident following virus infection and, crucially, inhibition of a critical protein involved in programmed necrosis also reduced ovarian cancer cell death following infection with Lister-dTK. In contrast, whilst features of both apoptosis and autophagy were evident following viral infection, inhibition of these pathways failed to attenuate cell death.

Infection with vaccinia virus leads to PARP cleavage, occasional caspase-3 cleavage (although this was not a consistent or particularly striking feature), phosphatidylserine externalisation and DNA fragmentation. Superficially, these observations imply that vaccinia virus induces apoptosis as a means of destroying ovarian cancer tumour cells. However, the actual percentage of cells expressing these markers was low, albeit significant. Moreover, inhibition of apoptosis by both Bcl2 overexpression and caspase inhibition failed to attenuate the cytotoxicity of Lister-dTK *in vitro*, despite inhibiting cisplatin induced cell death.

The results here tend to support that of previously established findings that, generally, infection with vaccinia does not lead to apoptotic cell death. Instead, necrotic areas are commonly seen in treated tumours, consistent with wild type infection which causes necrotic lesions in infected individuals, particularly where vaccinia necrosum (progressive vaccinia) develops due to immunodeficiency (Aragon, Ulrich et al. 2003). Reports of apoptosis in vaccinia treated tumours or cancer cell lines are rare; a double-deleted strain caused apoptosis in 4/5 multiple myeloma cell lines as detected solely by phosphatidylserine externalisation, although there are problems associated with using just one technique as is described later (Deng, Tang et al. 2008). However, induction of apoptosis did not appear to determine sensitivity to vaccinia as cell death was similar across all 5 cell lines, including those that had no or reduced levels of apoptosis (Deng, Tang et al. 2008). Induction of apoptosis can be induced by the expression of apoptotic proteins such as TRAIL from vaccinia in colorectal cancer (Ziauddin, Guo et al. 2010) or the addition of a prodrug converted by an activating enzyme encoded by vaccinia in breast cancer (Seubert, Stritzker et al. 2011), but these cause apoptosis on their own and control viruses showed limited evidence of initiating the process in the same cell lines.

The levels of apoptosis in ovarian cancer cells, as determined by DNA fragmentation and phosphatidylserine (PS) externalisation, were significantly higher than that of untreated cells in all 4 cell lines, with the exception of Igrov1 cells where there was a trend towards increased PS externalisation, although this was not significant. However, given the amount of cell death at the timepoints these markers were detected, 96hrs and 72hrs post-infection respectively, the actual percentage of cells exhibiting positive markers of apoptosis was lower than might be expected. The percentage of cells with fragmented DNA (<2n) ranged from 9-17% in Lister-dTK treated cells compared to a baseline of <3% in untreated cells at 96hrs post-infection. Similarly, the percentage of cells positive for external PS as detected by annexin V staining ranged from 10-25% in Lister-dTK treated cells at 72hrs post-infection over a baseline of 2-3% in untreated cells. Given that vaccinia anti-apoptotic genes such as F1L are expressed at early timepoints in infection (2-3hrs post-infection) and that in their absence apoptosis is induced with 36hrs (Postigo, Cross et al. 2006), it might be expected that apoptosis would occur at higher levels and earlier on if this were the main mechanism of cell death induced by Lister-dTK. However, there was no significant increase in either fragmented DNA or externalised PS at 48hrs post-infection in any of the cell lines tested. It is possible that earlier timepoints need to be studied. However, flow cytometry data indicate that significant cell death (DAPI positive cells) does not occur until after 48hrs. This then leads to the detection of annexin V positive cells at 72hrs post-infection, which are subsequently annexin V positive and DAPI positive 96hrs post-infection. This correlates with the expected pattern of apoptotic cells where PS is first externalised before cells lose membrane integrity, which can indicate either apoptotic or necrotic death (Vermes, Haanen et al. 1995). Recently however it has been reported that, unexpectedly, primary necrotic cells also demonstrate annexin V positive/PI negative staining before they become PI positive (Sawai and Domae 2011). This highlights the need to use more than one technique to determine apoptosis, particularly as PARP can also be cleaved during necrosis (Gobeil, Boucher et al. 2001) and the release of apoptosis-inducing factor (AIF) can also occur as a result of ATP depletion (Daugas, Susin et al. 2000) and during programmed necrosis, leading to some similar features of apoptosis (Boujrad, Gubkina et al. 2007; Delavallee, Cabon et al. 2011).

Caspase-3 cleavage was not detected in any of the four cell lines following infection with Lister-dTK except on one occasion upon long exposure in A2780 and A2780CP cells at 72hrs post-infection, further suggesting that apoptosis is not a critical mode of cell death in ovarian cancer cells. In addition, overexpression of Bcl2 and use of the pan-caspase inhibitor zVAD-fmk failed to significantly reduce Lister-dTK induced cytotoxicity. To exclude the possibility that caspase-3 was activated at earlier timepoints, a timecourse of infection was also performed from 24hrs to 72hrs post-infection and cleaved caspase-3 was not detected. The lack of caspase-3 activation was surprising given other markers of apoptosis are present, and that downstream PARP was cleaved in all four cell lines tested at 72hrs post-infection. However, PARP can be cleaved by other proteins besides caspase-3 (Gobeil, Boucher et al. 2001; Chaitanya, Steven et al. 2010) although these fragments tend to be of different molecular weights to the 89kDa protein resulting from Lister-dTK infection, and caspase-independent pathways of apoptosis have been described (Broker, Kruyt et al. 2005).

Apoptosis-inducing factor (AIF) is released into the cytosol from the mitochondria during apoptosis where it then translocates to the nucleus to aid in chromatin condensation and DNA fragmentation (Loeffler, Daugas et al. 2001). Crucially, release of AIF can be triggered by cathepsin D independent of the caspase-cascade (Bidere, Lorenzo et al. 2003) and the translocation of AIF to the nucleus is also caspase-independent (Loeffler, Daugas et al. 2001; Yu, Wang et al. 2002), can proceed in caspase-3$^{-/-}$ cells (Susin, Daugas et al. 2000) and is not prevented by either Bcl2 (Loeffler, Daugas et al. 2001) or zVAD (Daugas, Susin et al. 2000). Importantly, AIF mediates apoptosis in cancer cells with defective caspase activity following administration of either flavopiridol to glioblastoma cells (Alonso, Tamasdan et al. 2003) or staurosporine to non-small cell carcinoma cells (NSCLCs), that are resistant to a broad spectrum of apoptotic stimuli (Joseph, Marchetti et al. 2002). In addition, paclitaxel induced AIF mediated caspase-independent apoptosis in ovarian cancer cells (Ahn, Kim et al. 2004). Similar to the results presented here with Lister-dTK, paclitaxel resulted in DNA fragmentation and externalisation of PS in SKOV3 cells but a lack of caspase-3 activation (Ahn, Kim et al. 2004). It would be interesting to determine levels of AIF in the nucleus, cytosol and mitochondria in Lister-dTK treated ovarian cancer cells to see if this pathway is involved in the apparent induction of caspase-independent apoptosis observed here. Very recently, Bax mediated release of AIF has also been described as a critical step in programmed necrosis (Cabon, Galan-Malo et al. 2012), and it may well be that the markers of apoptosis observed here actually represent necrosis.

It is known that vaccinia encodes various inhibitors of apoptosis including F1L, E3L and N1L, and that these combine to prevent premature cell death that might restrict virus replication and spread. Consistent with the known functions of these proteins, minimal apoptosis was observed for the amount of overall cell death caused by Lister-dTK at the timepoints tested. However, although induction of apoptosis in infected cells may not be common it may be that danger signals released from infected cells lead to apoptosis in infected neighbouring cells, as has been demonstrated in colon cancer cells infected with vesicular stomatitis virus (VSV) (Breitbach, Paterson et al. 2007). In this series of experiments it was demonstrated that, whilst virus infection was sparse and limited to the tumour periphery following systemic delivery, extensive caspase-3 activation could be seen in the uninfected tumour core, which was associated with vascular shutdown (Breitbach, Paterson et al. 2007). These findings may offer an explanation for the results obtained here, whereby markers of apoptosis are observed yet do not appear to play a critical role in cell death. To determine the relevance of apoptosis in ovarian tumour cell death *in vivo*, staining for caspase-3 activation or other apoptotic markers would need to be performed on tumour tissue obtained from mice treated with Lister-dTK. This would also allow distinction between apoptosis in infected and uninfected cells, similar to the work of Breitbach *et al.*

Overall, detection of exposed PS, PARP cleavage and DNA fragmentation in all four ovarian cancer cells following infection with Lister-dTK indicates that apoptosis is at least initiated to some degree, although it remains to be seen if this is in infected cells themselves or in neighbouring cells. Furthermore, this does not appear to be through a caspase-dependent pathway. However, the low degree of apoptosis, coupled with the fact that neither zVAD-fmk nor Bcl2 overexpression was able to inhibit overall cell death, led to the conclusion that this is not a primary mechanism of cytotoxicity in ovarian cancer cells *in vitro*.

Similarly, limited markers of autophagy were detected following infection with Lister-dTK; LC3B cleavage was observed but autophagic flux was not evident, and there was only limited evidence of autophagosome formation by confocal microscopy that could not be confirmed by electron microscopy. In addition, inhibition of the pathway, either through overexpression of Bcl2 or the use of chloroquine or 3-methyladenine, did not attenuate the cytotoxicity of Lister-dTK in ovarian cancer cell lines. There is very little published on the involvement of autophagy in vaccinia-induced cell death, or indeed the vaccinia lifecycle. Autophagy can promote cell survival through its antiviral activity, including the direct degradation of virions and virion components, and through delivery of pathogen associated molecular patterns (PAMPS) to endosomal pathogen recognition receptors (PRRs) and toll-like receptors (TLRs) (reviewed in (Jordan and Randall 2011)). It is therefore not surprising that some viruses seek to block autophagy or to exploit the process for their own gain. It was previously hypothesised that vaccinia might hijack autophagy machinery for its own benefit, specifically for formation of the virion envelope, but this has been disproved by the discovery that vaccinia replicates and matures in Atg $5^{-/-}$ mouse embryonic fibroblasts and Beclin $1^{-/-}$ embryonic stem cells to the same degree as in the wild-type counterparts (Zhang, Monken et al. 2006).

Consistent with the results demonstrated here in ovarian cancer, it has also recently been shown that vaccinia initiates massive LC3 lipidation (conversion of LC3B-I to LC3B-II) in mouse fibroblast cells (Moloughney, Monken et al. 2011). Similar to the results obtained here, this was not accompanied by an increase in autophagic flux however. In addition, electron microscopy showed a complete absence of autophagosomes. Together, these data and the work presented here suggest that, whilst LC3B-I is readily converted to LC3B-II, an actual increase in the autophagic process ie. autophagic flux and autophagosome formation is not a predominant feature of vaccinia infection. Rather, Moloughney *et al* conclude that vaccinia actually disrupts cellular autophagy and leads to autophagosome deficiency, although this was not shown here in ovarian cancer cells. Blocking autophagy with 3-MA did not affect the cytotoxicity of vaccinia in any of the cell lines tested, either negatively or positively. Similarly, chloroquine also had no effect except at the higher concentrations when toxicity of the drug was significant. It is likely that these non-specific effects are responsible for the minor changes in EC50 value of Lister-dTK rather than any direct effect on autophagy. If it is true that vaccinia does not induce autophagosome formation (or in fact inhibits it), inhibitors such as 3-MA and chloroquine which both act upon the autophagosome at early and late stages respectively are likely to have no effect, as is seen here. The implications of modulation of LC3B cleavage by vaccinia are unclear, and it is not known what role this plays in infected cells if downstream autophagy does not take place.

Far more compelling is the induction of necrosis following vaccinia infection. Previously, this pathway has not been extensively explored but with the discovery and increasing knowledge of the pathways of programmed necrosis, necrosis is certainly far more complex than a form of accidental death. Infection with Lister-dTK leads to morphological changes indicative of necrosis, including ruptured membranes, swollen nuclei and cytoplasmic vacuoles in A2780 cells. Additionally, the release of HMGB1 was demonstrated and a sharp and significant decline in intracellular ATP levels was seen in all four cell lines infected with vaccinia. These data, consistent with the areas of necrosis observed *in vivo*, strongly suggest that necrosis is associated with vaccinia infection. Although the process of necrosis has not been investigated in detail in the context of oncolytic viral gene therapy, it is fairly well accepted that this occurs with wild-type vaccinia infection. However, the role of programmed necrosis and its implications in the efficacy and use of vaccinia as an oncolytic vector for ovarian cancer is of interest.

The work presented here suggests that key components of programmed necrosis, RIP1, caspase-8 and RIP3, associate during vaccinia infection of ovarian cancer cells. This is consistent with the finding that the RIP1/RIP3 complex forms in the liver of wild-type mice infected with vaccinia (Cho, Challa et al. 2009). Interestingly, RIP3 has been reported to determine sensitivity to other viruses such as cytomegalovirus (Brune 2011). Whilst levels of RIP3 were highest in TOV21G cells, the least sensitive of the cell lines tested, manipulation of RIP3 expression by targeted siRNA did not alter sensitivity to Lister-dTK. Similarly, knockdown of RIP1 or both proteins simultaneously also failed to effect vaccinia cytotoxicity in ovarian cancer cell lines. This is disappointing if programmed necrosis is a key pathway in vaccinia-induced cell death. However, necrostatin-1, a commercial inhibitor of RIP1 kinase activity significantly attenuated Lister-dTK in A2780CP, Igrov1 and Skov3ip1 cells. Conversely, this suggests that programmed necrosis does have a role in the cytotoxicity of Lister-dTK. In contrast to murine cytomegalovirus, which expresses the M45 protein that acts to inhibit necrosis through its interactions with RIP1 and RIP3 (Mack, Sickmann et al. 2008; Upton, Kaiser et al. 2008), no similar proteins encoded by vaccinia have yet been identified. Rather, the data here suggest that RIP1-mediated necrosis may contribute to vaccinia-induced cell death.

Viral inhibitors of programmed cell death (PCD) are generally believed to promote viral activity by preventing or delaying host cell death to allow virus replication and spread. Whilst apoptosis is the best known form of PCD, if this process is blocked a cell can proceed down the necrotic pathway, which is proposed also to limit and control viral infection. This is true for MCMV, which encodes M45 and suppresses both pathways of cell death (Upton, Kaiser et al. 2010). However, there is some evidence to suggest that the opposite may apply to vaccinia virus. Firstly, suppression of programmed necrosis by necrostatin-1 led to a decrease in cell death here. Secondly, expression of MC159, a viral FLIP that negatively regulates formation of the ripoptosome during programmed necrosis (Tenev, Bianchi et al. 2011), actually enhances the innate control of vaccinia virus (Challa, Woelfel et al. 2010). The different replication kinetics of the two viruses may explain this discrepancy in the role of programmed necrosis; vaccinia virus is a rapidly replicating virus unlike MCMV and so may not be as dependent on prolonged cell survival for efficient replication. Components of the ripotosome, such as RIP1, are also able to interact with key regulators of the immune response to infection, and inhibition of programmed necrosis was shown to facilitate NF-κB activation in mice infected with vaccinia (Challa, Woelfel et al. 2010). Potentially, the benefits to vaccinia of delayed cell death as a result of inhibiting programmed necrosis are outweighed by the corresponding increase in antiviral immune activity.

The impact of programmed necrosis on the immune response to vaccinia in ovarian cancer is yet to be determined. Similarly, whilst vaccinia-induced ovarian cancer cell death is decreased when programmed necrosis is inhibited, virus replication has net yet been studied. The findings here warrant further investigation into the role of programmed necrosis in oncolytic viral gene therapy, and whether manipulation of this process can enhance the therapeutic approach. Furthermore, increased understanding of ripoptosome formation and the regulation of this pathway by vaccinia merit attention of their own accord if the mechanism of viral vectors is to be truly deciphered.

Chapter 6

Final discussion

6. Final Discussion

The first oncolytic virus to be used clinically was based on the adenovirus type 5 backbone and, whilst a minimally modified version of this virus (termed H101) is now approved for use in China, its limitations were soon exposed. These include poor systemic delivery, slow replication that limits infection of tumour cells before virus clearance by the immune system, and a limited packaging capability for the expression of transgenes that might improve virus potency. Consequently, attention has moved towards other viruses as alternative vectors for oncolytic therapy. Today, a wide range of viruses are being explored, including vaccinia, measles, adenovirus, herpes simplex virus and reovirus, as well as lesser studied oncolytic viruses such as coxsackievirus, vesicular stomatitis virus and Newcastle disease virus. Naturally, these viruses each have their advantages and disadvantages, and expansion of the range of oncolytic viruses available may lead to advances in the field as a whole. Due to the differences between viruses, and the way they are used in individual studies, it is difficult to compare between the vast range of viruses available and determine which of these is the ideal oncolytic agent. A systematic review would be problematic, as choice of titre, model used and primary outcome to measure will favour some viruses over others. Nonetheless, there are certain characteristics that are desirable, or indeed essential, for a virus to be effective as an oncolytic agent and vaccinia, on paper at least, possesses many of these.

First and foremost, a novel therapy must be safe and vaccinia has a well characterised life cycle and toxicity profile (Lane, Ruben et al. 1969), with drugs available to control infection should adverse effects occur (De Clercq 2002; Wittek 2006). Furthermore, clinical trial experience so far has demonstrated that vaccinia is safe for the patient (Mastrangelo, Maguire et al. 1999; Park, Hwang et al. 2008; Breitbach, Burke et al. 2011) and the ability to engineer vaccinia by deleting genes required for replication in normal cells enhances the safety profile for healthcare workers and patient contacts. This engineering capability also allows the insertion of genes that enhance activity, with the insertion of GM-CSF the most clinically promising vaccinia virus to date (Park, Hwang et al. 2008; Breitbach, Burke et al. 2011).

The ideal oncolytic virus should also be able to infect and destroy a wide range of tumours and in this respect vaccinia is adept; vaccinia is able to infect almost every cell type and has shown activity against a range of tumour types in pre-clinical and clinical models. As such, its use as a therapy is not restricted to any one cancer. Conversely, the promiscuous nature of vaccinia is not without its own problems. The lack of a definitive receptor means that vaccinia does not demonstrate selective cell entry. Although tumour selective replication can be achieved by the deletion of certain genes, selective cell entry cannot be targeted and normal cells are still susceptible to virus infection, albeit with aborted replication. Another key requirement for an oncolytic virus is systemic delivery and immune avoidance. Vaccinia virus has a rapid cytoplasmic replication cycle (Hruby 1990) and an innate ability to spread systemically whilst evading immune detection (Vanderplasschen, Hollinshead et al. 1997; Vanderplasschen, Mathew et al. 1998). These features have enabled vaccinia to progress into clinical trials as a potential oncolytic agent and, crucially for the treatment of metastatic disease, it has demonstrated the ability to be delivered systemically to tumours (Breitbach, Burke et al. 2011). Furthermore, injection of virus into solid tumour lesions has seen a response in distant lesions throughout the body, suggesting that vaccinia has the potential to disseminate from the initial site of infection (Mastrangelo, Maguire et al. 2000).

Finally, the ability of a virus to stimulate an anti-tumour immune response and a long lasting effect to prevent relapse is essential if complete tumour destruction is not achieved on the first dose. Destruction of cancer stem cells, or cancer-initiating cells, may also be critical to achieve a complete response rather than a transient remission. Whilst there is some evidence to suggest that other oncolytic viruses may be able to target cancer stem cells (Cripe, Wang et al. 2009; Ahtiainen, Mirantes et al. 2010), this is not yet described for vaccinia virus.

Ultimately, despite the potential of vaccinia as a novel treatment for cancer, current data exist from phase II trials only and results from a planned phase III trial for the JX-594 virus in liver cancer (Schmidt 2011) will not be available for some time. The effectiveness of oncolytic vaccinia in a clinical setting remains to be proven and it may be that the limitations that apply to other vectors such as adenovirus may also be applicable to vaccinia. Whilst multiple doses of virus have been administered in clinical trials (Liu, Hwang et al. 2008; Park, Hwang et al. 2008), these studies were not primarily designed for efficacy, and the ability of subsequent doses to initiate tumour clearance in the face of a host immune response following the first dose is unclear. Repeated doses in pre-clinical models have demonstrated immune –mediated virus clearance that limits further virus efficacy (Chang, Ma et al. 2009). It is tempting to hope that results from pre-clinical models, where a single dose of virus leads to complete tumour regression (Zhang, Yu et al. 2007; Yu, Galanis et al. 2009), may translate into the clinic although ultimately, this may be asking too much. The likelihood of a virus propagating and destroying every tumour cell before immune clearance is slim, and therefore measures must be taken to increase virus spread, enable delivery of multiple doses and to combine oncolytic virotherapy with current treatments to amplify the overall response rate.

With these in mind, this work focused on the use of oncolytic virus for ovarian cancer, whose spread is largely limited to the peritoneal cavity. This affords the opportunity for intraperitoneal delivery of vaccinia, which achieves high concentrations of virus around the site of tumour deposits. Typically, in advanced disease there are multiple individual tumours throughout the peritoneal cavity and full surgical resection is not possible. As it may be difficult for oncolytic vaccinia also to seek out these numerous targets completely, combination of vaccinia with a platinum-based chemotherapy routinely used in the treatment of ovarian cancer is attractive. In order to enhance potential virus spread and efficacy, the effect of expressing decorin from an oncolytic strain was also investigated. Finally, the rational design of combination therapies and the ability to administer multiple doses of virus depends partly on a thorough understanding of the mechanisms of targeted tumour cell death.

Another vital consideration is the development of an immune response following the first dose of virus that prevents further re-infection, and several strategies already exist that aim to prevent this. These include consecutive dosing with a different virus to which the host has not developed a memory immune response (Le Boeuf, Diallo et al. 2010; Zhang, Tsai et al. 2010) and the use of anti-inflammatory drugs that have been shown to suppress the frequency of vaccinia virus-specific B cells and the production of neutralizing IgG, to enable repeated administration of vaccinia (Chang, Ma et al. 2009; Bernard, Bancos et al. 2010). Assuming that the immune response can be manipulated in such a way that repeated (and effective) doses of vaccinia may be given, the emergence of resistance to vaccinia is an area that has not yet been touched on. The life cycle of vaccinia is well understood, yet the mechanisms by which it kills target tumour cells is open to some debate; the general consensus is that vaccinia causes a primarily lytic death although there are some reports of apoptotic death in tumour cells (Liskova, Knitlova et al. 2011) and in immune cells (Baixeras, Cebrian et al. 1998; Engelmayer, Larsson et al. 1999; Humlova, Vokurka et al. 2002). Fully understanding the pathway of vaccinia-induced cell death is a step towards deciphering the mechanisms that might lead towards resistance to oncolytic virotherapy.

Work presented here has demonstrated the ability of vaccinia to specifically infect ovarian tumour tissue following systemic, intraperitoneal delivery and *in vitro* data suggest that it is capable of killing a range of ovarian cancer cell lines with a narrow range of sensitivity. This is promising if vaccinia is to progress as a generic treatment for ovarian cancer in the clinic, and may eliminate the costly and time consuming need to select suitable patients based on the presence of specific markers. Although efficacy could not be demonstrated in a challenging pre-clinical model of ovarian cancer, it is promising that cisplatin-resistant cells appear to respond to oncolytic vaccinia and exhibit a level of sensitivity similar to their non-resistant counterparts. The majority of patients treated with chemotherapy relapse and resistance ultimately develops to platinum-based therapy leaving limited treatment options. As these treatment-refractory patients are those most likely to be offered oncolytic vaccinia in the first instance, it is encouraging that cisplatin-resistant cells are sensitive to vaccinia, although great caution must be taken when attempting to extrapolate the results of a limited study *in vitro* to a clinical scenario. Disappointingly, vaccinia and cisplatin did not demonstrate synergy in the work presented within this thesis, unlike that recently suggested between vaccinia and paclitaxel (Huang, Sikorski et al. 2010). Although vaccinia and cisplatin do not synergise, that is not to say that there may not be an additive effect of using the two together, as has been reported against pancreatic cancer (Yu, Galanis et al. 2009). Further experiments to determine the effect of cisplatin on virus replication might rule out any antagonistic activity, and combination therapy in a less challenging *in vivo* model of ovarian cancer may yield favourable results over treatment with either therapy alone.

Attempts to improve the spread and efficacy of vaccinia virus by expressing the extracellular matrix protein decorin were unsuccessful. Vaccinia has already evolved for long range spread within the host and produces EEV which are resistant to both complement and neutralising IgG (Vanderplasschen, Hollinshead et al. 1997; Vanderplasschen, Mathew et al. 1998). Nonetheless, the fact that vaccinia has no definitive receptor means that efficient systemic delivery of an engineered oncolytic strain is hampered by infection of normal cells that do not support replication. Thus, only a small percentage of the dose injected is expected to reach the tumour and so efforts to maximise replication and spread are encouraged to maximise tumour cell destruction. Attempts to target various components of the extracellular matrix in combination with oncolytic viruses have shown to enhance viral activity and spread (Kim, Lee et al. 2006; Cheng, Sauthoff et al. 2007; Ganesh, Gonzalez Edick et al. 2007; Ganesh, Gonzalez-Edick et al. 2008; Watanabe, Kojima et al. 2010). Furthermore, collagen is a major component of the extracellular matrix and inhibits the spread of the large DNA virus herpes simplex (McKee, Grandi et al. 2006). As decorin is proposed to inhibit collagen fibril formation and also EGF, TGFβ1 and c-met receptor signalling pathways, all of which have been implicated in the progression and metastasis of ovarian cancer (Xu, Jiang et al. 2010; Mitra, Sawada et al. 2011; Yamamura, Matsumura et al. 2012), its expression from oncolytic vaccinia was hypothesised to enhance overall anti-tumour activity.

Crucially, levels of decorin released from infected cells were almost certainly too low to have an effect on these pathways. Robust models to quantify the spread of vaccinia *in vivo* were not available in this thesis but it is proposed that any advantage decorin might confer on the spread of other viruses such as adenovirus (Choi, Lee et al. 2010) is redundant in the case of vaccinia, which already has a rapid and efficient life cycle. In addition, although ECM modulating enzymes or proteins have shown efficacy previously, it might perhaps be more pertinent to target the ECM with regard to the specific nature of the tumour in question. With regards to ovarian cancer, the overwhelming barrier to increasing patient survival is the development of resistance to current therapeutics and the lack of alternative options. This is in contrast to other cancers where the physicality of the tumour microenvironment inhibits systemic delivery of chemotherapy, either by a poor blood supply and/or extensive stroma (Olive, Jacobetz et al. 2009). Combination of ECM modulating agents with viral therapy may require detailed knowledge of the ECM in question and a rational approach rather than a one-size fits all policy across all tumours.

Work focusing on the mechanism of ovarian cancer cell death revealed that markers of apoptosis, autophagy and necrosis were all present in infected cells, with an indication that necrosis is the predominant mode of death. Whilst vaccinia clearly interferes with the autophagic process, as indicated by increased LC3B-II following infection, an actual increase in autophagic flux was not seen and the relevance of this aberrant pathway to cell death could not be determined. Similarly, caspase-independent apoptosis was initiated but this too did not significantly contribute to cell death. The emergence of necrosis as a programmed form of cell death (Hitomi, Christofferson et al. 2008; Vandenabeele, Galluzzi et al. 2010) suggests that this process may be regulated during infection with viruses and certainly, there is an indication that this pathway may be initiated during the course of vaccinia infection. A logical next step in this body of work would be to study these same mechanisms in an *in vivo* setting. Whilst there is some work to suggest that replication efficiency *in vitro* corresponds to *in vivo* anti-tumour activity (Chen, Yu et al. 2011), other work reveals that the sensitivity of two different pancreatic cell xenografts to vaccinia is similar, despite wildly different profiles *in vitro* (Yu, Galanis et al. 2009), suggesting that the ability of cancer cells to die is in part dependent on their environment. Furthermore, there is some indication that different doses of West Nile virus can result in different modes of cell death (Chu and Ng 2003). As individual areas of tumour *in vivo* are likely to be subject to a whole range in number of infectious virions, it would be interesting to see how *in vivo* data corresponds to that described here of cells in culture.

Finally, the work presented here has focused on the mechanism of vaccinia-induced cell death in ovarian cancer cells that are all relatively similar in their sensitivity to vaccinia. Although Lister-dTK is an engineered strain designed to replicate in tumour cells only, it is capable of infecting both normal and tumour tissue. As has been demonstrated in normal ovarian surface epithelial cells, Lister-dTK is attenuated compared to the wild-type virus but still results in cell death. The mechanisms behind vaccinia-induced cell death in normal cells compared to that observed in ovarian tumour cells were not explored in this work. Given that tumour cells typically have aberrant cell death pathways, the mechanisms behind which vaccinia can override these to destroy cells warrants further investigation, and it is not yet clear if tumour and normal cells die by the same means. It would be interesting to examine if cells that are more resistant to vaccinia display similar characteristics to the ovarian cancer cells studied here. A larger panel of ovarian cancer cells is yet to be studied for sensitivity to vaccinia although, so far at least, they do not appear to vary as greatly in sensitivity to vaccinia as they do with other oncolytic viruses such as adenovirus (Flak, Connell et al. 2010). Recently, the potential for resistance to develop to viral gene therapy was described, where acquired resistance to an oncolytic strain of herpes simplex virus was associated with an altered gene expression signature (Song, Haddad et al. 2012). Microarray analysis revealed altered expression of genes that may be associated with viral attachment, entry and replication in resistant cells, as well as genes involved in the acute immune response. Persistent adenovirus expression in gut-associated lymphoid tissue has also been described in humans, and work in primates has hinted that chronic infection with virus shedding in stools may arise following initial exposure (Roy, Vandenberghe et al. 2009), which may cause some concern for repeated and prolonged exposure of patients to adenovirus vectors. To date, Song *et al* are the first to describe acquired resistance to oncolytic therapy and it is not yet known if resistance might develop to vaccinia, although this could be established fairly easily with exposure to increasing concentrations *in vitro*. The ability of vaccinia to induce cell death, and the mechanisms behind this, may vary across normal cells, sensitive tumour cells, inherently resistant tumour cells and in tumour cells that have acquired resistance through continued exposure to vaccinia. The work commenced here has attempted to decipher these pathways in ovarian cancer cells of similar sensitivity, and it would be interesting to expand this further to cover the above populations.

The field of oncolytic virotherapy as a whole has advanced hugely from the first designed vectors. Highly selective strains have been engineered as a result of increased understanding of the individual viral vectors and their target tumour cells. In addition, the generation of strains expressing further therapeutic genes has led to highly effective anti-tumour activity, in pre-clinical models at least. Currently, clinical trials have demonstrated the safety of vaccinia as a potential therapeutic agent and there are a number of key upcoming trials that will be critical for the future of viral gene therapy. Although in the early stages of clinical development, a phase I trial will explore the potential of repeated, intra-peritioneally delivered vaccinia virus (GL-ONC1) for the treatment of advanced peritoneal carcinomatosis, including that arising from ovarian cancer. A phase II trial from Jennerex seeks to show a survival advantage of the JX-594 strain plus best supportive care over best supportive care alone in hepatocellular carcinoma and, most exciting of all, a phase III trial of JX-594 as a first line therapy is planned for hepatocellular carcinoma, followed by additional therapy with sorafenib. Despite several setbacks in the field, and building on decades of work and historical observations, oncolytic vaccinia is now a serious consideration as a novel therapeutic for cancer.

Chapter 7

References

7. References

Adany, R., R. Heimer, et al. (1990). "Altered expression of chondroitin sulfate proteoglycan in the stroma of human colon carcinoma. Hypomethylation of PG-40 gene correlates with increased PG-40 content and mRNA levels." J Biol Chem **265**(19): 11389-96.

Adany, R. and R. V. Iozzo (1991). "Hypomethylation of the decorin proteoglycan gene in human colon cancer." Biochem J **276 (Pt 2)**: 301-6.

Ahn, H. J., Y. S. Kim, et al. (2004). "Mechanism of taxol-induced apoptosis in human SKOV3 ovarian carcinoma cells." J Cell Biochem **91**(5): 1043-52.

Ahtiainen, L., C. Mirantes, et al. (2010). "Defects in innate immunity render breast cancer initiating cells permissive to oncolytic adenovirus." PLoS One **5**(11): e13859.

Alcami, A. and G. L. Smith (1992). "A soluble receptor for interleukin-1 beta encoded by vaccinia virus: a novel mechanism of virus modulation of the host response to infection." Cell **71**(1): 153-67.

Alcami, A. and G. L. Smith (1995). "Vaccinia, cowpox, and camelpox viruses encode soluble gamma interferon receptors with novel broad species specificity." J Virol **69**(8): 4633-9.

Alcami, A., J. A. Symons, et al. (1998). "Blockade of chemokine activity by a soluble chemokine binding protein from vaccinia virus." J Immunol **160**(2): 624-33.

Alcami, A., J. A. Symons, et al. (2000). "The vaccinia virus soluble alpha/beta interferon (IFN) receptor binds to the cell surface and protects cells from the antiviral effects of IFN." J Virol **74**(23): 11230-9.

Alemany, R., K. Suzuki, et al. (2000). "Blood clearance rates of adenovirus type 5 in mice." J Gen Virol **81**(Pt 11): 2605-9.

Almoguera, C., D. Shibata, et al. (1988). "Most human carcinomas of the exocrine pancreas contain mutant c-K-ras genes." Cell **53**(4): 549-54.

Alonso, M., C. Tamasdan, et al. (2003). "Flavopiridol induces apoptosis in glioma cell lines independent of retinoblastoma and p53 tumor suppressor pathway alterations by a caspase-independent pathway." Mol Cancer Ther **2**(2): 139-50.

Amaravadi, R. K. (2008). "Autophagy-induced tumor dormancy in ovarian cancer." J Clin Invest **118**(12): 3837-40.

Andrade, A. A., P. N. Silva, et al. (2004). "The vaccinia virus-stimulated mitogen-activated protein kinase (MAPK) pathway is required for virus multiplication." Biochem J **381**(Pt 2): 437-46.

Andrea McCart, J., N. Mehta, et al. (2004). "Oncolytic Vaccinia Virus Expressing the Human Somatostatin Receptor SSTR2: Molecular Imaging after Systemic Delivery Using 111In-Pentetreotide." Mol Ther **10**(3): 553-561.

Aoyagi, M., D. Zhai, et al. (2007). "Vaccinia virus N1L protein resembles a B cell lymphoma-2 (Bcl-2) family protein." Protein Sci **16**(1): 118-24.

Aragon, T. J., S. Ulrich, et al. (2003). "Risks of serious complications and death from smallpox vaccination: a systematic review of the United States experience, 1963-1968." BMC Public Health **3**: 26.

Armstrong, D. K., B. Bundy, et al. (2006). "Intraperitoneal cisplatin and paclitaxel in ovarian cancer." N Engl J Med **354**(1): 34-43.

Baird, S. K., J. L. Aerts, et al. (2007). "Oncolytic adenoviral mutants induce a novel mode of programmed cell death in ovarian cancer." Oncogene **27**(22): 3081-3090.

Baixeras, E., A. Cebrian, et al. (1998). "Vaccinia virus-induced apoptosis in immature B lymphocytes: role of cellular Bcl-2." Virus Res **58**(1-2): 107-13.

Bankhead, C. R., C. Collins, et al. (2008). "Identifying symptoms of ovarian cancer: a qualitative and quantitative study." BJOG **115**(8): 1008-14.

Bartholomeusz, C., D. Rosen, et al. (2008). "PEA-15 induces autophagy in human ovarian cancer cells and is associated with prolonged overall survival." Cancer Res **68**(22): 9302-10.

Bartlett, N., J. A. Symons, et al. (2002). "The vaccinia virus N1L protein is an intracellular homodimer that promotes virulence." J Gen Virol **83**(Pt 8): 1965-76.

Bell, C. W., W. Jiang, et al. (2006). "The extracellular release of HMGB1 during apoptotic cell death." Am J Physiol Cell Physiol **291**(6): C1318-25.

Bengali, Z., A. C. Townsley, et al. (2009). "Vaccinia virus strain differences in cell attachment and entry." Virology **389**(1-2): 132-40.

Bernard, M. P., S. Bancos, et al. (2010). "Chronic inhibition of cyclooxygenase-2 attenuates antibody responses against vaccinia infection." Vaccine **28**(5): 1363-72.

Bhide, V. M., C. A. Laschinger, et al. (2005). "Collagen phagocytosis by fibroblasts is regulated by decorin." J Biol Chem **280**(24): 23103-13.

Bi, X., N. M. Pohl, et al. (2012). "Decorin-mediated inhibition of colorectal cancer growth and migration is associated with E-cadherin in vitro and in mice." Carcinogenesis.

Bialek, J., U. Kunanuvat, et al. (2011). "Relaxin enhances the collagenolytic activity and in vitro invasiveness by upregulating matrix metalloproteinases in human thyroid carcinoma cells." Mol Cancer Res **9**(6): 673-87.

Bidere, N., H. K. Lorenzo, et al. (2003). "Cathepsin D triggers Bax activation, resulting in selective apoptosis-inducing factor (AIF) relocation in T lymphocytes entering the early commitment phase to apoptosis." J Biol Chem **278**(33): 31401-11.

Billings, B., S. A. Smith, et al. (2004). "Lack of N1L gene expression results in a significant decrease of vaccinia virus replication in mouse brain." Ann N Y Acad Sci **1030**: 297-302.

Blansfield, J. A., D. Caragacianu, et al. (2008). "Combining agents that target the tumor microenvironment improves the efficacy of anticancer therapy." Clin Cancer Res **14**(1): 270-80.

Bluming, A. Z. and J. L. Ziegler (1971). "Regression of Burkitt's lymphoma in association with measles infection." Lancet **2**(7715): 105-6.

Bolton, K., D. Segal, et al. (2008). "Decorin is a secreted protein associated with obesity and type 2 diabetes." Int J Obes (Lond) **32**(7): 1113-21.

Bookman, M. A., K. M. Darcy, et al. (2003). "Evaluation of monoclonal humanized anti-HER2 antibody, trastuzumab, in patients with recurrent or refractory ovarian or primary peritoneal carcinoma with overexpression of HER2: a phase II trial of the Gynecologic Oncology Group." J Clin Oncol **21**(2): 283-90.

Bosman, F. T. and I. Stamenkovic (2003). "Functional structure and composition of the extracellular matrix." J Pathol **200**(4): 423-8.

Boujrad, H., O. Gubkina, et al. (2007). "AIF-mediated programmed necrosis: a highly regulated way to die." Cell Cycle **6**(21): 2612-9.

Boulter, E. A. (1969). "Protection against poxviruses." Proc R Soc Med **62**(3): 295-7.

Brader, P., K. J. Kelly, et al. (2009). "Imaging a Genetically Engineered Oncolytic Vaccinia Virus (GLV-1h99) Using a Human Norepinephrine Transporter Reporter Gene." Clin Cancer Res **15**(11): 3791-801.

Breitbach, C. J., J. Burke, et al. (2011). "Intravenous delivery of a multi-mechanistic cancer-targeted oncolytic poxvirus in humans." Nature **477**(7362): 99-102.

Breitbach, C. J., J. M. Paterson, et al. (2007). "Targeted inflammation during oncolytic virus therapy severely compromises tumor blood flow." Mol Ther **15**(9): 1686-93.

Broker, L. E., F. A. Kruyt, et al. (2005). "Cell death independent of caspases: a review." Clin Cancer Res **11**(9): 3155-62.

Brown, E., T. McKee, et al. (2003). "Dynamic imaging of collagen and its modulation in tumors in vivo using second-harmonic generation." Nat Med **9**(6): 796-800.

Broyles, S. S. (2003). "Vaccinia virus transcription." J Gen Virol **84**(Pt 9): 2293-303.

Brune, W. (2011). "Inhibition of programmed cell death by cytomegaloviruses." Virus Res **157**(2): 144-50.

Buller, R. M., S. Chakrabarti, et al. (1988). Deletion of the vaccinia virus growth factor gene reduces virus virulence. **62:** 866-874.

Buller, R. M., S. Chakrabarti, et al. (1988). "Deletion of the vaccinia virus growth factor gene reduces virus virulence." J Virol **62**(3): 866-74.

Buller, R. M., S. Chakrabarti, et al. (1988). "Cell proliferative response to vaccinia virus is mediated by VGF." Virology **164**(1): 182-92.

Buraschi, S., N. Pal, et al. (2010). "Decorin antagonizes Met receptor activity and down-regulates {beta}-catenin and Myc levels." J Biol Chem **285**(53): 42075-85.

Burdick, K. H. and W. A. Hawk (1964). "Vitiligo in a Case of Vaccinia Virus-Treated Melanoma." Cancer **17**: 708-12.

Burns, J. M., D. J. Dairaghi, et al. (2002). "Comprehensive mapping of poxvirus vCCI chemokine-binding protein. Expanded range of ligand interactions and unusual dissociation kinetics." J Biol Chem **277**(4): 2785-9.

Cabello-Verrugio, C. and E. Brandan (2007). "A novel modulatory mechanism of transforming growth factor-beta signaling through decorin and LRP-1." J Biol Chem **282**(26): 18842-50.

Cabon, L., P. Galan-Malo, et al. (2012). "BID regulates AIF-mediated caspase-independent necroptosis by promoting BAX activation." Cell Death Differ.

Campbell, S., B. Hazes, et al. (2010). "Vaccinia virus F1L interacts with Bak using highly divergent Bcl-2 homology domains and replaces the function of Mcl-1." J Biol Chem **285**(7): 4695-708.

CancerResearchUK. (2011, 23/03/11). "Ovarian cancer survival statistics." Retrieved 20/11/11, 2011, from http://info.cancerresearchuk.org/cancerstats/types/ovary/survival/.

CancerResearchUK. (2011, 04/11/11). "Ovarian Cancer-UK incidence statistics." Retrieved 20/11/11, 2011, from http://info.cancerresearchuk.org/cancerstats/types/ovary/incidence/.

Carroll, K., O. Elroy-Stein, et al. (1993). "Recombinant vaccinia virus K3L gene product prevents activation of double-stranded RNA-dependent, initiation factor 2 alpha-specific protein kinase." J Biol Chem **268**(17): 12837-42.

Carter, G. C., M. Law, et al. (2005). "Entry of the vaccinia virus intracellular mature virion and its interactions with glycosaminoglycans." J Gen Virol **86**(Pt 5): 1279-90.

Chaitanya, G. V., A. J. Steven, et al. (2010). "PARP-1 cleavage fragments: signatures of cell-death proteases in neurodegeneration." Cell Commun Signal **8**: 31.

Chalikonda, S., M. H. Kivlen, et al. (2008). "Oncolytic virotherapy for ovarian carcinomatosis using a replication-selective vaccinia virus armed with a yeast cytosine deaminase gene." Cancer Gene Ther **15**(2): 115-25.

Challa, S., M. Woelfel, et al. (2010). "Viral cell death inhibitor MC159 enhances innate immunity against vaccinia virus infection." J Virol **84**(20): 10467-76.

Chan, F. K., J. Shisler, et al. (2003). "A role for tumor necrosis factor receptor-2 and receptor-interacting protein in programmed necrosis and antiviral responses." J Biol Chem **278**(51): 51613-21.

Chang, C. L., B. Ma, et al. (2009). "Treatment with cyclooxygenase-2 inhibitors enables repeated administration of vaccinia virus for control of ovarian cancer." Mol Ther **17**(8): 1365-72.

Chang, E., S. Chalikonda, et al. (2005). "Targeting vaccinia to solid tumors with local hyperthermia." Hum Gene Ther **16**(4): 435-44.

Chang, H. W., J. C. Watson, et al. (1992). "The E3L gene of vaccinia virus encodes an inhibitor of the interferon-induced, double-stranded RNA-dependent protein kinase." Proc Natl Acad Sci U S A **89**(11): 4825-9.

Chen, N. G., Y. A. Yu, et al. (2011). "Replication efficiency of oncolytic vaccinia virus in cell cultures prognosticates the virulence and antitumor efficacy in mice." J Transl Med **9**: 164.

Cheng, J., H. Sauthoff, et al. (2007). "Human matrix metalloproteinase-8 gene delivery increases the oncolytic activity of a replicating adenovirus." Mol Ther **15**(11): 1982-90.

Cho, Y., T. McQuade, et al. (2011). "RIP1-dependent and independent effects of necrostatin-1 in necrosis and T cell activation." PLoS One **6**(8): e23209.

Cho, Y. S., S. Challa, et al. (2009). "Phosphorylation-driven assembly of the RIP1-RIP3 complex regulates programmed necrosis and virus-induced inflammation." Cell **137**(6): 1112-23.

Choi, I. K., Y. S. Lee, et al. (2010). "Effect of decorin on overcoming the extracellular matrix barrier for oncolytic virotherapy." Gene Ther **17**(2): 190-201.

Christofferson, D. E. and J. Yuan (2010). "Necroptosis as an alternative form of programmed cell death." Curr Opin Cell Biol **22**(2): 263-8.

Chu, J. J. and M. L. Ng (2003). "The mechanism of cell death during West Nile virus infection is dependent on initial infectious dose." J Gen Virol **84**(Pt 12): 3305-14.

Colombo, N., D. Guthrie, et al. (2003). "International Collaborative Ovarian Neoplasm trial 1: a randomized trial of adjuvant chemotherapy in women with early-stage ovarian cancer." J Natl Cancer Inst **95**(2): 125-32.

Connolly, D. C., R. Bao, et al. (2003). "Female mice chimeric for expression of the simian virus 40 TAg under control of the MISIIR promoter develop epithelial ovarian cancer." Cancer Res **63**(6): 1389-97.

Cooray, S., M. W. Bahar, et al. (2007). "Functional and structural studies of the vaccinia virus virulence factor N1 reveal a Bcl-2-like anti-apoptotic protein." J Gen Virol **88**(Pt 6): 1656-66.

Cripe, T. P., P. Y. Wang, et al. (2009). "Targeting cancer-initiating cells with oncolytic viruses." Mol Ther **17**(10): 1677-82.

Csordas, G., M. Santra, et al. (2000). "Sustained down-regulation of the epidermal growth factor receptor by decorin. A mechanism for controlling tumor growth in vivo." J Biol Chem **275**(42): 32879-87.

Danielson, K. G., H. Baribault, et al. (1997). "Targeted disruption of decorin leads to abnormal collagen fibril morphology and skin fragility." J Cell Biol **136**(3): 729-43.

Daugas, E., S. A. Susin, et al. (2000). "Mitochondrio-nuclear translocation of AIF in apoptosis and necrosis." FASEB J **14**(5): 729-39.

Davies, M. V., O. Elroy-Stein, et al. (1992). "The vaccinia virus K3L gene product potentiates translation by inhibiting double-stranded-RNA-activated protein kinase and phosphorylation of the alpha subunit of eukaryotic initiation factor 2." J Virol **66**(4): 1943-50.

De Clercq, E. (2002). "Cidofovir in the therapy and short-term prophylaxis of poxvirus infections." Trends Pharmacol Sci **23**(10): 456-8.

De Luca, A., M. Santra, et al. (1996). "Decorin-induced growth suppression is associated with up-regulation of p21, an inhibitor of cyclin-dependent kinases." J Biol Chem **271**(31): 18961-5.

De Wever, O. and M. Mareel (2003). "Role of tissue stroma in cancer cell invasion." J Pathol **200**(4): 429-47.

Degenhardt, K., R. Mathew, et al. (2006). "Autophagy promotes tumor cell survival and restricts necrosis, inflammation, and tumorigenesis." Cancer Cell **10**(1): 51-64.

Degterev, A., J. Hitomi, et al. (2008). "Identification of RIP1 kinase as a specific cellular target of necrostatins." Nat Chem Biol **4**(5): 313-21.

Delavallee, L., L. Cabon, et al. (2011). "AIF-mediated caspase-independent necroptosis: a new chance for targeted therapeutics." IUBMB Life **63**(4): 221-32.

Deng, H., N. Tang, et al. (2008). "Oncolytic virotherapy for multiple myeloma using a tumour-specific double-deleted vaccinia virus." Leukemia **22**(12): 2261-4.

Do, T. V., L. A. Kubba, et al. (2008). "Transforming growth factor-beta1, transforming growth factor-beta2, and transforming growth factor-beta3 enhance ovarian cancer metastatic potential by inducing a Smad3-dependent epithelial-to-mesenchymal transition." Mol Cancer Res **6**(5): 695-705.

Dobbelstein, M. and T. Shenk (1996). "Protection against apoptosis by the vaccinia virus SPI-2 (B13R) gene product." J Virol **70**(9): 6479-85.

Doceul, V., M. Hollinshead, et al. (2010). "Repulsion of superinfecting virions: a mechanism for rapid virus spread." Science **327**(5967): 873-6.

Doms, R. W., R. Blumenthal, et al. (1990). "Fusion of intra- and extracellular forms of vaccinia virus with the cell membrane." J Virol **64**(10): 4884-92.

Downward, J. (2003). "Targeting RAS signalling pathways in cancer therapy." Nat Rev Cancer **3**(1): 11-22.

Dranoff, G., E. Jaffee, et al. (1993). "Vaccination with irradiated tumor cells engineered to secrete murine granulocyte-macrophage colony-stimulating factor stimulates potent, specific, and long-lasting anti-tumor immunity." Proc Natl Acad Sci U S A **90**(8): 3539-43.

Droguett, R., C. Cabello-Verrugio, et al. (2006). "Extracellular proteoglycans modify TGF-beta bio-availability attenuating its signaling during skeletal muscle differentiation." Matrix Biol **25**(6): 332-41.

Efstathiou, E. and C. J. Logothetis (2010). "A New Therapy Paradigm for Prostate Cancer Founded on Clinical Observations." Clin Cancer Res.

Eguchi, Y., S. Shimizu, et al. (1997). "Intracellular ATP levels determine cell death fate by apoptosis or necrosis." Cancer Res **57**(10): 1835-40.

Engelmayer, J., M. Larsson, et al. (1999). "Vaccinia virus inhibits the maturation of human dendritic cells: a novel mechanism of immune evasion." J Immunol **163**(12): 6762-8.

Erbs, P., A. Findeli, et al. (2007). "Modified vaccinia virus Ankara as a vector for suicide gene therapy." Cancer Gene Ther **15**(1): 18-28.

Fang, Q., L. Yang, et al. (2005). "Host range, growth property, and virulence of the smallpox vaccine: vaccinia virus Tian Tan strain." Virology **335**(2): 242-51.

Feng, S., Y. Yang, et al. (2007). "Cleavage of RIP3 inactivates its caspase-independent apoptosis pathway by removal of kinase domain." Cell Signal **19**(10): 2056-67.

Feoktistova, M., P. Geserick, et al. (2011). "cIAPs block Ripoptosome formation, a RIP1/caspase-8 containing intracellular cell death complex differentially regulated by cFLIP isoforms." Mol Cell **43**(3): 449-63.

Fidler, I. J. (2003). "The pathogenesis of cancer metastasis: the 'seed and soil' hypothesis revisited." Nat Rev Cancer **3**(6): 453-8.

Fiedler, L. R. and J. A. Eble (2009). "Decorin regulates endothelial cell-matrix interactions during angiogenesis." Cell Adh Migr **3**(1).

Fishman, D. A., A. Kearns, et al. (1998). "Metastatic dissemination of human ovarian epithelial carcinoma is promoted by alpha2beta1-integrin-mediated interaction with type I collagen." Invasion Metastasis **18**(1): 15-26.

Flak, M. B., C. M. Connell, et al. (2010). "p21 Promotes oncolytic adenoviral activity in ovarian cancer and is a potential biomarker." Mol Cancer **9**: 175.

Foloppe, J., J. Kintz, et al. (2008). "Targeted delivery of a suicide gene to human colorectal tumors by a conditionally replicating vaccinia virus." Gene Ther **15**(20): 1361-1371.

Frentzen, A., Y. A. Yu, et al. (2009). "Anti-VEGF single-chain antibody GLAF-1 encoded by oncolytic vaccinia virus significantly enhances antitumor therapy." Proc Natl Acad Sci U S A **106**(31): 12915-20.

Galmiche, M. C., L. Rindisbacher, et al. (1997). "Expression of a functional single chain antibody on the surface of extracellular enveloped vaccinia virus as a step towards selective tumour cell targeting." J Gen Virol **78 (Pt 11)**: 3019-27.

Ganesh, S., M. Gonzalez Edick, et al. (2007). "Relaxin-expressing, fiber chimeric oncolytic adenovirus prolongs survival of tumor-bearing mice." Cancer Res **67**(9): 4399-407.

Ganesh, S., M. Gonzalez-Edick, et al. (2008). "Intratumoral coadministration of hyaluronidase enzyme and oncolytic adenoviruses enhances virus potency in metastatic tumor models." Clin Cancer Res **14**(12): 3933-41.

Gentile, A., L. Trusolino, et al. (2008). "The Met tyrosine kinase receptor in development and cancer." Cancer Metastasis Rev **27**(1): 85-94.

Gentschev, I., U. Donat, et al. (2010). "Regression of human prostate tumors and metastases in nude mice following treatment with the recombinant oncolytic vaccinia virus GLV-1h68." J Biomed Biotechnol **2010**: 489759.

Gentschev, I., M. Muller, et al. (2011). "Efficient colonization and therapy of human hepatocellular carcinoma (HCC) using the oncolytic vaccinia virus strain GLV-1h68." PLoS One **6**(7): e22069.

Girgis, N. M., B. C. Dehaven, et al. (2011). "The Vaccinia virus complement control protein modulates adaptive immune responses during infection." J Virol **85**(6): 2547-56.

Gnant, M. F., M. Puhlmann, et al. (1999). "Systemic administration of a recombinant vaccinia virus expressing the cytosine deaminase gene and subsequent treatment with 5-fluorocytosine leads to tumor-specific gene expression and prolongation of survival in mice." Cancer Res **59**(14): 3396-403.

Gobeil, S., C. C. Boucher, et al. (2001). "Characterization of the necrotic cleavage of poly(ADP-ribose) polymerase (PARP-1): implication of lysosomal proteases." Cell Death Differ **8**(6): 588-94.

Goldoni, S., A. Humphries, et al. (2009). "Decorin is a novel antagonistic ligand of the Met receptor." J Cell Biol **185**(4): 743-54.

Goldoni, S., D. G. Seidler, et al. (2008). "An antimetastatic role for decorin in breast cancer." Am J Pathol **173**(3): 844-55.

Gonzalez, V. M., M. A. Fuertes, et al. (2001). "Is cisplatin-induced cell death always produced by apoptosis?" Mol Pharmacol **59**(4): 657-63.

Gordon, A. N., N. Finkler, et al. (2005). "Efficacy and safety of erlotinib HCl, an epidermal growth factor receptor (HER1/EGFR) tyrosine kinase inhibitor, in patients with advanced ovarian carcinoma: results from a phase II multicenter study." Int J Gynecol Cancer **15**(5): 785-92.

Grant, D. S., C. Yenisey, et al. (2002). "Decorin suppresses tumor cell-mediated angiogenesis." Oncogene **21**(31): 4765-77.

Greiner, S., J. Y. Humrich, et al. (2006). "The highly attenuated vaccinia virus strain modified virus Ankara induces apoptosis in melanoma cells and allows bystander dendritic cells to generate a potent anti-tumoral immunity." Clin Exp Immunol **146**(2): 344-53.

Guedan, S., J. J. Rojas, et al. (2010). "Hyaluronidase expression by an oncolytic adenovirus enhances its intratumoral spread and suppresses tumor growth." Mol Ther **18**(7): 1275-83.

Guo, Z. S., A. Naik, et al. (2005). The Enhanced Tumor Selectivity of an Oncolytic Vaccinia Lacking the Host Range and Antiapoptosis Genes SPI-1 and SPI-2. **65:** 9991-9998.

Guo, Z. S., V. Parimi, et al. (2011). "The combination of immunosuppression and carrier cells significantly enhances the efficacy of oncolytic poxvirus in the pre-immunized host." Gene Ther **17**(12): 1465-75.

Guo, Z. S., S. H. Thorne, et al. (2008). "Oncolytic virotherapy: molecular targets in tumor-selective replication and carrier cell-mediated delivery of oncolytic viruses." Biochim Biophys Acta **1785**(2): 217-31.

Guse, K., M. Sloniecka, et al. (2010). "Antiangiogenic arming of an oncolytic vaccinia virus enhances antitumor efficacy in renal cell cancer models." J Virol **84**(2): 856-66.

Haddad, D., N. G. Chen, et al. (2011). "Insertion of the human sodium iodide symporter to facilitate deep tissue imaging does not alter oncolytic or replication capability of a novel vaccinia virus." J Transl Med **9**: 36.

Hanahan, D. and R. A. Weinberg (2000). "The hallmarks of cancer." Cell **100**(1): 57-70.

Hanahan, D. and R. A. Weinberg (2011). "Hallmarks of cancer: the next generation." Cell **144**(5): 646-74.

Hanna, E., J. Quick, et al. (2009). "The tumour microenvironment: a novel target for cancer therapy." Oral Dis **15**(1): 8-17.

Hannaford, P. C., L. Iversen, et al. (2010). "Mortality among contraceptive pill users: cohort evidence from Royal College of General Practitioners' Oral Contraception Study." BMJ **340**: c927.

Harrington, K., Vile, R., Pandha, H. (2008). Viral Therapy of Cancer, Wiley & Sons Inc.

He, S., L. Wang, et al. (2009). "Receptor interacting protein kinase-3 determines cellular necrotic response to TNF-alpha." Cell **137**(6): 1100-11.

Hellstrom, I., G. Goodman, et al. (2001). "Overexpression of HER-2 in ovarian carcinomas." Cancer Res **61**(6): 2420-3.

Hengstschlager, M., M. Knofler, et al. (1994). Different regulation of thymidine kinase during the cell cycle of normal versus DNA tumor virus-transformed cells. **269:** 13836-13842.

Heo, J., C. J. Breitbach, et al. (2011). "Sequential therapy with JX-594, a targeted oncolytic poxvirus, followed by sorafenib in hepatocellular carcinoma: preclinical and clinical demonstration of combination efficacy." Mol Ther **19**(6): 1170-9.

Hitomi, J., D. E. Christofferson, et al. (2008). "Identification of a molecular signaling network that regulates a cellular necrotic cell death pathway." Cell **135**(7): 1311-23.

Hruby, D. E. (1990). Vaccinia virus vectors: new strategies for producing recombinant vaccines. **3:** 153-170.

Hu, S., C. Vincenz, et al. (1997). "A novel family of viral death effector domain-containing molecules that inhibit both CD-95- and tumor necrosis factor receptor-1-induced apoptosis." J Biol Chem **272**(15): 9621-4.

Hu, Y., H. Sun, et al. (2009). "Decorin suppresses prostate tumor growth through inhibition of epidermal growth factor and androgen receptor pathways." Neoplasia **11**(10): 1042-53.

Huang, B., R. Sikorski, et al. (2010). "Synergistic anti-tumor effects between oncolytic vaccinia virus and paclitaxel are mediated by the IFN response and HMGB1." Gene Ther.

Huang, B., R. Sikorski, et al. (2011). "Synergistic anti-tumor effects between oncolytic vaccinia virus and paclitaxel are mediated by the IFN response and HMGB1." Gene Ther **18**(2): 164-72.

Huang, C. Y., T. Y. Lu, et al. (2008). "A novel cellular protein, VPEF, facilitates vaccinia virus penetration into HeLa cells through fluid phase endocytosis." J Virol **82**(16): 7988-99.

Humlova, Z., M. Vokurka, et al. (2002). "Vaccinia virus induces apoptosis of infected macrophages." J Gen Virol **83**(Pt 11): 2821-32.

Hung, C. F., Y. C. Tsai, et al. (2006). "Vaccinia virus preferentially infects and controls human and murine ovarian tumors in mice." Gene Ther **14**(1): 20-29.

Hunter-Craig, I., K. A. Newton, et al. (1970). "Use of vaccinia virus in the treatment of metastatic malignant melanoma." Br Med J **2**(5708): 512-5.

Huttenlocher, A., Z. Werb, et al. (1996). "Decorin regulates collagenase gene expression in fibroblasts adhering to vitronectin." Matrix Biol **15**(4): 239-50.

Ichimura, Y., T. Kirisako, et al. (2000). "A ubiquitin-like system mediates protein lipidation." Nature **408**(6811): 488-92.

Immonen, A., M. Vapalahti, et al. (2004). "AdvHSV-tk Gene Therapy with Intravenous Ganciclovir Improves Survival in Human Malignant Glioma: A Randomised, Controlled Study." Mol Ther **10**(5): 967-972.

Ingemarsdotter, C. K., S. K. Baird, et al. (2010). "Low-dose paclitaxel synergizes with oncolytic adenoviruses via mitotic slippage and apoptosis in ovarian cancer." Oncogene **29**(45): 6051-63.

Iozzo, R. V., F. Chakrani, et al. (1999). "Cooperative action of germ-line mutations in decorin and p53 accelerates lymphoma tumorigenesis." Proc Natl Acad Sci U S A **96**(6): 3092-7.

Iozzo, R. V., D. K. Moscatello, et al. (1999). "Decorin is a biological ligand for the epidermal growth factor receptor." J Biol Chem **274**(8): 4489-92.

Izmailyan, R. A., C. Y. Huang, et al. (2006). "The envelope G3L protein is essential for entry of vaccinia virus into host cells." J Virol **80**(17): 8402-10.

Jacobs, N., N. W. Bartlett, et al. (2008). "Vaccinia virus lacking the Bcl-2-like protein N1 induces a stronger natural killer cell response to infection." J Gen Virol **89**(Pt 11): 2877-81.

Jiang, H., E. J. White, et al. (2011). "Human adenovirus type 5 induces cell lysis through autophagy and autophagy-triggered caspase activity." J Virol **85**(10): 4720-9.

Jodele, S., L. Blavier, et al. (2006). "Modifying the soil to affect the seed: role of stromal-derived matrix metalloproteinases in cancer progression." Cancer Metastasis Rev **25**(1): 35-43.

Jordan, T. X. and G. Randall (2011). "Manipulation or capitulation: virus interactions with autophagy." Microbes Infect.

Joseph, B., P. Marchetti, et al. (2002). "Mitochondrial dysfunction is an essential step for killing of non-small cell lung carcinomas resistant to conventional treatment." Oncogene **21**(1): 65-77.

Kalamajski, S., A. Aspberg, et al. (2007). "The decorin sequence SYIRIADTNIT binds collagen type I." J Biol Chem **282**(22): 16062-7.

Katz, E., E. J. Wolffe, et al. (1997). "The cytoplasmic and transmembrane domains of the vaccinia virus B5R protein target a chimeric human immunodeficiency virus type 1 glycoprotein to the outer envelope of nascent vaccinia virions." J Virol **71**(4): 3178-87.

Kaur, B., T. P. Cripe, et al. (2009). ""Buy one get one free": armed viruses for the treatment of cancer cells and their microenvironment." Curr Gene Ther **9**(5): 341-55.

Kelly, K. J., Y. Woo, et al. (2008). "Novel oncolytic agent GLV-1h68 is effective against malignant pleural mesothelioma." Hum Gene Ther **19**(8): 774-82.

Kettle, S., A. Alcami, et al. (1997). "Vaccinia virus serpin B13R (SPI-2) inhibits interleukin-1beta-converting enzyme and protects virus-infected cells from TNF- and Fas-mediated apoptosis, but does not prevent IL-1beta-induced fever." J Gen Virol **78 (Pt 3)**: 677-85.

Kibler, K. V., T. Shors, et al. (1997). "Double-stranded RNA is a trigger for apoptosis in vaccinia virus-infected cells." J Virol **71**(3): 1992-2003.

Kim, J. H., Y. S. Lee, et al. (2006). "Relaxin expression from tumor-targeting adenoviruses and its intratumoral spread, apoptosis induction, and efficacy." J Natl Cancer Inst **98**(20): 1482-93.

Kim, J. H., J. Y. Oh, et al. (2006). "Systemic Armed Oncolytic and Immunologic Therapy for Cancer with JX-594, a Targeted Poxvirus Expressing GM-CSF." Mol Ther **14**(3): 361-370.

Kirn, D. H., Y. Wang, et al. (2007). "Targeting of interferon-beta to produce a specific, multi-mechanistic oncolytic vaccinia virus." PLoS Med **4**(12): e353.

Kirn, D. H., Y. Wang, et al. (2008). Enhancing Poxvirus Oncolytic Effects through Increased Spread and Immune Evasion. **68:** 2071-2075.

Kondo, Y., T. Kanzawa, et al. (2005). "The role of autophagy in cancer development and response to therapy." Nat Rev Cancer **5**(9): 726-34.

Koninger, J., N. A. Giese, et al. (2004). "Overexpressed decorin in pancreatic cancer: potential tumor growth inhibition and attenuation of chemotherapeutic action." Clin Cancer Res **10**(14): 4776-83.

Koninger, J., T. Giese, et al. (2004). "Pancreatic tumor cells influence the composition of the extracellular matrix." Biochem Biophys Res Commun **322**(3): 943-9.

Kotwal, G. J., S. N. Isaacs, et al. (1990). "Inhibition of the complement cascade by the major secretory protein of vaccinia virus." Science **250**(4982): 827-30.

Kotwal, G. J. and B. Moss (1989). "Vaccinia virus encodes two proteins that are structurally related to members of the plasma serine protease inhibitor superfamily." J Virol **63**(2): 600-6.

Kretzschmar, M., J. Wallinga, et al. (2006). "Frequency of adverse events after vaccination with different vaccinia strains." PLoS Med **3**(8): e272.

Kroemer, G., L. Galluzzi, et al. (2009). "Classification of cell death: recommendations of the Nomenclature Committee on Cell Death 2009." Cell Death Differ **16**(1): 3-11.

Kulbe, H., R. Thompson, et al. (2007). "The inflammatory cytokine tumor necrosis factor-alpha generates an autocrine tumor-promoting network in epithelial ovarian cancer cells." Cancer Res **67**(2): 585-92.

Kuznetsov, Y., P. D. Gershon, et al. (2008). "Atomic force microscopy investigation of vaccinia virus structure." J Virol **82**(15): 7551-66.

Labropoulou, V. T., A. D. Theocharis, et al. (2006). "Versican but not decorin accumulation is related to metastatic potential and neovascularization in testicular germ cell tumours." Histopathology **49**(6): 582-93.

Lafky, J. M., J. A. Wilken, et al. (2008). "Clinical implications of the ErbB/epidermal growth factor (EGF) receptor family and its ligands in ovarian cancer." Biochim Biophys Acta **1785**(2): 232-65.

Lane, J. M., F. L. Ruben, et al. (1969). "Complications of smallpox vaccination, 1968." N Engl J Med **281**(22): 1201-8.

Langhammer, S., R. Koban, et al. (2011). "Inhibition of poxvirus spreading by the anti-tumor drug Gefitinib (Iressa)." Antiviral Res **89**(1): 64-70.

Laster, S. M., J. G. Wood, et al. (1988). "Tumor necrosis factor can induce both apoptic and necrotic forms of cell lysis." J Immunol **141**(8): 2629-34.

Law, M., G. C. Carter, et al. (2006). "Ligand-induced and nonfusogenic dissolution of a viral membrane." Proc Natl Acad Sci U S A **103**(15): 5989-94.

Lazova, R., R. L. Camp, et al. (2011). "Punctate LC3B expression is a common feature of solid tumors and associated with proliferation, metastasis and poor outcome." Clin Cancer Res.

Le Boeuf, F., J. S. Diallo, et al. (2010). "Synergistic interaction between oncolytic viruses augments tumor killing." Mol Ther **18**(5): 888-95.

Le, X. F., W. Mao, et al. (2010). "Dasatinib induces autophagic cell death in human ovarian cancer." Cancer **116**(21): 4980-90.

Leist, M. and M. Jaattela (2001). "Four deaths and a funeral: from caspases to alternative mechanisms." Nat Rev Mol Cell Biol **2**(8): 589-98.

Levine, B. and G. Kroemer (2008). "Autophagy in the pathogenesis of disease." Cell **132**(1): 27-42.

Levine, B., S. Sinha, et al. (2008). "Bcl-2 family members: dual regulators of apoptosis and autophagy." Autophagy **4**(5): 600-6.

Li, M. and A. A. Beg (2000). "Induction of necrotic-like cell death by tumor necrosis factor alpha and caspase inhibitors: novel mechanism for killing virus-infected cells." J Virol **74**(16): 7470-7.

Lin, Y., A. Devin, et al. (1999). "Cleavage of the death domain kinase RIP by caspase-8 prompts TNF-induced apoptosis." Genes Dev **13**(19): 2514-26.

Liskova, J., J. Knitlova, et al. (2011). "Apoptosis and necrosis in vaccinia virus-infected HeLa G and BSC-40 cells." Virus Res **160**(1-2): 40-50.

Liu, T. C., T. Hwang, et al. (2008). "The targeted oncolytic poxvirus JX-594 demonstrates antitumoral, antivascular, and anti-HBV activities in patients with hepatocellular carcinoma." Mol Ther **16**(9): 1637-42.

Liu, X., M. Kremer, et al. (2004). "A natural vaccinia virus promoter with exceptional capacity to direct protein synthesis." J Virol Methods **122**(2): 141-5.

Locker, J. K., A. Kuehn, et al. (2000). "Entry of the two infectious forms of vaccinia virus at the plasma membane is signaling-dependent for the IMV but not the EEV." Mol Biol Cell **11**(7): 2497-511.

Loeffler, M., E. Daugas, et al. (2001). "Dominant cell death induction by extramitochondrially targeted apoptosis-inducing factor." FASEB J **15**(3): 758-67.

Lu, Z., R. Z. Luo, et al. (2008). "The tumor suppressor gene ARHI regulates autophagy and tumor dormancy in human ovarian cancer cells." J Clin Invest **118**(12): 3917-29.

Lun, X. Q., J. H. Jang, et al. (2009). "Efficacy of systemically administered oncolytic vaccinia virotherapy for malignant gliomas is enhanced by combination therapy with rapamycin or cyclophosphamide." Clin Cancer Res **15**(8): 2777-88.

Ma, X. H., S. Piao, et al. (2011). "Measurements of tumor cell autophagy predict invasiveness, resistance to chemotherapy, and survival in melanoma." Clin Cancer Res **17**(10): 3478-89.

Mack, C., A. Sickmann, et al. (2008). "Inhibition of proinflammatory and innate immune signaling pathways by a cytomegalovirus RIP1-interacting protein." Proc Natl Acad Sci U S A **105**(8): 3094-9.

Markman, M., B. N. Bundy, et al. (2001). "Phase III trial of standard-dose intravenous cisplatin plus paclitaxel versus moderately high-dose carboplatin followed by intravenous paclitaxel and intraperitoneal cisplatin in small-volume stage III ovarian carcinoma: an intergroup study of the Gynecologic Oncology Group, Southwestern Oncology Group, and Eastern Cooperative Oncology Group." J Clin Oncol **19**(4): 1001-7.

Mastrangelo, M. J., H. C. Maguire, Jr., et al. (1999). "Intratumoral recombinant GM-CSF-encoding virus as gene therapy in patients with cutaneous melanoma." Cancer Gene Ther **6**(5): 409-22.

Mastrangelo, M. J., H. C. Maguire, et al. (2000). "Intralesional vaccinia/GM-CSF recombinant virus in the treatment of metastatic melanoma." Adv Exp Med Biol **465**: 391-400.

McCart, J. A., M. Puhlmann, et al. (2000). "Complex interactions between the replicating oncolytic effect and the enzyme/prodrug effect of vaccinia-mediated tumor regression." Gene Ther **7**(14): 1217-23.

McCart, J. A., J. M. Ward, et al. (2001). Systemic Cancer Therapy with a Tumor-selective Vaccinia Virus Mutant Lacking Thymidine Kinase and Vaccinia Growth Factor Genes. **61:** 8751-8757.

McFarlane, S., J. Aitken, et al. (2011). "Early induction of autophagy in human fibroblasts after infection with human cytomegalovirus or herpes simplex virus 1." J Virol **85**(9): 4212-21.

McKee, T. D., P. Grandi, et al. (2006). "Degradation of fibrillar collagen in a human melanoma xenograft improves the efficacy of an oncolytic herpes simplex virus vector." Cancer Res **66**(5): 2509-13.

McNeish, I. A., S. Bell, et al. (2003). "Expression of Smac/DIABLO in ovarian carcinoma cells induces apoptosis via a caspase-9-mediated pathway." Exp Cell Res **286**(2): 186-98.

Mercer, J. and A. Helenius (2008). "Vaccinia virus uses macropinocytosis and apoptotic mimicry to enter host cells." Science **320**(5875): 531-5.

Mercer, J., S. Knebel, et al. (2009). "Vaccinia virus strains use distinct forms of macropinocytosis for host-cell entry." Proc Natl Acad Sci U S A **107**(20): 9346-51.

Merline, R., K. Moreth, et al. (2011). "Signaling by the Matrix Proteoglycan Decorin Controls Inflammation and Cancer Through PDCD4 and MicroRNA-21." Sci Signal **4**(199): ra75.

Michael T. Madigan, J. M. M., Jack Parker. (2000). Brock: Biology of Microorganisms, Prentice Hall.

Micheau, O. and J. Tschopp (2003). "Induction of TNF receptor I-mediated apoptosis via two sequential signaling complexes." Cell **114**(2): 181-90.

Mihaylova, M. M. and R. J. Shaw (2012). "The AMPK signalling pathway coordinates cell growth, autophagy and metabolism." Nat Cell Biol **13**(9): 1016-23.

Mitra, A. K., K. Sawada, et al. (2011). "Ligand-independent activation of c-Met by fibronectin and alpha(5)beta(1)-integrin regulates ovarian cancer invasion and metastasis." Oncogene **30**(13): 1566-76.

Mok, W., Y. Boucher, et al. (2007). "Matrix metalloproteinases-1 and -8 improve the distribution and efficacy of an oncolytic virus." Cancer Res **67**(22): 10664-8.

Moloughney, J. G., C. E. Monken, et al. (2011). "Vaccinia virus leads to ATG12-ATG3 conjugation and deficiency in autophagosome formation." Autophagy **7**(12).

Moscatello, D. K., M. Santra, et al. (1998). "Decorin suppresses tumor cell growth by activating the epidermal growth factor receptor." J Clin Invest **101**(2): 406-12.

Moser, T. L., S. V. Pizzo, et al. (1996). "Evidence for preferential adhesion of ovarian epithelial carcinoma cells to type I collagen mediated by the alpha2beta1 integrin." Int J Cancer **67**(5): 695-701.

Moss, B. (2001). Poxviridae: the viruses and their replication. Fields virology. P. M. H. D. M. Knipe, D. E. Griffin, R. A. Lamb, M. A. Martin, B. and a. S. E. S. Roizman. Philadelphia, Lippincott Williams & Wilkins**:** 2849–2883.

Moss, B. (2006). "Poxvirus entry and membrane fusion." Virology **344**(1): 48-54.

Moyer, R. W. (1987). "The role of the host cell nucleus in vaccinia virus morphogenesis." Virus Res **8**(3): 173-91.

Mueller, M. M. and N. E. Fusenig (2004). "Friends or foes - bipolar effects of the tumour stroma in cancer." Nat Rev Cancer **4**(11): 839-49.

Nagano, S., J. Y. Perentes, et al. (2008). "Cancer cell death enhances the penetration and efficacy of oncolytic herpes simplex virus in tumors." Cancer Res **68**(10): 3795-802.

Najarro, P., P. Traktman, et al. (2001). "Vaccinia virus blocks gamma interferon signal transduction: viral VH1 phosphatase reverses Stat1 activation." J Virol **75**(7): 3185-96.

Nash, M. A., M. T. Deavers, et al. (2002). "The expression of decorin in human ovarian tumors." Clin Cancer Res **8**(6): 1754-60.

Nash, M. A., A. E. Loercher, et al. (1999). "In vitro growth inhibition of ovarian cancer cells by decorin: synergism of action between decorin and carboplatin." Cancer Res **59**(24): 6192-6.

Neame, P. J., C. J. Kay, et al. (2000). "Independent modulation of collagen fibrillogenesis by decorin and lumican." Cell Mol Life Sci **57**(5): 859-63.

Neeman, M., R. Abramovitch, et al. (1997). "Regulation of angiogenesis by hypoxic stress: from solid tumours to the ovarian follicle." Int J Exp Pathol **78**(2): 57-70.

Ojeda, S., A. Domi, et al. (2006). "Vaccinia virus G9 protein is an essential component of the poxvirus entry-fusion complex." J Virol **80**(19): 9822-30.

Ojeda, S., T. G. Senkevich, et al. (2006). "Entry of vaccinia virus and cell-cell fusion require a highly conserved cysteine-rich membrane protein encoded by the A16L gene." J Virol **80**(1): 51-61.

Olive, K. P., M. A. Jacobetz, et al. (2009). "Inhibition of Hedgehog signaling enhances delivery of chemotherapy in a mouse model of pancreatic cancer." Science **324**(5933): 1457-61.

Pan, B. S., G. K. Chan, et al. (2010). "MK-2461, a Novel Multitargeted Kinase Inhibitor, Preferentially Inhibits the Activated c-Met Receptor." Cancer Res **70**(4): 1524-33.

Panicali, D., S. W. Davis, et al. (1981). "Two major DNA variants present in serially propagated stocks of the WR strain of vaccinia virus." J Virol **37**(3): 1000-10.

Park, B. H., T. Hwang, et al. (2008). "Use of a targeted oncolytic poxvirus, JX-594, in patients with refractory primary or metastatic liver cancer: a phase I trial." Lancet Oncol **9**(6): 533-42.

Pasquinucci, G. (1971). "Possible effect of measles on leukaemia." Lancet **1**(7690): 136.

Pattingre, S., A. Tassa, et al. (2005). "Bcl-2 antiapoptotic proteins inhibit Beclin 1-dependent autophagy." Cell **122**(6): 927-39.

Pellegata, N. S., F. Sessa, et al. (1994). "K-ras and p53 gene mutations in pancreatic cancer: ductal and nonductal tumors progress through different genetic lesions." Cancer Res **54**(6): 1556-60.

Pestell, K. E., S. M. Hobbs, et al. (2000). "Effect of p53 status on sensitivity to platinum complexes in a human ovarian cancer cell line." Mol Pharmacol **57**(3): 503-11.

Petit, A. M., J. Rak, et al. (1997). "Neutralizing antibodies against epidermal growth factor and ErbB-2/neu receptor tyrosine kinases down-regulate vascular endothelial growth factor production by tumor cells in vitro and in vivo: angiogenic implications for signal transduction therapy of solid tumors." Am J Pathol **151**(6): 1523-30.

Postigo, A., J. R. Cross, et al. (2006). "Interaction of F1L with the BH3 domain of Bak is responsible for inhibiting vaccinia-induced apoptosis." Cell Death Differ **13**(10): 1651-62.

Postigo, A., M. C. Martin, et al. (2009). "Vaccinia-induced epidermal growth factor receptor-MEK signalling and the anti-apoptotic protein F1L synergize to suppress cell death during infection." Cell Microbiol **11**(8): 1208-18.

Puhlmann, M., C. K. Brown, et al. (2000). "Vaccinia as a vector for tumor-directed gene therapy: biodistribution of a thymidine kinase-deleted mutant." Cancer Gene Ther **7**(1): 66-73.

Puhlmann, M., M. Gnant, et al. (1999). "Thymidine kinase-deleted vaccinia virus expressing purine nucleoside phosphorylase as a vector for tumor-directed gene therapy." Hum Gene Ther **10**(4): 649-57.

Ramsey-Ewing, A. and B. Moss (1998). "Apoptosis induced by a postbinding step of vaccinia virus entry into Chinese hamster ovary cells." Virology **242**(1): 138-49.

Raucci, A., R. Palumbo, et al. (2007). "HMGB1: a signal of necrosis." Autoimmunity **40**(4): 285-9.

Rauh-Hain, J. A., N. Rodriguez, et al. (2011). "Primary Debulking Surgery Versus Neoadjuvant Chemotherapy in Stage IV Ovarian Cancer." Ann Surg Oncol.

Reading, P. C., A. Khanna, et al. (2002). "Vaccinia virus CrmE encodes a soluble and cell surface tumor necrosis factor receptor that contributes to virus virulence." Virology **292**(2): 285-98.

Reed, C. C., J. Gauldie, et al. (2002). "Suppression of tumorigenicity by adenovirus-mediated gene transfer of decorin." Oncogene **21**(23): 3688-95.

Reed, C. C., A. Waterhouse, et al. (2005). "Decorin prevents metastatic spreading of breast cancer." Oncogene **24**(6): 1104-10.

Reynolds, L. P., A. T. Grazul-Bilska, et al. (2000). "Angiogenesis in the corpus luteum." Endocrine **12**(1): 1-9.

Ricciardelli, C., D. L. Russell, et al. (2007). "Formation of hyaluronan- and versican-rich pericellular matrix by prostate cancer cells promotes cell motility." J Biol Chem **282**(14): 10814-25.

Ritter, C. A., M. Perez-Torres, et al. (2007). "Human breast cancer cells selected for resistance to trastuzumab in vivo overexpress epidermal growth factor receptor and ErbB ligands and remain dependent on the ErbB receptor network." Clin Cancer Res **13**(16): 4909-19.

Roberts, K. L. and G. L. Smith (2008). "Vaccinia virus morphogenesis and dissemination." Trends Microbiol **16**(10): 472-9.

Roby, K. F., C. C. Taylor, et al. (2000). "Development of a syngeneic mouse model for events related to ovarian cancer." Carcinogenesis **21**(4): 585-91.

Rodriguez, G. (2003). "New insights regarding pharmacologic approaches for ovarian cancer prevention." Hematol Oncol Clin North Am **17**(4): 1007-20, x.

Rodriguez-Rocha, H., J. G. Gomez-Gutierrez, et al. (2011). "Adenoviruses induce autophagy to promote virus replication and oncolysis." Virology **416**(1-2): 9-15.

Roenigk, H. H., Jr., S. Deodhar, et al. (1974). "Immunotherapy of malignant melanoma with vaccinia virus." Arch Dermatol **109**(5): 668-73.

Roy, S., L. H. Vandenberghe, et al. (2009). "Isolation and characterization of adenoviruses persistently shed from the gastrointestinal tract of non-human primates." PLoS Pathog **5**(7): e1000503.

Salomaki, H. H., A. O. Sainio, et al. (2008). "Differential expression of decorin by human malignant and benign vascular tumors." J Histochem Cytochem **56**(7): 639-46.

Sancho-Martinez, S. M., F. J. Piedrafita, et al. (2011). "Necrotic concentrations of cisplatin activate the apoptotic machinery but inhibit effector caspases and interfere with the execution of apoptosis." Toxicol Sci **122**(1): 73-85.

Sandgren, K. J., J. Wilkinson, et al. (2010). "A differential role for macropinocytosis in mediating entry of the two forms of vaccinia virus into dendritic cells." PLoS Pathog **6**(4): e1000866.

Santra, M., I. Eichstetter, et al. (2000). "An anti-oncogenic role for decorin. Down-regulation of ErbB2 leads to growth suppression and cytodifferentiation of mammary carcinoma cells." J Biol Chem **275**(45): 35153-61.

Santra, M., D. M. Mann, et al. (1997). "Ectopic expression of decorin protein core causes a generalized growth suppression in neoplastic cells of various histogenetic origin and requires endogenous p21, an inhibitor of cyclin-dependent kinases." J Clin Invest **100**(1): 149-57.

Santra, M., C. C. Reed, et al. (2002). "Decorin binds to a narrow region of the epidermal growth factor (EGF) receptor, partially overlapping but distinct from the EGF-binding epitope." J Biol Chem **277**(38): 35671-81.

Santra, M., T. Skorski, et al. (1995). "De novo decorin gene expression suppresses the malignant phenotype in human colon cancer cells." Proc Natl Acad Sci U S A **92**(15): 7016-20.

Sarkar, S., A. Mazumdar, et al. (2010). "ZD6474, a dual tyrosine kinase inhibitor of EGFR and VEGFR-2, inhibits MAPK/ERK and AKT/PI3-K and induces apoptosis in breast cancer cells." Cancer Biol Ther **9**(8).

Satheshkumar, P. S. and B. Moss (2009). "Characterization of a newly identified 35-amino-acid component of the vaccinia virus entry/fusion complex conserved in all chordopoxviruses." J Virol **83**(24): 12822-32.

Sawai, H. and N. Domae (2011). "Discrimination between primary necrosis and apoptosis by necrostatin-1 in Annexin V-positive/propidium iodide-negative cells." Biochem Biophys Res Commun **411**(3): 569-73.

Scaffidi, P., T. Misteli, et al. (2002). "Release of chromatin protein HMGB1 by necrotic cells triggers inflammation." Nature **418**(6894): 191-5.

Scarlatti, F., R. Granata, et al. (2009). "Does autophagy have a license to kill mammalian cells?" Cell Death Differ **16**(1): 12-20.

Scarlatti, F., R. Maffei, et al. (2008). "Role of non-canonical Beclin 1-independent autophagy in cell death induced by resveratrol in human breast cancer cells." Cell Death Differ **15**(8): 1318-29.

Schilder, R. J., H. B. Pathak, et al. (2009). "Phase II trial of single agent cetuximab in patients with persistent or recurrent epithelial ovarian or primary peritoneal carcinoma with the potential for dose escalation to rash." Gynecol Oncol **113**(1): 21-7.

Schilder, R. J., M. W. Sill, et al. (2005). "Phase II study of gefitinib in patients with relapsed or persistent ovarian or primary peritoneal carcinoma and evaluation of epidermal growth factor receptor mutations and immunohistochemical expression: a Gynecologic Oncology Group Study." Clin Cancer Res **11**(15): 5539-48.

Schmidt, C. (2011). "Amgen spikes interest in live virus vaccines for hard-to-treat cancers." Nat Biotechnol **29**(4): 295-6.

Schmidt, F. I., C. K. Bleck, et al. (2011). "Vaccinia extracellular virions enter cells by macropinocytosis and acid-activated membrane rupture." Embo J **30**(17): 3647-61.

Schonherr, E., M. Broszat, et al. (1998). "Decorin core protein fragment Leu155-Val260 interacts with TGF-beta but does not compete for decorin binding to type I collagen." Arch Biochem Biophys **355**(2): 241-8.

Schorge, J. O., L. A. Garrett, et al. (2011). "Cytoreductive surgery for advanced ovarian cancer: quo vadis?" Oncology (Williston Park) **25**(10): 928-34.

Schramm, B. and J. K. Locker (2005). "Cytoplasmic organization of POXvirus DNA replication." Traffic **6**(10): 839-46.

Schweneker, M., S. Lukassen, et al. (2011). "The vaccinia virus O1 protein is required for sustained activation of the extracellular signal-regulated kinase (ERK) 1/2 and promotes viral virulence." J Virol.

Seglen, P. O. and P. B. Gordon (1982). "3-Methyladenine: specific inhibitor of autophagic/lysosomal protein degradation in isolated rat hepatocytes." Proc Natl Acad Sci U S A **79**(6): 1889-92.

Seidler, D. G., S. Goldoni, et al. (2006). "Decorin protein core inhibits in vivo cancer growth and metabolism by hindering epidermal growth factor receptor function and triggering apoptosis via caspase-3 activation." J Biol Chem **281**(36): 26408-18.

Senkevich, T. G. and B. Moss (2005). "Vaccinia virus H2 protein is an essential component of a complex involved in virus entry and cell-cell fusion." J Virol **79**(8): 4744-54.

Senkevich, T. G., B. M. Ward, et al. (2004). "Vaccinia virus entry into cells is dependent on a virion surface protein encoded by the A28L gene." J Virol **78**(5): 2357-66.

Sergina, N. V., M. Rausch, et al. (2007). "Escape from HER-family tyrosine kinase inhibitor therapy by the kinase-inactive HER3." Nature **445**(7126): 437-41.

Serrano-Olvera, A., A. Duenas-Gonzalez, et al. (2006). "Prognostic, predictive and therapeutic implications of HER2 in invasive epithelial ovarian cancer." Cancer Treat Rev **32**(3): 180-90.

Seubert, C. M., J. Stritzker, et al. (2011). "Enhanced tumor therapy using vaccinia virus strain GLV-1h68 in combination with a beta-galactosidase-activatable prodrug seco-analog of duocarmycin SA." Cancer Gene Ther **18**(1): 42-52.

Shen, S., O. Kepp, et al. (2012). "The end of autophagic cell death?" Autophagy **8**(1).

Shen, Y., D. D. Li, et al. (2008). "Decreased expression of autophagy-related proteins in malignant epithelial ovarian cancer." Autophagy **4**(8): 1067-8.

Shen, Y. and J. Nemunaitis (2005). "Fighting Cancer with Vaccinia Virus: Teaching New Tricks to an Old Dog." Mol Ther **11**(2): 180-195.

Shield, K., C. Riley, et al. (2007). "Alpha2beta1 integrin affects metastatic potential of ovarian carcinoma spheroids by supporting disaggregation and proteolysis." J Carcinog **6**: 11.

Shintani, K., A. Matsumine, et al. (2008). "Decorin suppresses lung metastases of murine osteosarcoma." Oncol Rep **19**(6): 1533-9.

Sinkovics, J. G. and J. C. Horvath (2008). "Natural and genetically engineered viral agents for oncolysis and gene therapy of human cancers." Arch Immunol Ther Exp (Warsz) **56 Suppl 1**: 3s-59s.

Skaznik-Wikiel, M. E., J. L. Lesnock, et al. (2011). "Intraperitoneal Chemotherapy for Recurrent Epithelial Ovarian Cancer Is Feasible With High Completion Rates, Low Complications, and Acceptable Patient Outcomes." Int J Gynecol Cancer.

Skulachev, V. P. (2006). "Bioenergetic aspects of apoptosis, necrosis and mitoptosis." Apoptosis **11**(4): 473-85.

Smith, E., J. Breznik, et al. (2011). "Strategies to enhance viral penetration of solid tumors." Hum Gene Ther **22**(9): 1053-60.

Smith, G. L. and B. Moss (1983). "Infectious poxvirus vectors have capacity for at least 25 000 base pairs of foreign DNA." Gene **25**(1): 21-8.

Smith, G. L., A. Vanderplasschen, et al. (2002). The formation and function of extracellular enveloped vaccinia virus. **83:** 2915-2931.

Song, T. J., D. Haddad, et al. (2012). "Molecular network pathways and functional analysis of tumor signatures associated with development of resistance to viral gene therapy." Cancer Gene Ther **19**(1): 38-48.

Song, X., Y. Zhou, et al. (2009). "Inhibition of retinoblastoma in vitro and in vivo with conditionally replicating oncolytic adenovirus H101." Invest Ophthalmol Vis Sci.

Steffensen, K. D., M. Waldstrom, et al. (2007). "The prognostic importance of cyclooxygenase 2 and HER2 expression in epithelial ovarian cancer." Int J Gynecol Cancer **17**(4): 798-807.

Stellrecht, C. M. and V. Gandhi (2009). "MET receptor tyrosine kinase as a therapeutic anticancer target." Cancer Lett **280**(1): 1-14.

Sulochana, K. N., H. Fan, et al. (2005). "Peptides derived from human decorin leucine-rich repeat 5 inhibit angiogenesis." J Biol Chem **280**(30): 27935-48.

Susin, S. A., E. Daugas, et al. (2000). "Two distinct pathways leading to nuclear apoptosis." J Exp Med **192**(4): 571-80.

Symons, J. A., A. Alcami, et al. (1995). "Vaccinia virus encodes a soluble type I interferon receptor of novel structure and broad species specificity." Cell **81**(4): 551-60.

Taqi, A. M., M. B. Abdurrahman, et al. (1981). "Regression of Hodgkin's disease after measles." Lancet **1**(8229): 1112.

Taylor, R. C., S. P. Cullen, et al. (2008). "Apoptosis: controlled demolition at the cellular level." Nat Rev Mol Cell Biol **9**(3): 231-41.

Tenev, T., K. Bianchi, et al. (2011). "The Ripoptosome, a Signaling Platform that Assembles in Response to Genotoxic Stress and Loss of IAPs." Mol Cell **43**(3): 432-48.

Tewari, M. and V. M. Dixit (1995). "Fas- and tumor necrosis factor-induced apoptosis is inhibited by the poxvirus crmA gene product." J Biol Chem **270**(7): 3255-60.

Thome, M., P. Schneider, et al. (1997). "Viral FLICE-inhibitory proteins (FLIPs) prevent apoptosis induced by death receptors." Nature **386**(6624): 517-21.

Thorne, S. H., D. L. Bartlett, et al. (2005). "The use of oncolytic vaccinia viruses in the treatment of cancer: a new role for an old ally?" Curr Gene Ther **5**(4): 429-43.

Thorne, S. H., T. H. Hwang, et al. (2007). "Rational strain selection and engineering creates a broad-spectrum, systemically effective oncolytic poxvirus, JX-963." J Clin Invest **117**(11): 3350-8.

Tian, S., J. Lin, et al. (2010). "Beclin 1-independent autophagy induced by a Bcl-XL/Bcl-2 targeting compound, Z18." Autophagy **6**(8): 1032-41.

Tian, Y., D. Sir, et al. (2011). "Requirement of Autophagy for HBV Replication in Transgenic Mice." J Virol.

Townsley, A. C. and B. Moss (2007). "Two distinct low-pH steps promote entry of vaccinia virus." J Virol **81**(16): 8613-20.

Townsley, A. C., T. G. Senkevich, et al. (2005). "The product of the vaccinia virus L5R gene is a fourth membrane protein encoded by all poxviruses that is required for cell entry and cell-cell fusion." J Virol **79**(17): 10988-98.

Townsley, A. C., T. G. Senkevich, et al. (2005). "Vaccinia virus A21 virion membrane protein is required for cell entry and fusion." J Virol **79**(15): 9458-69.

Trimbos, J. B., M. Parmar, et al. (2003). "International Collaborative Ovarian Neoplasm trial 1 and Adjuvant ChemoTherapy In Ovarian Neoplasm trial: two parallel randomized phase III trials of adjuvant chemotherapy in patients with early-stage ovarian carcinoma." J Natl Cancer Inst **95**(2): 105-12.

Troup, S., C. Njue, et al. (2003). "Reduced expression of the small leucine-rich proteoglycans, lumican, and decorin is associated with poor outcome in node-negative invasive breast cancer." Clin Cancer Res **9**(1): 207-14.

Tuefferd, M., J. Couturier, et al. (2007). "HER2 status in ovarian carcinomas: a multicenter GINECO study of 320 patients." PLoS One **2**(11): e1138.

Tysome, J. R., P. Wang, et al. (2011). "Lister vaccine strain of vaccinia virus armed with the endostatin-angiostatin fusion gene: an oncolytic virus superior to dl1520 (ONYX-015) for human head and neck cancer." Hum Gene Ther **22**(9): 1101-8.

Uhlen M, O. P., Fagerberg L, Lundberg E, Jonasson K, Forsberg M, Zwahlen M, Kampf C, Wester K, Hober S, Wernérus H, Björling L, Ponten F. (2010). "Towards a knowledge-based Human Protein Atlas." Nat Biotechnol **28**(12): 3.

Ulrich, T. A., E. M. de Juan Pardo, et al. (2009). "The mechanical rigidity of the extracellular matrix regulates the structure, motility, and proliferation of glioma cells." Cancer Res **69**(10): 4167-74.

Unemori, E. N., L. B. Pickford, et al. (1996). "Relaxin induces an extracellular matrix-degrading phenotype in human lung fibroblasts in vitro and inhibits lung fibrosis in a murine model in vivo." J Clin Invest **98**(12): 2739-45.

Upton, J. W., W. J. Kaiser, et al. (2008). "Cytomegalovirus M45 cell death suppression requires receptor-interacting protein (RIP) homotypic interaction motif (RHIM)-dependent interaction with RIP1." J Biol Chem **283**(25): 16966-70.

Upton, J. W., W. J. Kaiser, et al. (2010). "Virus inhibition of RIP3-dependent necrosis." Cell Host Microbe **7**(4): 302-13.

Vandenabeele, P., W. Declercq, et al. (2008). "Necrotic cell death and 'necrostatins': now we can control cellular explosion." Trends Biochem Sci **33**(8): 352-5.

Vandenabeele, P., L. Galluzzi, et al. (2010). "Molecular mechanisms of necroptosis: an ordered cellular explosion." Nat Rev Mol Cell Biol **11**(10): 700-14.

Vander Heiden, M. G., L. C. Cantley, et al. (2009). "Understanding the Warburg effect: the metabolic requirements of cell proliferation." Science **324**(5930): 1029-33.

Vanderplasschen, A., M. Hollinshead, et al. (1997). Antibodies against vaccinia virus do not neutralize extracellular enveloped virus but prevent virus release from infected cells and comet formation. **78:** 2041-2048.

Vanderplasschen, A., M. Hollinshead, et al. (1998). "Intracellular and extracellular vaccinia virions enter cells by different mechanisms." J Gen Virol **79 (Pt 4)**: 877-87.

Vanderplasschen, A., E. Mathew, et al. (1998). Extracellular enveloped vaccinia virus is resistant to complement because of incorporation of host complement control proteins into its envelope. **95:** 7544-7549.

Vanderplasschen, A. and G. L. Smith (1997). "A novel virus binding assay using confocal microscopy: demonstration that the intracellular and extracellular vaccinia virions bind to different cellular receptors." J Virol **71**(5): 4032-41.

Vermeer, P. D., J. McHugh, et al. (2007). "Vaccinia virus entry, exit, and interaction with differentiated human airway epithelia." J Virol **81**(18): 9891-9.

Vermes, I., C. Haanen, et al. (1995). "A novel assay for apoptosis. Flow cytometric detection of phosphatidylserine expression on early apoptotic cells using fluorescein labelled Annexin V." J Immunol Methods **184**(1): 39-51.

Vogel, K. G., M. Paulsson, et al. (1984). "Specific inhibition of type I and type II collagen fibrillogenesis by the small proteoglycan of tendon." Biochem J **223**(3): 587-97.

Wali, A. and D. S. Strayer (1999). "Infection with vaccinia virus alters regulation of cell cycle progression." DNA Cell Biol **18**(11): 837-43.

Wang, S. E., A. Narasanna, et al. (2006). "HER2 kinase domain mutation results in constitutive phosphorylation and activation of HER2 and EGFR and resistance to EGFR tyrosine kinase inhibitors." Cancer Cell **10**(1): 25-38.

Wasilenko, S. T., L. Banadyga, et al. (2005). "The vaccinia virus F1L protein interacts with the proapoptotic protein Bak and inhibits Bak activation." J Virol **79**(22): 14031-43.

Wasilenko, S. T., A. F. Meyers, et al. (2001). "Vaccinia virus infection disarms the mitochondrion-mediated pathway of the apoptotic cascade by modulating the permeability transition pore." J Virol **75**(23): 11437-48.

Wasilenko, S. T., T. L. Stewart, et al. (2003). "Vaccinia virus encodes a previously uncharacterized mitochondrial-associated inhibitor of apoptosis." Proc Natl Acad Sci U S A **100**(24): 14345-50.

Watanabe, Y., T. Kojima, et al. (2010). "A novel translational approach for human malignant pleural mesothelioma: heparanase-assisted dual virotherapy." Oncogene **29**(8): 1145-54.

Weibel, S., V. Raab, et al. (2011). "Viral-mediated oncolysis is the most critical factor in the late-phase of the tumor regression process upon vaccinia virus infection." BMC Cancer **11**: 68.

Weihua, Z., R. Tsan, et al. (2008). "Survival of cancer cells is maintained by EGFR independent of its kinase activity." Cancer Cell **13**(5): 385-93.

Whitbeck, J. C., C. H. Foo, et al. (2009). "Vaccinia virus exhibits cell-type-dependent entry characteristics." Virology **385**(2): 383-91.

Wileman, T. (2006). "Aggresomes and autophagy generate sites for virus replication." Science **312**(5775): 875-8.

Wittek, R. (2006). "Vaccinia immune globulin: current policies, preparedness, and product safety and efficacy." Int J Infect Dis **10**(3): 193-201.

Wu, H., S. Wang, et al. (2008). "Overexpression of decorin induces apoptosis and cell growth arrest in cultured rat mesangial cells in vitro." Nephrology (Carlton) **13**(7): 607-15.

Wu, I. C., D. C. Wu, et al. (2010). "Plasma decorin predicts the presence of esophageal squamous cell carcinoma." Int J Cancer **127**(9): 2138-46.

Xu, Z., Y. Jiang, et al. (2010). "TGFbeta and EGF synergistically induce a more invasive phenotype of epithelial ovarian cancer cells." Biochem Biophys Res Commun **401**(3): 376-81.

Yamaguchi, Y., D. M. Mann, et al. (1990). "Negative regulation of transforming growth factor-beta by the proteoglycan decorin." Nature **346**(6281): 281-4.

Yamamura, S., N. Matsumura, et al. (2012). "The activated transforming growth factor-beta signaling pathway in peritoneal metastases is a potential therapeutic target in ovarian cancer." Int J Cancer **130**(1): 20-8.

Yang, H., S. K. Kim, et al. (2005). "Antiviral chemotherapy facilitates control of poxvirus infections through inhibition of cellular signal transduction." J Clin Invest **115**(2): 379-87.

Yang, J., X. Liu, et al. (1997). "Prevention of apoptosis by Bcl-2: release of cytochrome c from mitochondria blocked." Science **275**(5303): 1129-32.

Yang, S., Z. S. Guo, et al. (2007). "A new recombinant vaccinia with targeted deletion of three viral genes: its safety and efficacy as an oncolytic virus." Gene Ther **14**(8): 638-647.

Yigit, R., L. F. Massuger, et al. (2010). "Ovarian cancer creates a suppressive microenvironment to escape immune elimination." Gynecol Oncol **117**(2): 366-72.

Young, L. S., P. F. Searle, et al. (2006). "Viral gene therapy strategies: from basic science to clinical application." J Pathol **208**(2): 299-318.

Yu, S. W., H. Wang, et al. (2002). "Mediation of poly(ADP-ribose) polymerase-1-dependent cell death by apoptosis-inducing factor." Science **297**(5579): 259-63.

Yu, Y. A., C. Galanis, et al. (2009). "Regression of human pancreatic tumor xenografts in mice after a single systemic injection of recombinant vaccinia virus GLV-1h68." Mol Cancer Ther **8**(1): 141-51.

Zafiropoulos, A., D. Nikitovic, et al. (2008). "Decorin-induced growth inhibition is overcome through protracted expression and activation of epidermal growth factor receptors in osteosarcoma cells." Mol Cancer Res **6**(5): 785-94.

Zeineldin, R., C. Y. Muller, et al. (2010). "Targeting the EGF receptor for ovarian cancer therapy." J Oncol **2010**: 414676.

Zhai, D., E. Yu, et al. (2010). "Vaccinia virus protein F1L is a caspase-9 inhibitor." J Biol Chem **285**(8): 5569-80.

Zhang, D. W., J. Shao, et al. (2009). "RIP3, an energy metabolism regulator that switches TNF-induced cell death from apoptosis to necrosis." Science **325**(5938): 332-6.

Zhang, H., C. E. Monken, et al. (2006). "Cellular autophagy machinery is not required for vaccinia virus replication and maturation." Autophagy **2**(2): 91-5.

Zhang, N., Y. Chen, et al. (2011). "PARP and RIP 1 are required for autophagy induced by 11'-deoxyverticillin A, which precedes caspase-dependent apoptosis." Autophagy **7**(6): 598-612.

Zhang, N., Y. Qi, et al. (2010). "FTY720 induces necrotic cell death and autophagy in ovarian cancer cells: a protective role of autophagy." Autophagy **6**(8): 1157-67.

Zhang, Q., Y. A. Yu, et al. (2007). "Eradication of solid human breast tumors in nude mice with an intravenously injected light-emitting oncolytic vaccinia virus." Cancer Res **67**(20): 10038-46.

Zhang, X. Y., X. Y. Xi, et al. (2011). "Autophagy inhibitor 3-MA decreases the production and release of infectious enterovirus 71 particles." Zhonghua Shi Yan He Lin Chuang Bing Du Xue Za Zhi **25**(3): 176-8.

Zhang, Y. Q., Y. C. Tsai, et al. (2010). "Enhancing the therapeutic effect against ovarian cancer through a combination of viral oncolysis and antigen-specific immunotherapy." Mol Ther **18**(4): 692-9.

Zhang, Z., M. R. Abrahams, et al. (2005). "The vaccinia virus N1L protein influences cytokine secretion in vitro after infection." Ann N Y Acad Sci **1056**: 69-86.

Zhou, Q., S. Snipas, et al. (1997). "Target protease specificity of the viral serpin CrmA. Analysis of five caspases." J Biol Chem **272**(12): 7797-800.

Zhu, J. X., S. Goldoni, et al. (2005). "Decorin evokes protracted internalization and degradation of the epidermal growth factor receptor via caveolar endocytosis." J Biol Chem **280**(37): 32468-79.

Ziauddin, M. F., Z. S. Guo, et al. (2010). "TRAIL gene-armed oncolytic poxvirus and oxaliplatin can work synergistically against colorectal cancer." Gene Ther **17**(4): 550-9.

Ziauddin, M. F., Z. S. Guo, et al. (2011). "TRAIL gene-armed oncolytic poxvirus and oxaliplatin can work synergistically against colorectal cancer." Gene Ther **17**(4): 550-9.

Zillhardt, M., J. G. Christensen, et al. (2010). "An orally available small-molecule inhibitor of c-Met, PF-2341066, reduces tumor burden and metastasis in a preclinical model of ovarian cancer metastasis." Neoplasia **12**(1): 1-10.

Zygiert, Z. (1971). "Hodgkin's disease: remissions after measles." Lancet **1**(7699): 593.